Fourth Annual Science Day
Faculty of Science-Sohag University

2019, March 5

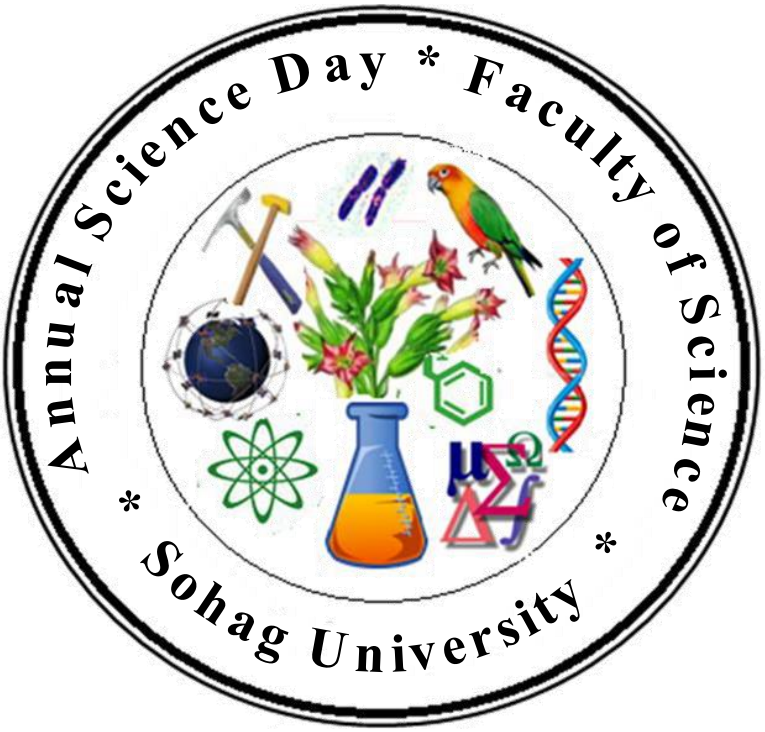

المؤتمر العلمى السنوى الرابع لكلية العلوم
جامعة سوهاج

Abstract Book for Papers Published by Staff Members of Faculty of Science during 2018

PREFACE

This abstract book is compiled of more than 260 papers published in estimated international journals by Staff members of Faculty of Science, Sohag University during 08. The book was made on the sidelines of the 4th Annual Science Day ceremony held on, 5 March, 2019 at Sohag Faculty of Science under the patronage of Dr. **Ahmed A. El-Ansary**, the Governor of Sohag, Prof. Dr. **Ahmed Aziz Abdel-Monem**, President of Sohag University, and Prof. Dr. **Ahmed Mohamed Soliman**, Dean of Faculty of Science.

Besides emerging the scientific research activities of staff members, the Abstract book as a whole is an important reference of the recent advances in research. Furthermore, the Annual Science Day meeting offers an opportunity for researchers from different departments who work on similar research problems but rarely cross paths, to connect with each other. Science Day event is also a great opportunity to share the value of our research with different sectors of community services.

Congratulations to all who participated, and thanks to everyone made this event such a huge success.

Dean of Faculty of Science
Prof. Dr. Ahmed M. Soliman

Organizing Committee

Prof. Dr. Ahmed M. Soliman	Dean of Faculty of Science
Prof. Dr. Ahmed M. Ahmed Ali	Vice-Dean for Graduate Students & Research Affairs
Prof. Dr. Kamal M. S. Khalil	Vice-Dean for Education & Students Affairs
Prof. Dr. Zakaria A. Mohamed	Chairman of Botany & Microbiology Department
Prof. Dr. Lobna A. E. Naser	Director of Quality Assurance Unit
Prof. Dr. Hazem Elmeshneb	Physics Department
Prof. Dr. Alaa Y. Fahmey	Zoology Department
Dr. Mohamed Ismael	Chemistry Department
Dr. Omar Elhady	Chemistry Department
Dr. Mostafa G. Redwan	Geology Department
Dr. Mahmoud Abdel Aleem Ali	Chemistry Department
Dr. Ahmed M. Abu-Dief	Chemistry Department
Dr. Naglaa Yousef	Botany & Microbiology Department
Dr. Mohamed Attef	Geology Department
Dr. Gamal Ismail	Mathematics & Computer Science Department
Dr. Hamdy Hassan	Mathematics & Computer Science Department
Dr. Mahmoud S. Bakheit	Botany & Microbiology Department
Dr. Alaa Elmeshneb	Physics Department
Dr. Mohamed Alaraby	Zoology Department
Mrs. Elham A. Abd El-Hameed	Quality Assurance Unit
Mr. Ahmed M. Abdel-Mawgoud	Quality Assurance Unit

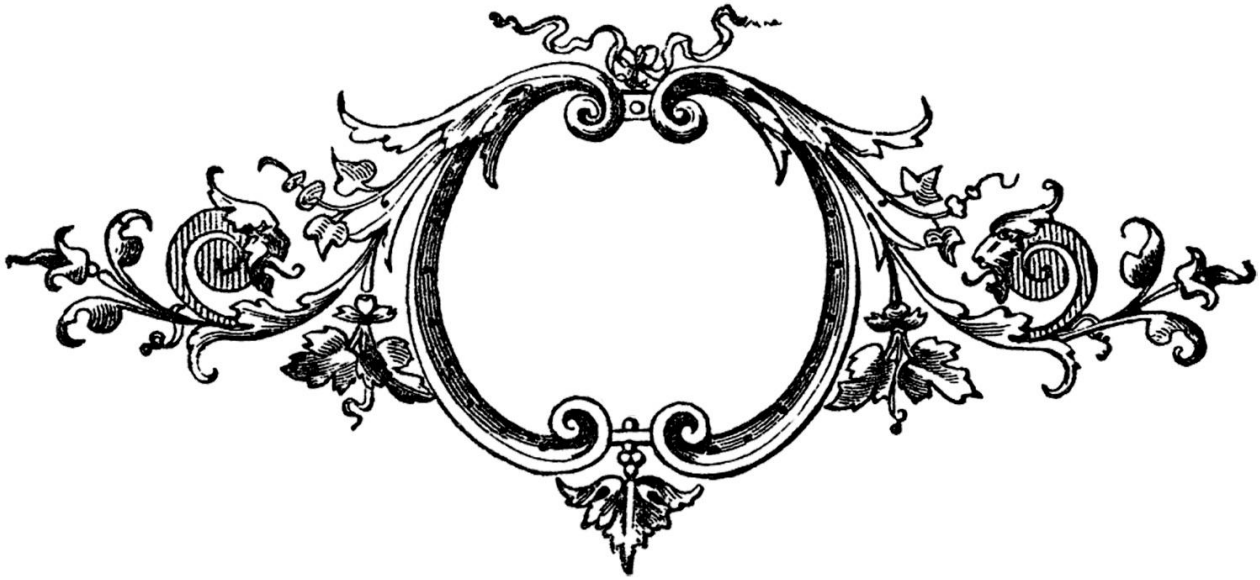

List of Publications

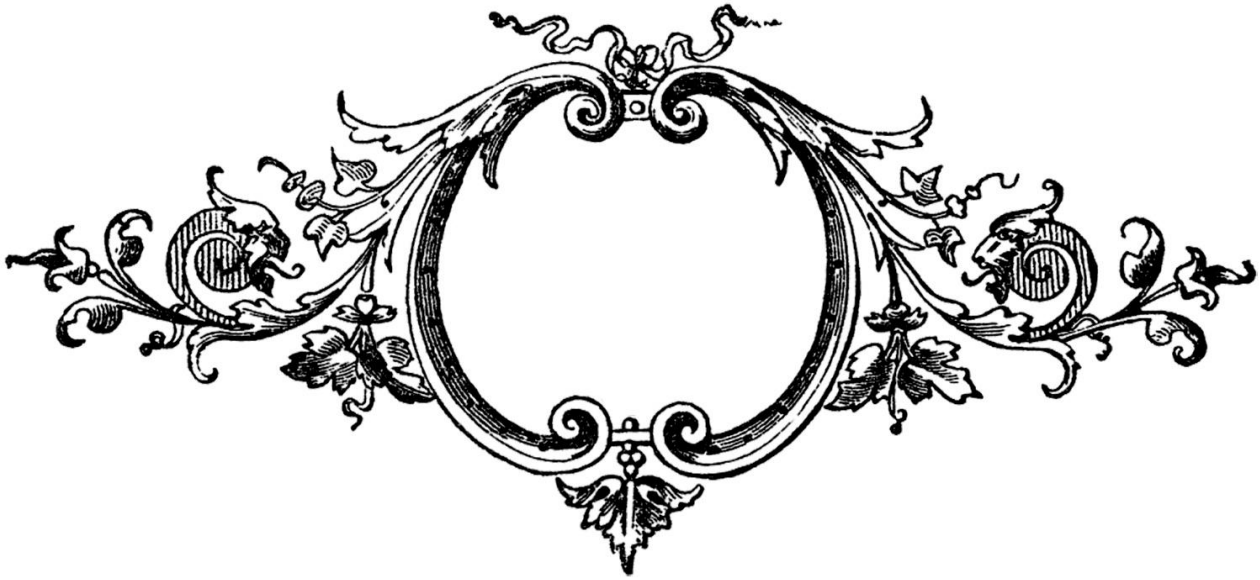

List of papers published by Staff members of Mathematics & Computer Science Department (Pages 1-38)

1	**Applied Mathematics & Information Sciences an International Journal** *Hamdy H .El-Sayed*
2	**Performance comparison of LEACH, SEP and Z-SEP protocols in WSN** *Hamdy H. El-Sayed*
3	**Performance Evaluation of Clustering EAMMH, LEACH, SEP, TEEN Protocols in WSN** *Hamdy H. El-Sayed*
4	**A Novel Algorithm based on Entanglement Measurement for Improving Speed of Quantum Algorithms** *Mohammed Zidan, Abdel-Haleem Abdel-Aty, A. Younes, E. A. Zanaty, I. El-khayat, Mahmoud Abdel-Aty*
5	**A Novelmetaheuristic Algorithm Based on Wave Function** *E.A. Zanaty, Khalid Abdel Wahab, Ali Qora*
6	**Generalized Hermite kernel function for support vector machine classifications** *E. A. Zanaty, Ashraf Afifi*
7	**Multi-Objective Optimization to Find the Shortest Paths Tree Problem in the Computer Networks** *Mahmoud A. Mofaddel, and Ahmed Y. Hamed*
8	**An Elliptical Boundary Skin Model For Hand Detection Based on HSV Color Space** *Usama Sayed, Mahmoud A. Mofaddel, Samy Bakheet, Zenab El-Zohry*
9	**Hiding Information using Secret Sharing Scheme Based on Gene Expression Programming** *Marghny H. Mohamed, Mahmoud A. Mofaddel, Tarek Y. Abd El-Naser*
10	**Text Message Encoding Based on Elliptic Curve Cryptography and a Mapping Methodology** *Omar Reyad*
11	**New SDN-Oriented Distributed Network Security System** *Fahad Nife, Zbigniew Kotulski and Omar Reyad*
12	**Multi-filter Score-Level Fusion for Fingerprint** *Muhammad Atta Othman Ahmed, Omar Reyad, Yasser AbdelSatar, Nahla F. Omran*
13	**Effect of rotation on the surface wave propagation in magneto-thermoelastic materials with voids** *AM Farhan, AM Abd-Alla*
14	**Effect of rotation and magnetic field on free vibrations in a spherical non-homogeneous embedded in an elastic medium** *F. S. Bayones and A. M. Abd-Alla*
15	**Eigenvalue approach to coupled thermoelasticity in a rotating isotropic medium** *F. S. Bayones and A. M. Abd-Alla*
16	**Effect of rotation and gravity on the reflection of P-waves from thermo-magneto-microstretch medium in the context of three phase lag model with initial stress** *S. M. Abo-Dahab, A. M. Abd-Alla, A. A. Kilany and M. Elsagheer*
17	**Reflection of plane waves in thermoelastic microstructured materials under the influence of gravitation** *S . M . Abo-Dahab, Adnan Jahangir and Abo-el-nour N. Abd-alla*
18	**Squeezing dynamics of a nanowire system with spin-orbit interaction** *R. I. Mohamed, A. Farouk, A. H. Homid4, O. H. El-Kalaawy, Abdel-Haleem Abdel-Aty4, M. Abdel-Aty3,5,6, and S. Ghose*
19	**New Design of Reversible Full Adder/Subtrac tor Using R Gate** *R. Montaser, A.Younes, and M. Abdel-Aty*
20	**Higher-Order Convolutions for Apostol-Bernoulli, Apostol-Euler and Apostol-Genocchi Polynomials** *Y. He, S. Araci, H. M. Srivastava and M. Abdel-Aty*
21	**Sub pico-second chirp-free optical solitons with Kaup-Newell equation using a couple of strategic algorithms** *S. Arshed, A. Biswas, M. Abdelaty, Q. Zhou, S. P. Moshokoa and M. Belic*

22	**Reflection and refraction of incident p-, T-, and SVwaves at interface between magnetized two solidliquid media with heat sources and initial stress with and without thermal relaxation times** *S. M. Abo-Dahaba,b, M. N. M. Allamc and M. Abdel-Atyd*
23	**Optical soliton perturbation with Kundu –Eckhaus equation by exp (− ϕ(ξ))-expansion scheme and G ′/G-expansion method** *S. Arsheda, A. Biswasb,c, M. Abdelatyd, Q. Zhouee, S. P. Moshokoacand M. Belicf*
24	**Analytical solution and applications of three qubits in three coupled modes without rotating wave approximation** *J. S. Zhang, L. J. Zhang, A. X. Chen,·and M. Abdel-Aty*
25	**Chirped singular and combo optical solitons for Gerdjikov –Ivanov equation using three integration forms** *A. J. M. Jawada, A. Biswasb,c, M. Abdelatyd, Q. Zhoue, S. P. Moshokoac and M. Belicf*
26	**The Population Inversion and the Entropy of a Moving Two-Level Atom in Interaction with a Quantized Field** *D. A. M. Abo-Kahlaa,b, M. Abdel-Aty3,4, and A. Farouke*
27	**Cavity control as a new quantum algorithms implementation treatment** *M. AbuGhanema,b, A. H. Homida,cand M. Abdel-Atya*
28	**Dynamical Controls for Improving Quantum Search Algorithm Through F lux Qubits System** *A . H . Homida,b, M. Abdel-Atyb,c, T El-Shahata, H. Eleuchd, and A. S. F. Obadae*
29	**A Novel Algorithm based on Entanglement Measurement for Improving Speed of Quantum Algorithms** *M. Zidan, Abdel-Haleem Abdel-Aty, A. Younes, E. A. Zanaty, I. El-khayat and M. Abdel-Aty*
30	**Robust general N user authentication scheme in a centralized quantum communication network via generalized GHZ states** *A. Farouk, J. Batle, M. Elhoseny, M. Naseri, M. Lone, A. Fedorov, M. Alkhambashi, S. H. Ahmed and M. Abdel-Aty*
31	**Entanglement o f a nonlinear two two-level atoms interacting with deformed fields in Kerr medium** *S. Abdel-Khalek, Y. S. El-Saman and M Abdel-Aty*
32	**Solving Deutsch's Problem using Entanglement Measurement Algorithm** *M. Zidan, Abdel-Haleem Abdel-Aty, A. S. A. Mohamed, I. El-khayat6 and M. Abdel-Aty*
33	**Finite Element Analysis of Thermoelastic Fiber-Reinforced Anisotropic Hollow Cylinder** *A. D. Hobiny, I. A. Abbas, and Fberto*
34	**A DPL model of photo-thermal interaction in an infinite semiconductor material containing a spherical hole** *A. D. Hobiny and I. A. Abbas*
35	**Fractional order photo-thermo-elastic waves in a two-dimensional semiconductor** *A. D. Hobiny and I. A. Abbas*
36	**Theoretical analysis of thermal damages in skin tissue induced by intense moving heat source** *A. D. Hobiny and I. A. Abbas*
37	**The influence of thermal and conductive temperatures in a nanoscale resonator** *A. D. Hobiny and I. A. Abbas*
38	**Analytical solutions of photo-thermo-elastic waves in a non-homogenous semiconducting material** *A. D. Hobiny and I. A. Abbas*
39	**Analytical solution of fractional order photo-thermoelasticity in a non-homogenous semiconductor medium** *A. D. Hobiny and I. A. Abbas*
40	**Stability of latent pathogen infection model with CTL immune response and saturated cellular infection** *A. M. Elaiw, A. A., Almatrafi, A. D. Hobiny and I. A. Abbas*
41	**Fractional Order Theory in a Semiconductor Medium Photogenerated by a Focused Laser Beam** *F. S. Alzahrani and I. A. Abbas*

42	**Generalized photo-thermo-elastic interaction in a semiconductor plate with two relaxation times** *F. S. Alzahrania and I. A. Abbas a,b,*
43	**Photo-thermoelastic interactions in a D semiconducting medium** *F. S. Alzahrani and I. A. Abbas*
44	**A Mode I Crack Problem for a Thermoelastic Fibre-Reinforced Anisotropic Material Using Finite Element Method** *I. A. Abbas a,b, and S. M. J. Razavic*
45	**Analytical and numerical solution of D problem for transversely isotropic generalized thermoelastic medium with Green-Naghdi model II** *I. A. Abbas, and M. I. A. Othman*
46	**Analytical Solutions of a Two-Dimensional Generalized Thermoelastic Diffusions Problem Due to Laser Pulse** *I. A. Abbas, and M. Marin*
47	**A Two-Temperature Photothermal Interaction in a Semiconductor Medium Containing a Cylindrical Hole** *I. A. Abbas, and A. Hobiny*
48	**Photo-thermal-elastic interaction in an unbounded semiconducting medium with spherical cavity due to pulse heat flux** *I. A. Abbas, and A. Hobiny*
49	**A DPL model of photothermal interaction in a semiconductor material** *I. A. Abbas, F. S. Alzahrani and A. Elaiw*
50	**The effect of fractional derivative on photo-thermoelastic interaction in an infinite semiconducting medium with a cylindrical hole** *I. A. Abbas, F. S. Alzahrani and F. Berto*
51	**A Green-Naghdi Model in a D Problem of a Mode I Crack in an Isotropic Thermoelastic Plate** *I. A. Abbas, and F. S. Alzahrani*
52	**Analytical Solutions of Plasma and Thermoelastic Waves Photogenerated by a Focused Laser Beam in a Semiconductor Material** *I. A. Abbas, K. A. Aly and A. Dahshan*
53	**A Study on Fractional Order Theory in Thermoelastic Half-Space under Thermal Loading** I. A. Abbas
54	**Free vibrations of nanoscale beam under two-temperature green and Naghdi model** I. A. Abbas
55	**Some Properties of Special Magnetic Curves** H. S. Abdel-Aziza, M. K. Saada,b and H. A. Alia,
56	**Estimation of R = P(Y < X) using k-Upper Record Values from Kumaraswamy Distribution** N. A. Abou-Elheggaga, A. A. Farghala, and H. A. Ramadanb
57	**Properties of Two Two-level Atoms Interacting with Intensity-Dependent Coupling** H. Bakry, A. S. A. Mohamed,3 and N. Zidan
58	**Quantum Fisher information of two sup erconducting charge qubits under dephasing noisy channel** *H. Abdel-Hameed, N. Zidan, and N. Metwally*
59	**Dynamics of Classical and Quantum Information on Spin-chains with Multiple Interactions** *A. Redwan, A. Abdel-Aty, N. Zidan, and T. El-Shahat*
60	**Dynamical properties and complex anti synchronization with applications to secure communications for a novel chaotic complex nonlinear model** *E. E. Mahmoud, and S. M. Abo-Dahaba,*
61	**High dimensional, four positive Lyapunov exponents and attractors with four scroll during a new hyperchaotic complex nonlinear model** *E. E. Mahmoud, K. M. Abualnaja and O. A. Althagafi*
62	**On phase and anti-phase combination synchronization of time delay nonlinear systems** *G. M. Mahmoud, A. A. Arafa and E. E. Mahmoud*

63	**Synchronization of time delay systems with non-diagonal complex scaling functions** *G. M. Mahmoud, E. E. Mahmoud, A. A. Arafa*
64	**Problem of Longitudinal and Secondary Vertically Waves Reflection and Transmission during Two Media in the Context of Three Magneto-thermoelastic Theories with Varies Fields** *S. M. Abo-Dahab, Emad E. Mahmoud*
65	**Stratified modeling in soft fuzzy topological structures** *S. E. Abbasa, E. El-sanowsyb, and A. Atefb*
66	**Connectedness in Fuzzy Soft T opological Spaces** *S. E. Abbasa, E. El-sanowsyb, and A. Atefb*
67	**A Solution of Random Nonlinear Integral Equation Via Random Hybrid Iterative Scheme** *R. A. Rashwana and H. A. Hammadb*
68	**Common Random Fixed Point Theorems of Integral Type of Akram-Contraction Mappings in Random Cone Metric Spaces** *R. A. Rashwana, D. Dhamodharanb, H. A. Hammadc, and R. Krishnakumard*
69	**C-class function on fixed point theorems for contractive mappings of integral type in n-banach spaces** *R. A. Rashwana, D. Dhamodharanb, H. A. Hammadc, and R. Krishnakumard*
70	**A common fixed point theorem for a pair of self mappings satisfying a general contractive condition of exponential type** *R. A. Rashwana and H. A. Hammadb,*
71	**Multi-filter Score-Level Fusion for Fingerprint Verification** *M. A. O. Ahmeda, O. Reyadb, Y. AbdelSatarc and N. F. Omranc*
72	**New SDN-Oriented Distributed Network Security System** *F. Nifea,b, Z. Kotulskia and O. Reyadc*
73	**Text Message Encoding Based on Elliptic Curve Cryptography and a Mapping Methodolog** *Omar Reyad*
74	**On Special Curves According to Darboux Frame in the Three Dimensional Lorentz Space** *H. S. Abdel-Aziz and M. Khalifa Saada*
75	**Some Geometric Invariants of Pseudo-Spherical Evolutes in the Hyperbolic 3-Space** *H. S. Abdel-Aziz, M. Khalifa Saad and A. A. Abdel-Salam*

List of papers published by Staff members of Physics Department (Pages 39-59)

1	**A Study of the Three-Body Force Effect on the EOS Properties of Asymmetric Nuclear Matter** *Mansour H. M. M., M. El-Zohry and A. E. Elmeshneb*
2	**Tensor target spin asymmetries in coherent π^0-photoproduction on the deuteron including intermediate ηNN interaction within a three-body approach** *E. M. Darwish, H. M. Abou-Elsebaa and Kh. S. A. Hassaneen*
3	**Cross Sections for the $\gamma d \rightarrow \pi NN$ Reaction Channels in the Photon Energy Range Between 300 and 500 MeV Including Final-State Interaction Effects** *E. M. Darwish and M. M. Almarashi*
4	**Explicit Solution for the Two-Body Scattering Problem a+b→c+d with High-Precision Interactions** *E. M. Darwish and E. M. Mahrous*
5	**Momentum Space Treatment of the Two-Body Problem** A+B→C+D **and Its Application to the** πN **Scattering with Realistic Interaction** *E. M. Darwish and E. M. Mahrous*
6	**Coherent Photoproduction of π^0-Meson from the Deuteron Including Polarization Effects** *E. M. Darwish*
7	**Tensor and Vector Analyzing Powers of Elastic Electron-Deuteron Scattering** *E. M. Darwish, E. M. Mahrous, and F. A. Alhazmi*
8	**Polarization Observables in the Reaction $\gamma d \rightarrow \pi^0 d$ Near η-Threshold** *E. M. Darwishand M. M. Almarashi*
9	**Coherent π^0-Photoproduction from the Deuteron Near Threshold** *E. M. Darwish, E. M. Mahrous and M. E. Alsehli*
10	**Effect of the carrier gas on morphological, optical and electrical properties of SnO nanostructures prepared by vapor transport** *N. M. A. Hadia, M. F. Hasaneen, Mohamed Asran Hassan and S. H. Mohamed*
11	**Examination of the kinetic reaction mechanisms of amorphous $As_{50}Se_{50}$ chalcogenide glass** *Mansour Mohamed, A. Y. Abdel-Latief, M. A. Abdel-Rahim, N. M. A. Hadia, E. R. Shaaban and Mohamed N. Abd-el Salam*
12	**Controlled synthesis, morphological, optical and electrical properties of copper-doped zinc oxysulfide nanostructures** *Mohammed S. Alqahtani, N. M. A. Hadia and S. H. Mohamed*
13	**Effect of oxidation time on structural, optical and electrical properties of mixed copper oxides nanocrystallites** *Mohammed S. Alqahtani, N. M. A. Hadia and S. H. Mohamed*
14	**Towards understanding the morphological, magnetic, optical and electrical properties of MnO nanowires for magneto-and optoelectronic applications** *M. A. Awad and N. M. A. Hadia*
15	**Tribo-Mechanical and Electrochemical Properties of Carbonitrided 36 Austenitic Stainless Steel by rf Plasma for Biomedical Applications** *F.M. El-Hossary, M. Raaif, A.M. Abd El-Rahman, M. Abo EL-Kassem*
16	**Optical and electrical performance of transparent conductive TiO/Cu/TiO multilayers prepared by magnetron sputtering** *M. A. Awad, M. Raaif*
17	**Effect of DC-pulsed magnetron sputtering power on structural, tribological and biocompatibility of Ti–Zr–N thin film** *F. M. El-Hossary, A. M. Abd El-Rahman, M. Raaif, Shuxin Qu, Junsheng Zhao, Manfred F. Maitz, M. Abo EL-Kassem*
18	**The disclosed transformation of pre-sputtered Ti films into nanoparticles via controlled thermal oxidation** *M. A. Awad, M. Raaif*

19	**Constructing and Characterizing TiAlN Thin Film by DC. Pulsed Magnetron Sputtering at Different Nitrogen/Argon Gas Ratios** *M. Raaif*
20	**Photonic crystal defective superconductor and black body radiations** *Arafa H. Aly, Ayman A. Ameen, Hussein A. ElSayed, S. H. Mohamed*
21	**Characterization of CuO/CuO nanowire arrays synthesized be by thermal method at various temperatures** *S. H. Mohamed and Kh. M. Al-Mokhtar*
22	**Effect of oxidation time on structural, optical and electrical properties of mixed copper oxides nanocrystallites** *Mohammed S. Alqahtani N. M. A. Hadia, S. H. Mohamed*
23	**Controlled synthesis, morphological, optical and electrical properties of copper *doped* zinc *oxysulfide* nanostructures** *Mohammed S. Alqahtani N. M. A. Hadia, S. H. Mohamed*
24	**Effect of the carrier gas on morphological, optical and electrical properties of SnO nanostructures prepared by vapor transport** *N. M. A. Hadia, M. F. Hasaneen, Mohamed Asran Hassan, S. H. Mohamed*
25	**Influence of Temperature Gradient on Surface properties of Nitriding AISI 304 Stainless Steel** *F. M. El-Hossary N. Z. Negm A. M. Abd El-Rahman A. A. Abd El-Moula, S.M. Khalil*
26	**Electric, thermoelectric and magnetic characterization of γ-FeO3 and Co3O4 nanoparticles synthesized by facile thermal decomposition of metal-Schiff base complexes** *E.M.M. Ibrahima, Laila H. Abdel-Rahmanb, Ahmed M. Abu-Diefb, A. Elshafaiea, Samar Kamel Hamdanb, A.M. Ahmeda*
27	**Magnetocaloric effect, electric, and dielectric properties of $Nd_{0.6}Sr_{0.4}Mn_xCo_xO_3$ composites** *I.A. Abdel-Latif a,b,c, A.M. Ahmed d, H.F. Mohamed d, S.A. Saleh d, J.A. Paixão e, Kh.A. Ziq f, M.Kh. Hamad f, E.G. Al-Nahari f, M. Ghozza g, S. Allam h*
28	**Thermopower and magnetocaloric properties in $NdSrMnO/CrO_3$ composites** *A.M. Ahmed, H.F. Mohamed, J.A. Paixão, Sara A. Mohamed*
29	**The electric and thermoelectric properties of Cu(II)-Schiff base nano-complexes** *E M M Ibrahim Laila H Abdel-Rahman Ahmed M Abu-Dief A Elshafaie Samar Kamel Hamdan and A M Ahmed*
30	**Theoretical study of ZnS/CdS bi-layer for thin-film CdTe solar cell** *H. A. Mohamed, A. S. Mohamed and H. M. Ali*
31	**Spectral functions of nuclear matter using self-consistent Green's function approach based on three-body force** *Khaled S. A. Hassaneen*
32	**Structural and optical properties of $CuIn_{-x}Ga_xSe$ thin films** *N.m.a hadia, m.m. wakkad, e.kh. Shokr, y. A. Taya*
33	**The Electric and Thermoelectric Properties of Cu(II)-Schiff base Nano-complexes** *E.M.M. Ibrahim, Laila H. Abdel-Rahman Ahmed M. Abu-Dief A. Elshafaie Samar Kamel Hamdan A. M. Ahmed*
34	**Electric, Thermoelectric and Magnetic Properties of Nickel(II) Imine Nanocomplexes** *A. Elshafaie Laila H. Abdel-Rahman Ahmed M. Abu-Dief Samar Kamel Hamdan A. M. Ahmed E.M.M. Ibrahim*
35	**Electric, thermoelectric and magnetic characterization of g-FeO_3 and Co_3O_4 nanoparticles synthesized by facile thermal decomposition of metal-Schiff base complexes** *E.M.M. Ibrahim, Laila H. Abdel-Rahman Ahmed M. Abu-Dief A. Elshafaie Samar Kamel Hamdan A. M. Ahmed*
36	**Optical And Thermoelectric Properties Of Nanocrystalline $Bi(Se_{-x}Te_x)_3$ Films** *A. M. Adam, E. M. M. Ibrahim, L. V. Panina, and P. Petkov*
37	**Effect of the synthesis conditions on the structural, morphological and optical properties of $BiTe_{.7}Se_{0.3}$ nanoparticles** *H.M. Ali, E.M.M. Ibrahim⁎, M.M. Wakkad, M.A.A. Mohamed*
38	**Thermoelectric properties of Te doped bulk $BiSe_3$ system** *A.M.A. dam, A. Elshafaie A.bd El-MoezA Mohamed, P. Petkov and E.M.M. Ibrahim*

39	**Correlation of structural and optical properties in as-prepared and annealed $BiSe_3$ thin films** *A.M. Adam, E. Lilovb, E.M.M. Ibrahim, P. Petkov, L.V. Paninaa, M.A. Darwish*
40	**Sonochemical synthesis, structural inspection and semiconductor behavior of three new nano sized Cu(II), Co(II) and Ni(II) chelates based on tri-dentate NOO imine ligand as precursors for preparing of metal oxides** *Laila H. Abdel Rahman, Ahmed M. Abu-Dief Rafat M. El-Khatib, Shimaa Mahdy Abdel-Fatah, A. M. Adam, E.M.M. Ibrahim*
41	**The synthesis of CuO and NiO nanoparticles by facile thermal decomposition of metal-Schiff base complexes and an examination of their electric, thermoelectric and magnetic Properties** *E.M.M. Ibrahim, Laila H. Abdel-Rahman Ahmed M. Abu-Dief A. Elshafaie Samar Kamel Hamdan A. M. Ahmed*
42	**The electric and thermoelectric properties of Cu(II)-schiff base nano-complexes** *Ibrahim, E.M.M., Abdel-Rahman, L.H.b, Abu-Dief, A.M., Elshafaie, A., Hamdan, S.K., Ahmed, A.M.*

List of papers published by Staff members of Chemistry Department (Pages 61-98)

1	**Cobalt ferrite nanoparticles with controlled composition-peroxymonosulfate mediated degradation of -phenylbenzimidazole-5-sulfonic acid** *Abdulaziz Al-Anazi, Wael H.Abdelraheem, ChangseokHan, Mallikarjuna N.Nadagouda, Labrini Sygellou, Michalis K.Arfanis, Polycarpos Falaras, Virender K.Sharma, Dionysios D.Dionysiou*
2	**Synthesis and Reactions of New Thiazoles and Pyrimidines Containing Sulfonate Moiety** *Khodairy, A.,Ali, A.M.,El-Wassimy, M.T.*
3	**Hematite Photoanodes with Size-controlled Nanoparticles for Enhanced Photoelectrochemical Water Oxidation** *Amira Y. Ahmed, Mahmoud G. Ahmed, Tarek A. Kandiel*
4	**New Method for Synthesis of Multi-substituted Imidazoles** *Marzouk, A.A.,Mohamed, S.K.,Aljohani, E.T.,Abdelhamid, A.A.*
5	**Artificial Macrocycles** *Abdelraheem, E.M.M., Shaabani, S.,Dömling, A.*
6	**Deazaflavins as photocatalysts for the direct reductive regeneration of flavoenzymes** *Van Schie, M.M.C.H., Younes, S.H.H., Rauch, M.C.R., Pesic, M., Paul, C.E., Arends, I.W.C.E., Hollmann,F.*
7	**Carbocation Catalyzed Bromination of Alkyl Arenes, a Chemoselective sp^3 vs. sp C−H functionalization** *Ni, S.,Mahmoud Abd El Aleem Ali El Remaily, Franzén, J.*
8	**Concise Synthesis of Macrocycles by Multicomponent Reactions** *Abdelraheem, E.M.M., Khaksar, S., Dömling, A.*
9	**Unexpected products from the reaction of chalcones with cyanoguanidine** *Moustafa, A.H.,Amer, A.A*
10	**Sonochemical synthesis, structural inspection and semiconductor behavior of three new nano sized $Cu^{(II)}$, $Co^{(II)}$ and $Ni^{(II)}$ chelates based on tri-dentate NOO imine ligand as precursors for metal oxides** *Laila H. Abdel Rahman, Ahmed M. Abu-Dief, Rafat M. El-Khatib, Shimaa Mahdy Abdel-Fatah, A.M. Adam, E.M.M. Ibrahim*
11	**New Route for the Synthesis of Hetaryl-,5-benzodiazepines: Part** *Ahmed, A.M.,Abdel-Ghany, H.,Moustafa, H.M.,Khodairy, A.*
12	**Utility of amino acid coupled,4-triazoles in organic synthesis: Synthesis of some new antileishmainal agents** *El-Saghier, A.M.M., Mohamed, M.A.A., Abdalla, O.A., Kadry, A.M.*
13	**The structure of 9-(3-bromo-6-chloro--hydroxyphenyl)-0-(-hydroxyethyl)-3,6-diphenyl-3,4,5,6,7,9-hexahydro- H-acridine-,8-dione** *Abdelhamid, A.A., Hawaiz, F.E., Mohamed, A.F., Mohamed, S.K., Simpson, J.*
14	**-Deoxy-d-ribose-5-phosphate aldolase (DERA): applications and modifications** *Haridas, M., Abdelraheem, E.M.M., Hanefeld, U.*
15	**Identification of some Bioactive Metabolites in a Fractionated Methanol Extract from Ipomoea aquatica (Aerial Parts) through TLC, HPLC, UPLC-ESI-QTOF-MS and LC-SPE-NMR Fingerprints Analyses** *Hefny Gad, M., Tuenter, E., El-Sawi, N., Younes, S., El-Ghadban, E.-M., Demeyer, K., Pieters, L., Vander Heyden, Y.,Mangelings, D.*
16	**Synthesis of Some New Polyfunctionalized Pyridines** *Amer, A.A.*
17	**Fabrication of oxidized graphite supported LaO_3/ZrOnanocomposite for the photoremediation of toxic fast green dye** *Gaurav Sharma Amit Kumar Shweta Sharma Sameerah I. Al-Saeedi Ghadah M. Al enani Ayman Nafady Tansir Ahamad Mu. Naushad Florian J. Stadler*

18	**Facile Approach to Graft Ionic Liquid into MOF for Improving the Efficiency of CO Chemical Fixation** *Yuxiu Sun, Hongliang Huang, Harsh Vardhan, Briana Aguila, Chongli Zhong, Jason A. Perman, Abdullah M. Al-Enizi, Ayman Nafady, and Shengqian Ma*
19	**A Multifunctional Zinc Oxide/Poly(Lactic Acid) Nanocomposite Layer Coated on Magnesium Alloys for Controlled Degradation and Antibacterial Function** *Hamouda M. Mousa, Abdalla Abdal-hay, Michal Bartnikowski, Ibrahim M. A. Mohamed, Ahmed S. Yasin, Sašo Ivanovski, Chan Hee Park and Cheol Sang Kim*
20	**$CoCr_7C_3$-like nanorods embedded on carbon nanofibers as effective electrocatalyst for methanol electro-oxidation** *Abdullah M.Al-Enizi Robert M. Brooks M.M. El-Halwany Ayman Yousef Ayman Nafady R.M. Abdel Hameed[f]*
21	**Lower Activation Energy for Catalytic Reactions through Host–Guest Cooperation within Metal–Organic Frameworks** *Briana Aguila, Dr. Qi Sun Xiaoliang Wang Erica O'Rourke, Ayman Nafady, Shengqian Ma*
22	**Sensitive and selective aggregation based colorimetric sensing of Fe^{3+} via interaction with acetyl salicylic acid derived gold nanoparticles** *Safia S. Memon Ayman Nafady Amber R. Solangi Abdullah M. Al-Enizi Sirajuddin Muhammad R. Shah Syed T.H. Sherazi Shabuddin Memon Munazza Arain Muhammad I. Abro Manzoor I. Khattak*
23	**Construction of an Ultrasensitive and Highly Selective Nitrite Sensor Using Piroxicam-Derived Copper Oxide Nanostructures** *Ali Alsalme, Munazza Arain, Ayman Nafady, and Sirajuddin*
24	**Cobalt nanoparticles incorporated into hollow doped porous carbon capsules as a highly efficient oxygen reduction electrocatalyst** *Feng Guo, Hui Yang, Briana Aguila, Abdullah M. Al-Enizi, Ayman Nafady, Mandeep Singh, Vipul Bansal and Shengqian Ma*
25	**Nanosized Samarium Modified Au-$Ce_{0.5}Zr_{0.5}O$ Catalysts for Oxidation of Benzyl Alcohol** *Alaa J. Faqeeh, Tarek T. Ali, Sulaiman N. Basahel, Katabathini Narasimharao*
26	**Acidic Peptizing Agent Effect on Anatase-Rutile Ratio and Photocatalytic Performance of TiO Nanoparticles** *Hatem A. Mahmoud, Katabathini Narasimharao, Tarek T. Ali and Kamal M. S. Khalil*
27	**Mechanisms of Photocatalytic Molecular Hydrogen and Molecular Oxygen Evolution over La-Doped $NaTaO_3$ Particles: Effect of Different Cocatalysts and Their Specific Activity** *Irina Ivanova, Tarek A. Kandiel, Young-Jin Cho, Wonyong Choi, and Detlef Bahnemann*
28	**Macrocycles: MCR synthesis and applications in drug discovery** *Abdelraheem, E.M.M., Shaabani, S., Dömling, A.*
29	**Synthesis, theoretical investigations, biocidal screening, DNA binding, *in vitro* cytotoxicity and molecular docking of novel Cu(II), Pd(II) and Ag(I) chlorobenzylidene Schiff base: Promising antibiotic and anticancer agents** *Laila H. Abdel-Rahman, Mohamed Shaker S. Adam, Ahmed M. Abu-Dief, H. Moustafa, Maram T. Basha, Ahmed S. Aboraia and Hanan El-Sayed Ahmed*
30	**Adsorption of the Heavy Metal Ions onto Bio sorbents: A review** *Ahmed M. Abu-Dief and Mallak Megalea Zikry*
31	**Electric, Thermoelectric and Magnetic Properties of Nickel(II) Imine Nanocomplexes** *A. Elshafaie, Laila H. Abdel-Rahman, Ahmed M. Abu-Dief, Samar Kamel Hamdan, A. M. Ahmed and E. M. M. Ibrahim*
32	**The synthesis of CuO and NiO nanoparticles by facile thermal decomposition of metal-Schiff base complexes and an examination of their electric, thermoelectric and magnetic Properties** *E.M.M. Ibrahim, Laila H. Abdel-Rahman, Ahmed M. Abu-Dief, A. Elshafaie, Samar Kamel Hamdan, A.M. Ahmed*

33	**Disposal of Heavy Transition Cd^{+} Ions from Aqueous Solution Utilizing Nanosized Flamboyant Pod (*Delonix regia*)** *Laila H. Abdel-Rahman, Ahmed M. Abu-Dief, M. A. Abd- ElSayed and Mallak Megalea Zikry*
34	**Electric, thermoelectric and magnetic characterization of γ-FeO3 and Co3O4 nanoparticles synthesized by facile thermal decomposition of metal-Schiff base complexes** *E.M.M. Ibrahim, Laila H. Abdel-Rahman, Ahmed M. Abu-Dief, A. Elshafaie, Samar Kamel Hamdan, A.M. Ahmed*
35	**The electric and thermoelectric properties of Cu(II)-Schiff base nano-complexes** *E M M Ibrahim, Laila H Abdel-Rahman, Ahmed M Abu-Dief, A Elshafaie, Samar Kamel Hamdan and A M Ahmed*
36	**Development and functionalization of magnetic nanoparticles as powerful and green catalysts for organic synthesis** *Ahmed M. Abu-Dief, Shimaa Mahdy Abdel-Fatah*
37	**Functionalization of Magnetic nanoparticles for drug delivery** *Ahmed M. Abu-Dief and Azza A. Hassan Abdel-Mawgoud*
38	**Hydrothermal Preparation and Characterization of $ZnFeO_4$ Magnetic Nanoparticles as an Efficient Heterogeneous Catalyst for the Synthesis of Multi-Substituted Imidazoles (MSI) and Study of their Anti-Inflammatory Activity** *Adel A. Marzouk, Ahmed M. Abu-Dief and Antar A. Abdelhamid*
39	**Synthesis, characterization and photocatalysis enhancement of EuO_3- ZnO mixed oxides nanoparticles** *W.S. Mohamed and Ahmed M. Abu-Dief*
40	**Two-Step Macrocycle Synthesis by Classical Ugi Reaction** *Abdelraheem, E.M.M, Khaksar, S, Kurpiewska, K, Kalinowska-Tuścik, J, Shaabani, S., Dömling,A*
41	**Catalytic activity of nickel(II), copper(II) and oxovanadium(II)-dihydroindolone complexes towards homogeneous oxidation reactions** *Mohamed Shaker S. Adam*
42	**Anionic oxide-vanadium Schiff base amino acid complexes as potent inhibitors and as effective catalysts for sulfides oxidation: Experimental studies complemented with quantum chemical calculations** *Mohamed Shaker S. Adam, Hany M. Abd El-Lateef, Kamal A. Soliman*
43	**Catalytic performance of binary and ternary oxovanadium complexes of dipyridinyl-urea in (ep)oxidation of *cis*-cyclooctene and -octene** *Mohamed Shaker S. Adam, Aly M. Hafez, Ibrahim El-Ghamry*
44	**Synthesis of polar unique 3d metal-imine complexes of salicylidene anthranilate sodium salt. Homogeneous catalytic and corrosion inhibition performance** *Hany M. Abd El-Lateef, Mohamed Shaker S. Adam, Mai M. Khalaf*
45	**Biological potential of oxo-vanadium salicylediene amino-acid complexes as cytotoxic, antimicrobial, antioxidant and DNA interaction** *Mohamed Shaker S. Adam, Hany Elsawy*
46	**Catalytic (ep)oxidation and corrosion inhibition potentials of Cu^{II} and Co^{II} pyridinylimino phenolate complexes** *Mohamed Shaker S. Adam, Ahmad Desoky M. Mohamad*
47	**Square wave voltammetric analysis of polyphenol content and antioxidant capacity of red wines using glassy carbon and disposable carbon nanotubes modified screen-printed electrodes** *Emad F. Newair, Paul A. Kilmartin, François Garcia*
48	**Mechanistic Pathways and Identification of the Electrochemically Generated Oxidation Products of Flavonoid Eriodictyol in the Presence of Glutathion** *Emad F. Newair, Refat Abdel-Hamid, Ayman Nafady, Abdullah M. Al-Enizi, Franc¸ois Garcia*

49	**Elucidating the Role of CO in the Soft Oxidative Dehydrogenation of Propane over Ceria-Based Catalysts** *Ewa Nowicka, Christian Reece, Sultan M. Althahban, Khaled M. H. Mohammed, Simon A. Kondrat, David J. Morgan, Qian He, David Willock, Stanislaw Golunski, Christopher J. Kiely and Graham J. Hutchings*
50	**Fine-template synthetic process of mesoporous TiO using ionic/nonionic surfactants as potential remediation of Pb(II) from contaminated soil** *Mai M. Khalaf, Naglaa Y. Abdallah, Hany M. Abd El-Lateef*
51	**A facile Synthetic Route to novel Polyamides-Based on Thieno[,3-*b*]thiophene and Their Application for Corrosion Inhibition Behavior** *Kamal I Aly, Amr H Moustafa, Hany M Abd El-lateef, Essam K Ahmed, Mohamed Gamal Mohamed and Sahar M Mohamed*
52	**Anionicoxide-vanadium Schiff base amino acid complexes as potent inhibitors and as effective catalysts for sulfides oxidation: Experimental studies complemented with quantum chemical calculations** *Mohamed Shaker S. Adam, Hany M. Abd El-Lateef, Kamal A. Soliman*
53	**Adsorption and Removal of Cationic and Anionic Surfactants Using Zero-Valent Iron Nanoparticles** *Hany M. Abd El-Lateef, Mai M. Khalaf Ali, Mahmoud M. Saleh*
54	**Polyhydrazide incorporated with thiadiazole moiety as novel and effective corrosion inhibitor for C-steel in pickling solutions of HCl and HSO_4** *Abdelwahed R. Sayed, Hany M Abd El-lateef, Ahmad Desoky M. Mohamad*
55	**Optical and photocatalytic measurements of Co-TiO nanoparticles thin films** *Mai M. Khalaf, Hany M. Abd El-Lateef, H. M. Ali*
56	**Chemical modification of commercial kaolin for mitigation of organic pollutants in environment via adsorption and generation of inorganic pesticides** *Mohamed Khairy, Haytham A. Ayoub, Farouk A. Rashwan, Hanan F. Abdel-Hafez*
57	**Pesticidal activity of nanostructured metal oxides for generation of alternative pesticide formulations** *Haytham Ayoub, Mohamed Khairy, Salaheldeen Elsaid, Farouk A. Rashwan, Hanan F. Abdel Hafez*
58	**Large-scale production of CdO/Cd(OH) nanocomposites for non-enzyme sensing and supercapacitor applications** *Mohamed Khairy, Haytham A. Ayoub and Craig E. Banks*
59	**Nanohexagonal FeO_3 Electrode for One-Step Selective Monitoring of Dopamine and Uric Acid in Biological Samples** *Mohammed Y. Emran, Mohamed A. Shenashen, Adel A. Abdelwahab, Mohamed Abdelmottaleb, Mohamed Khairy, Sherif A. El-Safty*
60	**Non-enzymatic electrochemical platform for parathion pesticide sensing based on nanometer-sized nickel oxide modified screen-printed electrodes** *Mohamed Khairy, Haytham A. Ayouba, Craig E. Banks*
61	**Simultaneous determination of codeine and its co-formulated drugs acetaminophen and caffeine by utilising cerium oxide nanoparticles modified screen-printed electrodes** *Mohamed Khairy, Bahaa G. Mahmoud, Craig E. Banks*
62	**Voltammetric determination of meclizine antihistamine drug utilizing graphite screen-printed electrodes in physiological medium** *Ahmed A. Khorshed, Mohamed Khairy, Craig E. Banks*
63	**Synthesis, Characterization, Modeling, and Antimicrobial Activity of Fe^{III}, CoII, Ni^{II}, Cu^{II}, and Zn^{II} Complexes Based on Tri-substituted Imidazole Ligand** *Mohamed Ismael, Aly Abdou, and A.-M. Abdel-Mawgoud*
64	**A promising electrodeposited iron oxide nanoparticles of very high saturation magnetization and superparamagnetic properties for remediation of polluted water with lead ions** *Mahmoud Elrouby, Nagwa Abo El-Maali, Rehab, Abd El-Rahman*
65	**Synthesis and characterization of titania nanoparticles and enhancement of photochemical, photoelectrochemical and electrochemical performance with zirconia nanoparticles** *Mahmoud Elrouby, Mai M. Khalaf*

66	**Facile synthesis of TiO/ZrO nanofibers/nitrogen co-doped activated carbon to enhance the desalination and bacterial inactivation via capacitive deionization** *Ahmed S. Yasin, Ibrahim M.A. Mohamed, Hamouda M Mousa, Chan Hee Park, Cheol Sang Kim*
67	**Electrocatalytic behavior of a nanocomposite of Ni/Pd supported by carbonized PVA nanofibers towards formic acid, ethanol and urea oxidation: A physicochemical and electro-analysis study** *Ibrahim M. A. Mohamed, Ahmed S. Yasin, Nasser A. M. Barakat, Seung A. Song, Ha Eun Lee, Seong Su Kim*
68	**Design of novel electrode for capacitive deionization using electrospun composite titania/zirconia nanofibers doped-activated carbon** *Ahmed S. Yasin, Ibrahim M.A. Mohamed, Chan Hee Park, Cheol Sang Kim*
69	**Sonochemical synthesis, structural inspection and semiconductor behavior of three new nano sized Cu(II), Co(II) and Ni(II) chelates based on tri-dentate NOO imine ligand as precursors for preparing of metal oxides** *Laila H. Abdel Rahman, Ahmed M. Abu-Dief, Rafat M. El-Khatib, Shimaa Mahdy Abdel-Fatah, A. M. Adam, E.M.M. Ibrahim*
70	**Identification of some Bioactive Metabolites in a Fractionated Methanol Extract from Ipomoea aquatica (Aerial Parts) through TLC, HPLC, UPLC-ESI-QTOF-MS and LC-SPE-NMR Fingerprints Analyses** *Hefny Gad M, Tuenter E, El-Sawi N, Younes S, El-Ghadban EM, Demeyer K, Pieters L, Vander Heyden Y, Mangelings D*
71	**Catalytic Oxidation of Benzyl Alcohol Using Nanosized Cu/Ni Schiff-Base Complexes and Their Metal Oxide Nanoparticles** *Sameerah I. Al-Saeedi, Laila H. Abdel-Rahman, Ahmed M. Abu-Dief, Shimaa M. Abdel-Fatah, Tawfiq M. Alotaibi, Ali M. Alsalme and Ayman Nafady*
72	**Synthesis, structural, thermal, optical and dielectric properties of chitosan biopolymer; influence of PVP and α-Fe2O3 Nanorods** *Sayed, A.M., Mohamad, A.D.M.*
73	**Ultrastructural, histochemical and biochemical effects of titanium dioxide nanoparticles on adult male albino rat liver and possible prophylactic effects of milk thistle seeds** *Abu-Dief, E.E., Abdel-Aziz, H.O., Nor-Eldin, E.K., Khalil, K.M., Ragab, E.E.*
74	**The electric and thermoelectric properties of Cu(II)-schiff base nano-complexes** *Ibrahim, E.M.M., Abdel-Rahman, L.H., Abu-Dief, A.M., Elshafaie, A., Hamdan, S.K., Ahmed, A.M.*
75	**Optimization of the pendant chain length in partially fluorinated aromatic anion exchange membranes for alkaline fuel cells** *Ahmed Mahmoud, A.M., Miyatake, K.*

List of papers published by Staff members of Botany&Microbiology Department (Pages 99-112)

1	***Phaeonectriella alba* sp. nov. from the River Nile, Egypt** *Ahmed E. Abdel-Aziz, Sabah S. Mohamed, Ahmed M. Abdel-Raheem†, Mohamed A. Abdel-Wahab*
2	***Khaleijomyces marinus gen. et sp. nov.* (Juncigenaceae, Torpedosporales) a new lignicolous marine fungus from Saudi Arabia** *Mohamed A. Abdel-Wahab, Abd El-Rahim M. A. El-Samawaty, Abdallah M. El Gorban, Mohamed A. Yassin & Marzouq H. Alsaadi*
3	**Four strains of yeasts: as effective biocontrol agents against both growth and mycotoxins formation by selected toxigenic fungi** *Zohri, A. A and Marwa Abdel-Kareem, M*
4	**Potentially harmful microalgae and algal blooms in the Red Sea: Current knowledge and research needs** *Zakaria A. Mohamed*
5	**Airborne fungi in outdoor air of riyadh city, kingdom of saudi arabia** *Abd El-Rahim M A El-Samawaty, Mohamed A Yassin, Mohamed A Abdel-Wahab*
6	**Concentrations of cylindrospermopsin toxin in water and tilapia fish of tropical fishponds in Egypt, and assessing their potential risk to human health** *Zakaria A. Mohamed & Asmaa Bakr*
7	**Grazing of the copepod *Cyclops vicinus* on toxic *Microcystis aeruginosa*: potential for controlling cyanobacterial blooms and transfer of toxins** *Zakaria A. Mohamed, Asmaa A. Bakr, Hamed A. Ghramh*
8	**Bioavailability of bound microcystins in mice orally fed with contaminated tilapia edible tissues: Implications to human health** *Zakaria A. Mohamed[a,*], Asmaa Bakra, Hamdy A. Soliman[b]*
9	**Gene expression and adventitious root formation on auxin containing medium as influenced by cytokinin type during the multiplication stage in micropropagation of moringa** *Ahmed Hassanein, Jehan Salem, Fayza Faheed, Abdullah El-nagish*
10	**Effect of anti-ethylene compounds on isoenzyme patterns and genome stability during long term culture of *Moringa oleifera*** *A. M. Hassanein · J. M. Salem · F. A. Faheed · A. El-nagish*
11	**Biosynthesis, Characterization, Optimization of Silver Nanoparticles from Marine *S. griseoflavus* and Their Role in Improving Antibiotic Susceptibility of Multidrug Resistance Pathogenic Fungi** *Muneera Al-Otaibia, Bahig El-Deebb, Nasser Mostafac*
12	**Biological Synthesis and Structural Characterization of Selenium Nanoparticles and Assessment of Their Antimicrobial Properties** *Bahig El-Deeba, Abdullah Al-Talhib, Nasser Mostafac, Rawan Abou-assyd*
13	**Antibiofilm Potential of Biogenic Silver Nanoparticles against Kocuria rosea and Kocuria rhizophila** *H. Elharirya, E. Gadoa, B. El-Deeba, and A. Altalhi*
14	**Interactions of physico-chemical properties of the River Nile water and fungal diversity in River Nile streams in Delta region** *Ahmed Mohamed Abdel-Raheem, Gamalat Abd-Aleem Abd-Elaah, Osman Mohamed El-Maghraby and Mahmoud Saad Eldin*
15	**Isolation and Molecular Identification of *Fusarium* Species from Some Cereal Grains and Their Products in Egypt** *Samia El-Rabbat, Osman El-Maghraby, Samah El-Debaiky[3] and Ashraf Haider[4]*
16	**Bio-monitoring of radionuclides air pollution using physiological responses of urban trees** *El-Khatib, A. A., Amany aboelkassem and H. Elzayat, M.*
17	**Characterisation of the Egyptian Pliocene bentonite from the Sohag region for pharmaceutical use** *Abdelhamid Elshater & Abdelaziz Elhaddad & Attef Elattaar & Magdy Abugharbia & Waffa Soliman*

18	**Heavy Metal Pollutants in Fresh Water** *Mohamed Youssef, Ebtesam Mohamed Morsy, Samia Mohamed Soliman, Abdel-Raheim El-Sayed Abdel-Latief*
19	**Fine-template synthetic process of mesoporous TiO using ionic/nonionic surfactants as potential remediation of Pb(II) from contaminated soil** *M. M. Khalaf · N. Y. Abdallah[3] · H. M. Abd El-Lateef*
20	**Impact of enzymes and toxins potentiality of four Aspergillus species to cause aspergillosis** *Mohamed Fawzy Adam, Abdel-Naser Zohri, Bassam Aboul-Nasr, Enas Mahmoud Amer*
21	**Isolation, antimicrobial resistance profile and molecular characterization of bacteria from broiler** *Aly E. Abo-Amer, Mohammed Y. Shobrak[3] and Abdullah D. Altalhi*
22	**Isolation and antimicrobial resistance of Escherichia coli isolated from farm chickens in Taif, Saudi Arabia** *Aly E. Abo-Amer, Mohammed Y. Shobrak, Abdullah D. Altalhi*
23	**Inhibition of fungal growth and mycotoxins formation of selected toxigenic fungi by different bacterial strains** *Zohri A A, Sabah S M, Youssef M and Marwa Abdel-Kareem M*
24	**Extracellular mycosynthesis of gold nanoparticles using *Trichoderma hamatum*: optimization, characterization and antimicrobial activity** *M. Marwa Abdel-Kareem and A.A. Zohri*
25	**The action mechanism and biocontrol potentiality of novel isolates of Saccharomyces cerevisiae against the aflatoxigenic *Aspergillus flavus*** *M. Marwa Abdel-Kareem, A.M. Rasme and A.A. Zohri*
26	**24-Epibrassinolide application enhances growth and biochemical aspects of squash under salt stress conditions** *Galal, A*
27	**The antibiotic peptaibol alamethicin from *Trichoderma permeabilises* Arabidopsis root apical meristem and epidermis but is antagonised by cellulase-induced resistance to alamethicin** *Dotson BR, Soltan D, Schmidt J, Areskoug M, Rabe K, Swart C, Widell S, Rasmusson AG.*

List of papers published by Staff members of Zoology Department (113-126)

1	**Long-Acting β-Adrenoceptor Agonists Enhance Glucocorticoid Receptor (GR)-Mediated Transcription by Gene-Specific Mechanisms Rather Than Generic Effects via GR** *Rider CF, Altonsy MO, Mostafa MM, Shah SV, Sasse S, Manson ML, Yan D, Kärrman-Mårdh C, Miller-Larsson A, Gerber AN, Giembycz MA, Newton R.*
2	**An Ethylenediamine-based Switch to Render the Polyzwitterion Cationic at Tumorous pH for Effective Tumor Accumulation of Coated Nanomaterials** *Abdul-Hackam Ranneh, Hiroyasu Takemoto, Shunya Sakuma, Aziz Awaad, Takahiro Nomoto, Yuki Mochida, Makoto Matsui, Keishiro Tomoda, Mitsuru Naito, and Nobuhiro Nishiyama.*
3	**Systematic in vivo study of NiO nanowires and nanospheres: biodegradation, uptake and biological impacts** *Alaraby M, Hernández A, Marcos R.*
4	**Toxic and Genotoxic Effects of Silver Nanoparticles in Drosophila.** *Alaraby M, Romero S, Hernández A, Marcos R.*
5	**Electrical excitability of roach (Rutilus rutilus) ventricular myocytes: effects of extracellular K^+, temperature and pacing frequency** *Badr, A., Abu-Amra, E.S., El-Sayed, M.F. and Vornanen, M.*
6	**Insulin-like 3 expression and fibrosis induction after intra-testicular injection of magnetic nanoparticles in rat testis and the ameliorative role of Echinacea purpurea extract** *Aziz Awaad, Mohamed A. Adly, Doaa Hosny*
7	**Effects of seasonal acclimatization on thermal tolerance of inward currents in roach (*Rutilus rutilus*) cardiac myocytes** *Badr, A., Korajoki, H., Abu-Amra, E.S., El-Sayed, M.F. and Vornanen, M.*
8	**Spleen immunotoxicities induced by intra-testicular injection of magnetic nanoparticles and the role of Echinacea purpurea extract: a histological and immunohistochemical study** *Aziz Awaad, Mohamed A. Adly, Doaa Hosny*
9	**Ameliorative effect of bee venom and its extracted bradykinin-potentiating factor on neurological alteration induced by acrylamide and chips administration** *Lashein, F.E.D.M., Amra, E.S.A., Seleem, A.A. and Badr, A.H.*
10	**Counter effect of bee venom and its extracted bradykinin-potentiating factor on acrylamide and chips administration-induced complications in the liver and kidney of male mice** *Amra, E.S.A., Lashein, F.E.D.M., Seleem, A.A. and Badr, A.H.*
11	**Histological and ultrastructural studies of spermatogenesis of freshwater mite, *Unionicola aegyptiaca* (Acari, Unionicolidae)** *Ramadan, S.A., Ismail, T.G. and Mustafa, A. N.*
12	**Expression of alpha-synuclein during eye development of Bufo arabicus.** *Seleem, A.A. and Lashein, F.E.D.M.*
13	**Ameliorative Roles of Vitamins C, E and DMSA on Hepatic and Renal Functions Against Lead Toxicity in Male Albino Rats** *Mohamed F.El-Sayed, Sarry Kh. Abdel – Kgaffar, Amin Abddou Seleem, Ramy A. Mohamed.*
14	**Description of two new species of aquatic oribatid mites (Family: Malaconothridae, Genus: Malaconothrus) from Sohag Governorate**, *Ramadan, S.A., Ismail, T.G. and Mustafa, A. N*
15	**Studies on the Abundance, Temporal Distribution and Diversity of Spiders (Arachnida: Araneae) Associated with Lemon Trees, Sohag Governorate, Egypt** *Fathey E. Soliman, Tarek G. Ismail, Alaa Y. Moustafa and Safa M. El-Masry*
16	**Spiders (Arachnida: Araneae) of Jazirat Shandweel District, Sohag Governorate, Egypt** *Fathey E. Soliman, Alaa Y. Moustafa, Tarek G. Ismail & Safa M. El-Masry*
17	**Identification of some trematode cercariae collected from six marine snail species of the genus nerita** *Amaal hassan, muslimah al-solami, sabah m. Hassan*

18	**Role of Parasitic Helminths in Bioremediating Some Heavy Metal Accumulation in the Tissues of Lethrinus mahsena** *Amaal Hassan, Samia Moharram, Hanan El Helaly*
19	**Meristic and Morphometric Characteristics of five-lined snapper, *Lutjanus quinquelineatus* (Bloch, 790) from the Red Sea, Egypt** *Faiza. M. Soliman, Sahar. F. Mehanna, Hamdy .A. Soliman and Taha. S. Baker*
20	**Oxidative stress and histomorphological markers in the offspring of *Poecilia reticulate* maternally exposed to metallic and nanoformulated copper** *Hamdy A. M. Soliman and Sohair M. M. Ragab*
21	**Modulatory effects of green tea extract against the hepatotoxic effects of 4-nonylphenol in catfish (Clarias gariepinus)** *Alaa El-Din H. Sayed, Hamdy A.M. Soliman*
22	**UVA-induced neurotoxicity in Japanese medaka (Oryzias latipes)** *Sayed AEH, Soliman HAM, Mitani H.*
23	**Effect of geographic location and sexual dimorphism on shield shape of the Red Sea hermit crab Clibanarius signatus using the geometric morphometric approach** *Ismail, T.G.,*
24	**Localization of connective tissue growth factor (CTGF) and transforming growth factor beta- (TGF-β) during eye development of four species of birds** *Seleem, A.A., Sultan, A.R.S., Said, A., Shahat, M.M. and Moustafa, M.A.*
25	**Zinc oxide nanoparticales induced histological, histochemical and genotoxicity effects in kidney of adult male rabbits** *Tito N Habib, Hekmat O Abdel-Aziz and Eman E Ragab*
26	**Synthesis and effect of a new Terbium Gibberellic complex on the histopathological alteration induced by Gibberellic acid on liver and kidney of mice Mus Musculus** *Seleem, A.A. and Hussein, B.H.*
27	**Antitumor effect of scorpion venom peptides in vivo of male rabbit and in vitro of DU45 cells of prostate cancer model** *Nadia S Mahrous, Hemely A Hassan, Fayza M Ali and Tito N Habib*
28	**Influences of olive leaf extract in the kidney of diabetic pregnant mice and their offspring** *Hend A. Mohammed, Hanan A. Okail, Mona A. Ibrahim, and Nahed M. Emam*

List of papers published by Staff members of Geology Departmen (127-134)

1	**Hydrocarbon type detection using the synthetic logs: A case study, Baba member, Gulf of Suez, Egypt** *Abudeif, A.M., Attia, M.M., Al-Khashab, H.M., Radwan, A.E.*
2	**A new species of Hypselaster (Echinoidea, Spatangoida) from the Middle Eocene Midawara Formation of the Eastern Desert, Egypt** *Elattaar, A.A.*
3	**Estimation of site effect using microtremor technique at 5th May City, Helwan, Egypt** *Mohammed, M.A., Abudeif, A.M., Omar, K.A., Attia, M.M.*
4	**Middle Eocene echinoids from El Sheikh Fadl-Ras Gharib stretch, Eastern Desert, Egypt: systematics, stratigraphy, palaeobiogeography** *Elattaar, A.A.*
5	**Detection of basaltic intrusion using geomagnetic survey on Kolit Fahdi, Eastern Desert, Egypt** *Abudeif, A.M., Alkhashab, M.H., Saad, S.E.*
6	**Karst Induced Geo-hazards in Egypt: Case study slope stability problems along some selected Desert Highways** *Youssef, A.M., El-Shater, A., El-Khashab, M.H., El-Haddad, B.A.*
7	**Engineering Applications of D Electrical Resistivity Tomography (TRT) For the proposed New Akhmim City, Sohag, Egypt** *Abudeif, A.M., FAT-HELBARY, R.E., El-khashab, H.M., Masoud, M.M.*
8	**Alteration parameters affecting the Luxor Avenue of the Sphinxes-Egypt** *El-Gohary M., Redwan M.*
9	**Evidence for rare-metal occurrences in the post-orogenic Pan-African Aswan pegmatite (southern Egypt): mineralogy, geochemistry and monazite dating** *Abdelfadil, K.M., Gharib, M.E., Putiš, M., Uher, P.*
10	**Provenance studies of Kalabsha kaolin deposits, Egypt: a petrographical and geochemical approach** *Saber, E.-S., Ali, M., El-Sheikh, A.*
11	**Late Neoproterozoic adakitic lavas in the Arabian-Nubian shield, Sinai Peninsula, Egypt** *Abdelfadil, K. M, Obeid, M. A, Azer, M. K, Asimow, P.D*
12	**Characterisation of the Egyptian Pliocene bentonite from the Sohag region for pharmaceutical use** *Elshater, A., Elhaddad, A., Elattaar, A., Abugharbia, M., Soliman, W.*
13	**Geotechnical properties of Precambrian carbonate, Saudi Arabia** *El-Sayed Sedek Abu Seif Abdulelah A. Bahabri, Abd El-Hamed El-Shater Abd El-Hamed*
14	**Pan-African rare-earth bearing paragneiss, South-eastern desert, Egypt: geochemistry and monazite age dating** *Abdelfadil, K.M. Putiš, M., Ondrejka, M., Saleh, G.*
15	**Hydrologic analysis of the challenges facing water resources and sustainable development of Wadi Feiran basin, southern Sinai, Egypt** *Ahmed, A.A., Diab, M.S.*
16	**Desertification risk assessment of sand dunes in middle Egypt: A geotechnical environmental study** *El-Sayed Sedek Abu Seif,, Mohamed H. El-Khashab*

Number of published papers by staff members of Faculty of Science during 2018

Department	Number
Mathematics	75
Physics	42
Chemistry	75
Botany & Microbiology	27
Zoology	28
Geology	16
Total	263

- **Collaborative publications within 2018 include:**

  Departments of Physics and Chemistry collaborate and success to publish 9 articles.

  Departments of Chemistry and Botany collaborate and success to publish one article.

  Departments of Botany and Geology collaborate and success to publish one article.

Mathematics

Applied Mathematics & Information Sciences an International Journal

Hamdy H .El-Sayed

Abstract:
WSNs are quickly gaining popularity due to they are potentially low cost solutions to a variety of real world challenges. They continue to grow day after day, so it needs the effective protocol mechanisms. There are various areas where research activities are going on in Wireless sensor networks. Data-centric technologies are needed that perform in network aggregation of data to yield energy-efficient dissemination. We examine changes of data aggregation energy and probability effects on the performance of Enhanced Distributed Energy Efficient Clustering (EDEEC) and Modified Low Energy Adaptive Clustering Hierarchy (MODLEACH) protocols. Our study uses Dead Nodes, Alive Nodes, Packet sends to BS Nodes and Count of Cluster Heads as a parameters. These parameters have been affected and changed with different data aggregation energy and probability. In this research work the results and observations made from the analyses of results about these protocols are presented.
Appl. Math. Inf. Sci. 12, No. 1, 171-177 (2018)

Performance comparison of LEACH, SEP and Z-SEP protocols in WSN

Hamdy H. El-Sayed

Abstract:
Wireless sensor networks (WSN) have major scope to monitor, and analyze the phenomena in the real world in details as much as possible, in places to a large degree, very dusky, very high, or very dangerous for researchers to go. Simulation could be great helpful to detect that the shortest possible time to minimize the cost of WSN when design. Simulation provides controlled environmental status for development and optimizing the design parameters and the configuration alternatives. It also represents a good prudence into the effects of the different parameters and so helps to identify those parameters to obtain the great importance for system operation and design. Some nodes transmit data directly to base station in Zonal Stable Election Protocol (Z-SEP) protocol whilst some clustering technique that used are send data to base station as well as in Stable Election Protocol (SEP) protocol. The Zonal Stable Election Protocol is implemented and compared with traditional Low Energy adaptive clustering hierarchy (LEACH) and Stable Election Protocol. Results of simulation showed that Zonal Stable Election Protocol is enhanced the stability period and end-to-end delay and less overhead than Low Energy adaptive clustering hierarchy and Stable Election Protocol. This article also tests the node density effects on dead nodes, alive nodes and packet to base station.
International Journal of Computer Applications (0975 – 8887), 180 – No.30, April 2018

Performance Evaluation of Clustering EAMMH, LEACH, SEP, TEEN Protocols in WSN

Hamdy H. El-Sayed

Wireless Sensor Networks (WSNs), are self-configured and infrastructure less wireless networks. That network consists of small devices which equipped with expert sensors and wireless transceivers. The main goal of a WSN is to make a connection data from the environment and send it to the base station (BS) where the data can be observed and analyzed. Wireless sensor devices also respond to queries sent from the base station (BS) to perform specific instructions. Finally, they can be equipped with actuators to "act" upon certain conditions. These networks are sometimes more specifically referred as Wireless Sensor and Actuator Networks. In the work of this paper work, clustering Energy aware multi-hop multi-path hierarchical protocol (EAMMH), Low-energy adaptive clustering hierarchy protocol (LEACH), Stable Election Protocol (SEP) and Threshold sensitive energy efficient sensor network protocol (TEEN) routing protocols for Wireless Sensor Network are compared. Average energy of node and number of dead nodes are used to measure the performance of theses protocols. Different values of number of nodes (node density) and energy of transmitter and receiver parameters are used. These routing algorithms have been developed in this regard. This article showed that the changes values of these parameters have clear effects on the performance of cluster protocols in WSN. In this research work the results and observations made from the analyses of results about these protocols are presented.
Inf. Sci. Lett. 7, No. 2, PP.35-40 (May 2018)

A Novel Algorithm based on Entanglement Measurement for Improving Speed of Quantum Algorithms

Mohammed Zidan, Abdel-Haleem Abdel-Aty, A. Younes, E. A. Zanaty, I. El-khayat, Mahmoud Abdel-Aty

Abstract:
In this paper, we draw attention to consider that the quantum entanglement measurement should be implemented as a key part during manufacturing the quantum processors and quantum micro-controllers. This paper aims to harness the complete power of quantum mechanics by the crossover between entanglement measurements and quantum gates to propose a novel quantum computer algorithms and protocols. One of these measurements that we apply is concurrence, used to measure entanglement in a two-qubit system to solve the problem under scrutiny in n-dimensional vector space. The general algorithm to reshape many of the existing quantum algorithms, and to propose a novel quantum algorithms and protocols based on entanglement measurement is proposed in this paper.
Appl. Math. Inf. Sci. 12, No. 1, 265-269 (2018)

A Novelmetaheuristic Algorithm Based on Wave Function

E.A. Zanaty, Khalid Abdel Wahab, Ali Qora

Abstract:
Aiming at the phenomenon of slow convergence rate and low accuracy of some metaheuristic algorithms , a novel metaheuristic algorithm based on wave function and swarm intelligence is proposed. Swarm intelligence is a collective intelligence of groups of simple agents deals with collective behaviors of decentralized and self-organized swarms, which result from the local interactions of individual components with one another and with their environment. Wave function is introduced to accelerate the convergence speed of proposed algorithm. Standard deviation can ensure the dispersion of the population to prevent premature convergence. The simulation results using Benchmark functions show that the proposed algorithm is effective.
International Journal of Advanced Research in Computer Science9, 2, March-April 2018

Generalized Hermite kernel function for support vector machine classifications

E. A. Zanaty , Ashraf Afifi

Abstract:
Support vector machines (SVMs) have proved to be promising methods for classification and regression analysis because of their solid mathematical foundations which convey several salient properties that other methods hardly provide. The critical SVMs problem is to select appropriate kernels as the performance of SVMs depends on this choice. In this paper, a set of new Hermite kernel functions is proposed for accurate SVMs classification. Besides clarifying how to apply the proposed Hermite kernel functions on vector inputs, we also enhanced the generalization capability of the proposed method when applied to a variety of classification problems. The generalized kernel functions are induced from Hermite polynomials which proved orthogonality and recurrence. The proposed generalized Hermite kernels satisfy Mercer's condition and are stated in the general form, allowing us to derive different kernel functions. The accuracy of the proposed kernels is compared with that of the existing kernels such as Universal, Chebyshev, Gaussian, and Polynomial by applying them to a variety of non-separable data sets with several attributes. It is shown that the proposed kernel gives good classification accuracy in nearly all the data sets, especially those of high dimensions.
International Journal of Computers and Applications, doi.org/10.1080/1206212X.2018.1489571

Multi-Objective Optimization to Find The Shortest Paths Tree Problem in The Computer Networks

Mahmoud A. Mofaddel, and Ahmed Y. Hamed

Abstract:
The shortest paths tree problem when considering cost and bandwidth constraints is addressed in this paper as multiobjective shortest paths tree problem. A multi-objective genetic algorithm is suitable to solve the presented problem. Therefore, this paper presents a multi-objective genetic algorithm based on Random Weighted Genetic Algorithm (RWGA) to solve the shortest paths tree problem subject to cost and bandwidth constraints. The objective of the proposed algorithm is to search the optimal set of edges connecting all nodes such that the sum of costs is minimized and the value bandwidth is maximized. The presented algorithm has been applied on two sample networks to illustrate their efficiency.
Appl. Math. Inf. Sci. 12, No. 1, 151-158 (2018)

An Elliptical Boundary Skin Model For Hand Detection Based on HSV Color Space

Usama Sayed, Mahmoud A. Mofaddel, Samy Bakheet, Zenab El-Zohry

Abstract:
Detection and tracking of human face and hands are curial for gesture recognition. In this paper, a skin segmentation framework is presented, where a robust elliptical model in HSV color space is developed, which promises not only to better model the skin color, but also to significantly lower the complexity of the hand detection process. In our approach, hand regions are identified and detected in Hue Saturation Value (HSV) color space that is proven to correspond closer to human perception of hand color than the traditional RGB color space. The obtained results show the potential of the method proposed and it yields good performance and has robustness with respect to illumination as well as with respect to image noise.
Information Sciences Letters, 7, No. 1, 13-17 (2018)

Hiding Information using Secret Sharing Scheme Based on Gene Expression Programming

Marghny H. Mohamed, Mahmoud A. Mofaddel, Tarek Y. Abd El-Naser

Abstract:
Undoubtedly, communication process is considered as one of the most important means which contributed in the technological development. Transfer the data between people rapidly and accurately has been appeared due to the development of the internet. However, these data may be very confidential and important and may be also found by the hackers who can steal, modify and misuse it. Therefore, it is important to transfer the data with ultimate security. Steganography is one of the techniques, which is designed to deal with such type of problems. In this paper, images have been used as a cover file, because of the difficulty of doubt of presence of any hidden data. Gene expression programming (GEP) algorithm has been used with LSB technique (it is based on replacing the LSBs of cover-image with secret-image bits giving a stego-image) for hiding data and secret-sharing scheme for protect it. We have been presented a secret sharing scheme based on which a user divides the secret-image vertically into parts such that each part is embedded randomly in one cover. Only authorized of parties can reconstruct the secret-image by comparing the variance between the left edges of the selected part of secret-image with the right edges of the other parts of secret-image and vice versa. The results of the comparison guide us to obtain the parts again of the secret image. The hiding of data needs a powerful and sophisticated method such as GEP where it chooses the best places to hide the secret-image in the cover-image through a set of processes to reduce attention of presence of confidential data by reducing the distortion and also besides hiding data we need strong protection method such as the SSC method where preventing hackers from easy access to the complete secret-image.
Inf. Sci. Lett. 7, No. 1, 19-28 (2018)

Text Message Encoding Based on Elliptic Curve Cryptography and a Mapping Methodology

Omar Reyad

Abstract:
Elliptic Curve Cryptography (ECC) is a public-key cryptosystem which can be used for message encryption, key agreement protocols and digital signature applications. ECC offers high level of security with smaller key sizes makes it ideal for applications which run on small devices that have power and memory constraints such as smart cards and cell phones. Encoding (converting a plaintext message to a point) and Decoding (converting a point to a plaintext message) are important functions in encryption and decryption schemes using ECC before transmission over public networks and unsecured channels. In this paper, we proposed a text message encoding scheme which is based on computational operations on points that lie on a predefined elliptic curve (EC). For any ECC-based encryption scheme, the mapping methodology of a plaintext message onto a coordinate on an affine curve is a mandatory prerequisite. ASCII character codes are considered for the mapping method to convert a plaintext message into coordinates of the predefined EC-points. Discussing the mapping methodology, creating the mapping table and the converting process are given in detail along with their implementations.
Inf. Sci. Lett.7, 1, 7-11 (2018)

New SDN-Oriented Distributed Network Security System

Fahad Nife, Zbigniew Kotulski and Omar Reyad

Abstract:
Software-Defined Network (SDN) is a network technology aimed to open new possibilities in network management and orchestration. This is important in future (especially mobile) networks, where virtualization of resources and network functions is the basic paradigm. SDN has been proposed to programmatically control networks, facilitating deployment of new applications and services, as well as tuning network policy and performance. It represents an important change in the way networks are architected, built, and managed. In this new networking paradigm, a network control plane is physically decoupled from a forwarding plane and is directly programmable. In SDN networks, the control plan e supports a logically centralized controller which has a global view of the entire network; it gathers information from the data plane to be processed by the management tasks which are implemented as applications running on the top of the controller. Based on the global view, these applications make packets processing decisions and distribute them to the data plane via the controller. However, security of such networks with their programmability and centralized points of control is not currently ensured on a sufficient level. In this paper, we present the concept of a new security system for SDN-based networks, which can be easily integrated with the existing network infrastructure as well as can provide security of all network components. It consists of two main subsystems: the network authentication and access control system to protect the network control and the distributed firewall system to protect data transmission. Such a system enables creating additional boundaries within the network to provide a multi-plane system of defense, solves the problem of a single point of failure, and makes it easy to protect the network from external attacks as well as from internal malicious users.
Appl. Math. Inf. Sci.12, 4, 673-683 (2018)

Multi-filter Score-Level Fusion for Fingerprint

Muhammad Atta Othman Ahmed, Omar Reyad, Yasser AbdelSatar, Nahla F. Omran

Abstract:
Biometric systems are widely used in various applications of today's authentication technology. The unimodal systems suffer from various stumbling blocks such as noisy inputs, non-universality, intra-class variability and imposter spoofing which affects the system performance and accuracy. To effectively handle these problems, two or more individual modalities are used. In this paper, we presented a multimodal approach for fingerprint verification based on a combination of score level fusion rules. In the preprocessing stage, Anisotropic Diffusion Filter (ADF) and Histogram Equalization (Hist-Eq) techniques were applied to overcome the main challenging drawbacks of fingerprint samples acquisition such as distortion, noise, rotation, etc. Supplementary, the Local Binary Pattern (LBP) was used for feature extraction. In score level fusion, the matching scores of individual fingerprints were combined via several fusion rules. Receiver Operating Characteristics (ROC) curves were formed for the multimodal approach that's why it is mainly used to evaluate our system. Experimental results shown improvements of the multimodal system using ADF and Hist-Eq versus the unimodal non-preprocessed fingerprint samples. The obtained results indicated that there is a significant increase in the performance of the proposed system due to the combination of scores, making it suitable for more applications relevant to identity verification.
Springer International Publishing AG, part of Springer Nature, A. E. Hassanien et al. (Eds.): AMLTA 2018, AISC 723, 624-633, 2018

Effect of rotation on the surface wave propagation in magneto-thermoelastic materials with voids

AM Farhan[1,2], AM Abd-Alla[3,*]
[1]*Physics Department, Faculty of Science, Jazan University, Saudi Arabia*
[2]*Physics Department, Faculty of Science, Zagzig University, Egypt.*
[3]*Mathematics Department, Faculty of Science, Sohag University, Egypt*

Abstract:
The present investigation is focused on studying the surface wave propagation in a generalized magneto-thermoelastic materials taking (Green Lindsay) model with voids. The general surface wave speed is derived to study the effects of magnetic field and rotation on surface wave in the presence of voids. In addition the present study can be comprehensively applied to the magneto-thermoelastic medium with voids. The possible non-dimensional frequency of surface wave propagation has been obtained as the solution of an algebraic equation involving a determinant whose elements contain the material parameters, the direction of applied magnetic field and rotation of surface wave propagation. The comparisons for the physical quantities are established numerically and represented graphically in different cases with respect to the used effects.
Journal of Ocean Engineering and Science 3 (2018): 334-342

Effect of rotation and magnetic field on free vibrations in a spherical non-homogeneous embedded in an elastic medium

F. S. Bayones[1] and A. M. Abd-Alla[2,*]
[1]*Mathematics Department, Faculty of Science, Taif University,888,Taif, Saudi Arabia,*
E-mail: F.S.Bayones@hotmail.com
[2]*Mathematics Department, Faculty of Science, Sohag University, 243, Sohag, Egypt,*

Abstract:
The prime objective of the present paper is to analyze the effect of magnetic field and rotation on the free vibrations of an elastic hollow sphere. The one-dimensional equation of motion is solved in terms of radial displacement. The frequency equation is obtained when the boundaries are free and fixed boundary conditions. The determination is concerned with the eigenvalues of the natural frequency of the free vibrations in the case of harmonic vibrations. The natural frequencies and the mode shapes are calculated numericall and the effects of rotation and magnetic field are discussed. It was shown that the dispersion curves of waves were significantly influenced by the magnetic field and rotation of the elastic sphere.
Results in Physics 9 (2018): 698-704.

Eigenvalue approach to coupled thermoelasticity in a rotating isotropic medium

F. S. Bayones[1] and A. M. Abd-Alla[2,*]
[1]Mathematics Department, Faculty of Science, Taif University, Saudi Arabia
[2]Mathematics Department, Faculty of Science, Sohag, Egypt

Abstract:
In this paper the linear theory of the thermoelasticity has been employed to study the effect of the rotation in a thermoelastic half-space containing heat source on the boundary of the half-space. It is assumed that the medium under consideration is traction free, homogeneous, isotropic, as well as without energy dissipation. The normal mode analysis has been applied in the basic equations of coupled thermoelasticity and finally the resulting equations are written in the form of a vector- matrix differential equation which is then solved by eigenvalue approach. Numerical results for the displacement components, stresses, and temperature are given and illustrated graphically. Comparison was made with the results obtained in the presence and absence of the rotation. The results indicate that the effect of rotation, non-dimensional thermal wave and time are very pronounced.
Results in physics 8 (2018): 7-15.

Effect of rotation and gravity on the reflection of P-waves from thermo-magneto-microstretch medium in the context of three phase lag model with initial stress

S. M. Abo-Dahab[1,2], A. M. Abd-Alla[3,*], A. A. Kilany[3] and M. Elsagheer[3]
[1]Department of Mathematics, Faculty of Science, South Valley University, Qena 83523, Egypt
[2]Department of Mathematics, Faculty of Science, Taif University, Taif, Saudi Arabia
[3]Department of Mathematics, Faculty of Science, Sohag University, Sohag 82524, Egypt

Abstract:
In this paper the linear theory of the thermoelasticity has been employed to study the effect the reflection of plane harmonic waves from a semi-infinite elastic solid under the effect of the magne ic field, rotation, initial stress and gravity. The medium under consider ation is traction free, homogeneous, isotropic , as well as with three-phase-lag. The normal mode analysis is used to solve the resulting non-dimensional coupled equations. The expressions for the reflection coefficients, which are the relations of the amplitudes of the reflected waves to the amplitude of the incident waves, are obtained similarly, the reflection coefficient ratio variations with the angle of incident under different conditions are shown graph ically. Comparisons are made with the results predicted by different theories Lord- Shulman theory (L-S), the GreenNaghdi theory of type III (G-N III) and the three-phase-lag model in the absence and presence of a magnetic field, rotation, initial stress and gravity. The results indicate that the effect of rotation, magnetic field, initial stress and gravity field are very pronounced.
Microsystem Technologies (2018) 1-13

Reflection of plane waves in thermoelastic microstructured materials under the influence of gravitation

S . M . Abo-Dahab[1], Adnan Jahangir[2] and Abo-el-nour N. Abd-alla[3,*]
[1]Department of Mathematics, Faculty of Science, South Valley University, Qena 83523, Egypt
[2]Department of Mathematics, COMSATS University Islamabad, Wah Cantonment, Pakistan
[3]Department of Mathematics, Faculty of Science, Sohag University, Sohâg, Egypt

Abstract:
This paper presents an analysis of wave propagation in a microstretch elastic medium in the context of the Green–Naghdi (GN) theory. Moreover, the dissipation and the influence of gravity on reflected waves have also been investigated. In the present article, five reflected waves propagate into the medium for any incident wave. The problem is solved numerically, and the amplitude ratios are graphically represented allowing for a comparison between the simple GN theory and the case in which one considers the effect of gravity on waves.

Continuum Mech. Thermodyn. (2018)

Squeezing dynamics of a nanowire system with spin-orbit interaction

R. I. Mohamed[1], A. Farouk[2], A. H. Homid[4], O. H. El-Kalaawy[1], Abdel-Haleem Abdel-Aty[4], M. Abdel-Aty[3,5,6,*] and S. Ghose[2]
[1]Department of Mathematics and Computer Science, Faculty of Science, Beni-Suef University,, Egypt.
[2]Department of Physics and Computer Science, Wilfrid Laurier University, Waterloo, Canada.
[3]University of Science and Technology, Zewail City for Science and Technology, Giza, Egypt.
[4]Faculty of science, Al-Azhar University, Assiut, 71524, Egypt.
[5]Department of Mathematics, Faculty of Science, Sohag University, Sohag, Egypt.
[6]Deanship of Scientifc Research and Graduate Studies, Applied Science University, Sitra, Bahrain.

Abstract:
We analyze the dynamics of squeezing in a ballistic quantum wire with Rashba spin-orbit interaction in the presence of both strong and weak magnetic felds and for diferent initial states of the system. Compared to the more standard measure of squeezing based on variances, we show that entropy squeezing is a more sensitive measure. Our results show that there is a strong relationship between the spin-orbit interaction and the strength of entropy squeezing. Furthermore, there is a relationship between the initial state and the number of squeezed components. This allows new knobs to control the strength and the component of entropy squeezing in a nanowire system.

Scientific Reports (2018) 8:10484

New Design of Reversible Full Adder/Subtrac tor Using R Gate

R. Montaser[1], A.Younes[1,2] and M. Abdel-Aty[3,4,*]
[1]*Department of Mathematics and Computer Science, Faculty of Science, Alexandria University, Egypt*
[2]*School of Computer Science, University of Birmingham, Birmingham, B15 2TT, UK*
[3]*University of Science and Technology, Zewail City of Science and Technology, Zewail, Egypt*
[4]*Department of Mathematics, Faculty of Science, Sohag University, Sohag, Egypt*

Abstract
Quantum computers require quantum processors. An important part of the processor of any computer is the arithmetic unit, which performs binary addition, subtraction, division and multiplication, however multiplication can be performed using repeated addition, while division can be performed using repeated subtraction . In this paper we present two designs using the reversible R3 gate to perform the quantum half adder/subtractor and the quantum full adder/subtractor. The proposed half adder/subtractor design can be used to perform different logical operations, such as AND, XOR, NAND, XNOR, NOT and copy of basis. The proposed design is compared with the other previous designs in terms of the number of gates used, the number of constant bits, the garbage bits, the quantum cost and the delay. The proposed designs are implemented and tested using GAP software.
International Journal of Theoretical Physics (2018)

Higher-Order Convolutions for Apostol-Bernoulli, Apostol-Euler and Apostol-Genocchi Polynomials

Y. He[1], S. Araci[2], H. M. Srivastava[3,4] and M. Abdel-Aty[5,*]
[1]*Faculty of Science, Kunming University of Science and Technology, Kunming 650500, Yunnan, China;*
[2]*Faculty of Economics, Administrative and Social Sciences, Hasan Kalyoncu University, Gaziantep TR-27410, Turkey*
[3]*Department of Mathematics and Statistics, University of Victoria, Victoria, BC V8W 3R4, Canada;*
[4]*Department of Medical Research, China Medical University, Taichung 40402, Taiwan*
[5]*Zewail City of Science andTechnology, University of Science and Technology, Cairo 82524, Egypt;*

Abstract:
In this paper, we present a systematic and unified investigation for the Apostol-Bernoulli polynomials, the Apostol-Euler polynomials and the Apostol-Genocchi polynomials. By applying the generating-function methods and summation-transform techniques, we establish some higher-order convolutions for the Apostol-Bernoulli polynomials, the Apostol-Euler polynomials and the Apostol-Genocchi polynomials. Some results presented here are the corresponding extensions of several known formulas
Mathematics (2018), 6, 329

Sub pico-second chirp-free optical solitons with Kaup-Newell equation using a couple of strategic algorithms

S. Arshed[1], A. Biswas[2,3], M. Abdelaty[4,*], Q. Zhou[5], S. P. Moshokoa[3] and M. Belic[6]

[1]Department of Mathematics, University of the Punjab, Lahore –54590, Pakistan
[2]Department of Physics, Chemistry and Mathematics, Alabama A&M University, Normal, AL –35762, USA
[3]Department of Mathematics and Statistics, Tshwane University of Technology, Pretoria–0008, South Africa
[4]Deanship of Research and Graduate Studies, Applied Science University, PO Box 5055, Bahrain
[5]School of Electronics and Information Engineering, Wuhan Donghu University, Wuhan 430212, People 's Republic of China
[6]Science Program, Texas A&M University at Qatar, PO Box 23874, Doha, Qatar

Abstract
This paper obtains bright, dark, singular and other combo optical soliton solutions to perturbed Kaup-Newell equation. Two strategic integration schemes are fruitfully applied to obtain these solutions. These solitons appear with constraint conditions on the soliton parameters that are also presented.
Optik - International Journal for Light and Electron Optics 172 (2018) 766-771

Reflection and refraction of incident p-, T-, and SVwaves at interface between magnetized two solidliquid media with heat sources and initial stress with and without thermal relaxation times

S. M. Abo-Dahab[a,b], M. N. M. Allam[c] and M. Abdel-Aty[d,*]
[a]Mathematics Department, Faculty of Science, South Valley University, Qena, Egypt; b [b]Mathematics Department, Faculty of Science, Taif University, Taif, Saudi Arabia; [c]Mathematics Department, Faculty of Science, Mansoura University, Mansoura, Egypt; [d]Deanship of Research and Graduate Studies, Applied Science University, Bahrain and Sohag University, Egypt

Abstract:
We investigate the problem of reflection and refraction of thermoelastic waves at a magnetized solid-liquid interface in presence of initial stress. In the context of Green-Lindsay and coupled thermoelastic theories of thermoelasticity, the problem has been solved and the effect of magnetic field, external heat sources, and initial stress on p-, T-, and SV-waves propagation have been discussed. The boundary conditions at the interface for displacement continuity, vanishing the tangential displacement, continuity of normal force, tangential force, and continuity of temperature are applied. The amplitudes ratios for the incident p-, T-, and SV-waves have been obtained. The effect of the initial stress, heat sources, and magnetic field on the reflection and transmitted coefficients for the incident waves have been discussed
Journal of Thermal Stresses (2018)

Optical soliton perturbation with Kundu –Eckhaus equation by exp (− ϕ(ξ))-expansion scheme and G ′/G²-expansion method

S. Arshed[a], A. Biswas[b,c], M. Abdelaty[d,*], Q. Zhoue[e], S. P. Moshokoa[c]and M. Belic[f]
[a]*Department of Mathematics, University of the Punjab, Lahore 54590, Pakistan*
[b]Department of Physics, Chemistry and Mathematics, Alabama A&M University, Normal, AL 35762, USA
[c]Department of Mathematics and Statistics, Tshwane University of Technology, Pretoria 0008, South Africa
[d]Deanship of Research and Graduate Studies, Applied Science University, PO Box 5055, Bahrain
[e]School of Electronics and Information Engineering, Wuhan Donghu University, Wuhan 430212, People's Republic of China
[f]Science Program, Texas A&M University at Qatar, PO Box 23874, Doha, Qatar

Abstract:
This paper reveals dark and singular optical solitons, as well as their combinations thereof, of the perturbed Kundu –Eckhaus equation. Two integration methodologies are adopted here. The existence criteria for these solitons are also presented.

Optik - International Journal for Light and Electron Optics 172 (2018) 79-85

Analytical solution and applications of three qubits in three coupled modes without rotating wave approximation

J. S. Zhang[1], L. J. Zhang[1], A. X. Chen[2,3]·and M. Abdel-Aty[4,5,6,*]
[1]Department of Applied Physics, East China Jiaotong University, Nanchang 330013, PRC
[2]Department of Physics, Zhejiang Sci-Tech University, Hangzhou 310018, PRC
[3]Institute for Quantum Computing, University of Waterloo, Ontario N2L3G1, Canada
[4]Applied Science University, Sitra, Bahrain
[5]Zewail City of Science and Technology, Giza, Egypt
[6]Sohag University, Sohag, Egypt

Abstract:
We study the dynamics of the three-qubit system interacting with multimode without rotating wave approximation (RWA). A physical realization of the system without direct qubits interactions with dephasing bath is proposed. It is shown that non-Markovian characters of the purity of the three qubits and the coupling strength of modes are stronger enough the RWA is no longer valid. The influences of the dephasing of qubits and interactions of modes on the dynamics of genuine multipartite entanglement and bipartite correlations of qubits are investigated. The multipartite and bipartite quantum correlations could be generated faster if we increase the coupling strength of modes and the RWA is not valid when the coupling strength is strong enough. The unitary transformations approach adopted here can be extended to other systems such as circuit or cavity quantum electrodynamic systems in the strong coupling regime.

Quantum Inf Process (2018) 17:125

Chirped singular and combo optical solitons for Gerdjikov –Ivanov equation using three integration forms

A. J. M. Jawad[a], A. Biswas[b,c], M. Abdelaty[d,*], Q. Zhou[e], S. P. Moshokoa[c] and M. Belic[f]
[a]Al-Rafidain University College, Baghdad 10014, Iraq
[b]Department of Physics, Chemistry and Mathematics, Alabama A&M University, Normal, AL 35762, USA
[c]Department of Mathematics and Statistics, Tshwane University of Technology, Pretoria 0008, South Africa
[d]Deanship of Research and Graduate Studies, Applied Science University, PO Box 5055, Bahrain[e] School of Electronics and Information Engineering, Wuhan Donghu University, Wuhan 430212, PRC
[f]Science Program, Texas A&M University at Qatar, PO Box 23874, Doha, Qatar

Abstract:
This study carries out the integration of Gerdjikov –Ivanov equation. The csch method, the extended tanh – coth method, and the modified simple equation method are utilized to extract the analytical soliton solutions.
Optik - International Journal for Light and Electron Optics 172 (2018) 144-149

The Population Inversion and the Entropy of a Moving Two-Level Atom in Interaction with a Quantized Field

D. A. M. Abo-Kahla[a,b], M. Abdel-Aty[3,4,*] and A. Farouk[e]
[a]Department of Mathematics, Faculty of Science, Taibah University, Madina, Saudi Arabia
[b]Department of Mathematics, Faculty of Education, Ain Shams University, Roxy, Cairo, Egypt
[c]Deanship of Scientific Research and Graduate Studies, Applied Science University, Sitra, Bahrain
[d]Sohag University, Sohag, Egypt
[e]Department of Physics and Computer Science, Faculty of Science, Wilfrid Laurier University, Waterloo, ON, Canada

Abstract:
An atom with only two energy eigenvalues is described by a two-dimensional state space spanned by the two energy eigenstates is called a two-level atom. We consider the interaction between a two-level atom system with a constant velocity. An analytic solution of the systems which interacts with a quantized field is provided. Furthermore, the significant effect of the temperature on the atomic inversion, the purity and the information entropy are discussed in case of the initial state either an exited state or a maximally mixed state. Additionally, the effect of the half wavelengths number of the field-mode is investigated.
Int J Theor Phys (2018)

Cavity control as a new quantum algorithms implementation treatment

M. AbuGhanem[a,b], A. H. Homid[a,c]and M. Abdel-Aty[a,*]
[a]*University of Science and Technology, Zewail City of Science and Technology, Giza, 12588, Egypt*
[b]*Department of Mathematics, Faculty of Science, Ain-Shams University, Cairo, 11566, Egypt*
[c]*Faculty of Science, Al-Azhar University, Assiut, 71524, Egypt*

Abstract:
Based on recent experiments [Nature 449, 438 (2007) and Nature Physics 6, 777 (2010)], a new approach for realizing quantum gates for the design of quantum algorithms was developed. Accordingly, the operation times of such gates while functioning in algorithm applications depend on the number of photons present in their resonant cavities. Multi-qubit algorithms can be realized in systems in which the photon number is increased slightly over the qubit number. In addition, the time required for operation is considerably less than the dephasing and relaxation times of the systems. The contextual use of the photon number as a main control in the realization of any algorithm was demonstrated. The results indicate the possibility of a full integration into the realization of multi-qubit multiphoton states and its application in algorithm designs. Furthermore, this approach will lead to a successful implementation of these designs in future experiments.
Front. Phys. 13(1), 130303 (2018)

Dynamical Controls for Improving Quantum Search Algorithm Through F lux Qubits System

A . H . Homid[a,b], M. Abdel-Aty[b,c,*], T El-Shahat[a], H. Eleuch[d], and A. S. F. Obada[e]
[a]*Faculty of Science Al-Azhar University Assiut 71524, Egypt*
[b]*University of Science and Technology Zewail City for Science and Technology Giza, Egypt*
[c]*Deanship of Scientific Research and Graduate Studies Applied Sciences University Kingdom of Bahrain*
[d]*Institute for Quantum Science and Engineering Texas A & M Universiy College Station, Texas 77843, USA*
[e]*Faculty of Science Al-Azhar University Nasrcity 11884, Cairo, Egypt*

Abstract:
A new technique was developed to generate the dynamical quantum gates, depend on the ferromagnetism and antiferromagnetism phenomena in the superconducting flux qubits system at the same interaction time. According to the dynamical controls techniques of such gates, we invoke and synthesize a new algorithm called the dynamical quantum search algorithm. The Grover algorithm was obtained at a specified time for the current algorithm. This algorithm was distinguished by accuracy in obtaining high probability of finding any marked state in a shorter time compared with Grover algorithm time. The algorithm performance was improved with respect to different values o f the dynamical controls.
Fortschr. P hys. (2018), 66, 1700080

A Novel Algorithm based on Entanglement Measurement for Improving Speed of Quantum Algorithms

M. Zidan[1,2], Abdel-Haleem Abdel-Aty[3], A. Younes[4], E. A. Zanaty[2], I. El-khayat[5] and M. Abdel-Aty[1,2,*]
[1]University of Science and Technology, Zewail City, Sheikh Zayed District, 12588, Giza, Egypt.
[2]Mathematics and Computer Science Department, Faculty of Sciences, Sohag University, Sohag, Egypt.
[3]Physics Department, Faculty of Science, Al-Azhar University, 71524 Assiut, Egypy
[4]Department of Mathematics & Computer Science, Faculty of Science, Alexandria University, Egypt
[5]Applied Sciences University, Kingdom of Bahrain.

Abstract:
In this paper, we draw attention to consider that the quantum entanglement measurement should be implemented as a key part during manufacturing the quantum processors and quantum micro-controllers. This paper aims to harness the complete power of quantum mechanics by the crossover between entanglement measurements and quantum gates to propose a novel quantum computer algorithms and protocols. One of these measurements that we apply is concurrence, used to measure entanglement in a two-qubit system to solve the problem under scrutiny in n-dimensional vector space. The general algorithm to reshape many of the existing quantum algorithms, and to propose a novel quantum algorithms and protocols based on entanglement measurement is proposed in this paper.
Applied Mathematics & Information Sciences (2018) 12: 265-269

Robust general N user authentication scheme in a centralized quantum communication network via generalized GHZ states

A. Farouk[1], J. Batle[3], M. Elhoseny[1], M. Naseri[4], M. Lone[5], A. Fedorov[6], M. Alkhambashi[7], S. H. Ahmed[8] and M. Abdel-Aty[2,*]
[1]Faculty of Computer and Information Sciences, Mansoura University, Egypt
[2]Applied Science University, Bahrain & Mathematics Dept. Sohag University, Egypt
[3]Departament de Física, Universitat de les Illes Balears, 07122 Palma de Mallorca, Balearic Islands, Spain
[4]Department of Physics, Kermanshah Branch, Islamic Azad University, Kermanshah, Iran
[5]Department of Physics, University of Kashmir, Srinagar-190006, India
[6]Russian Quantum Center, 100 Novaya Street, Skolkovo, Moscow 143025, Russia
[7]Information Technology Department, Al-Zahra College for Women, P.O. Box 3365, Muscat, Oman
[8]School of Computer Science & Engineering, Kyungpook National University, Daegu, Republic of Korea

Abstract:
Quantum communication provides an enormous advantage over its classical counterpart: security of communications based on the very principles of quantum mechanics. Researchers have proposed several approaches for user identity authentication via entanglement. Unfortunately, these protocols fail because an attacker can capture some of the particles in a transmitted sequence and send what is left to the receiver through a quantum channel. Subsequently, the attacker can restore some of the confidential messages, giving rise to the possibility of information leakage. Here we present a new robust General N user authentication protocol based on N-particle Greenberger–Horne–Zeilinger (GHZ) states, which makes eavesdropping detection more effective and secure, as compared to some current authentication protocols. The security analysis of our protocol for various kinds of attacks verifies that it is unconditionally secure, and that an attacker will not obtain any information about the transmitted key. Moreover, as the number of transferred key bits N becomes larger, while the number of users for transmitting the information is increased, the probability of effectively obtaining the transmitted authentication keys is reduced to zero.
Front. Phys. 13(2), 130306 (2018)

Entanglement o f a nonlinear t wo two-level a toms interacting with defo rmed fields in Kerr medium

S. ABDEL-KHALEK[1,2], Y. S. EL-SAMAN[1] and M ABDEL-ATY[3,4,*]
[1]Department of Mathematics, Faculty of Science, Sohag University, Sohag, Egypt
[2]Mathematics Department, Faculty of Science, Taif University, Taif, Saudi Arabia
[3]Scientific Research and Graduate Studies, Applied Science University, East Al-Kabir, Bahrain
[4]Mathematics Department, Faculty of Sciences, Sohag University and Zewail City of Science and Technology, Cairo, Egypt

Abstract:
In this paper we investigate the entanglement dynamics between two two-level atoms interacting with two coherent fields in two spatially separated cavities which are filled with a Kerr-like medium. We examine the effect of nonlinear medium on the dynamical properties of entanglement and atomic occupation probabilities in the case of even and odd deformed coherent states. The results show that the deformed fields play important roles in the evolution of entanglement. Also, the results demonstrate that entanglement sudden death, sudden birth and long-distance can be controlled by the deformation and nonlinear parameters.
Pramana – J. P hys. (2018) 90:1

Solving Deutsch's Problem using Entanglement Measurement Algorithm

M. Zidan[1,2], Abdel-Haleem Abdel-Aty[3], A. S. A. Mohamed[4,5], I. El-khayat[6] and M. Abdel-Aty[1,2,*]
[a]University of Science and Technology, Zewail City, Sheikh Zayed District, 12588, Egypt
[2]Mathematics and Computer Science Department, Faculty of Sciences, Sohag University, Sohag, Egypt.
[3]Physics Department, Faculty of Science, Al-Azhar University, 71524 Assiut, Egypt.
[4]University of Science and Technology, Zewail City, Sheikh Zayed District, 12588, Egypt
[5]Department of Engineering Mathematics and Physics, Faculty of Engineering, Cairo University, Egypt.
[6]Applied Sciences University, Kingdom of Bahrain.

Abstract:
Given a black-box representing an unknown Boolean function f , determining whether the unknown function f (x) has f (0) = f (1) or not using a single query to f is known as Deutsch's algorithm. Following [28], in this paper, we propose Deutsch's algorithm based on entanglement measurement. The proposed algorithm creates entanglement between the independent variable x represented by the test qubit and an ancilla qubit called detection qubit, where the entanglement is measured using concurrence measure to decide if the considered function f (x) has f (0) = f (1) or not.
Appl. Math. Inf. Sci. Lett. 6, No. 3, 1-5 (2018)

Finite Element Analysis of Thermoelastic Fiber-Reinforced Anisotropic Hollow Cylinder

A. D. Hobiny[a], I. A. Abbas [a,b,*] and Fberto[c]
[a]Department of Mathematics, King Abdulaziz University, Jeddah, Saudi Arabia
[b]Department of Mathematics, Faculty of Science, Sohag University, Sohâg 82524, Egypt [c]Department of Mechanical and Industrial Engineering, Norwegian University of Science and Technology (NTNU), Trondheim, Norway

Abstract:
In the present paper, we have constructed the equations for generalized thermoelasticity of a fiber-reinforced anisotropic hollow cylinder. The formulation is applied in the context of dualphase-lag model. An application of hollow cylinder is investigated for the outer surface is traction free and thermally isolated, while the inner surface is traction free and subjected to thermal shock. The problem is solved numerically using a finite element method. The results of displacement, temperature and radial and hoop stress are obtained and then presented graphically. Finally, the comparisons are made between the results predicted by the coupled theory, Lord and Shulman theory and dual-phase-lag model in presence and absence of reinforcement.
Strength of Materials (2018) 50: 396-405.

A DPL model of photo-thermal interaction in an infinite semiconductor material containing a spherical hole

A. D. Hobiny[a] and I. A. Abbas [a,b,*]
[a]Department of Mathematics, King Abdulaziz University, Jeddah, Saudi Arabia
[b]Department of Mathematics, Faculty of Science, Sohag University, Sohâg 82524, Egypt

Abstract:
The dual phase lag (DPL) heat transfer model is applied to study the photo-thermal interaction in an infinite semiconductor medium containing a spherical hole. The inner surface of the cavity was traction free and loaded thermally by pulse heat flux. By using the eigenvalue approach methodology and Laplace's transform, the physical variable solutions are obtained analytically. The numerical computations for the silicon-like semiconductor material are obtained. The comparison among the theories, i.e., dual phase lag (DPL), Lord and Shulman's (LS) and the classically coupled thermoelastic (CT) theory is presented graphically. The results further show that the analytical scheme can overcome mathematical problems by analyzing these problems.
European Physical Journal Plus (2018) 133

Fractional order photo-thermo-elastic waves in a two-dimensional semiconductor

A. D. Hobiny[a] and I. A. Abbas[a,b,*]
[a]*Department of Mathematics, King Abdulaziz University, Jeddah, Saudi Arabia*
[b]*Department of Mathematics, Faculty of Science, Sohag University, Sohâg 82524, Egypt*

Abstract:
This paper is devoted to the investigation of fractional order photo-thermo-elastic waves in a two-dimensional semiconductor using the eigenvalues approach. The formulations applied are based on the fractional order generalized thermo-elasticity in the context of the new model of heat conduction. The bounding surface of the plate is taken to be stress-free and exposed to a heat flux with the exponentially decaying pulse. By using Laplace's and Fourier's transformations and the eigenvalues approach methodology, the analytical solutions of variables have been obtained. A semiconducting material, such as silicon, has been investigated. In the conclusion, the results are graphically represented to show the effects of the thermal relaxation time and the fractional order parameters on the thermal, plasma and elastic waves.
European Physical Journal Plus (2018) 133

Theoretical analysis of thermal damages in skin tissue induced by intense moving heat source

A. D. Hobiny[a] and I. A. Abbas[a,b,*]
[a]*Department of Mathematics, King Abdulaziz University, Jeddah, Saudi Arabia*
[b]*Department of Mathematics, Faculty of Science, Sohag University, Sohâg 82524, Egypt*

Abstract:
In this paper, the analytical solution of hyperbolic bio-heat equation under intense moving heat source is presented. The exact solution in the domain of Laplace's transform is obtained. The thermal damages to the tissues are evaluated by the extent of the denatured protein employing with the Arrhenius equation. The results indicate that the hyperbolic bio-heat model reduces to the parabolic bio-heat model when the thermal relaxation time is zero. Numerical results for temperatures and thermal damages are represented graphically. The effects of heat source velocity on the temperature of skin tissue and thermal damages are studied. These results can be used as a confirmation part for studying the practical operations such as scanning laser treatment and other numerical solutions.
International Journal of Heat and Mass Transfer (2018) 124: 1011-1014

The influence of thermal and conductive temperatures in a nanoscale resonator

A. D. Hobiny[a] and I. A. Abbas[a,b,*]
[a]*Department of Mathematics, King Abdulaziz University, Jeddah, Saudi Arabia*
[b]*Department of Mathematics, Faculty of Science, Sohag University, Sohâg 82524, Egypt*

Abstract:
In this work, the thermoelastic interaction in a nano-scale resonator based on two-temperature Green-Naghdi model is established. The nanoscale resonator ends were simply supported. In the Laplace's domain, the analytical solution of conductivity temperature and thermodynamic temperature, the displacement and the stress components are obtained. The eigenvalue approach resorted to for solutions. In the vector-matrix differential equations form, the essential equations were written. The numerical results for all variables are presented and are illustrated graphically.
Results in Physics (2018) 9: 705-711

Analytical solutions of photo-thermo-elastic waves in a non-homogenous semiconducting material

A. D. Hobiny[a] and I. A. Abbas[a,b,*]
[a]*Department of Mathematics, King Abdulaziz University, Jeddah, Saudi Arabia*
[b]*Department of Mathematics, Faculty of Science, Sohag University, Sohâg 82524, Egypt*

Abstract:
In the present paper, the wave propagation on non-homogenous semiconductor through photo-thermal process has been studied by using the theory of coupled plasma and thermoelastic wave. Without neglecting the coupling between the plasma and thermoelastic wave that photo-generated through intensity modulated laser beamand tightly focused, a semiconducting isotropic elastic medium has non-homogeneityin thermal and elastic properties are considered. The analytical solutions in the domain of Laplace by the eigenvalues approach were observed through the transform techniques of Laplace. Silicon-like semiconductor was used to achieve the numerical computations.
Results in Physics (2018)10: 385-390

Analytical solution of fractional order photo-thermoelasticity in a non-homogenous semiconductor medium

A. D. Hobiny[a] and I. A. Abbas[a,b,*]
[a]*Department of Mathematics, King Abdulaziz University, Jeddah, Saudi Arabia*
[b]*Department of Mathematics, Faculty of Science, Sohag University, Sohâg 82524, Egypt*

Abstract:
Purpose: The purpose of this paper is to study the wave propagation in a non-homogenous semiconducting medium through the photothermal process using the fractional order photo-thermoelastic without neglecting the coupling between the plasma and thermoelastic waves that photogenerated through traction free and loaded thermally by exponentially decaying pulse boundary heat flux. Design/methodology/approach: The analytical solutions in the transformed domain by the eigenvalue approach were observed through the transform techniques of Laplace. Findings: Silicon-like semiconductor was used to achieve the numerical computations. Originality/value: Some comparisons are shown in the figures to estimate the effects of the fractional order and non-homogeneous parameters.

Multidiscipline Modeling in Materials and Structures (2018) 14: 1017-1030

Stability of latent pathogen infection model with CTL immune response and saturated cellular infection

A. M. Elaiw[a], A. A., Almatrafi[a,b], A. D. Hobiny[a] and I. A. Abbas[a,c,*]
[a]*Department of Mathematics, Faculty of Science, King Abdulaziz University, P.O. Box 80203, Jeddah, SA*
[a]*Department of Mathematics, Jamoum University College, Umm Al Qura University, Makkah, 21599, SA*
[c]*Department of Mathematics, Faculty of Science, Sohag University, Sohag, 82524, Egypt*

Abstract:
We propose a pathogen dynamics model with CTL immune response and both pathogenic and cellular infections. Both actively infected cells and latently infected cells are incorporated into the model. The infected-susceptible and pathogen-susceptible infection rates are given by saturated incidence. Three distributed time delays are considered. The existence and global stability of the equilibria are determined by two threshold parameters, the basic reproduction number and the CTL response activation number. The global stability of the three equilibria are proven using Lyapunov method. We solve the system of delay differential equations numerically to support the theoretical results.

AIP Advances (2018) 8(12), 125021-1:17

Fractional Order Theory in a Semiconductor Medium Photogenerated by a Focused Laser Beam

F. S. Alzahrani[a] and I. A. Abbas [a,b,*]
[a]*Nonlinear Analysis and Applied Mathematics Research Group, Department of Mathematics, King Abdulaziz University, Jeddah, 21589, Saudi Arabia*
[b]*Department of Mathematics, Faculty of Science, Sohag University, Sohag, 82524, Egypt*

Abstract:
In this paper, the fractional order theory has been applied for thermal, elastic and plasma waves to determine the carrier density, displacement, temperature and stress in a semiconductor medium. The thermal, elastic and plasma waves in a semi-infinite medium photogenerated by a focused laser beam were analyzed. The Laplace transformation is used to express the governing equation and solved analytically by applying eigenvalue approach methodology in that domain. A semiconducting material like as silicon was considered. According to the numerical results and graphics, the fractional order parameter and thermal relaxation time may play an important role in the behavior of all physical quantities.
Physical Mesomechanics (2018) 21: 117-123

Generalized photo-thermo-elastic interaction in a semiconductor plate with two relaxation times

F. S. Alzahrani[a] and I. A. Abbas [a,b,*]
[a]*Nonlinear Analysis and Applied Mathematics Research Group, Department of Mathematics, King Abdulaziz University, Jeddah, 21589, Saudi Arabia*
[b]*Department of Mathematics, Faculty of Science, Sohag University, Sohag, 82524, Egypt*

Abstract:
This study focuses on the effect of thermal relaxation times in a two-dimensional semiconductor medium by using eigenvalue approach. The formulation is applied under Green and Lindsay theory with two relaxation times. The bounding surface of the half-space is subjected to a heat flux with an exponentially decaying pulse and taken to be traction free. The variables solutions are obtained analytically by using Laplace-Fourier transformations and the eigenvalue approach methodology. A semiconducting material like as silicon is considered. The numerical computations are obtained and the outcomes are displayed graphically to assess the effects of the thermal relaxation times on the plasma, thermal, and elastic waves.
Thin-Walled Structures (2018) 129: 342-348

Photo-thermoelastic interactions in a 2D semiconducting medium

F. S. Alzahrani[a] and I. A. Abbas [a,b,*]
[a]*Nonlinear Analysis and Applied Mathematics Research Group, Department of Mathematics, King Abdulaziz University, Jeddah, 21589, Saudi Arabia*
[b]*Department of Mathematics, Faculty of Science, Sohag University, Sohag, 82524, Egypt*

Abstract:
Photo-thermoelastic interactions in a two-dimensional semiconductor medium are studied by using mathematical methods in the context of coupled thermoelastic theory and plasma waves with one thermal relaxation time. The Laplace-Fourier transformations and eigenvalues approach are used to obtain the general solutions for any set of boundary conditions. The medium is initially assumed to be at rest and due to a moving thermal source with a constant speed, which are traction free. A semiconductor medium like silicon has been considered. In the conclusion, the outcomes are represented graphically to show the influences of heat source speed and the relaxation time. The eigenvalues approach gives the analytical solution without any assumed restriction on the actual physical quantities.
European Physical Journal Plus (2018) 133 (15)

A Mode I Crack Problem for a Thermoelastic Fibre-Reinforced Anisotropic Material Using Finite Element Method

I. A. Abbas [a,b,*] and S. M. J. Razavi[c]
[a]*Department of Mathematics, Faculty of Science, Sohag University, Sohag, 82524, Egypt*
[b]*Nonlinear Analysis and Applied Mathematics Research Group, Department of Mathematics, King Abdulaziz University, Jeddah, 21589, Saudi Arabia*
[c]*Department of Mechanical and Industrial Engineering, Norwegian University of Science and Technology, Trondheim, 7491, Norway*

Abstract:
In this article, the theory of generalized thermoelasticity with one relaxation time is used to investigate the thermoelastic fiber-reinforced anisotropic material with a finite linear crack. The crack boundary is due to a prescribed temperature and stress distribution. By using the finite element method, the numerical solutions of the components of displacement, temperature and the stress components have been obtained. Comparisons of the results in the absence and presence of reinforcement have been presented.
Physical Mesomechanics (2018) 21(2) 135-139

Analytical and numerical solution of 2D problem for transversely isotropic generalized thermoelastic medium with Green-Naghdi model II

I. A. Abbas [a,b,*] and M. I. A. Othman[c,d]
[a]*Department of Mathematics, Faculty of Science, Sohag University, Sohag, Egypt*
[b]*Nonlinear Analysis and Applied Mathematics Research Group (NAAM), Department of Mathematics, King Abdulaziz University, Jeddah, Saudi Arabia*
[c]*Department of Mathematics, Faculty of Science, Zagazig University, Egypt*
[d]*Department of Mathematics, Faculty of Science, Taif University, Taif, 888, Saudi Arabia*

Abstract:
In this paper, a comparison was made between the analytical and numerical solution of a two-dimensional problem for a transversely isotropic generalized thermoelastic medium. The study is carried out in the context of generalized thermoelasticity proposed by Green and Naghdi's theory of type II. The problem has been solved analytically using the normal mode method with the eigenvalue approach and numerically using a finite element method. The accuracy of the finite element formulation was validated by comparing the analytical and numerical solutions for the field quantities.

International Journal of Acoustics and Vibrations (2018) 23(3): 294-301

Analytical Solutions of a Two-Dimensional Generalized Thermoelastic Diffusions Problem Due to Laser Pulse

I. A. Abbas [a,b,*] and M. Marin[c]
[a]*Nonlinear Analysis and Applied Mathematics Research Group (NAAM), Department of Mathematics, King Abdulaziz University, Jeddah, Saudi Arabia*
[b]*Department of Mathematics, Faculty of Science, Sohag University, Sohag, Egypt*
[c]*Department of Mathematics and Computer Sciences, Transilvania University of Brasov, Brasov, Romania*

Abstract:
In this paper, we apply the generalized thermoelastic theory with mass diffusion to a two-dimensional problem for a half-space. The surface of the half-space is taken to be traction-free and heated by laser pulse. The analytical solution is adopted for the temperature, the displacement components, concentration, the stress components and chemical potential. The nonhomogeneous basic equations have been written in the form of a vector–matrix differential equation, which is then solved using the eigenvalue approach. A comparison is made in the case of the absence and presence of a mass diffusion between the coupled and Lord–Shulman theories. The results obtained are presented graphically for the effects of the laser pulse and the mass diffusion to display the phenomena of physical significance.

Iranian J. Science and Technology - Transactions of Mechanical Engineering (2018) 42(1): 57-71

A Two-Temperature Photothermal Interaction in a Semiconductor Medium Containing a Cylindrical Hole

I. A. Abbas [a,b,*] and A. Hobiny[b]
[a]*Department of Mathematics, Faculty of Science, Sohag University, Sohag, Egypt*
[b]*Nonlinear Analysis and Applied Mathematics Research Group (NAAM), Department of Mathematics, King Abdulaziz University, Jeddah, Saudi Arabia*

Abstract:
Photothermoelastic interactions in an infinite semiconductor medium containing a cylindrical hole with two temperatures are studied using mathematical method under the purview of the coupled theory of thermal, plasma and elastic waves. The internal surface of the hole is constrained and the carrier density is photogenerated by bound heat flux with an exponentially decaying pulse. Based on Laplace transform and the eigenvalue approach methodology, the solutions of all variables have been obtained analytically. The numerical computations for silicon-like semiconductor material have been obtained. The results further show that the analytical scheme can overcome mathematical problems to analyze these problems.
International Journal of Thermophysics (2018) 39(1)

Photo-thermal-elastic interaction in an unbounded semiconducting medium with spherical cavity due to pulse heat flux

I. A. Abbas [a,b,*] and A. Hobiny[b]
[a]*Department of Mathematics, Faculty of Science, Sohag University, Sohag, Egypt*
[b]*Nonlinear Analysis and Applied Mathematics Research Group (NAAM), Department of Mathematics, King Abdulaziz University, Jeddah, Saudi Arabia*

Abstract:
In this work, the photothermal waves in an unbounded semiconducting medium with spherical cavity are studied. This problem is solved using the theory of coupled plasma, thermal, and elastic wave. An unbounded material, elastic semiconductor containing a spherical cavity with isotropic and homogeneous thermal and elastic properties has been considered. The inner surface of the cavity is taken traction-free and subjected to an exponentially decaying pulse boundary heat flux. Laplace transform techniques and eigenvalue approach were used to obtain the analytical solutions. Numerical computations have been done for silicon-like semiconductor material, and the results are presented graphically to estimate the effect of time and the coupling between the plasma, thermal, and elastic waves.
Waves in Random and Complex Media (2018) 28(4): 670-682

A DPL model of photothermal interaction in a semiconductor material

I. A. Abbas [a,b,*], F. S. Alzahrani [b] and A. Elaiw [b]
[a]*Department of Mathematics, Faculty of Science, Sohag University, Sohag, Egypt;*
[b]*Nonlinear Analysis and Applied Mathematics Research Group (NAAM), Department of Mathematics, King Abdulaziz University, Jeddah, Saudi Arabia*

Abstract
The generalized model for plasma, thermal, and elastic waves under dual phase lag model have been applied to determine the carrier density, the displacement, the temperature, and the stresses in a semiconductor medium. Using Laplace transform and the eigenvalue approach methodology, the solutions of all variables have been obtained analytically. A semiconducting material like as silicon was considered. The results were graphically represented to show the different between the dual phase model, Lord and Shulman's theory and the classical dynamical coupled theory.
Waves in Random and Complex Media (2018) 1-16

The effect of fractional derivative on photo-thermoelastic interaction in an infinite semiconducting medium with a cylindrical hole

I. A. Abbas [a,b,*], F. S. Alzahrani [b] and F. Berto [c]
[a]*Department of mathematics, Faculty of Science, Sohag University, Sohag, Egypt*
[b]*Nonlinear Analysis and Applied Mathematics Research Group (NAAM), Department of Mathematics, King Abdulaziz University, Jeddah, Saudi Arabia*
[c]*NTNU, Department of Engineering Design and Materials, Richard Birkelands vei 2b, Trondheim, 7491, Norway*

Abstract:
In the present paper, the theory of generalized photo-thermoelasticity under fractional order derivative was used to study the coupled of thermal, plasma, and elastic waves on unbounded semiconductor medium with a cylindrical hole during the photo-thermoelastic process. The bounding surface of the cavity was traction free and loaded thermally by exponentially decaying pulse boundary heat flux. The medium was considered to be a semiconductor medium homogeneous, and isotropic. In addition, the elastic and thermal properties were considered without neglecting the coupling between the waves due to thermal, plasma and elastic conditions. Laplace transform techniques were used to obtain the exact solution of the problem in the transformed domain by the eigenvalue approach and the inversion of Laplace transforms were carried out numerically. The results were displayed graphically to estimate the effect of the thermal relaxation time and the fractional order parameters on the plasma, thermal and elastic waves.
Engineering Solid Mechanics (2018) 6(3):275-284

A Green-Naghdi Model in a 2D Problem of a Mode I Crack in an Isotropic Thermoelastic Plate

I. A. Abbas [a,b,*] and F. S. Alzahrani [b]
[a]Department of Mathematics, Faculty of Science, Sohag University, Sohag, 82524, Egypt
[b]Nonlinear Analysis and Applied Mathematics Research Group, Department of Mathematics, King Abdulaziz University, Jeddah, 21589, Saudi Arabia

Abstract:
In this article, the generalized thermoelastic theory under Green and Naghdi models are used to study the thermoelastic interaction in an isotropic material containing a finite crack inside the material. The crack boundary is due to a prescribed temperature and stress distribution. Based on the Green-Naghdi type II and type III models, the formulation is applied to generalized thermoelasticity with an appropriate choice of parameters. Numerical solutions of the displacement components, temperature, and stress components are obtained using the finite element method. The results have been verified numerically and are represented graphically. Comparisons were made with expected results from Green and Naghdi model of type III and Green and Naghdi model of type II.

Physical Mesomechanics (2018) 21(2): 99-103

Analytical Solutions of Plasma and Thermoelastic Waves Photogenerated by a Focused Laser Beam in a Semiconductor Material

I. A. Abbas[a,b,*], K. A. Aly [c] and A. Dahshan [d]
[a]Department of Mathematics, Faculty of Science, Sohag University, Sohag, Egypt
[b]Nonlinear Analysis and Applied Mathematics Research Group (NAAM), Department of Mathematics, King Abdulaziz University, Jeddah, Saudi Arabia
[c]Department of Physics, Faculty of Science and Arts - Khulais, University of Jeddah, Jeddah, Saudi Arabia
[c]Department of Physics, Faculty of Science, Al-Azhar University, Assuit Branch, Assuit, Egypt
[d]The Research Center for Advanced Materials Science (RCAMS), King Khalid University, Abha, 61413, SA
[d]Department of Physics, Faculty of Science, Port Said University, Port Said, Egypt

Abstract:
In the present work, the coupled plasma theory (thermally and elasticity waves) was used to study the wave propagation of semiconducting sample through photothermal process. The coupled of the plasma, thermally, and elastic waves that photo-generated through intensity modulated laser beam and tightly focused has been considered to study an elastic homogeneous semiconducting medium with isotropic thermo-elastic properties. Laplace transformations were used to investigate analytically solutions in the transformed domain based on the approach of eigenvalue. Numerically calculations were carried out for silicon semiconductor sample. The results were graphical observed to show the influence the coupled wave of plasma, thermal, and elastic.

Silicon (2018) 10(6): 2609-2616

A Study on Fractional Order Theory in Thermoelastic Half-Space under Thermal Loading

I. A. Abbas
Department of Mathematics, Faculty of Science, Sohag University, Sohag, 82524, Egypt
Nonlinear Analysis and Applied Mathematics Research Group, Department of Mathematics, King Abdulaziz University, Jeddah, 21589, Saudi Arabia

Abstract:
In this study, the effect of fractional order derivative on a two-dimensional problem due to thermal shock with weak, normal and strong conductivity is established. The governing equations are taken in the context of Green and Naghdi of type III model (GNIII model) under fractional order derivative. Based on the Laplace and exponential Fourier transformations with eigenvalues approach, the analytical solutions has been obtained. For weak, normal and strong conductivity, the numerical computations for copper-like medium have been done and the results are shown numerically. The graphical results indicate that the effect of fractional order parameter has a major role on all physical quantities involved in the problem.
Physical Mesomechanics (2018) 21(2): 150-156

Free vibrations of nanoscale beam under two-temperature green and Naghdi model

I. A. Abbas
Department of Mathematics, Faculty of Science, Sohag University, Sohag, 82524, Egypt
Nonlinear Analysis and Applied Mathematics Research Group, Department of Mathematics, King Abdulaziz University, Jeddah, 21589, Saudi Arabia

Abstract:
The influence of the coupling between strain rate and temperature becomes domineering in the nanoscale beam. In this work, the free vibration of nanoscale beam resonators is analysed using Green and Naghdis theorem under the two-temperature model (2TGNIII). The influence of two-temperature parameters in a nanoscale beam is studied for beams under simply supported conditions. Exact expressions for frequency shift and the thermoelastic damping have been derived in the resonator, and calculation outcomes have been presented graphically with respect to frequency shift, natural frequency, and thermoelastic damping. The scale of length and thickness for a nanobeam equal to 15 × 10-9 m and equal to 1.3 × 10-12 s for time.
International Journal of Acoustics and Vibrations (2018) 23(3): 289-293

Some Properties of Special Magnetic Curves

H. S. Abdel-Aziz[a], M. K. Saad[a,b] and H. A. Ali[a,*]
[a]*Department of Mathematics, Faculty of Science, Sohag University, 82524 Sohag, Egypt*
[a,b]*Department of Mathematics, Faculty of Science, Islamic University of Madinah, 170 Madinah, KSA*

Abstract:
In the theory of curves, a magnetic field generates a magnetic flow whose trajectories are curves called magnetic curves. This paper aims at studying some properties for these curves which corresponding to the Killing magnetic fields in the 3-dimensional Euclidean space. We investigate the trajectories of the magnetic fields called T-magnetic and e-magnetic curves, also we give some characterizations of these curves. In addition, we determine all magnetic curves for new spherical images of a spherical curve and finally, we defray some examples to confirm our main results.

International Journal of Analysis and Applications (2018) 16(2) 177-192

Estimation of R = P(Y < X) using k-Upper Record Values from Kumaraswamy Distribution

N. A. Abou-Elheggag[a], A. A. Farghal[a,*] and H. A. Ramadan[b]
[a]*Mathematics Department, Faculty of science, Sohag University, Sohag 82524, Egypt*
[b]*Mathematics Department, Faculty of science, South Valley university, Qena, Egypt*

Abstract:
The problem of estimating the stress-strength R = P(Y < X) when X and Y are two independent ordinary samples was considered by many authors. In this paper, the problem of estimation of R = P(Y < X) when X and Y are two independent k-upper record values from the Kumaraswamy distribution is considered. Maximum likelihood (ML) and Bayes techniques are used for this purpose. The maximum likelihood estimator is used to construct both an exact confidence interval and percentile bootstrap confidence interval of the stress-strength. Bayes estimators have been developed under both symmetric (squared error) and asymmetric (LINEX) loss functions. Monte Carlo simulations are performed to compare the performances of the different methods.

J. Stat. Appl. Pro. 7, No. 2, 1-11 (2018)

Properties of Two Two-level Atoms Interacting with Intensity-Dependent Coupling

H. Bakry[1], A. S. A. Mohamed[2,3] and N. Zidan[1,*]
[1]*Mathematics Department, Faculty of Science, Sohag University, Sohag, Egypt*
[2]*Engineering Math and Physics Department, Faculty of Engineering, Cairo University, Giza, Egypt*
[3]*Zewail City of Science and Technology, University of Science and Technology, Giza, Egypt*

Abstract:
We discuss some new features of the model of two two-level atoms interacting with two single-mode thermal cavity field via multi-photon transitions under intensitydependent coupling. We examine the dynamics of quantum and classical correlations of the system initially exists in Werner states. The results show that the sudden death and sudden birth of quantum entanglement occur but the geometric measure of quantum discord remains non-zero. It is observed that, by increasing the number of photons, the periods become shorter and the quantum discord and entanglement become irregular.

Int J Theor Phys (2018) 57:539–548

Quantum Fisher information of two sup erconducting charge qubits under dephasing noisy channel

H. Abdel-Hameed[1,2], N. Zidan[1,3,*] and N. Metwally[4,5]
[1]*Mathematics Department, Faculty of Science, Sohag University, Sohag, Egypt*
[2]*Mathematics Department, Faculty of Science and Education, Al-Khurma Branch, Al-Taif University, SA*
[3]*Mathematics Department, College of Science, Jouf University, Saudi Arabia*
[4]*Department of Mathematics, College of Science, Bahrain University, Bahrain*
[5]*Department of Mathematics, Faculty of Science, Aswan University, Aswan, Egypt*

Abstract:
The Quantum Fisher information (QFI) of a two charged qubits system that interacts locally with a dephasing channel is quantified with respect to the charged qubits' and the channel's parameters. The behavior of Fisher information displays different phenomena as; the sudden changes (increasing/decreasing); the gradual decay and freezing of the QFI. It is shown that the QFI of the dephasing parameter decays gradually and vanishes completely as one increases the initial energies of the qubits and their mutual energy. The possibility of estimating the charged qubits' energies may be maximized at smaller values of the initial dephasing's parameter. The estimation degree of the mutual information reaches its upper bounds by increasing the initial energies. It is depicted that, by controlling the qubits' and the channel's parameters, the QFI may be frozen. We expect that this result may be interesting in the context of quantum encoding and quantum cryptography.

International Journal of Modern Physics B (2018) 32: 1850245

Dynamics of Classical and Quantum Information on Spin-chains with Multiple Interactions

A. Redwan[1], A. Abdel-Aty[2,3], N. Zidan[4,5,*] and T. El-Shahat[1]
[1]*Mathematics Department, Faculty of Science, Al-Azhar University, 71524 Assiut, Egypt*
[2]*Physics Department, College of Sciences, University of Bisha, Bisha, Saudi Arabia*
[3]*Physics Department, Faculty of Science, Al-Azhar University, 71524 Assiut, Egypt*
[4]*Mathematics Department, Faculty of Science, Sohag University, 82424 Soahg, Egypt*
[5]*Department of Mathematics, College of Science, Jouf University, Sakaka, Saudi Arabia*

Abstract:
The The classical and quantum information is very senstive to any internal and external noise. In this paper we invistigated the effcet of the Calogero-Moser (CM) type interaction, Dzyaloshinskii-Moriya (DM) interaction, thermalization and uniform and nonuniform magnetic fields on the dynamics of both classical and quantum information. The spin-chain model is used to describe the system in the thermal state. The egenerated correlation is quantified by the Shannon entropy for the classical information and the Von Neuman entropy for the quantum one. The obtained results showed that the quantum information is more influenced by the distance between the spins.
Inf. Sci. Lett. 7, No. 2, 29-33 (2018)

Dynamical properties and complex anti synchronization with applications to secure communications for a novel chaotic complex nonlinear model

E. E. Mahmoud[a,b,*] and S. M. Abo-Dahab[a,c]
[a]*Department of Mathematics, Faculty of Science, Taif University, Taif 888, Saudi Arabia*
[b]*Department of Mathematics, Faculty of Science, Sohag University, Sohag 82524, Egypt*
[c]*Department of Mathematics, Faculty of Science, South Valley University, Qena 83523, Egypt*

Abstract:
In this work, we present another chaotic (or hyperchaotic) complex nonlinear framework. This chaotic (or hyperchaotic) complex framework can be considered as a speculation of ”Guan” framework [1]. The new framework is a 5-dimensional nonstop real independent chaotic (or hyperchaotic) framework. The fundamental properties and elements of our framework are examined. Once with the all parameters are real and the other with one of these parameters is a complex parameter. When we examine the dynamics of the new framework and the parameters in real form, the conduct of the new framework is chaotic. While when one of these parameters is complex, our new framework is hyperchaotic. On the premise of Lyapunov capacity and dynamic control method, a scheme is designed to accomplish the complex anti-synchronization of two identical chaotic (or hyperchaotic) attractors of these frameworks. The effectiveness of the acquired outcomes will be delineated by a simulation case. Numerical outcomes are schemed to indicate state variables and errors of these chaotic attractors after synchronization to show that synchronization is accomplished. The above outcomes will give hypothetical establishment to the secure communication applications in light of the proposed scheme. In this secure communication scheme, synchronization between transmitter and receiver is accomplished and message signals will be recuperated. The encryption and rebuilding of the signals will be simulated numerically.
Chaos, Solitons and Fractals 106 (2018) 273–284

High dimensional, four positive Lyapunov exponents and attractors with four scroll during a new hyperchaotic complex nonlinear model

E. E. Mahmoud[1,2,*], K. M. Abualnaja[3] and O. A. Althagafi[4]
[1]*Department of Mathematics, Faculty of Science, Sohag University, Sohag 82524, Egypt*
[2]*Department of Mathematics, Faculty of Science, Taif University, Taif 888, Saudi Arabia*
[3]*Department of Mathematics, Umm Al-Qura University, P.O. Box 14949, Makkah, SA*
[4]*Department of Mathematics, College of Turabah, Taif University, Turabah 21478, SA*

Abstract:
New hyperchaotic nonlinear model inclusive complex variables have been introduced in this paper. This model has attributes that differentiate it from several of the models contemplated as of late in literature, for example, (i) this model is a high-dimension (9D), (ii) the new model has hyperchaotic conduct with four positive Lyapunov exponents, (iii) the attractors of our model has four scroll. Features and characteristics of this model containing Hamiltonian, invariance, dissipation, equilibria and their stability, Lyapunov exponents, Lyapunov dimension, bifurcation diagrams and chaotic (hyperchaotic) accomplishment are studied. On the confirmation of stability theory and active control technique, an approach is made to play out the complete and phase synchronizations of two identical hyperchaotic attractors of our model. The efficiency of the gained outcomes is revealed by a simulation illustration. The phase synchronization outcomes were utilized to build up a straightforward application in secure communication. Numerical effects computed to show the hyperchaotic synchronizations of a hyperchaotic model and to test the control powers scientific expressions gravity

AIP Advances. (2018), 8: 065018

On phase and anti-phase combination synchronization of time delay nonlinear systems

G. M. Mahmoud[1], A. A. Arafa[2] and E. E. Mahmoud[2,3,*]
[1]*Department of Mathematics, Faculty of Science, Assiut University, Assiut 71516, Egypt*
[1]*Department of Mathematics, Faculty of Science, Sohag University, Sohag 82524, Egypt*
[2]*Department of Mathematics, Faculty of Science, Taif University, Taif 888, Saudi Arabia*

Abstract:
Extensive studies have been done on the phenomenon of phase and anti-phase ynchronization between one drive and one response systems. As well as, combination synchronization for chaotic and hyperchaotic systems without delay also has been investigated. Thus, this paper aims to introduce the concept of phase and anti-phase combination synchronization (PCS and APCS) between two drive and one response time delay systems which are not studied in the literature as far as we know. The analysis of PCS and APCS are carried out using active control technique. An example is given to test the validity of the expressions of control forces to achieve the PCS and APCS of time delay systems. This example is between three different systems. When there is no control, the PCS does not occur where the phase difference is unbounded. The bounded phase difference appears when the control is applied which means that PCS is achieved. The special case which is the combination synchronization is studied as well

Journal of Computational and Nonlinear Dynamics. Vol. 13 (2018), 111001-1

Synchronization of time delay systems with non-diagonal complex scaling functions

G. M. Mahmoud[1], E. E. Mahmoud[2,3,*], A. A. Arafa[3]
[1]*Department of Mathematics, Faculty of Science, Assiut University, Assiut 71516, Egypt*
[2]*Department of Mathematics, Faculty of Science, Sohag University, Sohag, 82524, Egypt*
[3]*Department of Mathematics, Faculty of Science, Taif University, Kingdom of Saudi Arabia*

Abstract:
This paper deals with a kind of synchronization of dynamical systems with complex variables which is called generalized complex modified hybrid function projective synchronization (GCMHFPS) of time delay complex chaotic (hyperchaotic) systems. In other words, that the time delay complex systems can be synchronized up to a complex function transformation matrix. Moreover, the elements of the transformation matrix are complex functions of the states of drive system and time, where this matrix is not square. The idea of an active control method based on complex Krasovskii–Lyapunov functional is used to achieve GCMHFPS of time delay complex systems. Furthermore, based on the non-diagonal complex function transformation matrix, the modules and phases errors between one state of the complex response system and more than one of the states of the drive system are studied which have not been discussed before as far as we know. The analytical expression regarding the stability of this technique is derived and excellent agreement is found upon comparison with numerical calculations. In particular, we show through studying the time evolution of error, modulus and phase that the proposed scheme is effective for controlling time delay complex systems.
Chaos, Solitons and Fractals 111 (2018) 86-95

Problem of Longitudinal and Secondary Vertically Waves Reflection and Transmission during Two Media in the Context of Three Magneto-thermoelastic Theories with Varies Fields

S. M. Abo-Dahab[1,2], Emad E. Mahmoud[3,4,*]
[1]*Department of Mathematics, Faculty of Science, Taif University, Taif 888, Saudi Arabia* [2]*Department of Mathematics, Faculty of Science, SVU, Qena 83523, Egypt.*
[3]*Department of Mathematics, Faculty of Science, Taif University, Taif 888, Saudi Arabia.*
[4]*Department of Mathematics, Faculty of Science, Sohag University, Sohag 82524, Egypt.*

Abstract:
The aim of this paper is study the problem of longitudinal wave (p-wave) and secondary vertically (SV-wave) reflection and transmission during two media in the context of three magneto-thermoelastic theories with varies fields effects as magnetic field and initial stress.We deal the problem of reflection and transmission of thermoelastic waves at interface between two different media in the presence of initial stress and magnetic field, in the context of CT (Classical theory), GL (Green-Lindsay) and DPL (Dual Phase Lag). The boundary conditions applied at the interface as continuity of the displacement, neglecting the tangential displacement, continuity of normal force per unit initial area, neglecting the tangential stress and continuity of the temperature. The amplitudes ratios for the incident p- and SV- waves and so the refracted are obtained. The reflection and transmission coefficients ratios for the incident waves are computed numerically and the results are represented graphically to show the physical meaning of the phenomena.
Appl. Math. Inf. Sci. Vol. 12 (2018) 955-966.

Stratified modeling in soft fuzzy topological structures

S. E. Abbas[a], E. El-sanowsy[b,*] and A. Atef[b]
[a]*EgyptDepartment of Mathematics, Faculty of Science, Jazan University, Jazan, Saudi Arabia*
[b]*Department of Mathematics, Faculty of Science, Sohag University, Sohâg 82524, Egypt*

Abstract:
In this paper, we introduce the concepts of stratified fuzzy soft topogenous, stratified fuzzy soft filter, stratified fuzzy soft quasi-proximity and stratified fuzzy soft grill. Also, we introduce the concept of fuzzy soft topogenous structures by combining fuzzy soft topogenous with fuzzy soft filter and we introduce the concept of fuzzy soft quasi-proximity by combining fuzzy soft quasi-proximity with fuzzy soft grill and give their properties. Furthermore, we establish the relationship among these fuzzy soft topological structures and their s tratifications.

Soft Computing (2018) 22: 1603-1613.

Connectedness in Fuzzy Soft T opological Spaces

S. E. Abbas[a], E. El-sanowsy[b,*] and A. Atef[b]
[a]*EgyptDepartment of Mathematics, Faculty of Science, Jazan University, Jazan, Saudi Arabia*
[b]*Department of Mathematics, Faculty of Science, Sohag University, Sohâg 82524, Egypt*

Abstract:
In this paper, we define the f uzzy soft operator φ constructed from a fuzzy soft grill GE and a fuzzy soft topological space (X,τ_E). Also, we introduce and study the notion of connectedness to fuzzy soft topological spaces with fuzzy soft grills. Furthermore, we extend the notion of α-connectedness related to a fuzzy soft operator α on the set X.

Bull Braz Math Soc, New Series (2018)

A Solution of Random Nonlinear Integral Equation Via Random Hybrid Iterative Scheme

R. A. Rashwan[a] and H. A. Hammad[b,*]
[a]*Department of Mathematics, Faculty of Science, Assuit University, Assuit 71516, Egypt*
[b]*Department of Mathematics, Faculty of Science, Sohag University, Sohag 82524, Egypt*

Abstract:
In this paper, we introduce random Jungck-Picard-Krasnoselskii hybrid iterative process which is a hybrid of random Jungck, Picard and krasnoselskii iterative processes. We prove under $\phi-$contractive condition, our random hybrid iterative scheme converges faster than all of random Jungck-Picard, Jungck-Mann, JungckKrasnoselskii and Jungck-Ishikawa iterative processes. Finally, we use it to find a solution of random nonlinear integral equation. Our results generalize and improve several known results in stochastic and deterministic cases

J. Fixed Point Theory, 2018, 2018:4

Common Random Fixed Point Theorems of Integral Type of Akram-Contraction Mappings in Random Cone Metric Spaces

R. A. Rashwan[a], D. Dhamodharan[b], H. A. Hammad[c,*] and R. Krishnakumar[d]
[a]*Department of Mathematics, Faculty of Science, Assuit University, Assuit 71516, Egypt*
[b]*Department of Mathematics, Jamal Mohamed College (Autonomous),Tiruchirapplli-620020, India*
[c]*Department of Mathematics, Faculty of Science, Sohag University, Sohag 82524, Egypt*
[d]*Department of Mathematics,Urumu Dhanalakshmi College, Tiruchirappalli-620019, India*

Abstract:
In this paper, we prove a unique common random fixed point theorems in the framework of random cone metric spaces for generalized M_J-contraction and generalized $M_{J\psi}$-contraction conditions. An example to justify our theorems is given. Our results extend some previous work related to random cone metric spaces from the current existing literature.

J. Fixed Point Theory, 2018, 2018:7

C- class function on fixed point theorems for contractive mappings of integral type in n − banach spaces

R. A. Rashwan[a], D. Dhamodharan[b], H. A. Hammad[c,*] and R. Krishnakumar[d]
[a]Department of Mathematics, Faculty of Science, Assuit University, Assuit 71516, Egypt
[b]Department of Mathematics, Jamal Mohamed College (Autonomous),Tiruchirapplli-620020, India
[c]Department of Mathematics, Faculty of Science, Sohag University, Sohag 82524, Egypt
[d]Department of Mathematics,Urumu Dhanalakshmi College, Tiruchirappalli-620019, India

Abstract:
In this paper, we present some common fixed point theorems for class of mappings satisfying contractive condition of integral type in n−Banach spaces via C-Class function. Our results are version of some known results.

Adv. Fixed Point Theory, 8 (2018), No. 4, 384-400

New SDN-Oriented Distributed Network Security System

F. Nife[a,b], Z. Kotulski[a] and O. Reyad[c,*]
[a]Faculty of Electronics and Information Technology, Warsaw University of Technology, Poland
[b]Faculty of Science, Al-Muthanna University, Iraq
[c]Computer Science Branch, Faculty of Science, Sohag University, Egypt

Abstract:
Software-Defined Network (SDN) is a network technology aimed to open new possibilities in network management and orchestration. This is important in future (especially mobile) networks, where virtualization of resources and network functions is the basic paradigm. SDN has been proposed to programmatically control networks, facilitating deployment of new applications and services, as well as tuning network policy and performance. It represents an important change in the way networks are architected, built, and managed. In this new networking paradigm, a network control plane is physically decoupled from a forwarding plane and is directly programmable. In SDN networks, the control plane supports a logically centralized controller which has a global view of the entire network; it gathers information from the data plane to be processed by the management tasks which are implemented as applications running on the top of the controller. Based on the global view, these applications make packets processing decisions and distribute them to the data plane via the controller. However, security of such networks with their programmability and centralized points of control is not currently ensured on a sufficient level. In this paper, we present the concept of a new security system for SDN-based networks, which can be easily integrated with the existing network infrastructure as well as can provide security of all network components. It consists of two main subsystems: the network authentication and access control system to protect the network control and the distributed firewall system to protect data transmission. Such a system enables creating additional boundaries within the network to provide a multi-plane system of defense, solves the problem of a single point of failure, and makes it easy to protect the network from external attacks as well as from internal malicious users.

Appl. Math. Inf. Sci. 12, No. 4, 673-683 (2018)

Multi-filter Score-Level Fusion for Fingerprint Verification

M. A. O. Ahmed[a], O. Reyad[b,*], Y. AbdelSatar[c] and N. F. Omran[c]
[a]*Department of Electrical and Electronic Engineering, University of Cagliari, Piazza D'Armi, 09123 Cagliari, Italy*
[b]*Computer Science Branch, Faculty of Science, Sohag University, Egypt*
[c]*South Valley University, Qena, Egypt*

Abstract:
Biometric systems are widely used in various applications of today's authentication technology. The unimodal systems suffer from various stumbling blocks such as noisy inputs, non-universality, intra-class variability and imposter spoofing which affects the system performance and accuracy. To effectively handle these problems, two or more individual modalities are used. In this paper, we presented a multimodal approach for fingerprint verification based on a combination of score level fusion rules. In the preprocessing stage, Anisotropic Diffusion Filter (ADF) and Histogram Equalization (Hist-Eq) techniques were applied to overcome the main challenging drawbacks of fingerprint samples acquisition such as distortion, noise, rotation, etc. Supplementary, the Local Binary Pattern (LBP) was used for feature extraction. In score level fusion, the matching scores of individual fingerprints were combined via several fusion rules. Receiver Operating Characteristics (ROC) curves were formed for the multimodal approach that's why it is mainly used to evaluate our system. Experimental results shown improvements of the multimodal system using ADF and Hist-Eq versus the unimodal non-preprocessed fingerprint samples. The obtained results indicated that there is a significant increase in the performance of the proposed system due to the combination of scores, making it suitable for more applications relevant to identity verification.
AMLTA 2018, AISC 723, pp. 624–633, 2018

A common fixed point theorem for a pair of self mappings satisfying a general contractive condition of exponential type

R. A. Rashwan[a] and H. A. Hammad[b,*]
[a]*Department of Mathematics, Faculty of Science, Assuit University, Assuit 71516, Egypt*
[b]*Department of Mathematics, Faculty of Science, Sohag University, Sohag 82524, Egypt*

Abstract
In this paper, we prove a common fixed point theorem for a pair of self mappings satisfying a general contractive condition of exponential type in complete metric spaces. Our results extend and improve the results of Sharma and Ojha.
JP Journal of Fixed Point Theory and Applications

Text Message Encoding Based on Elliptic Curve Cryptography and a Mapping Methodology

Omar Reyad
Computer Science Branch, Faculty of Science, Sohag University, Egypt

Abstract:
Elliptic Curve Cryptography (ECC) is a public-key cryptosystem which can be used for message encryption, key agreement protocols and digital signature applications. ECC offers high level of security with smaller key sizes makes it ideal for applications which run on small devices that have power and memory constraints such as smart cards and cell phones. Encoding (converting a plaintext message to a point) and Decoding (converting a point to a plaintext message) are important functions in encryption and decryption schemes using ECC before transmission over public networks and unsecured channels. In this paper, we proposed a text message encoding scheme which is based on computational operations on points that lie on a predefined elliptic curve (EC). For any ECC-based encryption scheme, the mapping methodology of a plaintext message onto a coordinate on an affine curve is a mandatory prerequisite. ASCII character codes are considered for the mapping method to convert a plaintext message into coordinates of the predefined EC-points. Discussing the mapping methodology, creating the mapping table and the converting process are given in detail along with their implementations.
Inf. Sci. Lett. 7, No. 1, 7-11 (2018)

On Special Curves According to Darboux Frame in the Three Dimensional Lorentz Space

H. S. Abdel-Aziz[a,*] and M. Khalifa Saad[a,b]
[a]*Department of Mathematics, Faculty of Science, Sohag University, Egypt*
[b]*Faculty of Science, Islamic University of Madinah, 170 El-Madinah, KSA*
hsabdelaziz2005@yahoo.com

Abstract:
In the light of great importance of curves and their frames in many different branches of science, especially differential geometry as well as geometric properties and the uses in various fields, we are interested here to study a special kind of curves called Smarandache curves in Lorentz 3-space. Then, we present some characterizations for these curves and calculate their Darboux invariants. Moreover, we classify TP, TU, PU and TPU-Smarandache curves of a spacelike curve according to the causal character of the vector, curve and surface used in the study. Besides, we give some of differential geometric properties and important relations between that curves. Finally, to demonstrate our theoretical results a computational example is given with graph.
Computers, Materials and Continua 54, (2018) 229-249.

Some Geometric Invariants of Pseudo-Spherical Evolutes in the Hyperbolic 3-Space

H. S. Abdel-Aziz[a,*], M. Khalifa Saad[a,b] and A. A. Abdel-Salam[a]
[a]Department of Mathematics, Faculty of Science, Sohag University, Egypt
[b]Faculty of Science, Islamic University of Madinah, 170 El-Madinah, KSA
hsabdelaziz2005@yahoo.com

Abstract:

In this paper, we study the pseudo-spherical evolutes of curves in three dimensional hyperbolic space. We use techniques from singularity theory to investigate the singularities of pseudo-spherical evolutes and establish some relationships between singularities of these curves and geometric invariants of curves under the action of the Lorentz group. Besides, we defray with illustration some computational examples in support our main results.

Computers, Materials and Continua 57, (2018) 389-415.

قسم الفيزياء
Physics Department

Physics

قسم الفيزياء
Physics Department

A Study of the Three-Body Force Effect on the EOS Properties of Asymmetric Nuclear Matter

Mansour H. M. M.*1, M. El-Zohry[2] and A. E. Elmeshneb[2]

1 Physics Department, Faculty of Science, Cairo University, Cairo 12613, Egypt

2 Physics Department, Faculty of Science, Sohag University, Sohag 82524, Egypt

Abstract

Three-body effects are studied for both asymmetric nuclear matter and pure neutron matter to calculate the nuclear Equation of State (EOS). The Brueckner-Hartree-Fock (BHF) approximation is used using CD BonnB and Argonne V18 potentials. A two-body density dependent Skyrme potential is added to reproduce the empirical saturation point. Good agreement is obtained in comparison with exact calculation including three-body forces.

Armenian Journal of Physics, 2018, 11, 1, 1-10

Tensor target spin asymmetries in coherent π^0-photoproduction on the deuteron including intermediate ηNN interaction within a three-body approach

E. M. Darwish[1,2,*], H. M. Abou-Elsebaa[1,2] and Kh. S. A. Hassaneen[2]

[1]Physics Department, Faculty of Science, Taibah University, Medinah 41477, Saudi Arabia

[2]Physics Department, Faculty of Science, Sohag University, Sohag 82524, Egypt

Abstract

Motivated by the recent measurements from the VEPP-3 electron storage ring, we investigate the tensor target polarization asymmetries T_{2M} (M=0,1,2) in the reaction γd $\rightarrow \pi^0 d$ with a particular interest in the effect of the intermediate ηNN three-body approach. This approach is based on realistic separable representations of the driving two-body interaction in the πN, ηN, and NN subsystems. It is shown that the influence of rescattering effects in the intermediate state on the tensor target spin asymmetries is sizable at extreme backward pion angles. At forward angles, the contribution from the pure impulse approximation is dominated and the spin asymmetries show very little influence of rescattering effects. The sensitivity of results to the elementary pion photoproduction operator and to the NN potential model adopted for the deuteron wave function is investigated, and considerable dependences are found. The predicted spin asymmetries are also compared with available experimental data, and a satisfactory agreement with the recent data from VEPP-3 is obtained at photon energies below 400 MeV. At higher energies, the calculated spin asymmetries slightly underestimate the data.

Proceedings of the 6th

International Saudi Meeting on "Frontiers of Physics" (SIMFP2018), 19 American Institute of Physics (AIP) Conference Proceedings, Book of Abstracts, page 66.

Cross Sections for the $\gamma d \rightarrow \pi NN$ Reaction Channels in the Photon Energy Range Between 300 and 500 MeV Including Final-State Interaction Effects

E. M. Darwish[1,2,*] and M. M. Almarashi[1]

[1]*Physics Department, Faculty of Science, Taibah University, Medinah 41477, Saudi Arabia*

[2]*Physics Department, Faculty of Science, Sohag University, Sohag 82524, Egypt*

Abstract

Cross sections for the incoherent pion photoproduction reaction on the deuteron including final-state interaction effects are studied in the photon energy region from 300 to 500 MeV. For the elementary pion photoproduction operator on the free nucleon, the unitary isobar MAID2007 model is used. The interactions in the final two-body subsystems are taken from separable representations of realistic potentials. Numerical results for the unpolarized differential and total cross sections as well as for the doubly polarized differential and total cross sections for parallel and antiparallel helicity states of photon and deuteron for the $\gamma d \rightarrow \pi^- pp$, $\gamma d \rightarrow \pi^+ nn$, and $\gamma d \rightarrow \pi^0 np$ channels are given. Effects of final-state interaction are investigated and their role in these cross sections are found to be significant, especially for π^0 production.

International Journal of New Horizons in Physics, Vol. 5, No. 2 (2018) 21-30

Explicit Solution for the Two-Body Scattering Problem a+b→c+d with High-Precision Interactions

E. M. Darwish[1,2,*] and E. M. Mahrous[1]

[1]*Physics Department, Faculty of Science, Taibah University, Medinah 41477, Saudi Arabia*

[2]*Physics Department, Faculty of Science, Sohag University, Sohag 82524, Egypt*

Abstract

Explicit solution is given for the two-body scattering problem a+b→c+d with realistic and high-precision interactions. Formal expressions for the general two-fold differential cross section and the two-body scattering matrix are developed. In addition, the two-body scattering equation with a realistic two-body interaction is solved. The scattering phase shifts are calculated and compared with the data points form SAID analysis.

International Journal of New Horizons in Physics, Vol. 5, No. 2 (2018) 13-20

Momentum Space Treatment of the Two-Body Problem A+B→C+D and Its Application to the πN Scattering with Realistic Interaction

E. M. Darwish[1,2,*] and E. M. Mahrous[1]

[1]Physics Department, Faculty of Science, Taibah University, Medinah 41477, Saudi Arabia

[2]Physics Department, Faculty of Science, Sohag University, Sohag 82524, Egypt

Abstract

Based on a recently developed formalism for the two-body scattering problem A+B→C+D successfully applied to the nucleon-nucleon (NN) scattering problem [Int. J. New Horz. Phys. 5, No. 2, 13-20 (2018)], an explicit momentum space solution for the pion-nucleon (pN) scattering equation is given. The partial wave T-matrix for πN scattering is calculated with a realistic and high precision πN interaction. In addition, the πN scattering phase shifts for the important πN partial waves are predicted. These phase shifts are also compared with the data points form the Virginia Polytechnic Institute (VPI) partial wave analysis and a good description below 500 MeV is obtained.

Quantum Physics Letters, Vol. 7, No. 2 (2018) 29-34

Coherent Photoproduction of π^0-Meson from the Deuteron Including Polarization Effects

E. M. Darwish[1,2,*]

[1]Physics Department, Faculty of Science, Sohag University, Sohag 82524, Egypt

[2]Physics Department, Faculty of Science, Taibah University, Medinah 41477, Saudi Arabia

[*]E-Mail: darwish@science.sohag.edu.eg

Abstract

Coherent photoproduction of π^0-meson from the deuteron is investigated within an approach which includes the reaction amplitudes of the impulse approximation, two-step process with intermediate πN- and ηN-rescattering, and the higher order terms in the multiple scattering series for the intermediate ηNN interaction. This approach is based on realistic separable representations of the driving two-body interaction in the πN, ηN, and NN subsystems. For the elementary γN → πN operator, the unitary isobar model MAID2007 is used which describes well the elementary reaction. The radial deuteron wave function in the initial and final states are taken from the realistic CD-Bonn potential. Results for unpolarized and polarized cross sections as well as for all possible polarization observables with polarized photons and/or oriented deuterons are predicted and compared with available data, and differences with other theoretical models are analyzed. The contribution of γd → π0d to the deuteron spin asymmetry is calculated and its contribution to the Gerasimov-Drell-Hearn (GDH) integral is explicitly evaluated by integration up to a photon lab-energy of 900 MeV. The helicity E-asymmetry is also estimated. This work is motivated by the measurements of the CLAS Collaboration at Jefferson laboratory, where a cusp-like structure in the energy dependence of the differential cross section has been observed near η-production threshold at extremely backward pion angles, and the measurements of the VEPP-3 electron storage ring, where very recent data for the tensor-deuteron spin asymmetries have been measured. The effect of intermediate ηNN three-body interaction is significant in certain spin asymmetries, specially at extreme backward pion angles. It turns out that the inclusion of a full ηNN three-body contribution is quite essential. At forward angles, the contribution from the pure impulse approximation is dominated. The sensitivity of the obtained results to the elementary γN → πN amplitude and the choice of the NN potential model governs the deuteron wave function is investigated and considerable dependences are found. Compared to the experimental data from CLAS Collaboration for differential cross section, from YerPhi Collaboration for the linear photon asymmetry, and from VEPP-3 electron storage ring for the tensor target asymmetries, sizeable discrepancies are found.

Quarterly Physics Review, Vol. 4, No. 2 (2018) 1-38

Tensor and Vector Analyzing Powers of Elastic Electron-Deuteron Scattering

E. M. Darwish[1,2,*], E. M. Mahrous[1], and F. A. Alhazmi[1]
[1]*Physics Department, Faculty of Science, Taibah University, Medinah 41477, Saudi Arabia*
[2]*Physics Department, Faculty of Science, Sohag University, Sohag 82524, Egypt*

Abstract
Motivated by the measurements from NIKHEF, JLab and MIT-Bates with polarized beams and polarized targets, we study tensor and vector analyzing powers in the elastic *e-d* scattering process. Dependence of the obtained results on the realistic *NN* potential model adopted for the deuteron wave function is investigated. We found that the predicted analyzing powers agree with one another and with the experimental data up to $Q^2 \backsimeq 0.5$ $(\mathrm{GeV/c})^2$. At higher-Q^2 region, we found that the results are slightly diverged. The vector analyzing power T_{10} is found to be much smaller than T_{11}. Therefore, in addition to the tensor analyzing power T_{20}, the vector analyzing power T_{11} can be used as an another tool for extracting the deuteron electromagnetic form factors.
AIP Conference Proceedings, Vol. 1976, No. 1 (2018) 020008

Polarization Observables in the Reaction γd→π⁰d Near η-Threshold

E. M. Darwish[1,2,*]and M. M. Almarashi[1]
[1]*Physics Department, Faculty of Science, Taibah University, Medinah 41477, Saudi Arabia*
[2]*Physics Department, Faculty of Science, Sohag University, Sohag 82524, Egypt*

Abstract
Polarization observables in the reaction $\gamma d \rightarrow \pi^0 d$ near η-threshold with inclusion of rescattering effects are investigated. This work is motivated by the recent measurements for the tensor target spin asymmetry T_{20} from the VEPP-3 electron storage ring at Novosibirsk. Numerical results for the spin asymmetries T_{2m} (m=0,1,2) for tensor polarized deuterons and unpolarized photons are presented. It is shown that the influence of rescattering effects on the tensor target spin asymmetries is sizable, specially at extreme backward direction. We also compare our results with the recent measurements from VEPP-3, and find good agreement with data.
AIP Conference Proceedings, Vol. 1976, No. 1 (2018) 020031

Coherent π^0-Photoproduction from the Deuteron Near Threshold

E. M. Darwish[1,2,*], E. M. Mahrous[1], and M. E. Alsehli[1]

[1]Physics Department, Faculty of Science, Taibah University, Medinah 41477, Saudi Arabia

[2]Physics Department, Faculty of Science, Sohag University, Sohag 82524, Egypt

Abstract

Coherent photoproduction of π^0-meson from the deuteron near π^0-production threshold is investigated with special emphasize on single polarization observables. We report numerical results for the linear photon asymmetry Σ and tensor deuteron spin asymmetries $T_{2M}(M=0,1,2)$. The sensitivity of obtained results to the *D*-state contribution in the deuteron wave function of realistic *NN* potentials is studied. It is shown that the influence of *D*-state contribution on the predicted spin observables is sizable, and it provides important constraints for the extraction of the elementary neutron amplitude. Compared with the experimental data from TAPS collaboration for differential cross section, we obtain a satisfactory agreement.

AIP Conference Proceedings, Vol. 1976, No. 1 (2018) 020035

Effect of the carrier gas on morphological, optical and electrical properties of SnO_2 nanostructures prepared by vapor transport

N. M. A. Hadia, M. F. Hasaneen, Mohamed Asran Hassan and S. H. Mohamed

Abstract

The aim of the study was to explore the effects of carrier gas on the properties of SnO_2 nanostructures grown by vapor transport method for possible optoelectronic applications. Nanostructures of SnO_2 were synthesized via vapor transport method using Ar plus O_2 and N_2 plus O_2 gas mixtures. It was found that the carrier gas (Ar or N_2) has great influences on the properties of the resulting SnO2 nanostructures. Tetragonal single phase SnO_2 with nanowires (NWs) morphologies was obtained for Ar/O_2. The diameters of the NWs ranged from 10 to 162 nm and the lengths exceed 5 μm. While tetragonal single phase SnO2 with nanoparticles morphologies (diameters of 42–173 nm) was obtained for N_2/O_2. The calculated optical band gap values were 3.81 and 2.95 eV for samples prepared with Ar/O_2 and N_2/O_2, respectively. The conduction mechanism in the samples was found to be thermally activated. Single activation energy of 0.49 eV was evaluated for the sample prepared in Ar/O_2, while two activation energies (E_{AL} = 1.48 eV and E_{Ah} = 0.83 eV) were obtained for the sample prepared with N_2/O_2. The photoluminescence emission (intensity and shape) depended on the carrier gas. The observed emission peaks were assigned to the oxygen vacancies and the oxygen related defects. The obtained results may find applications in optoelectronics such as light emitting diodes.

Journal of Materials Science: Materials in Electronics (2018) 29:4155–4162

Examination of the kinetic reaction mechanisms of amorphous $As_{50}Se_{50}$ chalcogenide glass

Mansour Mohamed, A. Y. Abdel-Latief, M. A. Abdel-Rahim, N. M. A. Hadia, E. R. Shaaban and Mohamed N. Abd-el Salam

Abstract

The kinetic reactions mechanism of amorphous to crystalline transformation in the chalcogenide glasses of $As_{50}Se_{50}$ composition was investigated using differential scanning calorimetry (DSC) data measured under non-isothermal conditions at different heating rates (β = 5, 10, 20, 30 and 40 k min^{-1}). The DSC data were analyzed using the integral $g(\chi)$ and differential $f(\chi)$ forms which describes the solid-state reactions mechanism utilizing the Ozawa approach. The crystallization activation energy of $E_c(\chi)$ was determined using the iso-conversional methods proposed by Friedman, Flynn–Wall–Ozawa and Kissinger–Akahira–Sunose. The results revealed a slight increase of $E_c(\chi)$ with the conversion (χ). The results of $g(\chi)$, $f(\chi)$ and combination $g(\chi)f(\chi)$ master plots showed that the $As_{50}Se_{50}$ chalcogenide glasses is a combination of two- and three dimensional crystal growth

Applied Physics A (2018) 124:562

Controlled synthesis, morphological, optical and electrical properties of copper-doped zinc oxysulfide nanostructures

Mohammed S. Alqahtani, N. M. A. Hadia and S. H. Mohamed

Abstract

Zinc oxysulfide nanostructures may have physical and chemical properties that are different from ZnS or ZnO. Therefore, Cu-doped oxysulfide nanostructures were prepared by vapor transport and their properties were characterized by various techniques. EDAX analysis confirmed the presence of Zn, S, O and Cu in the samples. XRD revealed the formation of mixed phases of hexagonal ZnS, orthorhombic $ZnSO_4$, and hexagonal ZnO that is dependent on Cu content. The undoped sample has nanowire morphology. The increase in Cu doping changed the morphology form NWs to a mixture of NWs and nanoparticles (NPs), and then to NPs. The undoped oxysulfide sample has band gap of 4.08 eV, and the band gap decreased to 3.57 eV at 5% Cu doping. The PL intensity was enhanced upon Cu doping with 5 and 10 at% Cu while it weakened at higher Cu contents. The electrical resistivity decreased with Cu content and a thermally activated semiconducting behavior was reported for all samples.

Applied Physics A (2018) 124:617

Effect of oxidation time on structural, optical and electrical properties of mixed copper oxides nanocrystallites

Mohammed S. Alqahtani, N. M. A. Hadia and S. H. Mohamed

Abstract

Mixed nanocrystalline copper oxides were prepared from pre-sputtered copper films at 500 °C for various oxidation times. Mixed orthorhombic Cu64O and monoclinic CuO phases with CuO phase ration varied from 57.8 to 90.8% were obtained upon varying the oxidation time from 1 to 3 h. SEM observations revealed the nanocrystallites morphologies for the oxidized films. The film oxidized for 1 h have sizes in the range 39–69 nm and more coalescent nanocrystallites, with diameters in the ranges 45–157 nm and 47–251 nm, were observed for the films oxidized for 2 h and 3 h, respectively. The optical transmittance and reflectance as well as the optical constants were found to vary strongly with the variation of oxidation time. The optical band gap decreases from 2.58 to 2.49 eV with increasing oxidation time from 1 to 3 h. Semiconducting behavior and two distinct activation energies were reported for the films. The obtained results of the mixed copper oxides varied in a wide range which may find applications in optoelectronic devices.

Optik - International Journal for Light and Electron Optics,173 (2018) 101–109.

Towards understanding the morphological, magnetic, optical and electrical properties of MnO_2 nanowires for magneto-and optoelectronic applications

M. A. Awad and N. M. A. Hadia

Abstract

Mixed solutions of manganese sulfate and potassium permanganate were hydrothermally used to synthesis α-MnO_2 nanowires. Energy dispersive analysis of X-ray revealed the formation of stoichiometric MnO_2 and X-ray diffraction revealed the formation of single crystalline α-MnO_2. Examinations using both SEM and TEM yielded nanowires with diameters ranged from 40 to 50 nm and lengths ranged from 5 to 6 μm. The magnetic properties revealed that the α-MnO_2 NWs exhibit ferromagnetic/antiferromagnetic characteristics at liquid nitrogen and room temperatures. This kind of materials may be find usage in electromagnetic shielding applications. Direct optical band gap of 2.6 eV, that was blue shifted from the bulk value, was reported. Photoluminescence examinations displayed a strong emission peak around 395 nm and broad peak around 477 nm. The α-MnO_2 NWs showed a semiconducting behavior where the resistivity decreased with increasing temperature. Two activation energies were reported; the low temperature activation energy was 0.089 eV and the high temperature activation energy was 0.782 eV. Based on the observed high intensity UV emission peak, the obtained α-MnO_2 NWs may find applications in UV light emitting diodes.

Journal of Materials Science: Materials in Electronics (2018) 29:20695–20702.

Tribo-Mechanical and Electrochemical Properties of Carbonitrided 316 Austenitic Stainless Steel by rf Plasma for Biomedical Applications

F.M. El-Hossary, M. Raaif, A.M. Abd El-Rahman, M. Abo EL-Kassem

AISI 316 austenitic stainless steel was carbonitrided using rf plasma with purpose of using low-cost orthopedic implant materials in biomedical applications besides the manufacturing requests. The plasma treatment process was accomplished at low working gas pressure of 0.075 mbar in nitrogen-acetylene gaseous mixture. The plasma-processing time was fixed at 10 min while the plasma-processing power was varied from 450 to 650 watt. The effect of plasma treatment power on the structure, tribological, mechanical, electrochemical and biocompatibility of AISI 316 has been investigated. The structural results demonstrated the formation of nitrogen and carbon solid solutions, chromium nitride, iron carbide and iron nitride phases in the treated samples. The microhardness of the treated layer increases with increasing the processing power to reach a maximum value of approximately 1300 HV0.1 at 600 W which represents more than 6-folds increase in microhardness in comparison with the untreated matrix. The wear and corrosion resistance of the treated AISI 316 were enhanced compared to the untreated one. The friction coefficient was reduced from nearly 0.5 for the untreated substrate to nearly 0.3 for the carbonitrided sample. The surface energy and wettability of the carbonitrided samples were augmented as the plasma-processing power increased. Furthermore, the numbers of grown mesenchymal stem cells are higher for carbonitrided samples compared to the untreated one. The formation of nitrogen and carbon solid solution, chromium nitride, iron nitride and iron carbide hard phases after carbonitriding process is responsible for achieving good mechanical, tribological, biocompatibility and electrochemical properties for AISI 316 alloys.

Advances in Materials Physics and Chemistry, 2018, 8, 358-377

Optical and electrical performance of transparent conductive TiO2/Cu/TiO2 multilayers prepared by magnetron sputtering

M. A. Awad, M. Raaif

TiO_2/Cu/TiO_2 (TCT) multilayers were deposited by dc pulsed magnetron sputtering on glass substrates for the possible use as transparent conducting oxide (TCO). The thicknesses of copper (Cu_d) interlayers were 0, 8, 10, 12, 13 and 15 nm. The changes in structural, optical and electrical properties of the TCT multilayers were investigated as a function of Cu_d. XRD examination revealed that, all studied TCT multilayers have rutile TiO_2 crystalline structure with different orientations, whereas no peaks were indexed for the Cu. The refractive index (at 650 nm) of the TCT multilayers decreased from 2.39 to 1.90 and the optical band gap values decreased from 3.77 to 3.66 eV as the thickness of the Cu interlayer increased from 8 to 15 nm. It was found that the electrical resistivity of TCT multilayers decreased from 2.3×10^{-3} to 3.2×10^{-5} Ω cm with increasing Cu interlayer thickness from 8 to 15 nm. The TCT film with 10 nm Cu interlayer has a sheet resistance of 13.7 Ω/sq, an average transmittance value of 87.1% (in the wavelength ranging from 500 to 800 nm) and highest figure of merit value of 1.84×10^{-2} Ω^{-1}. Accordingly it can be considered as superlative TCT film which can be potentially used as transparent conductor electrode for solar cells and other optoelectronic applications.

J Mater Sci: Mater Electron (2018) 29:2815–2824

Effect of DC-pulsed magnetron sputtering power on structural, tribological and biocompatibility of Ti–Zr–N thin film

F. M. El-Hossary, A. M. Abd El-Rahman, M. Raaif, Shuxin Qu, Junsheng Zhao, Manfred F. Maitz, M. Abo EL-Kassem

The DC-pulsed magnetron sputtering was employed to deposit Ti–Zr–N thin film on AISI 316 substrates. All the plasma parameters were kept to be constant except the plasma-processing power which was varied from 125 to 250 W. The structure, tribological, electrochemical and biocompatibility properties of Ti–Zr–N films were investigated. X-ray patterns confirmed the formation of solid solution phase of Ti–Zr–N with different orientations. The results depicted that, the microhardness of Ti–Zr–N film increased with increasing the plasma-processing power to reach a maximum value of approximately 1050 HV0.015 at 200 W. Moreover, the tribological properties of AISI 316 coated with Ti–Zr–N were found to be superior compared with the uncoated sample. The wear rate of the coated sample at 225 W has a value of nearly 0.0034 mm^3/ Nm which is very low in comparison with AISI 316 substrate that has a value of 0.137 mm^3/ Nm. The biological properties of the examined samples were evaluated by investigating the proliferation of MC3T3-E1 osteoblast cells on the surface. The proliferation rate of the osteoblast cells was enhanced on Ti–Zr–N films prepared at low plasma power. It was demonstrated that the surface roughness and surface energy besides the surface chemical compositions affected the tribo-mechanical and biocompatibility features of Ti–Zr–N surfaces.

Applied Physics A (2018) 124:42

The disclosed transformation of pre-sputtered Ti films into nanoparticles via controlled thermal oxidation

M. A. Awad, M. Raaif

Nanoparticles of TiO_2 were successfully prepared from pre-sputtered Ti films using the controlled thermal oxidation. The effect of oxidation temperature on structural, morphological and optical properties in addition to photocatalysis activity of the sputtered films was tested and explained. Analysis of XRD and EDAX elucidated the enhancement in crystallization and oxygen content with the increase of oxidation temperature. SEM depicted the formation of very fine nanoparticles with no specific border on the films oxidized at 550 and 600 °C, whilst crystallites with larger size of approximately from 16 to 23 nm were observed for the film oxidized at 650 °C. Both optical transmission and refractive index were increased with increasing the oxidation temperature. A red shift in the absorption edge was obtained for the films oxidized at 650 °C compared to that oxidized at 600°C. The photocatalysis tests demonstrated the priority of 600 °C nanoparticle films to decompose methyl orange (MO) more than 650 °C treated film.

Applied Physics A (2018) 124:388

Constructing and Characterizing TiAlN Thin Film by DC. Pulsed Magnetron Sputtering at Different Nitrogen/Argon Gas Ratios

M. Raaif

In this survey, the magnetron sputtering with Dc. Pulsed mode was embroiled to deposit TiAlN thin film on AISI 316 as a substrate. All the plasma magnetron parameters were fixed excluding the nitrogen gas ratio which was varied from 10% to 50% with step interval of 10% with respect to argon. The structure, mechanical, tribological and electrochemical peculiarities of TiAlN films were studied. The TiAlN deposition rate is decreased in regard with increasing the nitrogen gas ratio where, the film thickness recorded a maximum value of 3 μm at nitrogen gas ratio of 10 %. X-ray configurations demonstrated the formation of solid solution phase of TiAlN with different orientations. The TiAlN coating has (111) preferred orientation at 10 and 20% nitrogen gas ratios while has (200) preferred orientation at 30-50% nitrogen gas ratios. The crystallite size was decreased with increasing the N_2 gas ratio. The results depicted that, the microhardness of TiAlN film was increased with decreasing the N_2 gas ratio and recorded a maximum value of approximately 850 HV0.015 at 10% N_2. Additionally, the tribological properties of the coated AISI 316 with TiAlN were enhanced compared with the uncoated sample. The wear volume loss of the coated sample at 10% N_2 has a value of nearly 9 $x10^4$ μm^3 which is low compared with the substrate that has a value of 4.5 $x10^6$ μm^3. The corrosion resistance of all TiAlN coatings was better than the uncoated sample. It was demonstrated; the change in nitrogen gas ratio regulated the physico-chemical features of the TiAlN coatings.

Journal of Advances in Physics 14(2018)5638-5652

Photonic crystal defective superconductor and black body radiations

Arafa H. Aly, Ayman A. Ameen, Hussein A. ElSayed, S. H. Mohamed

Abstract

In the present work, we have obtained a new design for sensing the black body radiation. In this work we designed one-dimensional photonic crystals incorporates that a high-temperature superconducting material as a defect layer. The numerical results are essentially obtained based on the fundamental characteristic matrix method. Also, the results show that the appearance of defect mode inside the photonic band gap. Moreover, the intensity of the defect mode could be tuned by the operating temperature as well as the black body temperature. The angle of incidence and the thickness of the superconductor are investigated. The present work could be potential use in many applications such as sensors for satellites thermal properties and spacecraft.

Optical and Quantum Electronics 50 (2018) 361.

Characterization of Cu_2O/CuO nanowire arrays synthesized be by thermal method at various temperatures

S. H. Mohamed[1] and Kh. M. Al-Mokhtar[2]

[1]Physics Department, Faculty of Science, Sohag University, 82524 Sohag, Egypt

[2]Department of Physics, Faculty of Science, Taibah University, Madinah, Saudi Arabia

Abstract

Cu_2O/CuO nanowires (NWs) were grown by thermal oxidation of copper sheet at various temperatures. The thickness and surface roughness of the oxide layers were measured using profilometer and it was found that they increase with increasing growth temperature. XRD patterns revealed the formation of mixed cubic Cu_2O and monoclinic CuO phases and the portion of the monoclinic CuO increased with growth temperature. SEM images revealed that the morphologies of all the samples have nanowires with diameters and lengths that depend on the growth temperature. A growth mechanism of these nanowires was proposed. The estimated optical band gap values for Cu_2O/CuO mixed NWs grown at 550, 600 and 650°C are 2.56, 2.40 and 2.27 eV, respectively. The Cu_2O/CuO NWs showed broad emission peaks in the range 335-480 nm, which can be a combination of several peaks. The room temperature resistivity values decreased with increasing growth temperature. The Cu_2O/CuO NWs have semiconducting behavior with two linear parts on Arrhenius plot for conductivity that gave two different activation energies.

Applied Physics A 124 (2018) 493.

Effect of oxidation time on structural, optical and electrical properties of mixed copper oxides nanocrystallites

Mohammed S. Alqahtani[1], N. M. A. Hadia[2,3], S. H. Mohamed[2,a]

[1]Department of physics and Astronomy, King Saud University, Riyadh 11451, Saudi Arabia

[2]Physics Department, Faculty of Science, Sohag University, 82524 Sohag, Egypt

[3]Department of physics, College of Science, Jouf University, Jouf, Saudi Arabia

Abstract

Mixed nanocrystalline copper oxides were prepared from pre-sputtered copper films at 500°C for various oxidation times. Mixed orthorhombic $Cu_{64}O$ and monoclinic CuO phases with CuO phase ration varied from 57.8 to 90.8% were obtained upon varying the oxidation time from 1 to 3 h. SEM observations revealed the nanocrystallites morphologies for the oxidized films. The film oxidized for 1 h have sizes in the range 39 - 69 nm and more coalescent nanocrystallites, with diameters in the ranges 45 – 157 nm and 47 – 251 nm, were observed for the films oxidized for 2 h and 3 h, respectively. The optical transmittance and reflectance as well as the optical constants were found to vary strongly with the variation of oxidation time. The optical band gap decreases from 2.58 to 2.49 eV with increasing oxidation time from 1 to 3 h. Semiconducting behavior and two distinct activation energies were reported for the films. The obtained results of the mixed copper oxides varied in a wide range which may find applications in optoelectronic devices.

Optik - International Journal for Light and Electron Optics 173 (2018) 101–109.

Controlled synthesis, morphological, optical and electrical properties of copper *doped* zinc *oxysulfide* nanostructures

Mohammed S. Alqahtani[1], N. M. A. Hadia[2,3], S. H. Mohamed[2,a]

[1]*Department of physics and Astronomy, King Saud University, Riyadh 11451, Saudi Arabia*

[2]*Physics Department, Faculty of Science, Sohag University, 82524 Sohag, Egypt*

[3]*Department of physics, College of Science, Jouf University, Jouf, Saudi Arabia*

Abstract

Zinc oxysulfide nanostructures may have physical and chemical properties that are different from ZnS or ZnO. Therefore, Cu doped oxysulfide nanostructurs were prepared by vapor transport and their properties were characterized by various techniques. EDAX analysis confirmed the presence of Zn, S, O and Cu in the samples. XRD revealed the formation of mixed phases of hexagonal ZnS, orthorhombic $ZnSO_4$, and hexagonal ZnO that is depend on Cu content. The undoped sample has nanowires morphology. The increase in Cu doping changed the morphology form NWs to a mixture of NWs and nanoparticles (NPs), and then to NPs. The undoped oxysulfide sample has band gap of 4.08 eV, and the band gap decreased to 3.57 eV at 5% Cu doping. The PL intensity was enhanced upon Cu doping with 5 and 10 at.% Cu while it weakened at higher Cu contents. The electrical resistivity decreased with Cu content and a thermally activated semiconducting behaviour was reported for all samples.

Applied Physics A 124 (2018) 617.

Effect of the carrier gas on morphological, optical and electrical properties of SnO_2 nanostructures prepared by vapor transport

N. M. A. Hadia, M. F. Hasaneen, Mohamed Asran Hassan, S. H. Mohamed

Abstract

The aim of the study was to explore the effects of carrier gas on the properties of SnO_2 nanostructures grown by vapor transport method for possible optoelectronic applications. Nanostructures of SnO_2 were synthesized via vapor transport method using Ar plus O_2 and N_2 plus O_2 gas mixtures. It was found that the carrier gas (Ar or N2) has great influences on the properties of the resulting SnO2 nanostructures. Tetragonal single phase SnO_2 with nanowires (NWs) morphologies was obtained for Ar/O2. The diameters of the NWs ranged from 10 to 162 nm and the lengths exceed 5 μm. While tetragonal single phase SnO_2 with nanoparticles morphologies (diameters of 42–173 nm) was obtained for N_2/O_2. The calculated optical band gap values were 3.81 and 2.95 eV for samples prepared with Ar/O_2 and N_2/O_2, respectively. The conduction mechanism in the samples was found to be thermally activated. Single activation energy of 0.49 eV was evaluated for the sample prepared in Ar/O_2, while two activation energies (E_{AL} = 1.48 eV and E_{Ah} = 0.83 eV) were obtained for the sample prepared with N_2/O_2. The photoluminescence emission (intensity and shape) depended on the carrier gas. The observed emission peaks were assigned to the oxygen vacancies and the oxygen related defects. The obtained results may find applications in optoelectronics such as light emitting diodes.

Journal of Materials Science: Materials in Electronics 29 (2018) 4155–4162

Influence of Temperature Gradient on Surface properties of Nitriding AISI 304 Stainless Steel

F. M. El-Hossary1, N. Z. Negm1, A. M. Abd El-Rahman1,2, A. A. Abd El-Moula, S.M. Khalil1,3,4*

[1]Physics Department, Faculty of Science, Sohag University, 82524-Sohag, Egypt

[2]Abdul-Aziz University, Jeddah, KSA.

[3]University College, Umm Al-Qura University, Alqunfadah, KSA.

[4]Umm Al-Qura University, Qunfadah Center for Scientific Research (QCSR), KSA

Abstract

AISI 304 austenitic substrates with different thicknesses were treated using rf plasma nitriding. This is to study the influence of the temperature gradient on the surface properties of the treated samples including nitrogen diffusivity and microstructure. X-ray diffraction, optical microscopy and scanning electron microscopy were used to characterize the treated samples. The results revealed that the surface temperature and temperature gradient of the nitrided substrate are substrate thickness dependent. It was found that the thickness of nitrided samples increases substantially as the temperature gradient increases from 1.93 x 10^5 to 10x10^{5o}C/m. The microstructure is characterized mainly by the nitride phases of nitrogen expanded austenite (γN) and chromium nitride (CrN). Furthermore, the iron nitride phase of Fe4N is detected at temperature gradient of 4.1x10^{5o}C/m and lower. A maximum value of the nitriding rate of 1.21 μm^2/s have been observed with the temperature gradient of 10x10^{5o}C/m.

Journal of Multidisciplinary Engineering Science and Technology (JMEST), 5 (10), 2018, 8671-8675

Electric, thermoelectric and magnetic characterization of γ-Fe2O3 and Co3O4 nanoparticles synthesized by facile thermal decomposition of metal-Schiff base complexes

E.M.M. Ibrahima,∗, Laila H. Abdel-Rahmanb, Ahmed M. Abu-Diefb, A. Elshafaiea,
Samar Kamel Hamdanb, A.M. Ahmeda

Using novel compounds for synthesis of metal oxide nanomaterials can tune their physical properties due to the associated variation in the shape, size and crystallinity. In this work, γ-Fe2O3 and Co3O4 nanoparticles were successfully prepared by a facile thermal decomposition route, employing [Fe(C32H22N4O2)]·2H2O and [Co(C16H11N3O4)].1 2H2O complexes, respectively as new precursors. The x-ray diffraction and high resolution transmission electron microscopy investigation confirmed that the materials consist of highly pure spinel γ-Fe2O3 and Co3O4 nanoparticles with average size of ∼9 and 30 nm, respectively. The electrical conduction is governed by the hopping mechanism. The thermoelectric power measurements confirmed that Co3O4 nanoparticles are non-degenerate semiconductor with Fermi energy ∼1.21 eV while γ-Fe2O3 nanoparticles showed a degenerate to non-degenerate transition. The Co3O4 nanoparticles showed a weak ferromagnetic ordering that could be attributed to uncompensated surface spins due to finite-size effects. But γ- Fe2O3 NPs show superparamagnetic behavior at room temperature.

Materials Research Bulletin, 99, (2018), 103-108

Magnetocaloric effect, electric, and dielectric properties of $Nd_{0.6}Sr_{0.4}Mn_xCo_{1}_xO_3$ composites

I.A. Abdel-Latif a,b,c, A.M. Ahmed d, H.F. Mohamed d, S.A. Saleh d, J.A. Paixão e, Kh.A. Ziq f, M.Kh. Hamad f, E.G. Al-Nahari f, M. Ghozza g, S. Allam h

a Physics Department, College of Sciences and Arts, Najran University, P.O. Box 1988, Najran 11001, Saudi Arabia

b Advanced Materials and Nano-Research Centre, Najran University, P.O. Box: 1988, Najran 11001, Saudi Arabia

c Reactor Physics Department, NRC, Atomic Energy Authority, Abou Zabaal, P.O. Box 13759, Cairo, Egypt

d Physics Department, Faculty of Science, Sohag University, Sohag 82524, Egypt

e CFisUC, Department of Physics, University of Coimbra, P-3004-516 Coimbra, Portugal

f Physics Department, College of Sciences, King Fahd University of Petroleum & Minerals, P.O. Box 5047, Dhahran 31261, Saudi Arabia

g Basic Science Department, High Institute of Engineering and Technology, El-Marg, Cairo, Egypt

h Physics Department, Faculty of Science, Cairo University, Giza, Egypt

The magnetocaloric effect (MCE) and electric-dielectric properties of the Nd-cobaltate perovskites Nd0.6Sr0.4Co1_xMnxO3 (x = 0, 0.3, 0.7 and 1) were investigated for possible use in magnetic cooling applications. Upon Mn substitution, the magnetic exchange interaction is affected by the (Mn4+/Mn3+) ratio, which in turn impacts several physical properties. The XRD patterns of the synthesized composites revealed a single phase with an orthorhombic structure with space group Pbnm (62). The orthorhombic lattice distortion increases linearly with the Mn content, reaching a maximum value (D = 7.377 _ 10_3) for Nd0.6Sr0.4MnO3. The temperature and frequency dependence of the dielectric permittivity was studied and analyzed using Maxwell-Wagner interfacial polarization and Koops phenomenological theory. The rapid increase in magnetic susceptibility around the paramagnetic (PM)–ferromagnetic (FM) transition temperature TC is greatly affected by Mn substitution. The decrease in susceptibility with increasing temperature can be attributed to a charge ordering effect. The PM-FM transition occurs in the temperature range of 150–200 K. Moreover, the presence of spontaneous magnetization with second-order phase transitions is observed from Arrott plot isotherms. The MCE was also investigated by determining DSM and the relative cooling power (RCP), and the maximum value is found for Nd0.6Sr0.4Co0.3 Mn0.7O3. These results compare favorably with those reported for similar materials, indicating our materials as a possible candidate for use in magnetocaloric refrigerators.

Journal of Magnetism and Magnetic Materials 457, ·February 2018

Thermopower and magnetocaloric properties in NdSrMnO/CrO_3 composites

A.M. Ahmed a, H.F. Mohamed a,⇑, J.A. Paixão b, Sara A. Mohamed a

a Physics Department, Faculty of Science, Sohag University, 82524 Sohag, Egypt

b CFisUC, Department of Physics, University of Coimbra, P-3004-516 Coimbra, Portugal

The thermoelectric power (TEP) and magnetocaloric effect (MCE) for (Nd0.6Sr0.4MnO3)1-x/(CrO3)x composites have been measured. The TEP measurements show a negative sign value of the Seebeck coefficient (S), in microvolts. TEP data construe in the low range of temperature by the magnon and phonon drag model, whereas at high temperature by small polaron conduction mechanism. Magnetic measurements exhibit that all composites show a paramagnetic–ferromagnetic transition with decreasing temperature. The Arrott plots of composites reveal the occurrence of a second order phase transition. The maximum value of magnetic entropy change (DS) is 2.37 J kg_1 K_1, achieved fore the composite with x = 0.015. Moreover, the maximum value of relative cooling power (RCP) is 122.1 J kg_1, achieved for the composite with x = 0.020. These composites may be appropriate for magnetic application near room temperature.

Journal of Magnetism and Magnetic Materials, 456, (2018), 217-222

The electric and thermoelectric properties of Cu(II)-Schiff base nano-complexes

E M M Ibrahim1, Laila H Abdel-Rahman2, Ahmed M Abu-Dief2, A Elshafaie1, Samar Kamel Hamdan2 and A M Ahmed1

1 Physics Department, Faculty of Science, Sohag University, Sohag, 82524, Egypt

2 Chemistry Department, Faculty of Science, Sohag University, Sohag, 82524, Egypt

Abstract

The physical properties, such as electric and optical properties, of metal-Schiff base complexes have been widely investigated. However, their thermoelectric (TE) properties remain unreported. This work presents Cu(II)-Schiff base complexes as promising materials for TE power generation. Therefore, three Cu(II)-Schiff base complexes (namely, [Cu(C32H22N4O2)].3 2H2O, [Cu(C23H17N4O7Br)], and [Cu(C27H22N4O8)].H2O) have been synthesized in nanosized scale. The electric and TE properties have been studied and comprehensive discussions have been presented to promote the nano-complexes (NCs) practical applications in the field of TE power generation. The electrical measurements confirm that the NCs are semiconductors and the electrical conduction process is governed by intermolecular and intramolecular transfer of the charge carriers. The TE measurements reveal that the Cu(II)-Schiff base NCs are nondegenerate P-type semiconductors. The measured Seebeck coefficient values were higher compared to the values reported in previous works for other organic materials indicating that the complexes under study are promising candidates for theremoelectric applications if the electrical conductivity could be enhanced.

Physica Scripta, 93 (5), 5801

Theoretical study of ZnS/CdS bi-layer for thin-film CdTe solar cell

H. A. Mohamed, A. S. Mohamed and H. M. Ali

Abstract

The performance of CdTe solar cells is strongly limited by the thickness of CdS window layer.A higher short-circuit current density might be achieved by decreasing the thickness of CdS layer as a result of reducing the absorption losses that take place in this layer. However, it is difficult to obtain uniform and pin-hole free CdS layers thinner than 50 nm. This problem can be solved through increasing the band gap of the window layer by adding a wide band gap semiconductor such as ZnS. In this work, bilayer ZnS/CdS film was studied as an improved window layer of ITO/ZnS/CdS/CdTe solar cell. The total thickness of ZnS/CdS layer was taken about 60 nm. The effect of optical losses due to reflection at different interfaces in the cell and absorption in ITO, ZnS, CdS as well as the recombination loss have been studied. Finally, the effects of the recombination losses in the space-charge region and the reflectivity from the back contact were taken into accounts. The results revealed that the optical losses of 23% were achieved at 60 nm thickness of CdS and theses losses minimized to 18% when ZnS layer of 30 nm thickness was added to CdS layer. The minimum optical and recombination losses of about 26% were obtained at 1 ns of electron life-time and∼0.4 μm width of the space-charge region. The maximum efficiency of 18.5% was achieved for ITO/CdS/CdTe cell and the efficiency increased up to 20% for ITO/ZnS/CdS/CdTe cell.

Materials Research Express, 5, (5), (2018), 056411.

Spectral functions of nuclear matter using self-consistent Green's function approach based on three-body force

Khaled S. A. Hassaneen

Abstract:
A self-consistent Green's Function approach is used to study the influence of short-range correlations beyond the mean-field approach of nuclear matter. The ladder equation, including both particle-particle and hole-hole propagation, is solved in nuclear matter for a realistic interaction derived from the CD-Bonn potential. The hole-hole interaction is used to calculate the spectral functions that describe the distribution of holes below Fermi level. The nucleon spectral functions are calculated from the momentum and energy-dependent self-energy. For comparison, the calculations are investigated by including nuclear three-body force. These spectral functions directly reflect the effects of the nucleon-nucleon correlations and can be explored by the analysis of nucleon knock-out experiments like (e, e′p).

THE EUROPEAN PHYSICAL JOURNAL PLUS (2018) 133: 484

Structural and optical properties of $CuIn_{1-x}Ga_xSe_2$ thin films

N.M.A HADIA, M.M. WAKKAD*, E.KH. SHOKR, Y. A. TAYA
Physics Department, Faculty of Science, Sohag University, Sohag, Egypt

Abstract
Bulk alloys of $CuIn_{1-x}Ga_xSe_2$ with Ga – incorporation ratio x= Ga / (Ga + In) equal to 0.1, 0.2, 0.3, 0.4 and 0.6 have been prepared by the melt quench technique. The $CuIn_{1-x}Ga_xSe_2$ (CIGS) thin films have been deposited on clean microscope glass substrates with different thickness (50, 100, 150, 200 and 250 nm) using the thermally evaporated technique in a vacuum of 3x10-4 mbar from the prepared bulk material. XRD, SEM and EDAX were utilized in order to examine the structure, surface morphology and composition stoichiometry of CIGS samples. Effects of Ga – ratio, film thickness and annealing at 573 K for different periods of time (5 – 60 min.) on structural and optical properties have been depicted and explained. Some important structural and optical parameters were calculated and discussed.

4th Confernece of young Researchers, Sohag 2018

The Electric and Thermoelectric Properties of Cu(II)-Schiff base Nano-complexes

E.M.M. Ibrahim[1*], Laila H. Abdel-Rahman[2], Ahmed M. Abu-Dief[2], A. Elshafaie[1], Samar Kamel Hamdan[2], A. M. Ahmed[1],

[1]Physics Department, Faculty of Science, Sohag University, Sohag 82524, Egypt

[2]Chemistry Department, Faculty of Science, Sohag University, Sohag 82524, Egypt

Abstract

The physical properties, such as electric and optical properties, of metal-Schiff base complexes have been widely investigated. However, their thermoelectric properties remain unreported. This work presents Cu(II)-Schiff base complexes as promising materials for thermoelectric power generation. Therefore, three Cu(II)-Schiff base complexes (namely, $[Cu(C_{32}H_{22}N_4O_2)].^3/_2H_2O$, $[Cu(C_{23}H_{17}N_4O_7Br)]$, and $[Cu(C_{27}H_{22}N_4O_8)].H_2O$) have been synthesized in nanosized scale. The electric and thermoelectric properties have been studied and comprehensive discussions have been presented to promote the nano-complexes practical applications in the field of thermoelectric power generation. The electrical measurements confirm that the nano-complexes are semiconductor and the electrical conduction process is governed by intermolecular and intramolecular transfer of the charge carriers. The thermoelectric measurements reveal that the Cu(II)-Schiff base nano-complexes are nondegenerate P-type semiconductors. The measured Seebeck coefficient values were higher compared to the values reported in previous works for other organic materials indicating that the complexes under study are promising candidate for theremoelectric applications if the electrical conductivity could be enhanced.

Physica Scripta 93 (2018) 055801 (8pp)

Electric, Thermoelectric and Magnetic Properties of Nickel(II) Imine Nanocomplexes

A. Elshafaie[1], Laila H. Abdel-Rahman[2], Ahmed M. Abu-Dief [2], Samar Kamel Hamdan[2], A. M. Ahmed[1], E.M.M. Ibrahim[1*]

[1]Physics Department, Faculty of Science, Sohag University, Sohag 82524, Egypt

[2]Chemistry Department, Faculty of Science, Sohag University, Sohag 82524, Egypt

Abstract

Production of novel organic semiconductor nanomaterials is essential for enabling the development of personal, portable, and flexible electronic modules. This work presents Ni(II)-Schiff base complexes with enhanced Seebek coefficient and weak ferromagnetic ordering for thermoelectric and magnetic devices. Four Ni(II)-Schiff base complexes (namely, $[Ni(C_{12}H_{10}N_3O_4Br)].2H_2O$, $[Ni(C_{16}H_{11}N_3O_4)].2H_2O$, $[Ni(C_{21}H_{14}N_5O_8Br)]$ and $[Ni(C_{25}H_{17}N_5O_8)].\frac{1}{2}H_2O$) have been synthesized in nanosized dimensions. The electrical and thermoelectric properties have been studied and comprehensive discussions have been presented to understand the electrical conduction mechanisms. The electrical conductivity measurements reveal that the conduction is due to the charge carriers hoping between the atomic sites of the same energy levels in the molecule as well as the transfer of the charge carriers between the neighboring complex molecules due to overlapping of their orbitals. The thermoelectric measurement confirms that the nanocomplexes are nondegenerate P-type semiconductors with enhanced Seebeck coefficient values compared to those reported for other organic materials. The nanocomplexes exhibit antiferromagnetic to paramagnetic transitions with the increase of temperature and weak ferromagnetic ordering at 300 K.

Nano, Vol. 13, No. 7 (2018) 1850074 (14 pages)

Electric, thermoelectric and magnetic characterization of g-Fe_2O_3 and Co_3O_4 nanoparticles synthesized by facile thermal decomposition of metal-Schiff base complexes

E.M.M. Ibrahim[1]*, Laila H. Abdel-Rahman[2], Ahmed M. Abu-Dief[2], A. Elshafaie[1], Samar Kamel Hamdan[2], A. M. Ahmed[1]

[1]Physics Department, Faculty of Science, Sohag University, Sohag 82524, Egypt

[2]Chemistry Department, Faculty of Science, Sohag University, Sohag 82524, Egypt

Abstract

Using novel compounds for synthesis of metal oxide nanomaterials can tune their physical properties due to the associated variation in the shape, size and crystallinity. In this work, g-Fe_2O_3 and Co_3O_4 nanoparticles were successfully prepared by a facile thermal decomposition route, employing $[Fe(C_{32}H_{22}N_4O_2)].2H_2O$ and $[Co(C_{16}H_{11}N_3O_4)].\frac{1}{2}H_2O$ complexes, respectively as new precursors. The x-ray diffraction and high resolution transmission electron microscopy investigation confirmed that the materials consist of highly pure spinel g-Fe_2O_3 and Co_3O_4 nanoparticles with average size of ~ 9 and 30 nm, respectively. The electrical conduction is governed by the hopping mechanism. The thermoelectric power measurements confirmed that Co_3O_4 nanoparticles are non-degenerate semiconductor with Fermi energy ~1.21 eV while g-Fe_2O_3 nanoparticles showed a degenerate to non-degenerate transition. The Co_3O_4 nanoparticles showed a weak ferromagnetic ordering that could be attributed to uncompensated surface spins due to finite-size effects. But g- Fe_2O_3 NPs show superparamagnetic behavior at room temperature.

Materials Research Bulletin 99 (2018) 103–108

Optical And Thermoelectric Properties Of Nanocrystalline $Bi_2(Se_{1-x}Te_x)_3$ Films

A. M. Adam[a,b,c], E. M. M. Ibrahim[b], L. V. Panina[c,d], and P. Petkov[a]

[a]Physics Department, University of Chemical Technology and Metallurgy, Sofia, Bulgaria;

[b]Physics Department, Faculty of Science, Sohag University, Sohag, Egypt; cDepartment of Engineering for Electronic Materials, National University of Science and Technology, MISiS, Moscow, Russia;

[d]Department of Design Methodology, Institute for Design Problems in Microelectronics RAS, Moscow, Russia

Abstract

Granular nanocrystalline $Bi_2(Se_{1-x}Te_x)_3$ films were prepared from highly crystalline bulk alloys used as source materials by means of thermal evaporation under vacuum (2×10^{-6} mbar). The nanofilms were deposited onto highly cleaned glass substrates of BK7 type. The structural characteristics, including surface morphology, roughness, and crystallite size, were studied by X-ray diffraction (XRD), atomic force microscopy (AFM), and transmission electron microscopy (TEM) analysis. Perfect crystallinity and nanoscalability of the prepared samples were asserted. Transmittance and reflectance spectra of the prepared nanofilms were investigated over the wavelength range of 400–2,700 nm. In the visible light region, all of the films showed an opaque behavior; however, as the wavelength increased into the infrared region, a growing transparency was observed. Based on the measured transmission and reflection spectra, the coefficients of absorbance and extinction as well as the optical band gap were determined. The refractive index was deduced from the reflectance measurements using the determined extinction coefficient. Direct allowed band transitions were confirmed in all films with a band gap energy of 0.85–1.05 eV, depending on the Te content. The possibility of an indirect band gap in the lower photon energy region was discussed. The Seebeck coefficient and electrical conductivity were measured in the temperature range of 300–500 K. Very large values of the power factor of 80 and $131x10^2\mu W$= m. K^2 were obtained for Be_2Se_3 films at room temperature and 473 K, respectively; the latter is three times larger than best previously reported values for similar film systems.

Nanoscale And Microscale Thermophysical Engineering, 22, 1, 2018, 21–38

Effect of the synthesis conditions on the structural, morphological and optical properties of $Bi_2Te_{2.7}Se_{0.3}$ nanoparticles

H.M. Ali, E.M.M. Ibrahim∗, M.M. Wakkad, M.A.A. Mohamed Physics Department, Faculty of Science, Sohag University, Sohag 82524, Egypt

Abstract

Beside their promising utility as thermoelectric generators, Bi_2Te_3 and related compounds have several applications in electronic and optoelectronic devices. In this work, $Bi_2Te_{2.7}Se_{0.3}$ nanoparticles (NPs) were successfully prepared via physical vapor deposition technique at different conditions of flow rate and temperature. The x-ray diffraction patterns show that, the NPs crystallize in a rhombohedral crystal structure with preferable growth along the (015) plane. Field-emission scanning electron microscope (FE-SEM) investigation shows that the NPs size depends significantly on the synthesis conditions of flow rate and temperature where it decreases with the decrease in the former or with the increase in the later. The effect of deposition conditions on the final morphology can be interpreted through the accompanied variation in the concentration of the gaseous precursors in the hot zone. The optical properties were studied using Kubelka-Munk theory. Optical band gaps of 0.52, 0.58, 0.53 eV were determined for the samples synthesized under different conditions.

Optik-International Journal for Light and Electron Optics, 158 (2018) 199–203

The synthesis of CuO and NiO nanoparticles by facile thermal decomposition of metal-Schiff base complexes and an examination of their electric, thermoelectric and magnetic Properties

E.M.M. Ibrahim[1]*, Laila H. Abdel-Rahman[2], Ahmed M. Abu-Dief[2], A. Elshafaie[1], Samar Kamel Hamdan[2], A. M. Ahmed[1]

[1]Physics Department, Faculty of Science, Sohag University, Sohag 82524, Egypt

[2]Chemistry Department, Faculty of Science, Sohag University, Sohag 82524, Egypt

Abstract

In this study, CuO and NiO NPs have been synthesized by facile thermal decomposition of Schiff base complexes and their physical properties have been examined. The synthesized CuO and NiO NPs are crystallized in polycrystalline monoclinic and cubic structures with average particle size 17±0.4 and 62±1 nm, respectively. The electrical conductivity measurements confirm that the conduction in the CuO NPs is a band-to-band type while the conduction in the NiO NPs is governed by the large polaron conduction mechanism. The thermoelectric measurements confirm that the CuO and NiO NPs are P-type degenerate semiconductors with room temperature Seebeck coefficients equal to 89.9 and 12.1 mV/K, respectively. The magnetic measurements exhibit that the NPs have weak ferromagnetic ordering and antiferromagnetic to paramagnetic transition with high dipolar interaction.

Materials Research Bulletin 107 (2018) 492–497

Thermoelectric properties of Te doped bulk Bi_2Se_3 system

A.M.A. dam[1,2,4] ,A. Elshafaie[1], A.bd El-MoezA Mohamed[1,3], P. Petkov[2] and E.M.M. Ibrahim1

[1] Physics Department, Faculty of Science, Sohag University, Sohag 82524, Egypt

[2] Physics Department, University of Chemical Technology and Metallurgy, Sofia 1000, Bulgaria

[3] Physics Department, Faculty of Science, Oviedo University, Oviedo 33007, Spain

[4] National University of Science and Technology MISiS, 119049, Moscow, Leninsky Prospekt, 4, Russia

Abstract

Polycrystalline bulk samples of $Bi_2(Se_{1-x}Te_x)_3$ system with x=0.0–0.9 were prepared by the conventional melting method. Successfully and cheaply, Se atoms were replaced by Te atoms to get Bi_2Se_3-Bi_2Te_3 or even Bi_2Te_3 alone. Difference of mass and size between Te and Se atoms is expected to result in interesting properties in the $Bi_2(Se_{1-x}Te_x)_3$ system. All compounds showed a metal semiconductor conductivity transition. The electrical conduction in the pristine Bi_2Se_3 compound increases with the low Te doping ratio (x=0.3) then decreases monotonically for further amounts of Te. The Seebeck coefficient of Bi_2Se_3 compound is positive showing up a p-type conduction. However, introducing Te content increases the n-type conduction with a decrease in the Seebeck coefficient absolute value. In addition, Bi_2Se_3 compound is found to exhibit relatively high room temperature power factor and figure of merit values of 2.13 $\mu W/m.k^2$. In an attempt to determine the figure of merit ZT, Bi_2Se_3 seems to be the best for room temperature, whereas, Te addition at high values makes the system just suitable for high temperature application.

Mater. Res. Express 5 (2018) 035514

Sonochemical synthesis, structural inspection and semiconductor behavior of three new nano sized Cu(II), Co(II) and Ni(II) chelates based on tri-dentate NOO imine ligand as precursors for preparing of metal oxides

Laila H. Abdel Rahman[a], Ahmed M. Abu-Dief [*a], Rafat M. El-Khatib [a], Shimaa Mahdy Abdel-Fatah [a], A. M. Adam[b], E.M.M. Ibrahim[b]

[a]Chemistry Department, Faculty of Science, Sohag University, 82534Sohag, Egypt

[b]Physics Department, Faculty of Science, Sohag University, 82534Sohag, Egypt

Three novel nanosized Cu(II), Co(II) and Ni(II) complexes of imine ligand attained from the condensation of 2-amino-3-hydroxypyridine and 3-methoxysalicylaldehyde have been prepared and investigated using diverse chemical methods such as NMR, CHN analysis, conductance, IR, Spectral studies, TGA and magnetic moment measurements. The obtained data confirmed that the synthesized complexes have metal: ligand ratio of 1:1 and octahedral geometry for Co(II) and Ni(II) complexes. Interestingly, The complexes are used as precursors for producing CuO, Co_2O_3 and NiO nanoparticles by calcination at 500 °C and their structures were described by powder x-ray and transmittance electron microscopy. Furthermore, to investigate the feasibility of using the synthesized materials for semiconductor based nanodevices, the electrical properties of the prepared imine complexes and their corresponding metal oxides were investigated by measuring the electrical conductivity over a temperature range 373-593K. The data confirm that the materials are semiconductor. The electrical conduction process in the complexes is governed by intermolecular and intramolecular transfer of the charge carriers. But, the conduction mechanism arises from the contribution of the phonon-assisted small polaron hopping in NiO nanoparticles and charge carrier hopping in CuO and Co_2O_3 nanoparticles. The results indicate that the complexes under study are promising candidates for wide scale of organic based semiconducting devices.

Applied organometalic chemistry (2018)

Correlation of structural and optical properties in as-prepared and annealed Bi_2Se_3 thin films

A.M. Adam[a,b,c], E. Lilovb, E.M.M. Ibrahim[b], P. Petkov[b], L.V. Paninaa, M.A. Darwish[a]

[a] *National University of Science and Technology, MISIS, Moscow, Russia*

[b] *Physics Department, University of Chemical Technology and Metallurgy, Sofia, Bulgaria*

[c] *Physics Department, Faculty of Science, Sohag University, Egypt*

Abstract

Bi_2Se_3 bulk alloys were synthesized using a standard mono-temperature melting process and used as source materials to deposit thin films on non-conductive super cleaned glass substrates by a vacuum thermal evaporation technique. Both bulk and thin-film samples were polycrystalline as confirmed by X-ray diffraction patterns. The film samples were subjected to the annealing process in air atmosphere at 250 and 300 ℃ for 3 h, aiming to boost the optical properties, in particular, to enhance the light transmission. The surface roughness, morphology and granular structure were investigated by atomic force microscope and scanning/transmission electron microscopes. The correlation between structural changes due to annealing and optical properties was observed. For a higher annealing temperature of 300 ℃, the coefficient of transmittance increased reaching 80–90% in the IR range. Consequently, the absorption coefficient greatly decreased by annealing, especially for low photon energies. The optical band gap corresponds to the direct transition and increased notably by annealing from 1.51 to 1.83 eV. The spectra of optical parameters including the refraction index, coefficient of extinction and complex-valued dielectric function were deduced from the transmittance/reflection measurements to evaluate the effect of annealing. The energy loss functions were also estimated demonstrating that the volume and surface energy losses are of the same order.

Journal of Materials Processing, doi.org/10.1016/j.jmatprotec.2018.09.005

The electric and thermoelectric properties of Cu(II)-schiff base nano-complexes

Ibrahim, E.M.M.[a], Abdel-Rahman, L.H.[b], Abu-Dief, A.M.[b], Elshafaie, A.[a], Hamdan, S.K.[b], Ahmed, A.M.[a]

[a]*Physics Department, Faculty of Science, Sohag University, Sohag, 82524, Egypt*

[b]*Chemistry Department, Faculty of Science, Sohag University, Sohag, 82524, Egypt*

The physical properties, such as electric and optical properties, of metal-Schiff base complexes have been widely investigated. However, their thermoelectric (TE) properties remain unreported. This work presents Cu(II)-Schiff base complexes as promising materials for TE power generation. Therefore, three Cu(II)-Schiff base complexes (namely, [Cu(C32H22N4O2)].3 2H2O, [Cu(C23H17N4O7Br)], and [Cu(C27H22N4O8)].H2O) have been synthesized in nanosized scale. The electric and TE properties have been studied and comprehensive discussions have been presented to promote the nano-complexes (NCs) practical applications in the field of TE power generation. The electrical measurements confirm that the NCs are semiconductors and the electrical conduction process is governed by intermolecular and intramolecular transfer of the charge carriers. The TE measurements reveal that the Cu(II)-Schiff base NCs are nondegenerate P-type semiconductors. The measured Seebeck coefficient values were higher compared to the values reported in previous works for other organic materials indicating that the complexes under study are promising candidates for theremoelectric applications if the electrical conductivity could be enhanced. © 2018 IOP Publishing Ltd Printed in the UK.

Physica Scripta, 93 (5), 2018, 055801

Chemistry

Cobalt ferrite nanoparticles with controlled composition-peroxymonosulfate mediated degradation of 2-phenylbenzimidazole-5-sulfonic acid

Abdulaziz Al-Anazi[a], Wael H.Abdelraheem[ab], ChangseokHan[a], Mallikarjuna N.Nadagouda[c], Labrini Sygellou[d], Michalis K.Arfanis[e], Polycarpos Falaras[e], Virender K.Sharma[f], Dionysios D.Dionysiou[a]*

[a]Environmental Engineering and Science Program, University of Cincinnati, Cincinnati, US, [b]Chemistry Department, Faculty of Science, Sohag University, Sohag 82524, Egypt, [c]Department of Mechanical and Materials Engineering, Wright State University, Dayton, Ohio 45324, US, [d]Foundation of Research and Technology Hellas, Institute of Chemical Engineering and High Temperature Chemical Processes (FORTH/ICE-HT), P.O. Box 1414, Gr-26504 Patras, Greece, [e]Institute of Nanoscience and Nanotechnology, NCSR Demokritos, 15310 Agia Paraskevi Attikis, Greece, [f]Program of the Environment and Sustainability, School of Public Health, Texas A&M University, 1266 TAMU College Station, TX 77843, United States

Abstract

Magnetic spinel cobalt ferrite nanoparticles with variable composition ($Co_xFe_{3-x}O_4$; x = 0.1, 0.5, 0.7 and 1.0) were synthesized. The nanoparticles were characterized by various surface techniques. Average sizes and surface areas of ferrites were determined in the ranges of 11–34 nm and 18.5–49.1 m^2/g, respectively. Surface analysis of the nanoparticles confirmed the spinel type structures in which Co(II) incorporated into the crystal lattice. The synthesized catalysts were used to dissociate peroxomonosulphate (PMS) into reactive sulfate radicals ($SO4^{\bullet-}$) and further into hydroxyl radicals ($HO^{\bullet}$) to degrade a target pollutant, 2-phenylbenzimidazole-5-sulfonic acid (PBSA) in absence of heat and light. As the molar ratio of cobalt (i.e., x) in the ferrite catalyst increased from 0.1 to 1.0, PBSA degradation enhanced from 24 to 75% in 240 min. The removal of PBSA increased significantly with the increase in PMS concentration up to 0.1 mM, followed by a decrease at PMS levels of >0.1 mM. Nitrogen content in PBSA was mineralized by the cobalt ferrite-PMS system mostly into NO_3^- and NH_4^+ ions with minor formation of NO_2^-. Only 32% TOC removal was observed over a 240 min reaction time, indicating carbon content in PBSA was not completely mineralized. A chemical probe method, based on free radical scavenging, revealed the contribution of both $SO4^{\bullet-}$ and $HO^{\bullet}$ species in PBSA degradation. Fifteen reaction intermediates were identified using LC/Q-TOF-ESI–MS analysis. Hydroxylation, elimination of sulfonate moiety, and ring cleavage processes were involved in the major degradation pathways. Catalyst reuse experiments demonstrated PBSA degradation efficiency either retained or increased with each subsequent reuse. The magnetic spinel Co-ferrite nanoparticles can be applied effectively to activate PMS without energy aiding for degrading harmful emerging organic contaminants in water.

Applied Catalysis B: Environmental, 221, 2018, 266-279

Synthesis and Reactions of New Thiazoles and Pyrimidines Containing Sulfonate Moiety

Khodairy, A.,Ali, A.M.,El-Wassimy, M.T.

Department of Chemistry, Faculty of Science, Sohag University, Sohag, 82524, Egypt

Abstract

Treatment of 2-tosyloxybenzylidinethiosemicarbazone (2) with active halo compounds afforded thiazoles 3–5. Moreover, reaction of compound 2 with acetic anhydride or dimethylformamide dimethylacetal gave N,N diacetyl 6 and dimethylamino derivatives 7, respectively. Cyclization of thiazole derivatives 3 with some arylidenemalononitriles yielded thiazolo[2,3-d]pyrans 8–12. Multicomponent reaction of 2-tosyloxybenzaldehyde (1) with urea, thiourea, or compound 2 and ethyl acetoacetate or acetylacetone afforded pyrimidines 13–14. The structures of compounds were elucidated by elemental and spectral analyses.

Journal of Heterocyclic Chemistry, 55, (4), 2018, 964-970

Hematite Photoanodes with Size-controlled Nanoparticles for Enhanced Photoelectrochemical Water Oxidation

Amira Y. Ahmed,[a] Mahmoud G. Ahmed,[a] and Tarek A. Kandiel[a,b]*

[a]*Department of Chemistry, Faculty of Science, Sohag University, Sohag 82524, Egypt*

[b]*Department of Chemistry, King Fahd University of Petroleum & Minerals (KFUPM), Dhahran 31261, SA*

The synthesis of hematite photoanodes with size-controlled nanoparticles is challenging due to the difficulty in finding the appropriate morphology-directing agents. In this paper, Ba^{2+} and Sr^{2+} ions were successfully employed to synthesize hematite photoanodes with size-controlled nanoparticles using a facile chemical bath deposition method. The synthesized electrodes were characterized by X-ray diffraction (XRD), scanning electron microscopy (SEM), inductively coupled plasma-optical emission spectrometry (ICP-OES), (photo)electrochemical impedance spectroscopy ((P)EIS), X-ray photoelectron spectroscopy (XPS) and intensity modulated photocurrent spectroscopy (IMPS) measurements. It was found that the average diameter of hematite nanoparticles is decreased by a factor of 13% and 35% by the addition of Ba^{2+} and Sr^{2+} ions into the chemical bath, respectively. In agreement with these results, the electroactive surface area of Ba- and Sr-modified hematite electrodes increased by 2.4 and 3.2 times, respectively, in comparison with that of bare hematite. The photoelectrochemical measurements under the standard illumination conditions revealed that the generated photocurrent at 1.23 V vs. RHE on Ba- and Sr-modified hematite photoanodes is 2.6 and 3 times higher than that of bare hematite, respectively. Moreover, the photocurrent onset potential for water oxidation on Ba- and Srmodified hematite photoanodes was shifted cathodically by about 150 and 220 mV, respectively. Based on these results, a good correlation between the photocurrent and the electroactive surface area was observed at high bias potential (i.e., 1.23 V vs. RHE) evincing that the photocurrent enhancement can be readily attributed to the enhanced electroactive surface area. The cathodic shift in the photocurrent onset potential of water oxidation was elucidated, however, by the higher density of surface states and the higher rate constant of charge transfer as proven by the PEIS and IMPS measurements, respectively.

Applied Catalysis B: Environ., 236 (2018) 117-124

New Method for Synthesis of Multi-substituted Imidazoles

Marzouk, A.A.[a],Mohamed, S.K.[b,c],Aljohani, E.T.[d],Abdelhamid, A.A.[e]

[a]*Pharmaceutical Chemistry Department, Faculty of Pharmacy, Al Azhar University, Cairo, Egypt*

[b]*Chemistry and Environmental Division, Manchester Metropolitan University, Manchester, M1 5GD, UK*

[c]*Chemistry Department, Faculty of Science, Minia University, El-Minia, 61519, Egypt*

[d]*Chemistry Department, College of Science, Majmaah University, Majmaah, 11952, Saudi Arabia*

[e]*Chemistry Department, Faculty of Science, Sohag University, Sohag, 82524, Egypt*

Abstract

Here, we reported two methods for the synthesis of multi-substituted imidazoles, firstly via four-component cyclocondensation reaction of benzil, aliphatic amines (allylamine or pentylamine), and aromatic aldehyde and ammonium acetate. Using an ionic liquid catalyst namely, diethyl ammonium hydrogen sulfate, and under solvent-free conditions. Secondly, via the alkylation of synthesized NH imidazoles with alkyl halide (allyl bromide and pentyl bromide) gave 8a–c in high yield (average 90%), the products can be purified by a non-chromatographic method, and these newly synthesized compounds have been characterized by spectral data: FTIR, IR, ^{1}H, ^{13}C nuclear magnetic resonance, the elemental analysis, and the X-ray structure

Journal of Heterocyclic Chemistry,Volume 55, Issue 7, July 2018, Pages 1775-1782

Artificial Macrocycles

Abdelraheem, E.M.M.[a,b],Shaabani, S.[a],Dömling, A.[a]

[a]*Biokatalyse, Afdeling Biotechnologie, Technische Universiteit Delft, Van der Maasweg 9, Netherlands*

[b]*Chemistry Department, Faculty of Science, Sohag University, Sohag, 82524, Egypt*

Abstract

Artificial macrocycles recently became popular as a novel research field in drug discovery. As opposed to their natural twins, artificial macrocycles promise to have better control on synthesizability and control over their physicochemical properties resulting in druglike properties. Very few synthetic methods allow for the convergent, fast but diverse access to large macrocycles chemical space. One synthetic technology to access artificial macrocycles with potential biological activity, multicomponent reactions, is reviewed here, with a focus on our own work. We believe that synthetic chemists have to acquaint themselves more with structure and activity to leverage the design aspect of their daily work. 1 Introduction 2 Macrocycle Properties and Receptor Binding 3 Synthetic Approaches towards Artificial Macrocycles Using MCR 4 Design Rules for Membrane Crossing Macrocycles 5 Design Rules for Libraries of Macrocycles 6 Computational Macrocyclic Methods 7 Future View.

Synlett, Volume 29, Issue 9, 1 June 2018, Pages 1136-1151

Deazaflavins as photocatalysts for the direct reductive regeneration of flavoenzymes

Van Schie, M.M.C.H.[a],Younes, S.H.H.[a,b],Rauch, M.C.R.[a],Pesic, M.[a],Paul, C.E.[c],Arends, I.W.C.E.[a],Hollmann, F.[a]

[a]*Department of Biotechnology, Delft University of Technology, van der Maasweg 9, Delft, HZ 2629, Netherlands*

[b]*Sohag University, Faculty of Sciences, Department of Chemistry, Sohag, 82524, Egypt*

[c]*Wageningen University and Research, Laboratory of Organic Chemistry, Stippeneng 4, Wageningen, WE 6708, Netherlands*

Abstract

Deazaflavins are potentially useful redox mediators for the direct, nicotinamide-independent regeneration of oxidoreductases. Especially the O_2-stability of their reduced forms have attracted significant interest for the regeneration of monooxygenases. In this contribution we further investigate the photochemical properties of deazaflavins and investigate the scope and limitations of deazaflavin-based photoenzymatic reaction systems.

Molecular Catalysis, Volume 452, June 2018, Pages 277-283

Carbocation Catalyzed Bromination of Alkyl Arenes, a Chemoselective sp^3 vs. sp^2 C−H functionalization

Ni, S.[a],Mahmoud Abd El Aleem Ali El Remaily[a,b], Franzén, J.[a]
[a]KTH, Royal Institute of Technology, School of Engineering Sciences in Chemistry, Biotechnology and Health, Department of Chemistry/Division of Organic Chemistry, Teknikringen 30, Stockholm, SE-100 44, Sweden
[b]Department of Chemistry, Faculty of Science, Sohag University, Sohag, 82524, Egypt

Abstract
The versatility of the trityl cation ($TrBF_4$) as a highly efficient Lewis acid organocatalyst is demonstrated in a light induced benzylic brominaion of alkyl-arenes under mild conditions. The reaction was conducted at ambient temperature under common hood light (55 W fluorescent light) with catalyst loadings down to 2.0 mol% using N-bromosuccinimide (NBS) as the brominating agent. The protocol is applicable to an extensive number of substrates to give benzyl bromides in good to excellent yields. In contrast to most previously reported strategies, this protocol does not require any radical initiator or extensive heating. For electron-rich alkyl-arenes, the trityl ion catalyzed bromination could be easily switched between benzylic sp^3 C−H functionalization and arene sp^2 C−H functionalization by simply alternating the solvent. This chemoselective switch allows for high substrate control and easy preparation of benzyl bromides and bromoarenes, respectively. The chemoselective switch was also applied in a one-pot reaction of 1-methylnaphthalene for direct introduction of both sp^3 C−Br and sp^2 C−Br functionality.
Advanced Synthesis and Catalysis, Volume 360, Issue 21, 5 November 2018, Pages 4197-4204

Concise Synthesis of Macrocycles by Multicomponent Reactions

Abdelraheem, E.M.M.[a,b],Khaksar, S.[a,c],Dömling, A.[a]
[a]Department of Drug Design, University of Groningen, A. Deusinglaan 1, Groningen, 9713 AV, Netherlands
[b]Chemistry Department, Faculty of Science, Sohag University, Sohag, 82524, Egypt
[c]Chemistry Department, Ayatollah Amoli Branch, Islamic Azad University, Amol, Iran

Abstract
A short reaction pathway was devised to synthesize a library of artificial 18-27-membered macrocycles. The five-step reaction sequence involves ring opening of a cyclic anhydride with a diamine, esterification, coupling with an amino acid isocyanide, saponification, and, finally, macro-ring closure using an Ugi or, alternatively, a Passerini multicomponent reaction. Three out of the five steps allow for the versatile introduction of linker elements, side chains, and substituents with aromatic, heteroaromatic, and aliphatic character. The versatile pathway is described for 15 different target macrocycles on a mmol scale. Artificial macrocycles have recently become of great interest due to their potential to bind to difficult post-genomic targets.
Synthesis ,Volume 50, Issue 5, 1 March 2018, Article number ss-2017-z0480-op, Pages 1027-1038

Unexpected products from the reaction of chalcones with cyanoguanidine

Moustafa, A.H.,Amer, A.A

Chemistry Department, Faculty of Science, Sohag University, Sohag, 82524, Egypt

Abstract

A new series of unexpected dihydrochalcones DHCs attached with cyanoiminopyrimidine moiety in addition to expected cyanoaminopyrimidines CAMPs were synthesized by efficient and facile method via reaction of cyanoguanidine with chalcone derivatives in the presence of EtONa

Tetrahedron, Volume 74, Issue 2, 11 January 2018, Pages 324-328

Sonochemical synthesis, structural inspection and semiconductor behavior of three new nano sized Cu(II), Co(II) and Ni(II) chelates based on tri - dentate NOO imine ligand as precursors for metal oxides

Laila H. Abdel Rahman, Ahmed M. Abu-Dief , Rafat M. El-Khatib, Shimaa Mahdy Abdel-Fatah, A.M. Adam, E.M.M. Ibrahim

[1] Chemistry Department, Faculty of, Science, Sohag University, 82534 Sohag, Egypt

[2] Physics Department, Faculty of Science, Sohag University, 82534 Sohag, Egypt

Three novel nanosized Cu(II), Co(II) and Ni(II) complexes of imine ligandattained from the condensation of 2-amino-3-hydroxypyridine and 3-methoxysalicylaldehyde have been prepared and investigated using diversechemical methods such as NMR, CHN analysis, conductance, IR, Spectral stud-ies, TGA and magnetic moment measurements. The obtained data confirmedthat the synthesized complexes have metal: ligand ratio of 1:1 and octahedralgeometry for Co(II) and Ni(II) complexes. Interestingly, The complexes are usedas precursors for producing CuO, $Co_2O_3$and NiO nanoparticles by calcinationat 500 °C and their structures were described by powder x-ray and transmit-tance electron microscopy. Furthermore, to investigate the feasibility of usingthe synthesized materials for semiconductor based nanodevices, the electricalproperties of the prepared imine complexes and their corresponding metaloxides were investigated by measuring the electrical conductivity over a temper-ature range 373-593 K. The data confirm that the materials are semiconductor.The electrical conduction process in the complexes is governed by intermolecu-lar and intramolecular transfer of the charge carriers. But, the conductionmechanism arises from the contribution of the phonon-assisted small polaronhopping in NiO nanoparticles and charge carrier hopping in CuO and Co2O3nanoparticles. The results indicate that the complexes under study are promis-ing candidates for wide scale of organic based semiconducting device

Appl Organometal Chem . 2018; 32 :e4174.

New Route for the Synthesis of Hetaryl-1,5-benzodiazepines: Part 2

Ahmed, A.M.,Abdel-Ghany, H.,Moustafa, H.M.,Khodairy, A.

Chemistry Department, Faculty of Science, Sohag University, Sohag, Egypt

Abstract

1,2,4-Triazin-3-ylthio-, 1,2,4-triazepin-3-ylthio-, 1,2,4-triazol-3-ylthio-, and 1,2,4,3-triazaphosphol-5-ylthio-1,5-benzodiazepines 4–20 were prepared via the reaction of 2-oxo-4-phenyl-2,3-dihydro-1H-1,5-benzodiazepin-3-ylhydrazonothiocarbamate (2) with halocompounds, dicarbonyl compounds, enaminones, 4-chlorobenzaldehyde, 4-chlorobenzylidenemalononitriles, N,N-dimethylformamide dimethylacetal, carbon disulfide, and 2,4-bis(4-methoxyphenyl)-1,3,2,4-dithiadiphosphetane-2,4-disulfide

Journal of Heterocyclic Chemistry, 2018

Utility of amino acid coupled 1,2,4-triazoles in organic synthesis: Synthesis of some new antileishmainal agents

El-Saghier, A.M.M.,Mohamed, M.A.A.,Abdalla, O.A.,Kadry, A.M.

Chemistry Department, Faculty of Science, Sohag University, Sohag, Egypt

Abstract

Starting from 3-amino-5-(2-hydroxyphenyl) amino acid coupled triazoles 1a-e, new 3-(2-hydroxyphenyl)-3H-imidazo[2,1-c][1,2,4]triazol-6(5H)-one 2a,b, 3b,d, 6a and 3-N-arly(alkyl) amino acid coupled triazoles 4b,d, 7a,c,d,e have been synthesized as potential antileishmanial agents. The structures of the newly synthesized compounds were confirmed using elemental and spectral analyses (FT-IR, ^{1}H-NMR, ^{13}C-NMR and MS). The in vitro antileishmanial potency of the synthesized compounds was evaluated compared to Amphotericin B deoxycholate and miltefosine as lead references. Compounds 2b, 7d and 7e showed perfect IC_{50} values corresponding to amphotericin B and more patent than miltefosine against L. aethiopica promastigotes.

Bulletin of the Chemical Society of Ethiopia, Volume 32, Issue 3, 2018, Pages 559-570

The structure of 9-(3-bromo-6-chloro-2-hydroxyphenyl)-10-(2-hydroxyethyl)-3,6-diphenyl-3,4,5,6,7,9-hexahydro-2 H-acridine-1,8-dione

Abdelhamid, A.A.[a],Hawaiz, F.E.[b]Email Author,Mohamed, A.F.[c],Mohamed, S.K.[d],Simpson, J.[e,f]

[a]Chemistry Department, Faculty of Science, Sohag University, Sohag, Egypt

[b]Chemistry Department, College of Education, Salahaddin University-Hawler, Erbil, Kurdistan Region, Iraq

[c]National Organization for Drug Control and Research (NODCAR), Giza, Egypt

[d]Chemistry and Environmental Division, Manchester Metropolitan University, Manchester, M1 5GD, UK

[e]Chemistry Department, Faculty of Science, Minia University, El-Minia, 61519, Egypt

[f]Department of Chemistry, University of Otago, PO Box 56, Dunedin, New Zealand

Abstract

In the structure of the title compound $C_{33}H_{29}BrClNO_4$, (I), the hexahydro-2H-acridine ring system has a hydroxyethyl substituent on the N atom and a 3-bromo-6-chloro-2-hydroxyphenyl substituent on the central C atom at the 9-position. An unusual feature of the molecule is that the substituents at the 3-and 5-positions of the outer cyclohexenone rings are phenyl rings rather than the more common dimethyl substituents. C atoms on both of the cyclohexenone rings are disordered over two sites. In the crystal structure, O-H..O, C-H..O and C-H..π(ring) hydrogen bonds combine with an Br-O and unusual C-Br..π(ring) halogen bonds to generate a three dimensional network with molecules stacked along the a-axis direction.

Acta Crystallographica Section E: Crystallographic Communications,Volume 74, 2018, 1218-1221

2-Deoxy-d-ribose-5-phosphate aldolase (DERA): applications and modifications

Haridas, M.[a], Abdelraheem, E.M.M.[a,b],Hanefeld, U.[a]

[a]Biokatalyse, Afdeling Biotechnologie, Technische Universiteit Delft, Van der Maasweg 9, Delft, 2629 HZ, Netherlands

[b]Chemistry Department, Faculty of Science, Sohag University, Sohag, 82524, Egypt

Abstract

2-Deoxy-d-ribose-5-phosphate aldolase (DERA) is a class I aldolase that offers access to several building blocks for organic synthesis. It catalyzes the stereoselective C–C bond formation between acetaldehyde and numerous other aldehydes. However, the practical application of DERA as a biocatalyst is limited by its poor tolerance towards industrially relevant concentrations of aldehydes, in particular acetaldehyde. Therefore, the development of proper experimental conditions, including protein engineering and/or immobilization on appropriate supports, is required. The present review is aimed to provide a brief overview of DERA, its history, and progress made in understanding the functioning of the enzyme. Furthermore, the current understanding regarding aldehyde resistance of DERA and the various optimizations carried out to modify this property are discussed.

Applied Microbiology and Biotechnology, Volume 102, Issue 23, 1 December 2018, Pages 9959-9971

Identification of some Bioactive Metabolites in a Fractionated Methanol Extract from Ipomoea aquatica (Aerial Parts) through TLC, HPLC, UPLC-ESI-QTOF-MS and LC-SPE-NMR Fingerprints Analyses

Hefny Gad, M.[a,b],Tuenter, E.[c],El-Sawi, N.[d],Younes, S.[d],El-Ghadban, E.-M.[b],Demeyer, K.[e],Pieters, L.[c],Vander Heyden, Y.[a]Email Author,Mangelings, D.[a]

[a]*Department of Analytical Chemistry and Pharmaceutical Technology, Centre for Pharmaceutical Research, Vrije Universiteit Brussel (VUB), Laarbeeklaan 103, Brussels, B-1090, Belgium*

[b]*Medicinal and Aromatic Plants Research Department, Horticulture Institute, Agriculture Research Centre, Dokki, Giza, Egypt*

[c]*Natural Products & Food Research and Analysis (NatuRA), Department of Pharmaceutical Sciences, University of Antwerp, Universiteitsplein 1, Antwerp, B-2610, Belgium*

[d]*Department of Chemistry, Faculty of Science, Sohag University, Sohag, Egypt*

[e]*Department of Toxicology, Dermato-Cosmetology and Pharmacognosy, Centre for Pharmaceutical Research, Vrije Universiteit Brussel (VUB), Laarbeeklaan 103, Brussels, B-1090, Belgium*

Abstract

Introduction: The plant species Ipomoea aquatica contains various bioactive constituents, e.g. phenols and flavonoids, which have several medical uses. All previous studies were executed in Asia; however, no reports are available from Africa, and the secondary metabolites of this plant species from Africa are still unknown. Objective: The present study aims finding suitable conditions to identify the bioactive compounds from different fractions. Methodology: Chromatographic fingerprint profiles of different fractions were developed using high-performance liquid chromatography (HPLC) and then these conditions were transferred to thin-layer chromatography (TLC). Subsequently, the chemical structure of some bioactive compounds was elucidated using ultra-performance liquid chromatography-quadrupole time of flight-tandem mass spectrometry (UPLC-QTOF-MS) and liquid chromatography-solid phase extraction-nuclear magnetic resonance (LC-SPE-NMR) spectroscopy. Results: The HPLC fingerprints, developed on two coupled Chromolith RP-18e columns, using a gradient mobile phase (methanol/water/trifluoroacetic acid, 5:95:0.05, v/v/v), showed more peaks than the TLC profile. The TLC fingerprint allows the identification of the types of chemical constituents, e.g. flavonoids. Two flavonoids (nicotiflorin and ramnazin-3-O-rutinoside) and two phenolic compounds (dihydroxybenzoic acid pentoside and di-pentoside) were tentatively identified by QTOF-MS, while NMR confirmed the structure of rutin and nicotiflorin. Conclusion: The HPLC and TLC results showed that HPLC fingerprints give more and better separated peaks, but TLC helped in determining the class of the active compounds in some fractions. Bioactive constituents were identified as well using MS and NMR analyses. Two flavonoids and two phenolic compounds were tentatively identified in this species for the first time, to the best of our knowledge.

Phytochemical AnalysisVolume 29, Issue 1, January/February 2018, Pages 5-15

Synthesis of Some New Polyfunctionalized Pyridines

Amer, A.A.

Department of Chemistry, Faculty of Science, Sohag University, Sohag, 82524, Egypt

Abstract

5-Methyl-2,4-dihydro-3H-pyrazol-3-one and/or 5-methyl-2-phenyl-2,4-dihydro-3H-pyrazol-3-one was reacted with arylidenemalononitrile in the presence of sodium alkoxide to give 2-amino-6-alkoxy-4-arylpyridine-3,5-dicarbonitrile 4a–e instead of the reported pyrazolo[3,4-b]pyridine-5-carbonitriles. The same products 4a–e were prepared via reaction of arylidenemalononitrile with sodium alkoxide in an appropriative alcohol. However, the new synthetic route for preparation of their positional isomer 4-amino-6-alkoxy-2-arylpyridine-3,5-dicarbonitrile 7a–j has been achieved via reaction of 2-aminoprop-1-ene-1,1,3-tricarbonitrile with different aromatic aldehydes under the same conditions.

Journal of Heterocyclic Chemistry, Volume 55, Issue 1, January 2018, Pages 297-301

Fabrication of oxidized graphite supported La_2O_3/ZrO_2nanocomposite for the photoremediation of toxic fast green dye

GauravSharma[abc]AmitKumar[abc]ShwetaSharma[c]Sameerah I.Al-Saeedi[d]Ghadah M.Al-enani[d]AymanNafady[e]TansirAhamad[e]Mu.Naushad[e]Florian J.Stadler

College of Materials Science and Engineering, Shenzhen Key Laboratory of Polymer Science and Technology, Guangdong Research Center for Interfacial Engineering of Functional Materials, Nanshan District Key Lab. for Biopolymers and Safety Evaluation, Shenzhen University,,PR China

[b] Key Laboratory of Optoelectronic Devices and Systems of Ministry of Education and Guangdong Province, College of Optoelectronic Engineering, Shenzhen University, Shenzhen 518060, PR China

[c]School of Chemistry, Shoolini University, Solan 173212, Himachal Pradesh, India

[d] Department of Chemistry, College of Science, Princess Nourah bint Abdul Rahman University, Riyadh, SA

[e]Department of Chemistry, College of Science, King Saud University, Riyadh 11451, SA

The dyes are one of major pollutants discharged to water bodies without any premeditation. Their undesirable detection in aqueous bodies has created a menace as they tend to disturb the complete aquatic ecosystem by directly hindering the photosynthetic process of aquatic flora. Thus pre and post discharge remediation of these dyes are of immense significance. In the present study, novel OG/La_2O_3/ZrO_2nanocomposite having high photocatalytic ability was prepared by co-precipitationmethod. Visible photocatalytic ability of the nanocomposite was employed for the degradation of fast green dye as a target pollutant. The OG/La_2O_3/ZrO_2nanocomposite was well characterized using various techniques as FTIR, XRD, SEM, TEM and XPS etc. The nanocomposite also exhibited adsorption capability due to the presence of oxidized graphite (OG) sheets those provided high surface area for the fast green molecules to get adsorb onto them. High degradation efficiency (89%) was obtained within 90 min of visible light irradiation. Effect of pH, photocatalyst amount and light intensity was also studied. Superoxide and hydroxyl radicals; were found to be the major reacting species as confirmed by the scavenging studies. Furthermore, OG/La_2O_3/ZrO_2 nanocomposite exhibited high reusability interpreting the nanocomposite as a proficient photocatalyst with active utilization for treating industrial waste water.

Journal of Molecular Liquids, accepted manuscript, 27 December 2018

Facile Approach to Graft Ionic Liquid into MOF for Improving the Efficiency of CO_2 Chemical Fixation

Yuxiu Sun[†‡], Hongliang Huang[†] , Harsh Vardhan[‡], Briana Aguila[‡], Chongli Zhong[†], Jason A. Perman*[‡] , Abdullah M. Al-Enizi[§], Ayman Nafady[§‖], and Shengqian Ma*[‡]

[†] State Key Laboratory of Separation Membranes and Membrane Processes, Tianjin Polytechnic University, 399 Binshui West Road, Tianjin 300387, China

[‡] Department of Chemistry, University of South Florida, 4202 E. Fowler Avenue, Tampa, Florida 33620, United States

[§] Chemistry Department, College of Science, King Saud University, Riyadh 11451, Saudi Arabia

[‖] Chemistry Department, Faculty of Science, Sohag University, Sohag 82524, Egypt

This work describes a facile approach to modify metal–organic frameworks (MOFs) with ionic liquids (ILs), rendering them as useful heterogeneous catalysts for CO2 chemical fixation. An amino-functionalized imidazolium-based ionic liquid is firmly grafted into the porous MOF, MIL-101–SO3H by the acid–base attraction between positively charged ammonium groups on the IL and negatively charged sulfonate groups from the MOF. Analyses by Fourier transform infrared spectroscopy, X-ray photoelectron spectroscopy, 1H NMR, and N2 sorption experiments reveal the MOF-supported ionic liquid (denoted as IL@MOF) material remains intact while functioning as a recyclable heterogeneous catalyst that can efficiently convert CO2 and epichlorohydrin into chloropropene carbonate without the addition of a cocatalyst.

ACS Appl. Mater. Interfaces, 2018, 10 (32), pp 27124–27130

A Multifunctional Zinc Oxide/Poly(Lactic Acid) Nanocomposite Layer Coated on Magnesium Alloys for Controlled Degradation and Antibacterial Function

Hamouda M. Mousa[a,b], Abdalla Abdal-hay[b,c], Michal Bartnikowski [b,c], Ibrahim M. A. Mohamed[a,d], Ahmed S. Yasin[a], Sašo Ivanovski[c], Chan Hee Park[a] and Cheol Sang Kim[a]

[a] *Department of Bionanosystem Engineering, Chonbuk National University, Jeonju, Jeonbuk 561-756, RK*
[b] *Department of Engineering Materials and Mechanical Design, Faculty of Engineering, SVU, Qena,, Egypt*
[c] *The University of Queensland, School of Dentistry, Oral Health Centre Herston, Australia*
[d] *Department of Chemistry, Faculty of Science, Sohag University, Sohag 82524, Egypt*

Abstract:
In the present work, magnesium (Mg) AZ31 alloy was coated with a multifunctional membrane layer composed of ZnO nanoparticles (NPs) embedded in a poly(lactic acid) (PLA) matrix. We aimed to produce a stable coating that would be used to control the degradation rate of the Mg alloy and promote a local antibacterial activity. ZnO NPs were dispersed at 5 and 10 wt % in a PLA solution and dip-coatedontotheAZ31substrate. Surface topography, chemical composition, thickness, electrochemical corrosion performance, mass variation, antibacterial activity, adhesion performance, and cytotoxicity of an uncoated control and coated alloys were investigated. The results indicated that the incorporation of ZnO NPs at various concentrations affords a dramatic control over surface topography and degradation rates under in vitro and in vivo environmental conditions when compared to the uncoated Mg alloy control. In addition, the results confirmed that the coated layer exerts antibacterial properties and supports cell growth, indicating this system may have utility for bone tissue engineering applications.
ACS biomaterials science & engineering, 4 (2018) 2169-2180.

$CoCr_7C_3$-like nanorods embedded on carbon nanofibers as effective electrocatalyst for methanol electro-oxidation

Abdullah M.Al-Enizi[a]Robert M.Brooks[b]M.M.El-Halwany[cd]AymanYousef[de]AymanNafady[a]R.M. AbdelHameed[f]

[a]Department of Chemistry, College of Science, King Saud University, Riyadh 11451, Saudi Arabia
[b]Department of Civil and Environmental Engineering, Temple University, Philadelphia, PA, 19122, USA
[c]Engineering Mathematics and Physics Department, Faculty of Engineering, Mansoura University, Egypt
[d]Department of Chemical Engineering, Jazan University, Jazan 45142, Saudi Arabia
[e]Department of Mathematics and Physics Engineering, Faculty of Engineering at Mataria, Helwan University, Cairo 11718, Egypt
[f]Chemistry Department, Faculty of Science, Cairo University, Giza, Egypt

$CoCr_7C_3$-like nanorods encapsulated in carbon nanofibers shell [$CoCr_7C_3$-CNFs] were prepared using a simple electrospinning technique. The as-prepared nanocompositewas physically characterized using XRD, SEM, TEM and EDX analysis techniques. The electrocatalytic activity of $CoCr_7C_3$-CNFs was examined for methanol electro-oxidation in alkaline medium using cyclic voltammetry and chronoamperometry. The fabricated $CoCr_7C_3$-CNFs revealed good electroactivity towards methanol oxidation reaction. The measured low onset potential value [−80 mV (Ag/AgCl)] implied a marked enhancement in the oxidation kinetics at $CoCr_7C_3$-CNFs surface. Chronoamperometry test also displayed an increased steady state oxidation current density value of 18.42 mA cm^{-2} at 400 mV after 1800 s. This synthesized low cost, highly active and stable nanocomposite could be widely employed as a promising anode material in direct methanol fuel cells.
International Journal of Hydrogen Energy, **43, 21, 24, 2018, 9943-9953**

Lower Activation Energy for Catalytic Reactions through Host–Guest Cooperation within Metal–Organic Frameworks

Briana Aguila , Dr. Qi Sun Xiaoliang Wang Erica O'Rourke, Ayman Nafady, Shengqian Ma

Industrial synthesis is driven by a delicate balance of the value of the product against the cost of production. Catalysts are often employed to ensure product turnover is economically favorable by ensuring energy use is minimized. One method, which is gaining attention, involves cooperative catalytic systems. By inserting a flexible polymer into a metal–organic framework (MOF) host, the advantages of both components work synergistically to create a composite that efficiently fixes carbon dioxide to transform various epoxides into cyclic carbonates. The resulting material retains high yields under mild conditions with full reusability. By quantitatively studying the kinetic rates, the activation energy was calculated, for a physical mixture of the catalyst components to be about 50 % higher than that of the composite. Through the unification of two catalytically active components, a new opportunity opens up for the development of synergistic systems in multiple applications.

Angewandte Chemie, Volume130, Issue32, Pages 10264-10268

Sensitive and selective aggregation based colorimetric sensing of Fe^{3+} via interaction with acetyl salicylic acid derived gold nanoparticles

Safia S.Memon[a]AymanNafady[bc]Amber R.Solangi[a]Abdullah M.Al-Enizi[b]Sirajuddin[a]Muhammad R.Shah[d]Syed T.H.Sherazi[a]ShabuddinMemon[a]MunazzaArain[e]Muhammad I.Abro[f]Manzoor I.Khattak[g]

[a]National Centre of Excellence in Analytical Chemistry, University of Sindh, Jamshoro, 76080, Pakistan
[b]Department of Chemistry, College of Science, King Saud University, Riyadh 11451, Saudi Arabia
[c]Chemistry Department, Faculty of Science, Sohag University, Sohag 82524, Egypt, [d]International Centre for Chemical and Biological Sciences, HEJ Research Institute of Chemistry, University of Karachi, Karachi 75270, Pakistan, [e]Dr. MA Kazi Institute of Chemistry, University of Sindh, Jamshoro, 76080 Pakistan
[f]Department of Metallurgy & Materials Engineering, Mehran University of Engineering & Technology, Jamshoro, Pakistan, [g]Department of Chemistry, University of Balochistan, Quetta, Pakistan

Here we highlight a single pot green synthetic protocol for gold nanoparticles (AuNps) using acetyl salicylic acid (ASA) drug as reducing and capping agent. These nanoparticles were characterized using UV–Vis (UV–Vis) spectroscopy, Fourier Transform Infrared (FT-IR) Spectroscopy, X-ray diffractometry (XRD) and Atomic Force Microscopy (AFM). The estimated average size of AuNps was 33 nm. These ASA-AuNps were employed to develop a highly selective and sensitive colorimetric sensor for Fe^{3+} detection. This sensor responded linearly to Fe^{3+} in the range of 0.3–2.1 μmol L^{-1}. The limit of detection (LOD) and limit of quantification (LOQ) of sensor was 0.051 and 0.17 μmol L^{-1} respectively. The response of the developed sensor to the interfering ions like Ni^{2+}, Hg^{2+}, Cd^{2+}, Cr^{3+}, Co^{2+}, As^{3+}, Pb^{2+}, Fe^{2+} and Zn^{2+} was negligible. The sensor was used successfully to detect Fe^{3+} in real water samples collected from various locations of the Sindh River.

Sensors and Actuators B: Chemical, 259, 15, Pages 1006-1012

Construction of an Ultrasensitive and Highly Selective Nitrite Sensor Using Piroxicam-Derived Copper Oxide Nanostructures

Ali Alsalme, Munazza Arain , Ayman Nafady, andSirajuddin

[1]*Department of Chemistry, College of Science, King Saud University, P.O. Box 2455, Riyadh 11451, SA*

[2]*Dr. M. A. Kazi Institute of Chemistry, University of Sindh, Jamshoro 76080, Pakistan*

[3]*Chemistry Department, Faculty of Science, Sohag University, Sohag 82524, Egypt*

[4]*National Center of Excellence in Analytical Chemistry, University of Sindh, Jamshoro 76080, Pakist*

In this work, piroxicam-based copper oxide nanostructures (Px-CuO NSs) were synthesized via hydrothermal precipitation in the presence of ammonia. The prepared Px-CuO NSs were subjected to scanning electron microscopy (SEM) and X-ray diffraction (XRD) to obtain morphology and crystallinity, respectively. The SEM study reveals that these Px-CuO NSs are in the form of porous rose-like nanopetals with dotted particles on their surface, while the XRD study confirms their crystalline nature. The Px-CuO NS-based sensors were fabricated by drop-casting them onto the surface of a glassy carbon electrode (GCE) and they were tested for nitrite detection using voltammetry and amperometry. The results show these Px-CuO NSs to be highly stable on the GCE surface with linear amperometric (current vs. time) responses to wide range of nitrite concentrations from 100 to 1800 nM, with limits of detection (LOD) and quantification (LOQ) being 12 nM and 40 nM, respectively. Importantly, the fabricated sensor showed negligible effects for a 10-fold higher concentration of common interfering agents and exhibited excellent selectivity. It was applied successfully for nitrite detection in water samples such as river water, mineral water, and tap water

Catalysts **2018, *8*(1), 29**

Cobalt nanoparticles incorporated into hollow doped porous carbon capsules as a highly efficient oxygen reduction electrocatalyst

Feng Guo [ab], Hui Yang [b], Briana Aguila[b], Abdullah M. Al-Enizi [c], Ayman Nafady [cd], Mandeep Singh [e], Vipul Bansal [e] and Shengqian Ma *[bc]

[a]*Chongqing Key Laboratory of Inorganic Special Functional Materials, College of Chemistry and Chemical Engineering, Yangtze Normal University, 16 Juxian Rd, Fuling, ChongQing, 408100 China*

[b]*Department of Chemistry, University of South Florida, CHE205A, 4202E. Fowler Avenue, Florida 33620, USA*

[c]*Chemistry Department, College of Science, King Saud University, Riyadh, 11451, Saudi Arabia*

[d]*Chemistry Department, Faculty of Science, Sohag, 82524, Egypt*

[e]*Ian Potter NanoBioSensing Facility, NanoBiotechnology Research Laboratory, School of Science, RMIT University, Melbourne, VIC 3000, Australia*

Platinum-based materials have been the dominant and best electrocatalysts for promoting the oxygen reduction reaction (ORR). However, going beyond state-of-the-art catalysts remains a great challenge. Recently, nanostructured composites of conductive carbons and earth-abundant metals have emerged as promising electrocatalysts. Herein, we report a facile and practical approach for the synthesis of cobalt nanoparticles embedded into hollow nitrogen/cobalt-doped porous carbon capsules (Co@NPCC). The fabrication of this material was achieved *via* the thermal decomposition of sacrificial metal–organic framework nanocrystals coated with a metal–tannic acid coordination polymer shell, upon pyrolysis, which delivers zerovalent cobalt nanoparticles embedded in the walls of hollow capsules. Co@NPCC proved to be a superb catalyst for the electrochemical ORR, showing a highly positive onset potential (~1.02 V *vs.* RHE) and current density (~5.2 mA cm^{-2}) in 0.1 M KOH electrolyte. These values are in excellent agreement with those reported for the state-of-the-art Pt/C catalyst. Significantly, materials produced *via* this approach can be manufactured on a large scale, thereby providing access to next-generation catalysts for important electrochemical processes.

Catal. Sci. Technol., 2018, 8**, 5244-5250**

Nanosized Samarium Modified Au-$Ce_{0.5}Zr_{0.5}O_2$ Catalysts for Oxidation of Benzyl Alcohol

Alaa J. Faqeeh, Tarek T. Ali*, Sulaiman N. Basahel, Katabathini Narasimharao

In this study, Au-$Ce_{0.5}Zr_{0.5}O_2$ (Au-CeZr) and Sm modified AuCeZr catalysts were synthesized by organic deposition-precipitation method using gold acetate and samarium acetate as Au and Sm precursors and tetrapropyl ammonium hydroxide as precipitating agent. The synthesized nanocrystalline Au-CeZr and Sm modified Au-CeZr materials found be effective catalysts for benzyl alcohol oxidation at low reaction temperatures. The catalysts were characterized by XRD, SEM, TEM, DRIFT spectra after pyridine adsorption, N_2-physisorption, XPS and H_2-TPR techniques. The Au nanoparticles are highly dispersed on CeZr support and XRD reflections due to presence of Au metal were not observed for the samples which contained less than 1.0 wt% Au. The XPS and H_2-TPR results revealed that at lower Au loadings, strong Au-CeZr interaction resulted an easy exclusion of surface oxygen ions in Au-CeZr and Sm-Au-CeZr catalysts. Pyridine adsorption results indicated an increase of Lewis acid sites of the CeZr support after Au deposition and Sm modification. The 2.0 Sm-0.5Au-CeZr catalyst is most active and selective catalysts for benzyl alcohol oxidation among the synthesized catalysts due to optimum loading of Au and Sm. An optimal surface acidity and redox properties is accountable for the improved catalytic activity of 2.0 Sm-0.5Au-CeZr catalyst in the benzyl alcohol oxidation.

Mol. Cat., 456 (2018) 10–21

Acidic Peptizing Agent Effect on Anatase-Rutile Ratio and Photocatalytic Performance of TiO_2 Nanoparticles

Hatem A. Mahmoud, Katabathini Narasimharao, Tarek T. Ali and Kamal M. S. Khalil,

TiO_2 nanoparticles were synthesized from titanium isopropoxide by a simple peptization method using sulfuric, nitric, and acetic acids. The effect of peptizing acid on physicochemical and photocatalytic properties of TiO_2 powders was studied. The structural properties of synthesized TiO_2 powders were analyzed by using XRD, TEM, N_2-physisorption, Raman, DR UV-vis, FTIR, and X-ray photoelectron spectroscopy techniques. The characterization results showed that acetic acid peptization facilitated the formation of pure anatase phase after thermal treatment at 500 °C; in contrast, nitric acid peptization led to a major rutile phase formation (67%). Interestingly, the sample peptized using sulfuric acid yielded 95% anatase and 5% rutile phases. The photocatalytic activity of synthesized TiO_2 nanoparticles was evaluated for degradation of selected organic dyes (crystal violet, methylene blue, and p-nitrophenol) in aqueous solution. The results confirmed that the TiO_2 sample peptized using nitric acid (with rutile and anatase phases in 3:1 ratio) offered the highest activity for degradation of organic dyes, although, TiO_2 samples peptized using sulfuric acid and acetic acid possessed smaller particle size, higher band gap energy, and high surface area. Interestingly, TiO_2 sample peptized with nitric acid possessed relatively high theoretical photocurrent density (0.545 $mA\ cm^{-2}$) and pore diameter (150 Å), which are responsible for high electron-hole separation efficiency and diffusion and mass transportation of organic reactants during the photochemical degradation process. The superior activity of TiO_2 sample peptized with nitric acid is due to the effective transfer of photogenerated electrons between rutile and anatase phases.

Nanoscale Res. Lett., 13:48 (2018) 1 – 13

Mechanisms of Photocatalytic Molecular Hydrogen and Molecular Oxygen Evolution over La-Doped $NaTaO_3$ Particles: Effect of Different Cocatalysts and Their Specific Activity

Irina Ivanova[1], Tarek A. Kandiel[2,3]*, Young-Jin Cho[4], Wonyong Choi[4], and Detlef Bahnemann[1,5]*

[1]Institut für Technische Chemie, Leibniz University Hannover, Callinstr. 3, Hannover, Germany. [2]Department of Chemistry, Faculty of Science, Sohag University, Sohag 82524, Egypt .[3]Department of Chemistry, King Fahd University of Petroleum & Minerals (KFUPM), Dhahran 31261, SA, [4]Division of Environmental Science and Engineering, Pohang University of Science and Technology (POSTECH), Pohang 37673, Korea. [5]Laboratory for "Photoactive Nanocomposite Materials", Saint-Petersburg State University, Ulyanovskaya str. 1, Peterhof, Saint-Petersburg, 198504 Russia.

A better understanding of the mechanisms of H_2 and O_2 evolution over cocatalyst-loaded photocatalysts is an essential step in constructing efficient artificial systems for the overall water splitting. In this paper, La-doped $NaTaO_3$ particles loaded with different cocatalysts (i.e., noble metals and metal oxides) have been synthesized and used as model photocatalysts to study the mechanisms of photocatalytic H_2 and/or O_2 evolution from pure water, aqueous methanol solution, and aqueous silver nitrate solution. It was found that the photocatalytic activity and selectivity toward H_2 and/or O_2 evolution strongly depend on the nature of the cocatalyst and the investigated system. For pure water and aqueous silver nitrate systems, the affinity of the cocatalyst nanoparticles to react with the photogenerated charge carriers (electrons or holes) was found to be the main reason for the observed selective behavior for H_2 and O_2 evolution. The creation of active sites and subsequent decrease in activation energy is thought to play a secondary role. In the presence of methanol, when the dark injection of an electron into the conduction band of the photocatalyst is possible, the catalytic roles of the investigated cocatalysts toward the formation of H_2 gas were found to be decisive, in addition to the charge separation and interfacial electron transfer processes. No overall water splitting into H_2 and O_2 can be achieved utilizing La-doped $NaTaO_3$ loaded with only one cocatalyst; however, it was found that the loading of La-doped $NaTaO_3$ with two different cocatalysts, i.e. RuO_2 and CoO, enables the simultaneous formation of H_2 and O_2 from pure water. The modification of photocatalyst with two different cocatalysts seems to be essential for enhancing the efficiency of overall photocatalytic splitting. The interfacial electron transfer on the cocatalyst-loaded La-doped $NaTaO_3$ was determined by measuring the cathodic and anodic photocurrents in the presence of Fe^{2+}/Fe^{3+} electron shuttle. Methanol and bromate were used as electron donors and electron acceptors during the cathodic and anodic photocurrent measurements, respectively. By correlation of the photocurrent with the activity of the investigated cocatalysts, it was concluded that the creation of active sites and subsequent decrease in activation energy for H2 evolution is the main requirement for efficient H_2 evolution from the aqueous methanol system, whereas the interaction with the photogenerated holes and the formation of intermediates allowing a multielectron transfer process seems to be an essential step for the water oxidation and O_2 evolution. This information appears to be crucial for a rational design of a highly active photocatalyst for overall water splitting under UV−vis illumination.

ACS Catal., (2018) 2313-2325

Macrocycles: MCR synthesis and applications in drug discovery

Abdelraheem, E.M.M.[a,b], Shaabani, S.[a], Dömling, A.[a]

[a]Biokatalyse, Afdeling Biotechnologie, Technische Universiteit Delft, Van der Maasweg 9, Netherlands
[b]Chemistry Department, Faculty of Science, Sohag University, Sohag, 82524, Egypt

Abstract

Macrocycles are an emerging and largely underexploited part of chemical space where potential drugs for difficult genomic targets can be discovered. Macrocycles can have advantages over their natural twins such as better control over synthesis, physicochemical properties and target binding. Fast and convergent synthesis pathways are underdeveloped. Multicomponent reaction (MCR) chemistry is very well suited for the synthesis of a diverse range of macrocycles and is also able to generate great levels of molecular diversity and complexity at low synthetic costs

Drug Discovery Today: Technologies, Volume 29, November 2018, Pages 11-17

Synthesis, theoretical investigations, biocidal screening, DNA binding, *in vitro* cytotoxicity and molecular docking of novel Cu(II), Pd(II) and Ag(I) chlorobenzylidene Schiff base: Promising antibiotic and anticancer agents

Laila H. Abdel-Rahman[1], Mohamed Shaker S. Adam[1, 2], Ahmed M. Abu-Dief[1]*, H. Moustafa[3], Maram T. Basha[4], Ahmed S. Aboraia[5] and Hanan El-Sayed Ahmed[1]

[1]Chemistry Department, Faculty of Science, Sohag University, Sohag 82534, Egypt

[2]Department of Chemistry, College of Science, King Faisal University, P.O. Box 380, Al Hufuf, SA

[3]Chemistry Department, Faculty of Science, Cairo University, 12613 Giza, Egypt

[4]Depart ment of Chemistry, Faculty of Science, King Abdulaziz University, Jeddah, Saudi Arabia

[5] Medicinal Chemistry Department, Faculty of Pharmacy, Assiut University, Assiut, Egypt

Abstract

Three new Cu(II), Pd(II) and Ag(I) complexes with bi-dentate Schiff base ligand "HL" namely 2-[(4-Chloro-benzylidene)-amino]-phenol were synthesized. The stoichiometric ratios and physicochemical properties of these complexes were determined using elemental analyses (C, H, and N), magnetic measurements, IR, UV-Vis spectra, molar conductivity and thermal analyses. The results revealed that the metal ions coordinated with ligand HL through azomethine nitrogen and phenolic oxygen atoms. AgL and PdL complexes are present in a 1:1 molar ratio with square planar and tetrahedral geometry, respectively while CuL_2 complex is present in a 1:2 molar ratio with octahedral (Oh) geometry. The electronic structure and nonlinear optical parameters (NLO) of the titled ligand HL and the studied 1:1 and 1:2 complexes were investigated theoretically at the DFT-B3LYP/6-311G** level of theory. The compounds were screened against various strains of bacteria and fungi. They displayed good results of inhibition against the studied pathogenic microorganism. The absorption spectroscopic, viscosity and gel electrophoresis measurements were used for studying the interaction of the investigated complexes with calf thymus DNA (CT-DNA). The studied complexes showed a good interaction with CT-DNA *via* intercalation and groove modes. Moreover, molecular docking of these complexes was studied to understand the drug–DNA interactions and calculate the potential binding mode and energy. Furthermore, the anticancer effects of HL and its complexes, on selected human carcinoma cell lines, were determined. The cytotoxic results showed that the prepared complexes are more potent than its Schiff base ligand**.**

Appl Organometal Chem. 2018,32, e4527.

Adsorption of the Heavy Metal Ions onto Bio sorbents: A review

Ahmed M. Abu-Dief[1*] and Mallak Megalea Zikry[2]

[1]Chemistry Department, Faculty of Science, Sohag University, 82534 Sohag, Egypt.

[2]Medicinal and Aromatic Plants Researches Department, Horticulture Research Institute (HRI), Agri. Res. Center (ARC), Giza, Egypt.

Abstract:

Heavy metal pollution possess a great potential threat to the environment and has its own damaging effects to plants, animals and ultimately to human health, because of its release into the environment and water bodies results in a variety of illnesses related with the risk of dermal damage, respiratory problems and several kinds of cancer. The removal of heavy metals from aqueous solutions by using biomass to reduce the problem of limited and scarce water resources which is considered the most important obstacles at all that prevent the continued implementation of plans State's expansion, maximize benefit from the available water resources and reduce the growing gap between available water resources and the required water needs to maintain international water security and the health of the human. Thus, our study is to investigate the ability of natural bio sorbents for removing heavy metal aqueous solution.

Int. J. Nano. Chem. 4, No. 3, 27-39 (2018) 27

Electric, Thermoelectric and Magnetic Properties of Nickel(II) Imine Nanocomplexes

A. Elshafaie*, Laila H. Abdel-Rahman†, Ahmed M. Abu-Dief†, Samar Kamel Hamdan†, A. M. Ahmed* and E. M. M. Ibrahim*

**Physics Department, Faculty of Science Sohag University, Sohag 82524, Egypt*

†Chemistry Department, Faculty of Science Sohag University, Sohag 82524, Egypt

Abstract:

Production of novel organic semiconductor nanomaterials is essential for enabling the development of personal, portable and °exible electronic modules. This work presents Ni(II)-Schi® base complexes with enhanced Seebeck coe±cient and weak ferromagnetic ordering for thermoelectric and magnetic devices. Four Ni(II)-Schi® base complexes (namely $[Ni(C_{12}H_{10}N_3O_4Br)].2H_2O$, $[Ni(C_{16}H_{11}N_3O_4].2H_2O$, $[Ni(C_{21}H_{14}N_5O_8Br)]$ and $[Ni(C_{25}H_{17}N_5O_8].1/2H_2O)$ have been synthesized in nanosized dimensions. The electrical and thermoelectric properties have been studied, and comprehensive discussions have been presented to understand the electrical conduction mechanisms. The electrical conductivity measurements reveal that the conduction is due to the charge carriers hoping between the atomic sites of the same energy levels in the molecule as well as the transfer of the charge carriers between the neighboring complex molecules due to overlapping of their orbitals. The thermoelectric measurement con¯rms that the nanocomplexes (NCs) are non-degenerate P-type semiconductors with enhanced Seebeck coe±cient values compared with those reported for other organic materials. The NCs exhibit antiferromagnetic to paramagnetic transitions with the increase of temperature and weak ferromagnetic ordering at 300 K.

NANO: Brief Reports and Reviews Vol. 13, No. 7 (2018) 1850074 (14 pages)

The synthesis of CuO and NiO nanoparticles by facile thermal decomposition of metal-Schiff base complexes and an examination of their electric, thermoelectric and magnetic Properties

E.M.M. Ibrahim[a], Laila H. Abdel-Rahman[b], Ahmed M. Abu-Dief[b], A. Elshafaie[a], Samar Kamel Hamdan[b], A.M. Ahmed[a]

[a] Physics Department, Faculty of Science, Sohag University, Sohag 82524, Egypt

[b] Chemistry Department, Faculty of Science, Sohag University, Sohag 82524, Egypt

Abstract:

In this study, CuO and NiO NPs have been synthesized by facile thermal decomposition of Schiff base complexes and their physical properties have been examined. The synthesized CuO and NiO NPs are crystallized in polycrystalline monoclinic and cubic structures with average particle size 17 ± 0.4 and 62 ± 1 nm, respectively. The electrical conductivity measurements confirm that the conduction in the CuO NPs is a band-to-band type while the conduction in the NiO NPs is governed by the large polaron conduction mechanism. The thermoelectric measurements confirm that the CuO and NiO NPs are P-type degenerate semiconductors with room temperature Seebeck coefficients equal to 89.9 and 12.1 mV/K, respectively. The magnetic measurements exhibit that the NPs have weak ferromagnetic ordering and antiferromagnetic to paramagnetic transition with high dipolar interaction.

Materials Research Bulletin 107 (2018) 492–497

Disposal of Heavy Transition Cd^{2+} Ions from Aqueous Solution Utilizing Nanosized Flamboyant Pod (*Delonix regia*)

Laila H. Abdel-Rahman[a], Ahmed M. Abu-Dief [a]*, M. A. Abd- ElSayed [b] and Mallak Megalea Zikry [b]

[a] *Chemistry Department, Faculty of Science, Sohag University, 82534 Sohag, Egypt*

[b] *Medicinal and Aromatic Plants Researches Department, Horticulture Research Institute (HRI), Agri. Res. Center (ARC), Giza, Egypt*

Abstract:

The absorption of toxic heavy metal by natural adsorbents from water were indicated by investigation the effect of nano sized (*Delonix regia* (DR)) and (CADR) citric acid *Delonix regia* chemically modified adsorbent for removing the Cd^{2+} ions. Different techniques were employed for characterizing the adsorbent (*Delonix regia*) such energy dispersive analysis of X-ray (EDAX), Fourier transform infrared spectroscopy (FT-IR), Transmission electron microscopy (TEM), X-ray powder diffraction (XRD) and scanning electron microscopy (SEM). The effect of temperature, dosage of adsorbent, contact time, pH and Cd^{2+} ion concentration on adsorption process were studied. (q_m) the maximum adsorption capacity of Cd^{2+} ions by *Delonix regia* was 37.2 mg g^{-1}. The highest removal efficiency (R.E.) was 96.00 % at pH 4.0. FT-IR peaks indicated that the main functional groups are hydroxyl and carboxylic groups are responsible for Cd^{2+} ions binding in the adsorption. The adsorption process was endothermic. The adsorption process was best described by pseudo second order kinetics model. The Freundlich isotherm has a better fit with the experimental data compared to Langmuir isotherm. These results indicated that *Delonix regia i*s environment friendly, available and low cost adsorbent for adsorbing the Cd^{2+} ions.

Journal of Transition Metal Complexes Vol. 1 (2018), Article ID 236055, 10 pages

Electric, thermoelectric and magnetic characterization of γ-Fe2O3 and Co3O4 nanoparticles synthesized by facile thermal decomposition of metal-Schiff base complexes

E.M.M. Ibrahim[a], , Laila H. Abdel-Rahman[b], Ahmed M. Abu-Dief[b], A. Elshafaie[a], Samar Kamel Hamdan[b], A.M. Ahmed[a]

[a] *Physics Department, Faculty of Science, Sohag University, Sohag 82524, Egypt*

[b] *Chemistry Department, Faculty of Science, Sohag University, Sohag 82524, Egypt*

Abstract

Using novel compounds for synthesis of metal oxide nanomaterials can tune their physical properties due to the associated variation in the shape, size and crystallinity. In this work, γ-Fe_2O_3 and Co_3O_4 nanoparticles were successfully prepared by a facile thermal decomposition route, employing $[Fe(C_{32}H_{22}N_4O_2)]\cdot 2H_2O$ and [Co ($C_{16}H_{11}N_3O_4$)].1/2H_2O complexes, respectively as new precursors. The x-ray diffraction and high resolution transmission electron microscopy investigation confirmed that the materials consist of highly pure spinel γ-Fe_2O_3 and Co_3O_4 nanoparticles with average size of ∼9 and 30 nm, respectively. The electrical conduction is governed by the hopping mechanism. The thermoelectric power measurements confirmed that Co_3O_4 nanoparticles are non-degenerate semiconductor with Fermi energy ∼1.21 eV while γ-Fe_2O_3 nanoparticles showed a degenerate to non-degenerate transition. The Co_3O_4 nanoparticles showed a weak ferromagnetic ordering that could be attributed to uncompensated surface spins due to finite-size effects. But γ- Fe_2O_3 NPs show superparamagnetic behavior at room temperature

Materials Research Bulletin 99 (2018) 103–108

The electric and thermoelectric properties of Cu(II)-Schiff base nano-complexes

E M M Ibrahim[1], Laila H Abdel-Rahman[2], Ahmed M Abu-Dief[2], A Elshafaie[1], Samar Kamel Hamdan[2] and A M Ahmed[1]

[1]Physics Department, Faculty of Science, Sohag University, Sohag 82524, Egypt

[2]Chemistry Department, Faculty of Science, Sohag University, Sohag 82524, Egypt

Abstract

The physical properties, such as electric and optical properties, of metal-Schiff base complexes have been widely investigated. However, their thermoelectric properties remain unreported. This work presents Cu(II)-Schiff base complexes as promising materials for thermoelectric power generation. Therefore, three Cu(II)-Schiff base complexes (namely, $[Cu(C_{32}H_{22}N_4O_2)].\frac{3}{2}H_2O$, $[Cu(C_{23}H_{17}N_4O_7Br)]$, and $[Cu(C_{27}H_{22}N_4O_8)].H_2O$) have been synthesized in nanosized scale. The electric and thermoelectric properties have been studied and comprehensive discussions have been presented to promote the nano-complexes practical applications in the field of thermoelectric power generation. The electrical measurements confirm that the nano-complexes are semiconductor and the electrical conduction process is governed by intermolecular and intramolecular transfere of the charge carriers. The thermoelectric measurements reveal that the Cu(II)--Schiff base nano-complexes are nondegenerate P-type semiconductors. The measured Seebeck coefficient values were higher compared to the values reported in previous works for other organic materials indicating that the complexes under study are promising candidate for theremoelectric applications if the electrical conductivity could be enhanced.

Phys. Scr. 93 (2018) 055801 (8pp)

Development and functionalization of magnetic nanoparticles as powerful and green catalysts for organic synthesis

Ahmed M. Abu-Dief, Shimaa Mahdy Abdel-Fatah

Chemistry Department, Faculty of Science, Sohag University, 82534 Sohag, Egypt

Abstract

Magnetic nanoparticles are a highly worthy reactant for the correlation of homogeneous inorganic and organic containing catalysts. This review deals with the very recent main advances in the development of various nano catalytic systems by the immobilization of homogeneous catalysts onto magnetic nanoparticles. Catalytic fields include the use of mainly cobalt, nickel, copper, and zinc ferrites, as well as their mixed-metal combinations with Cr, Cd, Mn and sometimes some lanthanides. The ferrite nanomaterials are obtained mainly by co-precipitation and hydrothermal methods, sometimes by the sonochemical technique, micro emulsion and flame spray synthesis route. Catalytic processes with application of ferrite nanoparticles include degradation (in particular photocatalytic), reactions of dehydrogenation, oxidation, alkylation, C–C coupling, among other processes. Ferrite nano catalysts can be easily recovered from reaction systems and reused up to several runs almost without loss of catalytic activity. Finally, we draw conclusions and present a futurity outlook for the further development of new catalytic systems which are immobilized onto magnetic nanoparticles

Beni-Suef University Journal of Basic and Applied Sciences 7 (2018) 55–67

Int. J. Nano. Chem. 4, No. 1, 1-17 (2018) 1

Functionalization of Magnetic nanoparticles for drug delivery

Ahmed M. Abu-Dief* and Azza A. Hassan Abdel-Mawgoud
Chemistry Department, Faculty of Science, Sohag University-82524, Egypt

Abstract
Magnetic nanoparticles (MNPs) possess unique magnetic properties and the ability to function at the cellular and molecular level of biological interactions making them an attractive platform as carriers for drug delivery. Recent advances in nanotechnology have improved the ability to specifically tailor the features and properties of MNPs for these biomedical applications. To better address specific clinical needs, MNPs with higher magnetic moments, non-fouling surfaces, and increased functionalities are now being developed for applications in the detection, diagnosis, and treatment of malignant tumors, cardiovascular disease, and neurological disease. Through the incorporation of highly specific targeting agents and other functional ligands, such as fluorophores and permeation enhancers, the applicability and efficacy of these MNPs have greatly increased. This review provides a background on applications of MNPs as carriers for drug delivery and an overview of the recent developments in this area of research.
SF J. Nanochem. Nanotechnol. 2018; 1(1)1-6

Hydrothermal Preparation and Characterization of $ZnFe_2O_4$ Magnetic Nanoparticles as an Efficient Heterogeneous Catalyst for the Synthesis of Multi-Substituted Imidazoles (MSI) and Study of their Anti-Inflammatory Activity

Adel A. Marzouk[a], Ahmed M. Abu-Dief*[b] and Antar A. Abdelhamid[b]
[a]*Pharmaceutical Chemistry Department, Faculty of Pharmacy, Al Azhar University, Egypt*
[b]*Department of Chemistry, Faculty of Science, Sohag University, 82524 Sohag, Egypt.*

Abstract:
Nanoparticles are key focus of research for a wide elongated novel applications. From this point of view, $ZnFe_2O_4$ magnetic nanoparticles was synthesized hydrothermally and characterized via SEM, TEM, HR-TEM, powder X-ray, EDAX, IR, TGA as well as magnetic measurements. Moreover, it was used as a robust catalyst for the synthesis of the biologically active series of multi-substituted imidazoles (MSI) by a multicomponent reaction by the reaction between of benzil with different aromatic aldehydes, ammonium acetate, and aliphatic amine (N,N-Dimethyl-1,3-propanediamine and 1-amino-2-propanol) under solvent-free conditions. The key advantages of this method are shorter reaction times, very high yield, and ease of establishment. The thermally and chemically stable, benign and economical catalyst was easily recovered using an external magnet and reused in at least five successive runs without an appreciable loss of activity**.** All of these novel synthesized compounds have been characterized from spectral data and their purity were checked by TLC and give one spot. Furthermore, the prepared compounds were tested for their anti-inflammatory activity.
Appl Organometal Chem. 2018, 32(1), e3794.

Synthesis, characterization and photocatalysis enhancement of Eu_2O_3- ZnO mixed oxides nanoparticles

W.S.Mohamed[a] and Ahmed M. Abu-Dief[b]

[a]Physics Department, Faculty of Science, Sohag University, 82524 Sohag, Egypt

[b]Chemistry Department, Faculty of Science, Sohag University, 82524 Sohag, Egypt

Abstract

Pure zinc oxide nanoparticles (ZnO NPs) and europium oxide mixed ZnO nanoparticles (Eu_2O_3 mixed ZnO NPs) at different Eu_2O_3 ratios (5, 10 and 15 %) were synthesized by precipitation method at optimum conditions. The synthesized samples have been characterized by means of X-ray diffraction (XRD), scanning electron microscopic (SEM) with energy dispersive X-ray spectroscopy (EDXS), transmission electron microscope (TEM), Fourier transfer infrared spectroscopy (FTIR), Raman spectroscopy and UV–Vis diffuse reflectance spectroscopy (UV–Vis DRS). We found that the as-synthesized ZnO NPs exhibit high phase purity and well crystalline wurtzite ZnO structure. The Eu_2O_3- ZnO NPs exhibit Eu_2O_3 zinc blend phase in addition to the wurtzite phase of pure ZnO confirming a high purity and good crystallinity of the as-synthesized samples. The high-purity formation of ZnO and Eu_2O_3 phases were confirmed by FTIR and Raman spectra. Microstructural analysis by SEM and TEM confirms the sphere-like morphology with different particle sizes (29-40 nm) of the as-synthesized samples. The photocatalytic activities of pure ZnO NPs and Eu_2O_3- ZnO NPs, for the degradation of methylene blue (MB), were evaluated under Ultraviolet (UV) light irradiation. The results show that the Eu_2O_3 played an important role in the enhancement of photocatalytic properties of ZnO NPs. We found that 5% Eu_2O_3 mixed ZnO nanoparticles exhibit the highest photocatalytic activity (degradation efficiency is 96.5% after 180 min of UV light irradiation), as compared with pure ZnO NPs (degradation efficiency is 80.3% after 180 min of UV light irradiation). The improved photocatalytic activity of optimum Eu_2O_3 mixed ZnO is due to its high crystallinity, high surface area with small particle size and narrow energy gap.

Journal of Physics and Chemistry of Solids 116 (2018) 375–385

Two-Step Macrocycle Synthesis by Classical Ugi Reaction

Abdelraheem, E.M.M[a,b],Khaksar, S[a],Kurpiewska, K[c],Kalinowska-Tuścik, J[c],Shaabani, S.[a],Dömling, A[a]

[a]Department of Drug Design, University of Groningen, A. Deusinglaan 1, Groningen, 9713 AV, Netherlands

[b]Chemistry Department, Faculty of Science, Sohag University, Sohag, 82524, Egypt

[c]Faculty of Chemistry, Jagiellonian University, Gronostajowa 2, Krakow, 30-387, Poland

Abstract

The direct nonpeptidic macrocycle synthesis of α-isocyano-ω-amines via the classical Ugi four-component reaction (U-4CR) is introduced. Herein an efficient and flexible two-step procedure to complex macrocycles is reported. In the first step, the reaction between unprotected diamines and isocyanocarboxylic acids gives high diversity of unprecedented building blocks in high yield. In the next step, the α-isocyano-ω-amines undergo a U-4CR with high diversity of aldehydes and carboxylic acids in a one-pot procedure. This synthetic approach is short and efficient and leads to a wide range of macrocycles with different ring sizes

Journal of Organic Chemistry, Volume 83, Issue 3, 2 February 2018, Pages 1441-1447

Catalytic activity of nickel(II), copper(II) and oxovanadium(II)-dihydroindolone complexes towards homogeneous oxidation reactions

Mohamed Shaker S. Adam[1,2*]

[1]*Department of Chemistry, College of Science, King Faisal University, P.O. Box 380 Al Hufuf , SA.*

[2]*Department of Chemistry, Faculty of Science, Sohag University, Sohag-82534, Egypt.*

Abstract:

Three novel paramagnetic metal complexes (MH_2ID) of Ni^{2+}, Cu^{2+} and VO^{2+} ions with 3-hydroxy-3,3'-biindoline-2,2'-dione (dihydroindolone, H_4ID) were synthesized and characterized by different spectroscopic methods. The ligand (H_4ID) was synthesized *via* homocoupling reaction of isatin in presence of phenylalanine in methanol. Complexation of low valent Ni^{2+}, Cu^{2+} ions and high valent VO^{2+} ions with H_4ID carried out in 1 : 2 molar ratios. A comparison in the catalytic potential of paramagnetic complexes of low and high valent metal ion was explored in the oxidation processes of *cis*-cyclooctene, benzyl alcohol and thiophene by an aqueous H_2O_2, as a green terminal oxidant, in the presence and absence of acetonitrile, as an organic solvent, at 85 °C. NiH_2ID, CuH_2ID and VOH_2ID show good catalytic activity, *i.e.* good chemo- and regioselectivity. VOH_2ID has the highest catalytic potential compared to both Ni^{2+}- and Cu^{2+}-species in the same homogenous aerobic atmosphere. Catalytic oxidation of other alkenes and alcohols was also studied using NiH_2ID, CuH_2ID or VOH_2ID as a pre-catalyst by an aqueous H_2O_2. A mechanistic pathway for those oxidation processes was proposed.

Applied Organometallic Chemistry, 32 (2018) e4234.

Anionic oxide-vanadium Schiff base amino acid complexes as potent inhibitors and as effective catalysts for sulfides oxidation: Experimental studies complemented with quantum chemical calculations

Mohamed Shaker S. Adam[a,b*], Hany M. Abd El-Lateef[a,b*], Kamal A. Soliman[c]

[a] *Department of Chemistry, College of Science, King Faisal University, P.O. Box 380 Al Hufuf, SA*

[b] *Chemistry Department, Faculty of Science, Sohag University, Sohag-82534, Egypt.*

[c] *Chemistry Department, Faculty of Science, Benha University, 13518Benha, Egypt.*

Abstract:

Three anionic oxide-vanadium Schiff base *N*-salicylidene amino acid complexes are derived from the reaction of sodium salicylaldehyde-5-sulfonate with phenylalanine (VO-1), alanine (VO-2) or glycine (VO-3), followed by mixing with vanadyl sulfate monohydrate. Inhibition effect of VO-1, VO-2 and VO-3 is investigated for the corrosion of carbon steel in chloride acid solution. From the electrochemical measurements, VO-complexes protect carbon steel form corrosion, yielding maximum inhibition efficiency up to 94.7% in the presence of 1.0 mM VO-1 inhibitor. All VO-complexes act as mixed-type inhibitors. The SEM and EDX investigations provided the appearance of an inhibitor layer encasement the steel surface. Catalytic efficiency of VO-complexes is measured in the symmetric and asymmetric oxidation of sulfides by using an aqueous H_2O_2. All complexes show high catalytic potentials towards sulfides oxidation. VO-1, VO-2 and VO-3 are optimized at B3LYP/GEN and B3LYP/LANL2DZ levels of theory in gas and aqueous phases. Theoretical results agree with the experimental reactivity of the VO-complexes, as corrosion inhibitors and catalysts for sulfides oxidation.

Journal of Molecular Liquids, 250 (2018) 207-322

Catalytic performance of binary and ternary oxovanadium complexes of dipyridinyl-urea in (ep)oxidation of *cis*-cyclooctene and 1-octene

Mohamed Shaker S. Adam[a,b]*, Aly M. Hafez, Ibrahim El-Ghamry[c]

[a] *Department of Chemistry, College of Science, King Faisal University, Al Hufuf 31982 Al Hassa, SA*

[b] *Chemistry Department, Faculty of Science, Sohag University, Sohag-82534, Egypt.*

[c] *Chemistry Department, Faculty of Science, Benha University, 13518Benha, Egypt.*

Abstract:

Two novel ternary and binary mono-oxovanadium (IV) complexes of acetylacetonate (ac) and 1,3-dipyridin-2-yl-urea (HL) are synthesized, as VO(acac)(L) (1 : 1) and $VO(L)_2$ (1 : 2). They are characterized by various physico-chemical spectroscopic tools. The formation constants K_f are calculated from the spectrophotometric measurements. The catalytic potential of VO(acac)(L) and $VO(L)_2$ has been examined in the (ep)oxidation of alkenes (*cis*-cyclooctene and 1-octene) by an aqueous hydrogen peroxide, H_2O_2, and *tert*-butyl hyderoperoxide, TBHP. The effects of temperature, solvent and oxidant/alkene molar ratio are studied in order to get the optimized reaction conditions. Most of the catalytic (ep)oxidation products of *cis*-cyclooctene and 1-octene are determined qualitatively and quantitatively using gas chromatographic analysis. The increase of the catalyst amount to double time reduces the (ep)oxidation process time with improvement of the amount of the chemoselective epoxy product.

Reaction Kinetics, Mechanisms and Catalysis, 124 (2018) 779-805

Synthesis of polar unique 3d metal-imine complexes of salicylidene anthranilate sodium salt. Homogeneous catalytic and corrosion inhibition performance

Hany M. Abd El-Lateef[a,b], Mohamed Shaker S. Adam[a,b], Mai M. Khalaf[a,b]

[a] *Department of Chemistry, College of Science, King Faisal University, P.O. Box 380 Al Hufuf 31982 Al Hassa, Saudi Arabia.*

[b] *Chemistry Department, Faculty of Science, Sohag University, Sohag-82534, Egypt.*

Abstract:

Three polar Ni(II)-, Cu(II)- and Zn(II)-complexes (M-SSA) of salicylidene anthranilate sodium salt ligand were synthesized. The ligand (H_2SSA) and its corresponding metal-complexes are characterized by alternative physico-cehmical tools in which H_2SSA acts as tridentate bi-basic chelating agent. Catalytic potential of M-SSA was investigated in the homogenous oxidation of 1,2-cyclohexene at 80 °C in acetonitrile, water or under solvent-free condition. M-complexes exhibit high catalytic reactivity with high chemoselectivity in acetonitrile. Cu-SSA shows the highest catalytic potential for the oxidation of 1,2-cyclohexene than Ni-SSA or Zn-SSA. The lowest yield of the epoxy-product was obtained in water due to the hydrolysis ring opening reaction affording 1,2-cyclohexanediol. The inhibition performance of H_2SSA and M-SSA on the carbon steel corrosion (CS) in HCl was studied using electrochemical techniques. The inhibition capability was increased with increasing inhibitor dose. The adsorption of inhibitors on the surface of CS obeyed the Langmuir isotherm paradigm. Surface characterizations (SEM/EDX) revealed that the investigated compounds adsorbed on CS surface and form protective layer that shield the surface from direct corrosion attack. The experimental data have been completed by density functional theory treatment. The obtained theoretical results are exceedingly in agreement with empirical results catalytically and inhibitory.

Journal of the Taiwan Institute of Chemical Engineers 88 (2018) 286–304

Biological potential of oxo-vanadium salicylediene amino-acid complexes as cytotoxic, antimicrobial, antioxidant and DNA interaction

Mohamed Shaker S. Adam[1,2]*, Hany Elsawy[1,3]

[1] Department of Chemistry, College of Science, King Faisal University, Al Hufuf 31982 Al Hassa, SA

[2] Department of Chemistry, Faculty of Science, Sohag University, Sohag-82534, Egypt.

[3] Department of Chemistry, Faculty of Science, Tanta University, Tanta-31527, Egypt.

Abstract:

New series of oxo-vanadium N-salicyledieneamino acid Schiff base complexes are synthesized and characterized. They are synthesized from the reaction of sodium salicylaldehyde-5-sulfonate, some amino acids, alanine (VOHL1), leucine (VOHL2) or glycine (VOHL3) in an aqueous media, and leucine (VOHLpy1) or tryptophan (VOHLpy2) in pyridine with vanadyl acetylacetonate. The complexes are characterized by EA, TGA, IR, UV-Visible and mass spectra, conductivity and magnetic measurements. The biological activity of the VO-complexes shows that VOHL1, VOHL2 and VOHL3 exhibit anti-proliferative effect and may be used as anticancer drugs. VO-complexes manifest high toxicity, except VOHL2 is less toxic, and could be applied for the human being. VOHL1, VOHL2 and VOHL3 display a remarkable SOD like potential and act as high inhibiting reagents. VOHLpy1 and VOHLpy2 show low inhibiting potentials. All VO-complexes have good anti-oxidant effect, in which VOHL3 affords the best antioxidant activity. The interaction between VO-complexes and DNA is studied spectrophotometrically and by gel electrophoresis. Binding constants and spectrophotometric parameters indicate a strong interaction between VO-complexes and DNA. All VO-complexes have respectable anti–bacterial and antifungal activities, where VOHL3 shows the maximum potential. DFT calculations of VOHL1 and VOHL3 were discussed in the light of their biological activity, which are convenient with the obtained results.

Journal of Photochemistry & Photobiology, B: Biology 184 (2018) 34–43

Catalytic (ep)oxidation and corrosion inhibition potentials of Cu^{II} and Co^{II} pyridinylimino phenolate complexes

Mohamed Shaker S. Adam[a,b]*, Ahmad Desoky M. Mohamad[b]

[a] Department of Chemistry, College of Science, King Faisal University, Al Hufuf 31982 Al Hassa, SA

[b] Department of Chemistry, Faculty of Science, Sohag University, Sohag-82534, Egypt.

Abstract:

The coordination chemical behavior of pyridinylimino phenolate sodium sulfonate (HPSS) was examined with Cu^{II} and Co^{II} ions to give two novel para-magnetic complexes, CuPSSACl and $Co(PSS)_2$, respectively. In CuPSSACl, Cu^{2+} ion reacts with HPSS in 1 : 1 and 1 : 2 of Co^{2+} ion to HPSS in $Co(PSS)_2$, respectively. Various physico-chemical spectroscopic tools were applied to characterize their molecular structures. The spectrophotometric measurements were used to determine the formation constants, K_f. CuPSSACl and $Co(PSS)_2$ exhibited performed catalytic potential towards the (ep)oxidation of 1,2-cyclooctene by an aqueous H_2O_2 under alternative conditions. The catalytic sufficiency of CuPSSACl and $Co(PSS)_2$ was influenced by other parameters (temperature, solvent and oxidant). CuPSSACl is more effective catalyst than $Co(PSS)_2$. The corrosion inhibition of HPSS and its chelates (CuPSSCl and $Co(PSS)_2$) on carbon steel (CS) in HCl solution were studied using electrochemical (potentiodynamic polarization, PDP and electrochemical impedance spectroscopy, EIS) and surface (SEM and EDX) techniques. The inhibition efficiency incremented with the inhibiting agent concentrations following the sequence: CuPSSCl > $Co(PSS)_2$ > HPSS. Thermodynamically, those compounds act as mixed-type inhibiting agents and obeyed Langmuir adsorption isotherm *via* chemisorption. SEM and EDX investigations confirmed the protective efficiency of the titled inhibiting agents on CS in HCl.

Polyhedron 151 (2018) 118–130

Square wave voltammetric analysis of polyphenol content and antioxidant capacity of red wines using glassy carbon and disposable carbon nanotubes modified screen-printed electrodes

Emad F. Newair[a], Paul A. Kilmartin[b], François Garcia[c]

[a]*Unit of Electrochemistry Applications (UEA), Department of Chemistry, Faculty of Science, University of Sohag, Sohag 82524, Egypt*

[b]*School of Chemical Sciences, University of Auckland Private Bag 92019, Auckland, New Zealand*

[c] *SPO, INRA, Montpellier Supagro, Univ Montpellier, Montpellier, France*

Abstract:

The polyphenols present in different French red wines were characterized electrochemically using square wave voltammetry (SWV). The voltammetric measurements were carried out using a glassy carbon electrode and disposable screen-printed carbon electrodes unmodified and modified with single- and multi-walled carbon nanotubes. The single-walled carbon nanotubes-modified screen-printed carbon electrode (SWCNTs-SPCE) showed the best results for the voltammetric analysis of polyphenols in red wine samples, allowing using disposable electrodes to perform measurements. The obtained voltammograms contained three characteristic oxidation peaks. The first peak at the lowest potential was ascribed to oxidation of catechol and galloyl groups of polyphenols (on the flavonoid B-ring), the second peak to the oxidation of malvidin anthocyanins and the third peak was due mainly to the second oxidation wave of flavonoid phenolic groups. The total polyphenols content was determined by spectrophotometric and chromatographic methods as well as antioxidant capacity by the ABTS method, and were in good agreement with the SWCNTs-SPCE results. Thus, SWV is a satisfying fast electrochemical technique for the polyphenol characterization and antioxidant capacity determination of red wine compared to the more frequently used cyclic voltammetry or differential pulse voltammetry, especially using SWCNTs-SPCE.

European Food Research and Technology 2018, 244, 1225–1237.

Mechanistic Pathways and Identification of the Electrochemically Generated Oxidation Products of Flavonoid Eriodictyol in the Presence of Glutathion

Emad F. Newair[a], Refat Abdel-Hamid[a], Ayman Nafady[a,b], Abdullah M. Al-Enizi[b], Franc¸ois Garcia[c]

Unit of Electrochemistry Applications (UEA), Department of Chemistry, Faculty of Science, University of Sohag, Sohag 82524, Egypt

[b]*Department of Chemistry, College of Science, King Saud University, Riyadh 11451, Saudi Arabia*

[c] *SPO, INRA, Montpellier Supagro, Univ Montpellier, Montpellier, France*

Abstract:

The metabolic oxidation pathways of dietary flavonoid eriodictyol (Er) are not very well-probed. In the present work, the electrochemical oxidation behavior of Er was studied in aqueous Britton-Robinson (B-R) buffer solution using cyclic voltammetry (CV), chronoamperometry (CA), and bulk-electrolysis (BE). The oxidation products and reaction pathways of Er in the absence and the presence of glutathione (GSH) were proposed and identified in view of the results obtained by ultra-highperformance liquid chromatography coupled with mass spectrometry (UPLC-MS). In the absence of GSH, eriodictyol shows one quasi-reversible oxidation process at E1/2=0.305 V, followed by a totally irreversible anodic peak at a more positive potential (E_p^a=1.05 V vs. Ag/AgCl, 3 M KCl). Putatively, the first process correspondsto the oxidation of the catechol moiety on the B ring of Er while the second one is attributed to the oxidation of the resorcinol moiety on the A ring. In the presence of GSH, however, the anodic oxidation of Er was proposed to be an ECEC-type mechanism. The Er molecule first underwent a two-electron oxidation coupled with loss of two-proton to generate the corresponding quinone, which was either reduced to the original Er molecule by GSH, or further interacted with GSH to produce mono- and biglutathione conjugates of Er. The proposed mechanism was confirmed by digital simulation of the cyclic voltammograms.

Electroanalysis 2018, 30, 1706 – 1714

Elucidating the Role of CO_2 in the Soft Oxidative Dehydrogenation of Propane over Ceria-Based Catalysts

Ewa Nowicka[a,b], Christian Reece[a], Sultan M. Althahban[c], Khaled M. H. Mohammed[d,e,f], Simon A. Kondrat[a,g], David J. Morgan[a], Qian He[a], David Willock[a], Stanislaw Golunski[a], Christopher J. Kiely[a,c] and Graham J. Hutchings[a].

[a]School of Chemistry, Cardiff University, Main Building, Park Place, Cardiff CF10 3AT, U.K., [b]Institut für Chemie, Technische Universität Berlin, Straße des 17. Juni 124, 10623 Berlin, Germany, [c]Department of Materials Science and Engineering, Lehigh University, 5 East Packer Avenue, US, [d]Chemistry Department, Faculty of Science, Sohag University, Sohag 82524, Egypt, [e]UK Catalysis Hub, Research Complex at Harwell, RAL, Harwell, Oxfordshire OX110FA, U.K., [f]Department of Chemistry, University College London, 20 Gordon Street, London WC1H 0AJ, U.K., [g]Department of Chemistry, Loughborough University, Loughborough, Leicestershire LE11 3TU, U.K

Abstract:

A mixed oxide support containing Ce, Zr, and Al was synthesized using a physical grinding method and applied in the oxidative dehydrogenation of propane using CO_2 as the oxidant. The activity of the support was compared with that of fully formulated catalysts containing palladium. The $Pd/CeZrAlO_x$ material exhibited long-term stability and selectivity to propene (during continuous operation for 140 h), which is not normally associated with dehydrogenation catalysts. From temperature-programmed desorption of NH_3 and CO_2 it was found that the catalyst possessed both acidic and basic sites. In addition, temperature-programmed reduction showed that palladium promoted both the reduction and reoxidation of the support. When the role of CO_2 was investigated in the absence of gas-phase oxidant, using a temporal analysis of products (TAP) reactor, it was found that CO_2 dissociates over the reduced catalyst, leading to formation of CO and selective oxygen species. It is proposed that CO_2 has the dual role of regenerating selective oxygen species and shifting the equilibrium for alkane dehydrogenation by consuming H_2 through the reverse water-gas-shift reaction. These two mechanistic functions have previously been considered to be mutually exclusive.

ACS Catalysis, 8(4) (2018) 3454-3468.

Fine-template synthetic process of mesoporous TiO_2 using ionic/nonionic surfactants as potential remediation of Pb(II) from contaminated soil

Mai M. Khalaf*[1,3], Naglaa Y. Abdallah[2], Hany M. Abd El-Lateef*[1,3]

[1]Chemistry Department, Faculty of Science, Sohag University, 82524 Sohag, Egypt

[2]Botany & Microbiology Department, Faculty of Science, Sohag University, 82524 Sohag, Egypt

[3]Department of Chemistry, College of Science, King Faisal University, Al Hufuf, 31982 Al Hassa, SA

This trend of research deals with preparation of mesoporous TiO_2 by a simple approach using sol gel method by various surfactant templates. The designed nano adsorbents TiO_2 were featured by various characterization methods of Fourier Transform Infrared (FT-IR), X-ray diffraction (XRD), Surface area analysis (Brunauer-Emmett-Teller, BET), Transmission electron microscope (TEM), and Scanning electron microscope (SEM). These obtained nano adsorbents are examined as functional adsorbents for lead ions up taking from contaminated soil specimens. The results presented the effect of ionic and nonionic surfactant templates on the texture of the three types of mesoporous TiO_2 nano adsorbents. The effects of the temperature, pH and amount of nano adsorbents TiO_2 on the adsorption process were studied. The optimum conditions of 25 °C, 5, and 0.1 g were obtained for temperature, pH and amount of adsorbents, respectively. The obtained results revealed that about 97.6, 99.1, and 95.3 % of total adsorptive capacity were obtained for Ti C, Ti S, and Ti P, respectively at 100 mg/L of Pb (II) ions in soil solutions during 120 min. The Adsorption Isotherm and the thermodynamic parameters were further illustrated. These findings recommended these nano adsorbent TiO_2 as adequate adsorbents in remediation process of Pb enriched soil.

International Journal of Environmental Science and Technology (2018)

A facile Synthetic Route to novel Polyamides-Based on Thieno[2,3-*b*]thiophene and Their Application for Corrosion Inhibition Behavior

Kamal I Aly[a], Amr H Moustafa*[b], Hany M Abd El-lateef [b, c], Essam K Ahmed[d], Mohamed Gamal Mohamed[a] and Sahar M Mohamed[d]

[a]*Polymer Research Lab , Chemistry Department, Faculty of Science, Assiut University, Assiut 71516, Egypt*
[b]*Chemistry Department, Faculty of Science, Sohag University ,Sohag 82524, Egypt*
[c]*Chemistry Department, College of Science, King Faisal university, Al Hufuf, 31982 Al Hassa, Saudi Arabia*
[d]*Chemistry Department, Faculty of Science, Minia University, El-Minia 61519 Egypt*

Polyamides containing thieno[2,3-*b*]thiophene moiety have been prepared *via* a simple polycondensation reaction of the diaminothieno[2,3-*b*]thiophene monomer **1a** with different kinds of diacid chlorides (including, oxaloyl, adipoyl, sebacoyl, isophthaloyl, terephthaloyl, 4,4′-azodibenzoyl, 3,3′-azodibenzoyl, *p*-phenylene diacryloyl) in the presence of LiCl anhydrous as a catalyst and NMP as solvent through low-temperature solution polycondensation technique. The chemical structures of model compound and synthesized polyamides have been confirmed by FT-IR, nuclear magnetic resonance spectroscopy (including, ^{1}H-NMR and ^{13}C-NMR) and elemental analysis. In addition, the thermal stability, crystallinity structure and surface morphology of synthesized polyamides were characterized *via* Thermogravametric analysis (TGA), Wide-angle X-ray diffraction analysis (WXRD) and scanning electron microscope (SEM). Also, the corrosion inhibition behavior of selected examples of polyamides was studied; the inhibitive effect of the investigated polymers for carbon steel in 1.0 M HCl was studied using potentiodynamic polarization (PDP) and electrochemical impedance spectroscopy (EIS) methods. PDP results displayed that the polyamides containing thieno[2,3-*b*]thiophene moiety can be act as mixed-type inhibitors. The inhibition efficiency (*P* %) was found to be in the range 67.13-96.01%. There is an increase in *P*% by the synthesized polymers in comparison to the starting monomer. The adsorption of these polymers was found to obey Langmuir adsorption isotherm.

Chinese J. Polym. Sci. 2018, 36, 835–847

Anionicoxide-vanadium Schiff base amino acid complexes as potent inhibitors and as effective catalysts for sulfides oxidation: Experimental studies complemented with quantum chemical calculations

Mohamed Shaker S. Adam[a,b]*, Hany M. Abd El-Lateef[a,b]*, Kamal A. Soliman[c]

[a] *Chemistry Department, Faculty of Science, Sohag University, Sohag-82534, Egypt.*
[b] *Department of Chemistry, College of Science, King Faisal University, Al Hufuf 31982 Al Hassa, SA*
[c] *Chemistry Department, Faculty of Science, Benha University, 13518Benha, Egypt.*

Abstract

Three anionic oxide-vanadium Schiff base *N*-salicylideneamino acid complexes are derived from the reaction of sodium salicylaldehyde-5-sulfonate with phenylalanine (VO-1), alanine (VO-2) or glycine (VO-3), followed by mixing with vanadyl sulfate monohydrate. Inhibition effect of VO-1, VO-2 and VO-3 is investigated for the corrosion of carbon steel in chloride acid solution. From the electrochemical measurements, VO-complexes protect carbon steel form corrosion, yielding maximum inhibition efficiency up to 94.7% in the presence of 1.0 mM VO-1 inhibitor. All VO-complexes act as mixed-type inhibitors. The SEM and EDX investigations provided the appearance of an inhibitor layer encasement the steel surface. Catalytic efficiency of VO-complexes is measured in the symmetric and asymmetric oxidation of sulfides by using an aqueous H_2O_2. All complexes show high catalytic potentials towards sulfides oxidation.VO-1, VO-2 and VO-3 are optimized at B3LYP/GEN and B3LYP/LANL2DZ levels of theory in gas and aqueous phases. Theoretical results agree with the experimental reactivity of the VO-complexes, as corrosion inhibitors and catalysts for sulfides oxidation.

Journal of Molecular Liquids 250 (2018) 307–322

Adsorption and Removal of Cationic and Anionic Surfactants Using Zero-Valent Iron Nanoparticles

Hany M. Abd El-Lateef [1,3*], Mai M. Khalaf Ali [1, 3], Mahmoud M. Saleh[2,3 *]

[1]*Department of Chemistry, Faculty of Science, Sohag University, Sohag, Egypt.*

[2] *Department of Chemistry, Faculty of Science, Cairo University, Cairo, Egypt.*

[3] *Chemistry Department, College of Science, King Faisal University, Al-Hassa, KSA*

This study is dedicated for adsorption of surfactants on Zero-Valent Iron (nZVI). As a nano-adsorbent, nZVI is synthesized by simple and economic method then characterized using various surface and structural techniques. These include; transmission electron micrograph (TEM), field emission scanning electron microscopy (FE-SEM), X-ray diffraction spectroscopy (XRD), BET surface area determination and Zeta potential (ζ–potential) of the nZVI. Nano-ZVI is tested as potential adsorbent for the removal of a cationic surfactant, hexadecylpyridinium chloride surfactant (HDPCl) and anionic surfactant, sodium dodecylbenzene sulfonate (DBS) from dilute solutions. The effects of different experimental parameters such as the amount of nZVI, the initial surfactant concentration, pH, shaking speed, and temperature on the system performance have been studied. The equilibrium adsorption isotherms of the HDPCl and DBS on the nZVI have been fitted with Langmuir model. The obtained thermodynamic parameters demonstrate the easiness and spontaneity of the adsorption process with favorable adsorption extent to the HDPCl compared to the DBS. This was attributed to the difference in the molecular structures. Kinetic studies show that the experimental data for HDPCl and DBS follows the Lagergren first-order kinetics. Reusing of spent nZVI is possible with adequate removal efficiencies of the surfactant molecules through multiple regeneration cycles.

Journal of Molecular Liquids 268 (2018) 497–505

Polyhydrazide incorporated with thiadiazole moiety as novel and effective corrosion inhibitor for C-steel in pickling solutions of HCl and H_2SO_4

Abdelwahed R. Sayed[a, c], Hany M Abd El-lateef[*a, b], Ahmad Desoky M. Mohamad[b]

[a] *Chemistry Department, Faculty of Science, Sohag University ,Sohag 82524, Egypt*

[b] *Chemistry Department, College of Science, King Faisal university, Al Hufuf, 31982 Al Hassa, SA*

[c] *Chemistry Department, Faculty of Science, Beni-Suef University, Beni-Suef, Egypt*

In this paper polyhydrazide incorporated with thiadiazole moiety (**S5**) was prepared and its chemical configuration was confirmed by spectroscopic methods (FTIR, ^{1}NMR and ^{13}CNMR). The inhibitive action of **S5** polymer and its monomer 2,5-dihydrazinyl-1,3,4-thiadiazole (**M1**) on the C-steel corrosion in pickling acids solution was investigated by weight loss, potentiodynamic polarization (PDP) and electrochemical impedance spectroscopy (EIS) measurements. PDP method exhibited that the investigated polymer is mixed-type corrosion inhibitor in both acids (HCl and H_2SO_4). The data revealed that S5 compound is a good inhibitor for C-steel in studied acids, and protection efficiency (*P*%) follows this sequence: H_2SO_4<HCl. Also, it was found that, the *P*% of the S5 polymer is higher than that obtained for its monomer (M1). Adsorption of the titled polymer obeyed the isotherm of Langmuir and involves both chemical and physical adsorptions. Scanning electron microscopy (SEM) investigations established the protective layer formation from the studied polymer on the metal substrate and shield it from direct Cl^- and/ or SO_4^{--} attack.

Macromolecular Research, 26 (2018) 882–891

Optical and photocatalytic measurements of Co-TiO_2 nanoparticles thin films

Mai M. Khalaf [1, 3], Hany M. Abd El-Lateef [1, 3]*H. M. Ali[2]

[1]*Chemistry Department, Faculty of Science, 82524 Sohag, Sohag University, Egypt*

[2]*Physics Department, Faculty of Science, 82524 Sohag, Sohag University, Egypt*

[3]*Department of Chemistry, College of Science, King Faisal University, Al Hufuf, 31982 Al Hassa, SA*

Abstract

Nanoparticles Co-TiO_2 thin films were synthesized by sol-gel method. The structural properties of the synthesized sample were studied including FTIR, XRD and TEM. The XRD confirmed the presence of double phase anatase/rutile for the TiO_2 nanoparticles. Effect of annealing temperature and exposure to microwave energy on the optical properties were studied for transparent conductive oxide (TCO) application. The optical energy gap and refractive index were determined. It was found that microwave treatment is an effective method for reinforced the optical properties of films. The photocatalytic properties were studied by determining the absorbance of methylene blue (MB) using UV source as a function of illumination time.

Plasmonics (2018) 13:1795–1802

Chemical modification of commercial kaolin for mitigation of organic pollutants in environment via adsorption and generation of inorganic pesticides

Mohamed Khairy, Haytham A. Ayoub, Farouk A. Rashwan, Hanan F. Abdel-Hafez

Contamination of water supplies with different organic pollutants from industrial and agricultural activities has received high concern recent years. Thus, efficient removal of these organic pollutants and minimize their usage in environment are highly recommended. Herein, we report hydrothermal chemical modifications of commercial kaolin (CK) in presence of sodium hydroxide (alkaline-modified kaolin; AMK) and disodium hydrogen phosphate (phosphate-modified kaolin; PMK) reagents. Interestingly, these chemical modifications altered the physico-chemical characteristics of CK in term of morphology, surface area and functionality which enhanced the adsorption capability of organic pollutants (i.e. methylene blue; MB) as well as offered an alternative inorganic pesticide that might reduce the consumption of organic pesticides. The results showed that, the equilibrium of MB adsorption is well described by Langmuir isotherm with maximum monolayer capacity of 434.78 and 476.19 mg/g for AMK and PMK, respectively. Furthermore, AMK and PMK revealed reasonable latent entomotoxic effect against cotton leafworm (S. littoralis) compared to a highly toxic organic pesticide (i.e. Methomyl). Therefore, the naturally abundant kaolin can be utilized efficiently to mitigate the organic pollutants in environment through sequestering of organics and generation of alternative inorganic pesticides for green plant protection.

Applied Clay Science 153 (2018) 124–133

Pesticidal activity of nanostructured metal oxides for generation of alternative pesticide formulations

Haytham Ayoub, Mohamed Khairy, Salaheldeen Elsaid, Farouk A. Rashwan, Hanan F. Abdel Hafez

Herein, nanostructured metal oxides of essential soil nutrient elements (i. e. CuO and CaO) with definite shape and size were simply synthesized and their pesticidal activities against cotton leafworm (Spodoptera littoralis) were explored for the first time. These metal oxide nanostructures represented novel economic and eco-friendly nano-pesticides for sustainable plant protection and might boost the nutrient content of soil. The results showed that CuO NPs and CaO NPs exhibited potential entomotoxic effects against S. littoralis. Interestingly, CuO NPs exhibited fast entomotoxic effect with LC50 = 232.75 mg/L after 3 days, while CaO NPs showed a slow entomotoxic effect with LC50 = 129.03 mg/L after 11 days of post-treatments. The difference in the pesticidal activity of the metal oxides is related to their physical characteristics and interfacial surfaces upon insect midgut and cuticle layer of insect body wall. Thus, nanoengineered metal oxides might be utilized to generate an alternative and cost effective pesticide formulation in the next future.
Journal of Agriculture and Food Chemistry, 66, 2018, 5491–5498

Large-scale production of $CdO/Cd(OH)_2$ nanocomposites for non-enzyme sensing and supercapacitor applications

Mohamed Khairy, Haytham A. Ayoub and Craig E. Banks

Recent advancements in electrode design are substantially linked to state-of-the-art nanomaterial fabrications. Herein, we report a simple one-pot hydrothermal synthesis of $Cd(OH)_2$ with a platelet-like morphology, which was subsequently annealed at relatively high temperatures to produce a $CdO/Cd(OH)_2$ nanocomposite for the first time. It was found that the control of thermal treatment allowed tunable charge transport across the nanometre scale due to the presence of CdO and $Cd(OH)_2$ mixed nanocrystals. The $CdO/Cd(OH)_2$ nanocrystals offer interesting prospects for the electrocatalytic oxidation of nitrite ions and for supercapacitor applications. The $CdO/Cd(OH)_2$ nanocomposite was blended with a trace amount of gold NPs for enhancing the electrochemical conductivity and electrocatalytic capability for nitrite oxidation with a sensitivity of 32.9 mA mM^{-1} . It afforded a promising electrocatalyst in a wide concentration range up to 10 mM with a low detection limit of 0.87 mM. Furthermore, the $CdO/Cd(OH)_2$ nanocomposite electrode was showed to be a highly active and stable supercapacitor, achieving a high specific capacitance in an alkaline medium of about 145 F g^{-1} at a discharge current of 2.0 A g^{-1}. These results have revealed that the presence of mixed oxide/hydroxide nanocrystals in nanoscale dimensions will be very interesting for various electrochemical applications and provide for a new class of nanodevices based on electrochemistry with unique capabilities.
RSC Adv., 2018, 8,921-930

Nanohexagonal Fe_2O_3 Electrode for One-Step Selective Monitoring of Dopamine and Uric Acid in Biological Samples

Mohammed Y. Emran, Mohamed A. Shenashen, Adel A. Abdelwahab, Mohamed Abdelmottaleb, Mohamed Khairy, Sherif A. El-Safty

Fabrication of nonenzymatic biosensors based on the nanomaterials for highly sensitive and selective detection of single or multiple molecules coexisting in one biological sample is extremely challenging. Design of the hierarchical nanohexagonal Fe_2O_3 platelets (HFP) via one-pot hydrothermal treatment was employed for selective signaling of dopamine (DA) and uric acid (UA) in the presence of ascorbic acid (AA) with high sensitivity. Electrode design with the nanosized structure of parallel hexagonal platelets (20–40 nm), high surface area, multiactive site, smooth surface, and pore distribution inside/outside the surfaces renders excellent sensitivity and selectivity of DA and UA during the catalytic oxidation process. Simultaneous monitoring and selective signaling of DA and UA were successfully achieved by HFP with detection limits as low as 16 nM and 0.218 μM with a wide linear range from 1 to 200 μM and from 20 to 400 μM for DA and UA, respectively. HFP provides high stability and reproducibility with relative standard deviations in the range of 2.5–5.29% to monitor DA and UA. Furthermore, continuous monitoring of DA and UA in real human saliva/serum samples was realized with high sensitivity and selectivity. The designed HFP can be employed as a nonenzymatic biosensor for simultaneous detection of mono-bioactive molecules in the biological samples.

***Electrocatalysis*, 9, 2018, 514–525.**

Non-enzymatic electrochemical platform for parathion pesticide sensing based on nanometer-sized nickel oxide modified screen-printed electrodes

Mohamed Khairy, Haytham A. Ayouba, Craig E. Banks

Nanozyme-based electrochemical sensors have attracted much attention because of their low cost, sensitivity and remarkable stability under extensive environmental and industrial conditions. Interestingly, the physical characteristics of the nanomaterials in terms of size, shape, composition, surface area and porosity dominate the electrochemical processes at electrode surfaces. Herein, we explore nickel oxide nanoplatelets (NPs) modified screen-printed electrode-based nanozyme sensor that displays high electrochemical activity including stability, sensitivity, selectivity and applicability for organophosphate pesticide (Parathion) determination. Differential pulse voltammogram of NiO-SPE in presence of parathion showed a characteristic peak current at −1.0 V (vs. Ag/AgCl). The NiO-SPE platform allows determination of parathion over the concentration range of 0.1–30 μM with a limit of detection (LOD) of 0.024 μM. The sensing platform is found to detect parathion of interferences without compromising the sensitivity of the sensor. Such interesting features offer sensitive determination of parathion in water, urine and vegetable samples.

Food Chemistry 255 (2018) 104–111

Simultaneous determination of codeine and its co-formulated drugs acetaminophen and caffeine by utilising cerium oxide nanoparticles modified screen-printed electrodes

Mohamed Khairy, Bahaa G. Mahmoud, Craig E. Banks

We report a facile and low-cost methodology for the simultaneous determination of codeine (COD) and its common co-formulated drugs acetaminophen (APAP) and caffeine (CAF) utilising cerium oxide nanoparicles modified screen-printed electrodes (CeO_2-SPEs) for the first time. Interestingly, CeO_2-SPEs offer a promising, sensitive, robust and chemically stable non-enzymatic electrochemical sensor for the simultaneous determination of APAP, COD and CAF without any interference / overlapping of voltammetric peaks/signals. The electro-analytical sensing of APAP, COD and CAF were explored using CeO_2-SPEs over a wide concentration range with competitively low detection limits (3S/N) of 0.051, 0.043 and 2.4 μmol L^{-1} respectively. The CeO_2-SPEs with nanoscale CeO_2 architectures exhibit practical analytical utility for the accurate and simultaneous determination of APAP, COD and CAF in human serum samples with excellent recoveries. The results show exceptional electrochemical performance of CeO_2-SPEs in term of simplicity, stability and sensing abilities that can effectively reduce processing costs for scalable production and routine analysis.

Sensors and Actuators B 259 (2018) 142–154

Voltammetric determination of meclizine antihistamine drug utilizing graphite screen-printed electrodes in physiological medium

Ahmed A. Khorshed, Mohamed Khairy, Craig E. Banks

Several classes of antihistamine drugs are widely distributed over the world's medication although their intensive side effects are in the high dosages. In the present manuscript, we report a simple, cost-effective and sensitive voltammetric determination of the meclizine antihistamine drug using unmodified/bare graphite screen-printed electrodes (GSPE) within physiological micellar medium of sodium dodecyl sulphate (SDS). The GSPE show an electrochemical oxidation peak of meclizine at +1.0 V vs. Ag/AgCl. It was found that, the voltammetric peak height of meclizine was markedly increased almost three-times in B. R. Buffer of pH 7.0 containing 0.067 g/L of SDS. This significant enhancement is due to their uniform assemblage of SDS molecules on the graphite surface which promotes the electrostatic interactions of the meclizine drug with GSPE. Under the optimum experimental conditions, the determination of meclizine were explored in a wide concentration range of 33×10^{-8} –29.13×10^{-6} mol/L with a nanomolar detection limit (LOD) of 80×10^{-9} mol/L. Furthermore, the GSPE was utilized for determination of meclizine within pharmaceutical tablets and human fluids with satisfactory accuracy and precision.

Journal of Electroanalytical Chemistry 824 (2018) 39–44

Synthesis, Characterization, Modeling, and Antimicrobial Activity of Fe^{III}, CoII, Ni^{II}, Cu^{II}, and Zn^{II} Complexes Based on Tri-substituted Imidazole Ligand

Mohamed Ismael*, Aly Abdou, and A.-M. Abdel-Mawgoud

Chemistry Department, Faculty of Science, Sohag University, Sohag 82524, Egypt

The reaction of the synthesized 2-(4,5-diphenyl-1H-imidazol-2-yl) phenol, (HL) ligand with Fe^{III}, Co^{II}, Ni^{II}, Cu^{II}, and Zn^{II} ions at room temperature resulted in the formation of the five complexes; $[Fe(L)_2(H_2O)(Cl)]\cdot 2H_2O$ and $[M(L)_2)]\cdot nH_2O$ [M = Co, Zn (n = 2), Ni, Cu (n = 1)]. The ligand and its complexes were characterized based on elemental analyses, spectral, magnetic and molar conductance measurements. The molecular and electronic structure of the ligand and its complexes was optimized theoretically and the quantum chemical parameters were calculated. The results revealed an interesting geometrical variation; octahedral for FeL, seesaw for CoL, distorted square planar for NiL and CuL, as well a tetrahedral arrangement for ZnL. The HL ligand and its metal complexes were screened against the growth of pathogenic bacteria [*Escherichia coli* (G^-) and *Bacillus cereus* (G^+)] and fungi (*Aspergillus fumigatus*) in terms of the minimum inhibitory concentration (MIC). The metal complexes showed high enhancement as antimicrobial candidates with lower MIC values compared with their parent ligand. Structure activity relationship formula was quantified by correlating the experimental MIC values with theoretical electronic chemical properties. Molecular docking of the complexes against CYP51B protein of A. fumigatus, the target enzyme for the antimicrobial reagents, was achieved to find the best orientation of the substrate, which would form a stable complex with overall minimum energy. The docking results enhanced the activity of the imidazole-based complexes as promising antimicrobial candidates.

Zeitschrift für anorganische und allgemeine Chemie (Z. Anorg. Allg. Chem) 2018, 644, 1203-1214

A promising electrodeposited iron oxide nanoparticles of very high saturation magnetization and superparamagnetic properties for remediation of polluted water with lead ions

Mahmoud Elrouby* [a], Nagwa Abo El-Maali [b], Rehab, Abd El-Rahman [a]

[a] *Sohag University, Faculty of Science, Chemistry Department, Sohag 82524, Egypt*

[b] *Assiut University, Faculty of Science, Chemistry Department, Assiut 71515, Egypt*

For the first time, iron oxide nanoparticles (NPs) with very high saturation magnetization (Ms=283 emu/g) and superparamagnetic properties compared with other published data are successfully obtained via a facile electrochemical method. Iron oxide nanoparticles (NPs) are fabricated by electro-reduction of the ferric-triethanolamine complex in an alkaline medium but at certain optimized conditions. Here, the electro-deposition pathway of iron oxide NPs is traced and detected via cyclic voltammetry and X-ray powder diffraction (XRD) techniques. The scanning electron microscopy (SEM) and the high-resolution transmission electron microscopy (HR-TEM) are used for morphological characterization of the electrodeposits. These nanostructured iron oxides exhibited high efficiency towards the removal of lead ions. The capacity (Q_m) of the removal of Pb^{2+} for these smart oxides is found to be 134.77 mg/g. Moreover, these materials give high uptake of about 96.58%.

Journal of the Taiwan Institute of Chemical Engineers, Vol. 93, 2018, 379-387.

Synthesis and characterization of titania nanoparticles and enhancement of photochemical, photoelectrochemical and electrochemical performance with zirconia nanoparticles

Mahmoud Elrouby*[a], Mai M. Khalaf[a,b]
[a] *Chemistry Department, Faculty of Science, Sohag University, 82524, Sohag, Egypt*
[b] *Department of Chemistry, College of Science, King Faisal University, Al Hufuf, 31982, Al Hassa, SA*

Nanosized Zr-doped TiO_2 with improved structural stability and photocatalytic properties was synthesized by the sol-gel method. The physicochemical and morphological properties of the catalyst were investigated by transmission electron microscopy, thermo-gravimetric analysis, differential thermal analysis, X-ray diffraction, and Brunauer-Emmett-Teller analysis. Zr-doped TiO_2 possessed a mesoporous structure and a noticeably increased surface area (90 m^2g^{-1}) as compared with pristine TiO_2 (28 m^2g^{-1}). On doping with Zr, TiO_2 exhibited reinforced texture, improved thermal stability, and enhanced photocatalytic properties. The electrochemical and photoelectrochemical characteristics of the samples were examined by Mott-Schottky analysis and sweep voltammetry under both dark and light conditions.
Journal of Physics and Chemistry of Solids, Vol. 122, 2018, 227-233.

Facile synthesis of TiO_2/ZrO_2 nanofibers/nitrogen co-doped activated carbon to enhance the desalination and bacterial inactivation via capacitive deionization

Ahmed S. Yasin[a], Ibrahim M.A. Mohamed[a,c], Hamouda M Mousa[a,d], Chan Hee Park[a,b], Cheol Sang Kim[a,b]
[a]*Department of Bionanosystem Engineering, Chonbuk National University, Jeonju, Jeonbuk 561-756, RK*
[b]*Division of Mechanical Design Engineering, Chonbuk National University, Jeonju, Jeonbuk 561-756, R K*
[c]*Chemistry Department, Faculty of Science, Sohag University, Sohag 82524, Egypt,* [d]*Department of Engineering Materials and Mechanical Design, Faculty of Engineering, SVU, Qena, 83523, Egypt*
Abstract:
Capacitive deionization, as a second generation electrosorption technique to obtain water, is one of the most promising water desalination technologies. Yet; in order to achieve high CDI performance, a well-designed structure of the electrode materials is needed, and is in high demand. Here, a novel composite nitrogen-TiO_2/ZrO_2 nanofibers incorporated activated carbon (NACTZ) is synthesized for the first time with enhanced desalination efficiency as well as disinfection performance towards brackish water. Nitrogen and TiO_2/ZrO_2 nanofibers are used as the support of activated carbon to improve its low capacitance and hydrophobicity, which had dramatically limited its adequacy during the CDI process. Importantly, the as-fabricated NACTZ nanocomposite demonstrates enhanced electrochemical performance with significant specific capacitance of 691.78 F g^{-1}, low internal resistance and good cycling stability. In addition, it offers a high capacitive deionization performance of NACTZ yield with electrosorptive capacity of 3.98 mg g^{-1}, and, good antibacterial effects as well. This work will provide an effective solution for developing highly performance and low-cost design for CDI electrode materials.
Scientific Reports, 8 (2018) 541-554.

Electrocatalytic behavior of a nanocomposite of Ni/Pd supported by carbonized PVA nanofibers towards formic acid, ethanol and urea oxidation: A physicochemical and electro-analysis study

Ibrahim M. A. Mohamed[a,b], Ahmed S. Yasin[c], Nasser A. M. Barakat[d,e], Seung A. Song[d], Ha Eun Lee[d], Seong Su Kim[a]

[a]*Department of Mechanical Engineering, KAIST, 291 Daehak-ro, Youseong-gu, Daejeon, Republic of Korea*
[b]*Department of Chemistry, Faculty of Science, Sohag University, Sohag, 82524, Egypt*
[c]*Bionanosystem Engineering Department, Chonbuk National University, Jeonju 561-756, Republic of Korea*
[d]*Department of Organic Materials and Fiber Engineering, Chonbuk National University, 567 Baekje-daero, Deokjin-gu, Jeonju-si, Jeollabuk-do, Republic of Korea*
[e]*Chemical Engineering Department, Faculty of Engineering, Minia University, Minia, Egypt*

Abstract:
A nanocomposite of Ni/Pd supported by carbonized poly-vinyl alcohol (PVA) nanofibers (NFs) was synthesized via electrospinning followed by calcination under an argon atmosphere. The as-synthesized NFs were studied using physicochemical analyses, such as field-emission scanning electron microscopy (FESEM), Transmission electron microscopy (TEM), X-ray diffraction (XRD), Fourier transform infrared spectroscopy (FTIR) and X-ray photoelectron spectroscopy (XPS), to investigate the morphology, crystallinity, effect of carbonization and surface chemistry of the NFs, respectively. Cyclic voltammetry (CV) and chronoamperometry (CA) were utilized to study the performance of the NFs towards electrooxidation reactions. The designed NFs present superior electrocatalytic behavior in an acid medium towards formic acid oxidation, as well as urea and ethanol oxidation in an alkaline medium. The electrocatalytic performance of the bimetallic NFs appears to arise from the assembly of bimetallic Ni/Pd@NFs based on PVA, which has hydroxyl groups. These hydroxyl groups can decrease the negative processes that occur as a result of metal-metal interactions, such as the aggregation process. This study introduces a novel non-precious electrocatalyst to facilitate the commercialization of fuel cells based on formic acid, urea and ethanol.

Applied Surface Science, 435 (2018) 122-129.

Design of novel electrode for capacitive deionization using electrospun composite titania/zirconia nanofibers doped-activated carbon

Ahmed S. Yasin[a], Ibrahim M.A. Mohamed[a,c], Chan Hee Park[a,b], Cheol Sang Kim[a,b]

[a]*Department of Bionanosystem Engineering, Chonbuk National University, Jeonju, Jeonbuk 561-756, RK*
[b]*Division of Mechanical Design Engineering, Chonbuk National University, Jeonju, Jeonbuk 561-756, RK*
[c] *Chemistry Department, Faculty of Science, Sohag University, Sohag 82524, Egypt*

Abstract:
Well-dispersed TiO_2/ZrO_2 nanofibers-doped activated carbon (AC/TiZr) were successfully synthesized as an electrode for the capacitive deionization (CDI) technique via electrospinning that was followed by a hydrothermal treatment. SEM, TEM, XRD, XPS and EDX measurements were employed to characterize the morphology, crystal structure and chemistry composition of the as-synthesized material. The electrochemical performance of the AC/TiZr nanocomposite modified electrode was measured using systematic cyclic voltammetry (CV) experiments. The highest specific capacitance for the AC/TiZr-based electrode is 251.3 Fg/g, which is higher than those of the AC (207.4 Fg/g) and TiO2/ZrO2 NFs (0.4 Fg/g)-based electrodes, and the interior resistance was also reduced. A desalination performance enhancement was obtained in the case of the AC/TiZr and the electrosorptive is 2.96 mg g−1. The implementation of the AC/TiZr nanocomposite provided a high potential for improving the efficiency of CDI.

Materials Letters, 213 (2018) 62-66.

Sonochemical synthesis, structural inspection and semiconductor behavior of three new nano sized Cu(II), Co(II) and Ni(II) chelates based on tri-dentate NOO imine ligand as precursors for preparing of metal oxides

Laila H. Abdel Rahman[a], Ahmed M. Abu-Dief [*a], Rafat M. El-Khatib [a], Shimaa Mahdy Abdel-Fatah [a], A. M. Adam[b], E.M.M. Ibrahim[b]

[a]*Chemistry Department, Faculty of Science, Sohag University, 82534Sohag, Egypt*

[b]*Physics Department, Faculty of Science, Sohag University, 82534Sohag, Egypt*

Three novel nanosized Cu(II), Co(II) and Ni(II) complexes of imine ligand attained from the condensation of 2-amino-3-hydroxypyridine and 3-methoxysalicylaldehyde have been prepared and investigated using diverse chemical methods such as NMR, CHN analysis, conductance, IR, Spectral studies, TGA and magnetic moment measurements. The obtained data confirmed that the synthesized complexes have metal: ligand ratio of 1:1 and octahedral geometry for Co(II) and Ni(II) complexes. Interestingly, The complexes are used as precursors for producing CuO, Co_2O_3 and NiO nanoparticles by calcination at 500 °C and their structures were described by powder x-ray and transmittance electron microscopy. Furthermore, to investigate the feasibility of using the synthesized materials for semiconductor based nanodevices, the electrical properties of the prepared imine complexes and their corresponding metal oxides were investigated by measuring the electrical conductivity over a temperature range 373-593K. The data confirm that the materials are semiconductor. The electrical conduction process in the complexes is governed by intermolecular and intramolecular transfer of the charge carriers. But, the conduction mechanism arises from the contribution of the phonon-assisted small polaron hopping in NiO nanoparticles and charge carrier hopping in CuO and Co_2O_3 nanoparticles. The results indicate that the complexes under study are promising candidates for wide scale of organic based semiconducting devices.

Applied organometalic chemistry (2017)

Identification of some Bioactive Metabolites in a Fractionated Methanol Extract from Ipomoea aquatica (Aerial Parts) through TLC, HPLC, UPLC-ESI-QTOF-MS and LC-SPE-NMR Fingerprints Analyses.

Hefny Gad M, Tuenter E, El-Sawi N, Younes S, El-Ghadban EM, Demeyer K, Pieters L, Vander Heyden Y, Mangelings D

Abstract

The plant species Ipomoea aquatica contains various bioactive constituents, e.g. phenols and flavonoids, which have several medical uses. All previous studies were executed in Asia; however, no reports are available from Africa, and the secondary metabolites of this plant species from Africa are still unknown. The present study aims finding suitable conditions to identify the bioactive compounds from different fractions. Chromatographic fingerprint profiles of different fractions were developed using high-performance liquid chromatography (HPLC) and then these conditions were transferred to thin-layer chromatography (TLC). Subsequently, the chemical structure of some bioactive compounds was elucidated using ultra-performance liquid chromatography-quadrupole time of flight-tandem mass spectrometry (UPLC-QTOF-MS) and liquid chromatography-solid phase extraction-nuclear magnetic resonance (LC-SPE-NMR) spectroscopy. The HPLC fingerprints, developed on two coupled Chromolith RP-18e columns, using a gradient mobile phase (methanol/water/trifluoroacetic acid, 5:95:0.05, v/v/v), showed more peaks than the TLC profile. The TLC fingerprint allows the identification of the types of chemical constituents, e.g. flavonoids. Two flavonoids (nicotiflorin and ramnazin-3-O-rutinoside) and two phenolic compounds (dihydroxybenzoic acid pentoside and di-pentoside) were tentatively identified by QTOF-MS, while NMR confirmed the structure of rutin and nicotiflorin. The HPLC and TLC results showed that HPLC fingerprints give more and better separated peaks, but TLC helped in determining the class of the active compounds in some fractions. Bioactive constituents were identified as well using MS and NMR analyses. Two flavonoids and two phenolic compounds were tentatively identified in this species for the first time, to the best of our knowledge.
Copyright © 2017 John Wiley & Sons, Ltd.

Phytochem Anal. 2018 Jan;29(1):5-15

Catalytic Oxidation of Benzyl Alcohol Using Nanosized Cu/Ni Schiff-Base Complexes and Their Metal Oxide Nanoparticles

Sameerah I. Al-Saeedi, Laila H. Abdel-Rahman, Ahmed M. Abu-Dief, Shimaa M. Abdel-Fatah, Tawfiq M. Alotaibi, Ali M. Alsalme and Ayman Nafady

Abstract

In this work, nanosized Cu and Ni Schiff-base complexes, namely ahpvCu, ahpnbCu, and ahpvNi, incorporating imine ligands derived from the condensation of 2-amino-3-hydroxypyridine, with either 3-methoxysalicylaldehyde (ahpv) or 4-nitrobenzaldehyde (ahpnb), were synthesized using sonochemical approach. The structure and properties of the new ligands and their complexes with Ni(II) and Cu(II) were determined via infrared (IR), nuclear magnetic resonance (NMR), electronic spectra (UV-Vis), elemental analysis (CHN), thermal gravimetric analysis (TGA), molar conductivity (Λ_m), and magnetic moment (μ_{eff}). The combined results revealed the formation of 1:1 (metal: ligand) complexes for ahpvCu and ahpvNi and 1:2 for ahpnbCu. Additionally, CuO and NiO nanoparticles were prepared by calcination of the respective nanosized Cu/Ni complexes at 500 °C, and characterized by powder X-ray diffraction (XRD) and transmission electron microscopy (TEM). Significantly, the as-prepared nanosized Schiff-base Cu/Ni complexes and their oxides showed remarkable catalytic activity towards the selective oxidation of benzyl alcohol (BzOH) in aqueous H_2O_2/ dimethylsulfoxide (DMSO) solution. Thus, catalytic oxidation of BzOH to benzaldehyde (BzH) using both ahpvCu complex and CuO nanoparticles in H_2O_2/DMSO media at 70 °C for 2 h yielded 94% and 98% BzH, respectively, with 100% selectivity.

Catalysts 2018, 8(10), 452

Synthesis, structural, thermal, optical and dielectric properties of chitosan biopolymer; influence of PVP and α-Fe_2O_3 Nanorods

Sayed, A. M.[a,b], Mohamad, A.D.M.[c,d]

[a]Department of Physics, Faculty of Science, Fayoum University, Fayoum, 63514, Egypt

[b]Department of Physics, Faculty of Science, Northern Border University, Arar, 91431, Saudi Arabia

[c]Department of Chemistry, Faculty of Science, Sohag University, Sohag, 82534, Egypt

[d]Department of Chemistry, Faculty of Science, Northern Border University, Arar, 91431, Saudi Arabia

The present work reports the influence of Polyvinylpyrrolidone (PVP) and hematite (α-Fe_2O_3) nanorods (NRs) on the physicochemical properties of chitosan (Cs), as an approach to broaden its medical and technological applications. Hematite NRs of 11.4 nm diameter and 87.9 nm crystallite size were prepared by a free-template chemical method. Cs, PVP/Cs and blend loaded with hematite NRs were prepared by solution casting. Significant changes in the films' surface were clarified using the scanning electron microscope (SEM). Fourier transformation infrared spectroscopy (FT-IR) confirmed the interaction between the NRs and the NH_2 and OH functional groups of Cs. DSC measurements showed one endothermic peak assigned to the water elimination, and an exothermic one, in the range 268–287 °C, attributed to the decomposition of saccharine structure in Cs. The swelling properties of the films were sensitive to the pH of the solution. PVP/Cs film showed ~ 85% transmittance in the visible region and its optical band gap narrowed from 5.4 eV to 4.05 eV after loading with 2.0 wt.% hematite. The influence of NRs content on the optical constants of the films is discussed. The dielectric properties depend on the film' structure. The large Polaron tunneling (LPT) model is the best suitable mechanism for the electric conduction. Due to their high thermal stability and decomposition temperature, transmittance and high conductivity, the prepared films are a candidate for the packaging industry, for use in some medical applications such as treating some chronic wounds, and optical windows and fibers. © 2018, Springer Nature B.V.

J Polymer Research, 25 (2018), 175

Ultrastructural, histochemical and biochemical effects of titanium dioxide nanoparticles on adult male albino rat liver and possible prophylactic effects of milk thistle seeds

Abu-Dief, E.E.[a], Abdel-Aziz, H.O.[a], Nor-Eldin, E.K.[a], Khalil, K.M.[b], Ragab, E.E.[a]

[a]*Department of Histology, Faculty of Medicine, Sohag University, Sohag, Egypt*

[b]*Department of Chemistry, Faculty of Science, Sohag University, Sohag, Egypt*

Introduction: Titanium dioxide nanoparticles (Tio2 NPs) are manufactured worldwide in large quantities for use in a wide range of applications. TiO2 NPs proved to damage liver function and induce an oxidative stress attack leading to liver toxicity. Milk thistle is an herbal supplement used to treat liver and biliary disorders. Silymarin, an active ingredient of milk thistle, is a strong antioxidant that promotes liver cell regeneration and stabilizes cell membranes. Aim: To investigate the biochemical, the histological and the histochemical changes in the liver after administration of different doses of Tio2 NPs and to evaluate the possible protective role of Milk thistle against these effects. Materials and Methods: Fifty adult male rats were divided into five groups; group I control, groups IIa and IIIa injected IP by 100mg/kg and 150mg/kg TiO2 for 2 weeks, respectively and groups IIb and 111b treated by oral milk thistle 4 weeks; one week prior, 2 weeks concomitant with IP 100mg/kg and 150mg/kg TiO2, respectively and the forth week after injection. Thereafter, rats were sacrificed and liver as well as blood samples were collected for estimation of serum alanine aminotransferase (ALT) and alkaline phosphatase (ALPs). Liver samples were processed for examination by TEM and immunohistochemical staining with P53 and PCNA antibodies counted statistically positive cells. Results: There was an increase in ALT and ALPs activities. Groups 11a and 111a treated by TiO2 showed signs of apoptosis and degeneration in the hepatocytes with nuclear changes and a significant increase in P53 and PCNA antibodies positive cells. These changes were ameliorated by concomitant injection with milk thistle with TiO2 in groups IIb and IIIb. Conclusion: The alterations observed might be an indication of hepatocyte injury due to TiO2 NPs toxicity that interacts with proteins and enzymes in hepatic tissue leading to generation of reactive oxygen species induce hepatocytes apoptosis. Milk thistle, has a hepatoprotective effect probably by its antioxidant effect.

Egyptian Journal of Histology, 41(2018),1-10

The electric and thermoelectric properties of Cu(II)-schiff base nano-complexes

Ibrahim, E.M.M.[a], Abdel-Rahman, L.H.[b], Abu-Dief, A.M.[b], Elshafaie, A.[a], Hamdan, S.K.[b], Ahmed, A.M.[a]

[a]*Physics Department, Faculty of Science, Sohag University, Sohag, 82524, Egypt*

[b]*Chemistry Department, Faculty of Science, Sohag University, Sohag, 82524, Egypt*

The physical properties, such as electric and optical properties, of metal-Schiff base complexes have been widely investigated. However, their thermoelectric (TE) properties remain unreported. This work presents Cu(II)-Schiff base complexes as promising materials for TE power generation. Therefore, three Cu(II)-Schiff base complexes (namely, [Cu(C32H22N4O2)].3 2H2O, [Cu(C23H17N4O7Br)], and [Cu(C27H22N4O8)].H2O) have been synthesized in nanosized scale. The electric and TE properties have been studied and comprehensive discussions have been presented to promote the nano-complexes (NCs) practical applications in the field of TE power generation. The electrical measurements confirm that the NCs are semiconductors and the electrical conduction process is governed by intermolecular and intramolecular transfer of the charge carriers. The TE measurements reveal that the Cu(II)-Schiff base NCs are nondegenerate P-type semiconductors. The measured Seebeck coefficient values were higher compared to the values reported in previous works for other organic materials indicating that the complexes under study are promising candidates for theremoelectric applications if the electrical conductivity could be enhanced. © 2018 IOP Publishing Ltd Printed in the UK.

Physica Scripta, 93 (5), 2018, 055801

Optimization of the pendant chain length in partially fluorinated aromatic anion exchange membranes for alkaline fuel cells

Ahmed Mahmoud, A.M.a,b, Miyatake, K.aEmail Author View Correspondence

[a]*Clean Energy Research Center, University of Yamanashi, 4 Takeda, Kofu, 400-8510, Japan*

[b]*Chemistry Department, Faculty of Science, Sohag University, Sohag, 825 24, Egypt*

For robust anion exchange membranes, we have investigated the effect of aliphatic side chains on the properties of partially fluorinated aromatic copolymers (QPAFs) with ammonium groups. A new series of QPAF membranes with various interstitial aliphatic side chain lengths (QPAF-Cx) where x = 2-6 were successfully synthesized. QPAF-C3 with a propylene side chain and ion exchange capacity (IEC = 1.24 meq. g^{-1}) showed balanced properties with the highest hydroxide ion conductivity (99 mS cm^{-1} at 80 °C in water) and relatively low water uptake, based on a well-developed phase separated morphology. Moreover, the QPAF-C3 membrane exhibited excellent alkaline stability to maintain high ion conductivity (98% remaining) and high mechanical properties after 1000 h in 1 M KOH at 80 °C. The QPAF-C3 membrane also revealed reasonable stability even in 4 M and 8 M KOH at 80 °C. In fuel cell operation, the QPAF-C3 membrane exhibited a higher power density (224 mW cm^{-2}) than those of our previous QPAF-C1 (138 mW cm^{-2}), QPAF-C1B (167 mW cm^{-2}), and Tokuyama A-201 (122 mW cm^{-2}) membranes. In the durability test for 62 h, QPAF-C3 maintained 69% of its initial voltage with minor structural degradation. © 2018 The Royal Society of Chemistry.

Journal of Materials Chemistry AVolume 6, Issue 29, 2018, Pages 14400-14409

Botany Department
قسم النبات

Botany

Botany Department
قسم النبات

Phaeonectriella alba sp. nov. from the River Nile, Egypt

Ahmed E. Abdel-Aziz, Sabah S. Mohamed, Ahmed M. Abdel-Raheem†, Mohamed A. Abdel-Wahab

Department of Botany and Microbiology, Faculty of Science, Sohag University, Sohag 82524, Egypt

Abstract

A new species, *Phaeonectriella alba*, collected from the River Nile, Aswan Governorate, Egypt, is described and illustrated. Phylogenetic analyses of LSU rDNA sequences placed the new species with *P. lignicola* (the type species) in a highly supported clade. *Phaeonectriella alba* is characterized by conical, superficial, hyaline, membranous ascomata; 4- or 8-spored asci that are persistent, clavate, with a truncate apical thickening and a simple pore and cytoplasmic retraction below apex; early deliquescing catenophyses; and ascospores that are ellipsoid to broad ellipsoid, thin-walled, 1–3 septate, hyaline when young, becoming brown at maturity, with an apical germ pore in each cell and without appendages.

Mycotaxon (2018) Volume 133, pp. 597–605

Khaleijomyces marinus gen. et sp. nov. (Juncigenaceae, Torpedosporales) a new lignicolous marine fungus from Saudi Arabia

MOHAMED A. ABDEL-WAHAB[1,2*], ABD EL-RAHIM M. A. EL-SAMAWATY[1,3], ABDALLAH M. EL GORBAN[1,3], MOHAMED A. YASSIN[1,3] & MARZOUQ H. ALSAADI[1]

Abstract

During an ongoing study of marine fungi from Saudi Arabia, an undescribed taxon was recorded on driftwood collected from intertidal zone at El Khobar sea front, Dammam city, Saudi Arabia. A new taxon, *Khaleijomyces*, is described in here as a new genus and a new species, *K. marinus* is established. Phylogenetic analyses of a combined SSU and LSU rDNA dataset position the new genus within the family Juncigenaceae, Torpedosporales. Other phylogenetic related genera are: *Fulvocentrum*, *Juncigena* and *Marinokulati*. The morphology of *Khaleijomyces* is different from the above three genera and it is characterized by apricot to reddish-brown, membranous, superficial to immersed ascomata with long, periphysate necks; faint apricot-color ascomatal venter, a common character in members of Torpedosporales; hamathecium consists of pseudoparenchymatous tissue that breaks down into catenophyses; cymbiform to fusiform, thin-walled asci, without apical apparatus; hyaline, multi-guttulate and unicellular ascospores when young becoming light-brown to brown in color and 1-4 septate in old specimens.

Phytotaxa (2018). 340 (3): 277–285

Four strains of yeasts: as effective biocontrol agents against both growth and mycotoxins formation by selected 11 toxigenic fungi

Zohri, A. A[1] and Marwa Abdel-Kareem, M[2]

Abstract:
Spoilage and poisoning of foods by fungi is a major problem, especially in developing countries. The need thus arises for natural preservatives that could be used for semi processed and processed foods. One of these possibilities is the use of yeast strains to control mycotoxigenic fungi. Four yeast strains (*Candida krusei* AUMC 8161, *Pichia anomala* AUMC 2674, *Pichia guilliermondii* AUMC 2663 and *Saccharomyces cerevisiae* AUMC 3875) were selected as a biocontrol agents against both growth and mycotoxins production by different 11 toxigenic fungal isolates; five local isolates from different Egyptian food sources and six isolates obtained from CBS (Central Bureau voor Schimmel cultures, Holland). *Candida krusei* AUMC 8161 completely inhibited the growth and toxin formation of all the 11 tested toxigenic isolates. *Pichia anomala* AUMC 2674 completely inhibited the growth and toxin production by 6 fungal isolates and strongly reduced the growth as well as toxin formation by the other tested toxigenic fungi. *Pichia guilliermondii* AUMC 2663 strongly reduced the growth and toxin production by the 11 toxigenic fungi. *Saccharomyces cerevisiae* AUMC 3875 completely inhibited the growth of 5 fungal isolates and strongly reduced the growth of the others.
Global Advanced Research Journal of Microbiology (2018) Vol. 7(8) pp. 132-135.

Airborne fungi in outdoor air of riyadh city, kingdom of saudi arabia

Abd El-Rahim M A El-Samawaty[1,2], Mohamed A Yassin[1,2,*,] Mohamed A Abdel-Wahab[1]

Abstract
This is a qualitative and quantitative study of the culturable airborne fungi at different districts of the fast-growing Riyadh city. Airborne fungi were surveyed in outdoor environment using portable personal volumetric air sampler. One cubic meter of air was sampled from 12 sampling points at each district. A total of 552 air samples were collected from 46 districts in Riyadh city and analyzed. After incubation and identification, concentrations of airborne fungi were calculated as CFU/m3. A total of 2735 colony forming unit (CFU) were isolated which belong to 102 fungal species representing 35 genera. The most common genus was *Aspergillus* that collected from all studied sites and represented by 19 species. *Cladosporium* and *Emericella* were frequent genera, while *Penicillium*, *Alternaria*, *Ulocladium*, *Cochliobolus*, *Rhizopus*, *Paecilomyces*, *Nattrassia* and *Fusarium* were common genera. Fungal communities recorded from the 46 districts were classified into three distinct groups: (1) Districts with less than 20 CFU/m3. *Aspergillius niger* dominated the fungal communities at these districts. (3) Districts ranged between 20 and 100 CFU/m3. These districts are intermediate in size, age, population density and standard of livings. *Cladosporium*, *Aspergillus flavus*, *A. niger*, and *Emericella* dominated the fungal communities at those districts.
Fresenius Environmental Bulletin (2018) Volume 27 – No. 5/ pages 2943-2950

Potentially harmful microalgae and algal blooms in the Red Sea: Current knowledge and research needs

Zakaria A. Mohamed

Department of Botany and Microbiology, Faculty of Science, Sohag University, Sohag 82524, Egypt

Abstract

Harmful algal blooms (HABs) have increased throughout the world's coastal oceans during the last century mostly due to water eutrophication and climate change. These blooms are often accompanied by extreme extensive negative impacts to fisheries, coastal resources, public health and local economies. However, limited studies have reported HAB events in Red Sea coastal waters. This article reviews potentially harmful microalgae in the Red Sea, based on available published information during the last 3 decades. Five harmful algal blooms were recorded in the Red Sea; of which 3 blooms are formed by dinoflagellates (*Noctiluca scintillans, Pyrodinuium bahamense, Protoperidinium quinquecorne*), one by raphidophytes (*Heterosigma akashiwo*) and one by cyanobacteria (*Trichodesmium erythraeum*). Additionally, mangrove swamps in the Red Sea were occupied by cyanobacterial mats, which contain microcystin and saxitoxin-producing species. The existing data in this review could be a catalyst for the establishment of monitoring and management program for HABs and their toxins in Red Sea coastal waters. This review also identifies current research gaps and suggests future research directions.

Marine Environmental Research 140 (2018) 234–242

Concentrations of cylindrospermopsin toxin in water and tilapia fish of tropical fishponds in Egypt, and assessing their potential risk to human health

Zakaria A. Mohamed1 & Asmaa Bakr1

Abstract

Unlike microcystin, cylindrospermospin (CYN) concentrations in fishpond water and their accumulation in fish tissues have been largely unexplored. This study determined CYN levels in water and tilapia fish organs from three tropical fishponds in southern Egypt. Water and fish samples were collected monthly from fishponds for 12 months (Oct 2012 to Sep 2013). The results revealed that six CYN-producing species of cyanobacteria dominated phytoplankton populations and formed blooms in these fishponds during warm months. Among these species, Anabaena affinis, *Planktothrix agardhii*, *Cylindrospermopsis catemaco*, and C. *philippinensis* were assigned as CYN producers for the first time in the present study. The highest cell densities of CYN producing species in fishponds were recorded in August and September 2013, correlating with high temperature, pH and nutrient concentrations. Dissolved CYN was found in fishpond waters at levels (0.3–2.76 μg L−1) very close to those of particulate CYN (0.4–2.37 μg L−1). CYN was also estimated in tilapia fish organs at levels up to 417 ng g−1 in the intestines, 1500 ng g−1 in the livers, and 280 ng g−1in edible muscles. Compared to the recommended guideline (0.03 μg kg−1 day−1), the estimated daily intake (EDI) of CYN in our samples of edible muscles exceeded this limit by a factor of 1.3–14 during summer and autumn. This might represent a risk to human health upon consumption of such contaminated fish muscles. Therefore, fishponds worldwide should be monitored for the presence toxic cyanobacteria to protect humans from their potent toxins.

Environmental Science and Pollution Research (2018) 25:36287–36297

Grazing of the copepod *Cyclops vicinus* on toxic *Microcystis aeruginosa*: potential for controlling cyanobacterial blooms and transfer of toxins

Zakaria A. Mohamed[1,*], Asmaa A. Bakr[1], Hamed A. Ghramh[2]

Abstract:

Grazing of zooplankton on phytoplankton may contribute to a reduction of harmful cyanobacteria in eutrophic waters. However, the feeding capacity and interaction between zooplankton and toxic cyanobacteria vary among grazer species. In this study, laboratory feeding experiments were designed to measure the grazing rate of the copepod *Cyclops vicinus* on *Microcystis aeruginosa* and the potential microcystin (MC) accumulation in the grazer. Copepods were fed a mixed diet of the edible green alga *Ankistrodesmus falcatus* and toxic *M. aeruginosa* for 10 days. The results showed that C. *vicinus* e_ ciently ingested toxic *Microcystis* cells with high grazing rates, varying during the feeding period (68.9–606.3 *Microcystis* cells animal−1 d−1) along with *Microcystis* cell density. *Microcystis* cells exhibited a remarkable induction in MC production under grazing conditions with concentrations 1.67–12.5 times higher than those in control cultures. Furthermore, C. *vicinus* was found to accumulate MCs in its body with concentrations increasing during the experiment (0.05–3.21 μg MC animal−1). Further in situ studies are needed to investigate the ability of *Cyclops* and other copepods to assimilate and detoxify MCs at environmentally relevant concentrations before deciding on the biocontrol of *Microcystis* blooms by copepods.

Oceanological and Hydrobiological Studies (2018) 47, 3, pages (296-302)

Bioavailability of bound microcystins in mice orally fed with contaminated tilapia edible tissues: Implications to human health

Zakaria A. Mohamed[a,*], Asmaa Bakra, Hamdy A. Soliman[b]

Abstract:

This study investigates for the first time in vivo potential release of bound microcystins (MCs) from edible fish tissues. Bound MCs were released in the mouse digestive system and reached the liver (2.1–14.3 ng g−1) and blood (1–5 ngml−1). The released MCs were active and negatively affected liver functions of treated mice. The estimated daily intake (EDI) for bound MCs (93.5 μg kg−1 day−1) is about 2300 times higher than the WHO safe EDI (0.04 μg kg−1 day−1), compared to lower EDI for free MCs (0.002 μg kg−1 day−1). Therefore, bound MCs in fish tissues should be considered when fish are monitored for human consumption.

Toxicon 151 (2018) 34–36

Gene expression and adventitious root formation on auxin containing medium as influenced by cytokinin type during the multiplication stage in micropropagation of moringa

Ahmed Hassanein, Jehan Salem, Fayza Faheed, Abdullah El-nagish

Abstract:

To study gene expression during root formation, cotyledonary nodal segments of aseptically germinated seedlings were used for induction of shoot formation on cytokinin containing medium followed by induction of root formation on auxin containing medium. Nodal segments free of cotyledons showed a low tendency to form shoots on basal MS medium. Shoot formation increased signifcantly when cotyledonary nodes with two complete cotyledons were used. Further increase in shoot formation and growth were detected when they were cultured on MS containing 0.56 mg/l of BAP. When the suitable concentration of IAA (0.5 mg/l), IBA (1.0 mg/l) and NAA (0.5 mg/l) for induction of root formation was the isoenzyme pattern of both isoenzymes, with the darker staining isoenzyme forms being those with the higher activity under specifc conditions. Root formation and expression of antioxidant enzymes (SOD, POX and CAT) on IAA containing medium were influenced by cytokinin type during the shoot formation stage. They were higher when 0.56 mg/l BAP was used for shoot multiplication and followed by 0.5 mg/l IAA for root formation as compared to the use of 0.56 mg/l KIN followed by 0.5 mg/l IAA. In addition, polypeptides specifc for each cytokinin type were detected when shoots were subcultured on auxin containing medium for root formation

Phyton; annales rei botanicae (2018). 58(2):175-184

Effect of anti-ethylene compounds on isoenzyme patterns and genome stability during long term culture of *Moringa oleifera*

A. M. Hassanein[1] · J. M. Salem[1] · F. A. Faheed[1] · A. El-nagish[1]

Abstract:

Multiplication of *Moringa oleifera* shoots on MS medium supplemented with 2.5 μM BAP for 3 weeks resulted in shoot vitrification which led to chlorosis, retardation of shoot formation, reduction in shoot length, necrosis of shoot tips and formation of friable calli on the base of cultured explants. Vitrification symptoms decreased when MS medium containing 2.5 μM BAP in combination with 10 μM AgNO3, 50 μM salicylic acid (SA) or 200 μM CoCl2 was used. Studying isoenzyme patterns of SOD, POX, CAT, GOT and EST indicated that moringa shoots multiplied without obvious variation in isoenzyme patterns up to 7 subcultures. Moringa shoots subjected to 14 subcultures and anti-ethylene compounds showed variation in isoenzyme patterns and were associated with the disappearance of vitrification which facilitated root formation and acclimatization. Under long term cultures, RAPD, ISSR and SSR indicated that AgNO3 was the optimal anti-ethylene substance for avoidance of vitrification in moringa but it resulted in high somaclonal variation. Application of SA decreased vitrification as well as somaclonal variation compared to CoCl2 under long term culture. Consequently, SA was recommended for moringa clonal multiplication.

Plant Cell Tiss Organ Cult (2018) 132:201-212

Biosynthesis, Characterization, Optimization of Silver Nanoparticles from Marine *S. griseoflavus* and Their Role in Improving Antibiotic Susceptibility of Multidrug Resistance Pathogenic Fungi

Muneera Al-Otaibia*, Bahig El-Deebb, Nasser Mostafac*

Abstract

Green synthesis of silver nanoparticles using marine microorganisms has gained profound interest because of their potential to synthesize nanoparticles of various size, shape and morphology. In the present investigate, 25 silver resistant bacterial isolates were isolated from different sites of red sea cost at Jeddah city, , bacterial strain BM3 was selected on the basis of its ability to produce stable extracellular silver nanoparticles (AgNPs). Biochemical and Molecular characterization of this isolate indicated that BM3 strain is belonged to *Streptomyces* and identified as *S. griseoflavus*. The biosynthesis of AgNPs was monitored by UV–Visible spectrum that showed surface plasmon resonance (SPR) peak at 420 nm. Further characterization of synthesized AgNPs was carried out using the XRD, TEM and FTIR spectroscopy. TEM and XRD analysis revealed that the AgNPs synthesized by MB was spherical in shape with a size range of 5-45. nm FTIR confirmed the presence of proteins as the stabilizing agent surrounding the nanoparticles. Optimization of silver nanoparticles synthesis has been studied and the results demonstrated that the biosynthesis of AgNPs by bacterial supernatant increased with the increasing of the temperature, pH and Ag+ ions concentration. All tested antibiotics showed synergistic inhibition against growth of the pathogenic bacteria. The biocide actions of AgNPs studied using SEM. The results showed damage in membrane and some pits that have been created cause inter cellular components leakage and finally cell death.

American Scientific Research Journal for Engineering, Technology, and Sciences (2018) 46, 160-177

Biological Synthesis and Structural Characterization of Selenium Nanoparticles and Assessment of Their Antimicrobial Properties

Bahig El-Deeba, Abdullah Al-Talhib , Nasser Mostafac, Rawan Abou-assyd*

Abstract

Biological synthesis of selenium nanoparticles (SeNPs) using microorganisms has received profound interest because of their potential to synthesize nanoparticles of various size, shape and morphology. In the current study, 206 selenium resistant bacterial isolates were isolated from 18 samples from different environmental sources of Saudi Arabia. Among These isolates, bacterial strain BGRW was selected on the basis of its ability to produce stable extra/intracellular SeNPs. Molecular characterization of this isolate indicated that BGRW strain belongs to the *Providencia vermicola*. BGRW was found to be highly resistant to selenium dioxide up to 20 mM.The biosynthesis of SeNPs was monitored by UV–Visible spectrum that showed surface plasmon resonance (SPR) peak at 295 nm. Further characterization of synthesized SeNPs was carried out using the XRD, TEM and FTIR spectroscopy. TEM and XRD analysis revealed that the SeNPs synthesized by BGRW was hexagonal in shape with a size range of ~3 to 50 nm with average 28nm. FTIR spectroscopy confirmed the presence of proteins as the stabilizing agent surrounding the nanoparticles. In the present study six antibiotics were investigated to explore their synergistic effect when combined with SeNPs against various pathogenic. All tested antibiotics showed synergistic inhibition against a growth of the pathogenic bacteria. The biocide actions of SeNPs on Gram-negative and Gram-positive pathogens were studied using SEM. The results showed damage, blebs, fusion, clumps and randomly distribution in the cell wall of the tested microbes resulting the death of cells.

American Scientific Research Journal for Engineering, Technology, and Sciences (2018) 45, 135-170

Antibiofilm Potential of Biogenic Silver Nanoparticles against Kocuria rosea and Kocuria rhizophila1

H. Elharirya, [b], *, E. Gadoa, [c], B. El-Deeba, [d], and A. Altalhia

Abstract:
The present study aims at biosynthesizing, characterizing and evaluating the biogenic silver nanoparticles (AgNPs) as antimicrobial and antibiofilm against Kocuria rosea and Kocuria rhizophila. Cellfree supernatant of Proteus mirabilis culture was used for biosynthesizing AgNPs, which confirmed by visualizing color change and X-ray diffraction. Transmission electron microscopy showed the formation of AgNPs in the range of 5–40 nm. ART-FTIR spectra provided evidence for presence of proteins as possible biomolecules responsible for stability of AgNPs and act as capping agent. AgNPs had ability to inhibit growth of K. rosea and K. rhizophila. The minimum inhibitory concentration (MIC90) of AgNPs against both strains was 25 μg/mL. Antiadhesive effect of AgNPs was verified at sub-MIC90 dose (12.5 μg/mL). The AgNPs concentrations up to 100 μg/mL were not effective for complete removing the already established biofilms with maximum removing percentage of 30.5–34.9%. In conclusion, the present study demonstrated an unprecedented green process for biosynthesizing stable spherical-shaped AgNPs. Early control is suggested by preventing biofilm formation using low AgNPs concentration (12.5 μg/mL) as a potential ingredient for formulating effective chemical sanitizers.
Microbiology, 2018, Vol. 87, No. 1, pp. 9–20.

Interactions of physico-chemical properties of the River Nile water and fungal diversity in River Nile streams in Delta region

Ahmed Mohamed Abdel-Raheem, Gamalat Abd-Aleem Abd-Elaah, Osman Mohamed El-Maghraby and Mahmoud Saad Eldin
Botany department, Faculty of Science, Sohag University.

Abstract
Water pollution in Egypt is increasing over time, with constant supply of pollutant effluents to the water system from several sources. Water samples were collected for hydrochemical analysis during four successive seasons from some irrigation canals and streams of River Nile in Delta region governorates. There are various correlations patterns between fungal communities and physico-chemical parameters. Air and water temperature were major factors that affect fungal distribution. Calcium and magnesium have inverse correlation on fungal diversity. There was no significant correlation of $SO4^{2-}$ and $NO2^{-}$ with distribution of freshwater fungi. Ammonia and phosphate encouraged fungal growth. Salinity played active role in determining fungal diversity and community composition. Changes in species composition were correlated positively with elevated concentrations of NH3 +, and pH in some governorates.
Journal of Environmental Studies [JES] 2018. 18: 33-45

Isolation and Molecular Identification of *Fusarium* Species from Some Cereal Grains and Their Products in Egypt

Samia El-Rabbat[1], Osman El-Maghraby[2], Samah El-Debaiky[3] and Ashraf Haider[4]

Abstract:

18 strains of *Fusarium* species were isolated from cereal grains and their products (wheat, rice, barely, flour, corn flour and starch) collected from different locations in Cairo and El-Gharbia governorates, Egypt, using sample dilution and direct culture methods. The isolated *Fusarium* strains were identified morphologically as: 4 isolates *F. oxysporum*, 2 isolates from each of *F. solani*, *F. equiseti*, *F. fujikuroi*, *F. chlamydosporum and F. brachygibbosum* and 1 isolate of each of *F. verticillioides*, *F. subglutinans*, *F. anthophylum* and *F. moniliforme*. The identification of *Fusarium* species was confirmed genetically. Molecular identification based on ITS1 and ITS4 regions indicated PCR fragments ranged from 500 to 600 bp. PCR fragments of conserved ribosomal ITS regions were sequenced, aligned and deposited in NCBI GenBank with the following accession numbers. *F. fujikuroi* (MG211161), *F. fujikuroi* (MG211162), *F. verticillioides* (XM 018895258.1), *F. sporotrichioides* (MG211163), *F. solani* (MG211159), *F. solani* (MG211160) and *F. equiseti* (KM246255.1).

International Journal of Innovative Science, Engineering & Technology, Vol. 5 Issue 2, February 2018

Bio-monitoring of radionuclides air pollution using physiological responses of urban trees

El-Khatib, A. A., Amany aboelkassem and H. Elzayat, M.

Abstract:

Contamination of environment by radionuclides in territories under urboecosystem conditions is an actual problem. The search for new express methods for radioactivity determination of environment is an important task of research. The present work evaluated the ability to use Eucalyptus globulus leaves to act as bio-monitor for environmental radionuclides air pollution. On the basis of radionuclides analysis, leaves of E. globulus exhibited different accumulation coefficients according to the distance from the quarry. The relationship between the radionuclides concentrations in leaf deposited dust and soil samples was estimated by Pearson coefficients to resolve two main mechanisms of radionuclide accumulation, atmospheric deposition, and root uptak**e.**

Journal of Current Research (2018). ***10, Issue, 02, pp.65279-65286***

Characterisation of the Egyptian Pliocene bentonite from the Sohag region for pharmaceutical use

Abdelhamid Elshater[1] & Abdelaziz Elhaddad1 & Attef Elattaar[1] & Magdy Abugharbia[2] & Waffa Soliman[1]

Abstract

This paper aims to prepare purified Na-bentonite with improved properties for its use in the pharmaceutical industry. Calcium bentonite from the Sohag region of Egypt was activated with various proportions of sodium carbonate (2, 3, 5 and 8 wt.%). Additionally, bentonite was purified by sedimentation to eliminate impurities, especially quartz. The results of X-ray diffraction (XRD) and swelling volume data confirmed that raw bentonite was converted to sodium bentonite using 5% Na2CO3. The sodium bentonite (M5) obtained by activation met the chemical and microbiological requirements set by the pharmacopoeias regarding toxic trace elemental contents (As, Pb and Cd), the absence of E. coli, the total contents of aerobic microbes and physicochemical properties such as swelling volume, pH and sedimentation volume. Therefore, (M5) bentonite can be designated as being potentially appropriate for pharmaceutical applications. The cation exchange capacity (CEC), surface area, porosity, pH, gel formation and swelling volume data indicated that M5 bentonite could be used to formulate oral suspensions and in topical application.

Arabian Journal of Geosciences (2018) 11: 385

Heavy Metal Pollutants in Fresh Water

Mohamed Youssef[1], Ebtesam Mohamed Morsy[2], Samia Mohamed Soliman[1], Abdel-Raheim El-Sayed Abdel-Latief[2]

[1]Botany and Microbiology Department, Faculty of Science, Sohag University, Sohag, Egypt
[2]Soil, Water and Environment Res. Institute, Agric. Res. Center (ARC), Giza, Egypt

Abstract:

Water quality is one of the most important concerns. This study focused on screening of the most dangerous heavy metals (cadmium, chromium, copper, lead and nickel)in fresh water sources (surface and groundwater) of study area, Sohag governorate, Egypt. Ninety samples were collected from 15 sites along the study area extending from Tima to Dar-Elsalam cities; 12 wells and 3 Nile river local sites, 6 samples for each site, three during winter and three during summer. Results indicated that, total dissolved solids (TDS) and electric conductivity (EC) parameters in all samples increased significantly in summer than winter. While pH increased in winter than summer. All tested physical parameters of samples were within the safe limit of drinking water as prescribed by WHO, except pH in samples S1 and S3. The concentration of metals in the study area showed that all tested samples were free from Cr during winter or summer season. Also, Cu was not recorded in winter but appeared during summer season within permissible limit. Nickel (Ni) was recorded in all tested samples within permissible limit. On the other hand, Cd and Pb were recorded over than permissible limit in some samples. This study may represent dangerous alarm for the potential threats to the fresh water resources in study area.

Journal of Biomaterials. Vol. 2, No. 2, 2018, pp. 46-50

Fine-template synthetic process of mesoporous TiO2 using ionic/nonionic surfactants as potential remediation of Pb(II) from contaminated soil

M. M. Khalaf[1,2] · N. Y. Abdallah[3] · H. M. Abd El-Lateef[1,2]

Abstract

This trend of research deals with preparation of mesoporous TiO2 by a simple approach using sol–gel method by various surfactant templates. The designed nano-adsorbents TiO2 were featured by various characterization methods of Fourier transform infrared, X-ray diffraction, surface area analysis (Brunauer–Emmett–Teller), transmission electron microscope, and scanning electron microscope. These obtained nano-adsorbents are examined as functional adsorbents for lead ions up taking from contaminated soil specimens. The results presented the effect of ionic and nonionic surfactant templates on the texture of the three types of mesoporous TiO2 nano-adsorbents. The effects of the temperature, pH, and amount of nanoadsorbents TiO2 on the adsorption process were studied. The optimum conditions of 25 °C, 5, and 0.1 g were obtained for temperature, pH, and amount of adsorbents, respectively. The obtained results revealed that about 97.6, 99.1, and 95.3% of total adsorptive capacity were obtained for Ti C, Ti S, and Ti P, respectively, at 100 mg L−1 of Pb(II) ions in soil solutions during 120 min. The adsorption isotherm and the thermodynamic parameters were further illustrated. These findings recommended these nano-adsorbent TiO2 as adequate adsorbents in remediation process of Pb-enriched soil.

International Journal of Environmental Science and Technology (2018)

Impact of enzymes and toxins potentiality of four Aspergillus species to cause aspergillosis

Mohamed Fawzy Adam, Abdel-Naser Zohri, Bassam Aboul-Nasr, Enas Mahmoud Amer

Abstract

Aspergilli are the main causal agent of invasive apergillosis chest disease. A total of 80 isolates of *Aspergillus flavus* ,(٢٠)*A. fumigatus* (15), *A. niger* (30) and *A. terreus* (15) isolates, previously recovered from aspergillosis suspected patients at Assiut university hospitals, were assayed for their enzymes and toxins profile. The results revealed that, all of the tested isolates had the ability to utilize calf lung tissue in addition, to produce catalase, peroxidase. Meanwhile, 82.5-90% isolates produced protease, lipase, urease, phospholipase whereas, 70% of isolates exhibited hemolytic activities. TLC of the cleaned extracts of the tested isolates exhibited the ability of all A. flavus isolates assayed to produce aflatoxins B1 & G1, 53%, moreover, *A. fumigatus* isolates produced fumagillin and gliotoxin. On the other side, 43.3 % & 23.3% of *A. niger* isolates produced ochratoxins & gliotoxin respectively. Virulence assay of 10 µl of gliotoxin standard and cleaned extracts of A. fumigatus toxic isolates showed necrotic area on Guinea Pigs lungs compared to the control. Thus, opportunistic fungi isolated from aspergillosis patients possess high enzymatic and toxic profile that might play an important role in their mycopathy.

European Respiratory Journal 2018 52: PA2657

Isolation, antimicrobial resistance profile and molecular characterization of bacteria from broiler

Aly E. Abo-Amer[1,2]*, Mohammed Y. Shobrak[3] and Abdullah D. Altalhi[1]

Abstract:

Currently, poultry is a main source of food in the world. However, it is one of the most purchases commonly associated with food-borne disease. Drug-resistant bacteria can be transmitted to humans directly by contact with poultry wastes or indirectly by contaminated poultry foodstuffs, therefore contributing to the existed increasing crisis of antimicrobial resistance. This project was aimed to determine the incidence of antimicrobial resistant bacteria isolated from chicken and the genes responsible of this resistance. One hundred cloacal swabs were aseptically obtained from chickens from different farms. The results indicated that 78.8 % of bacterial isolates belonged to *E. coli*. Moreover, 5.5%, 4.4% and 3.3% of bacterial isolates were *Pseudomonas aeruginosa*, *Klebsiella pneumonia* and *Kluyvera intermedia*, respectively. Antimicrobial susceptibility testing of bacterial isolates was carried out using the Kirby-Bauer disk diffusion method. Most of bacterial isolates were resistant to Oxacillin, Oxytetracycline, Chloramphenicol and Lincomycin. However, most of isolates were only sensitive to Colistin. The greatest of bacterial isolates were resistant to ~4-26 antimicrobials indicative multidrug resistant isolates. The resistance genes *bla*SHV, *aac(3)-IV*, *tet*(A) and *tet*(B); *aadA1*, *catA1*, and *cmlA*, *ere*(A) and *sul1* were nearly detected in most *E. coli* isolates. 16S rRNA analysis confirmed that the most multidrug resistant isolates belonged to *E. coli*. These results revealed emergence multiple drug resistant-bacteria from poultry. This study recommends that it should be a strict regulatory procedure for the use of antimicrobials in human and animals to minimize the emergence and distribution of antimicrobial resistant bacteria.

BIOSCIENCE RESEARCH, 2018 15(2): 900-912.

Isolation and antimicrobial resistance of Escherichia coli isolated from farm chickens in Taif, Saudi Arabia

Aly E. Abo-Amer[a,b],*, Mohammed Y. Shobrakc, Abdullah D. Altalhia

Abstract:

Objectives: Poultry is one of the main sources of food in the world. Antimicrobial-resistant Escherichia coli can be transmitted to humans by contact with poultry waste or by contaminated poultry products, contributing to the increasing crisis of antimicrobial resistance. This study aimed to determine the incidence of antimicrobial resistance in E. coli isolated from chickens in Taif province, Saudi Arabia, and to identify the genes responsible for any resistance observed. Methods: A total of 150 cloacal swabs were aseptically obtained from chickens from different farms, from which 180 colonies of E. coli were identified using standard microbiology procedures. Antimicrobial susceptibility testing was performed by the Kirby–Bauer disk diffusion method. The genes blaSHV, aac(3)- IV, tet(A), tet(B), aadA1, catA1, cmlA, ere(A) and sul1 were detected by PCR. Results: Most of the E. coli isolates showed resistance to oxacillin (99%), lincomycin (98%) and oxytetracycline (97%). The prevalence of resistance to chloramphenicol (73%), ciprofloxacin (59%) and ampicillin (51%) was lower. Genes conferring resistance to β-lactams (blaSHV) and tetracyclines [tet(A) and tet(B)] were observed at prevalences of 96% and 95%, respectively, among the E. coli isolates. Chloramphenicol (catA1 and cmlA) and erythromycin [ere(A)] resistance genes showed prevalences of 72% and 15%, respectively, whereas gentamicin [aac(3)-IV], streptomycin (aadA1) and sulfonamide (sul1) resistance genes were detected in 20%, 20% and 10% of the studied isolates, respectively. Conclusion: A significant prevalence of antimicrobial resistance genes was observed among E. coli isolates from farm chickens, supporting strict regulatory procedures for the use of antimicrobial agents.

Journal of Global Antimicrobial Resistance 15 (2018) 65–68

Inhibition of fungal growth and mycotoxins formation of selected toxigenic fungi by different bacterial strains

Zohri A A[1], Sabah S M[2], Youssef M[2] and Marwa Abdel-Kareem M [2]

1Botany & Microbiology Department, Faculty of Science, Assiut University, Egypt;
2Botany Department, Faculty of Science, Sohag University, Egypt

Abstract

Four bacterial strains (*Bacillus amyloliquefaciens* BICS 08b, *B. subtilis* AUMC 63, *Lactococcus lactis* BICS 081b and *Pseudomonas fluorescence* BICS 0149b) were tested for their ability to inhibit both growth and mycotoxins production by different 11 toxigenic fungi; five local isolates from different Egyptian food sources and six standard strains obtained from CBS, Central Bureau voor Schimmelcultures, Holland. *Pseudomonas fluorescence* BICS 0149b completely inhibited growth of nine fungi and completely inhibited toxin production by the 11 tested fungi. *Bacillus subtilis* AUMC 63 reduced fungal growth of the 11 fungal isolates under study by 40-100%, and reduced their toxins formation by 20- 100%. *Lactococcus lactis* BICS 081b highly reduced both fungal growth and mycotoxins production by 76-100% and 60-100%, respectively. *Bacillus amyloliquefaciens* BICS 08b completely inhibited toxins formation by almost fungi while it was not highly affected their growth. From this result, some bacterial strains may be successfully used as a biological control agent of food contamination with molds and mycotoxins

GPH - Journal of Applied Science (2018). Volume-1 | Issue-1 |

Extracellular mycosynthesis of gold nanoparticles using *Trichoderma hamatum*: optimization, characterization and antimicrobial activity

M. Marwa Abdel-Kareem[1] and A.A. Zohri[2]

Abstract

Synthesis of gold nanoparticles (AuNPs) has become a needed domain of applied science. Biological method for synthesis of AuNPs by *Trichoderma hamatum* SU136 aqueous mycelial extract was achieved. The culture filtrate of the fungus was exposed to three different concentrations of gold chloride. The culture filtrate of the fungus was exposed to three different concentrations of gold chloride (0.25, 0.5 and 1.0 mmol l^{-1}). In all cases, the gold ions (Au3+) were reduced to Au0, leading to the formation of stable AuNPs. The AuNPs were identified by UV–visible spectrometry, TEM and FT-IR. The presence of a surface plasmon band around 530 nm indicates AuNPs synthesis. *Trichoderma hamatum* SU136 synthesized 5–30 nm sized; spherical, pentagonal and hexagonal morphologies of AuNPs by TEM. The existence and binding of proteins with nanoparticles was approved by FT-IR study. Parameters optimization showed the smallest size of AuNPs was obtained with (0.5 mmol l _1 gold chloride, pH 7 at 38°C). Interestingly, AuNPs exhibited antimicrobial activity against four pathogenic bacterial strains in the presence of the standard antibiotic, streptomycin.

Letters in Applied Microbiology (2018). 67, 465--475

The action mechanism and biocontrol potentiality of novel isolates of Saccharomyces cerevisiae against the aflatoxigenic *Aspergillus flavus*

M. Marwa Abdel-Kareem[1] , A.M. Rasmey[2] and A.A. Zohri[3]

Abstract

Inhibition of Aspergillus flavus growth and its aflatoxins production using the biocontrol agent Saccharomyces cerevisiae as well as to explore its mode of action was studied. Eight strains of S. cerevisiae strains were able to suppress the growth of A. flavus Z103. The maximum growth inhibition of A. flavus Z103 was obtained by living cells of S. cerevisiae EBF101 and *S. cerevisiae* 117 with 85 and 83%, respectively. The sporulation inhibition and hyphae deterioration of A. flavus Z103 by *S. cerevisiae* cells adhesion were observed under SEM; up to 99_8% inhibition of aflatoxins biosynthesis by *A. flavus* Z103 was resulted when the fungus was treated by autoclaved extracellular crude of S. cerevisiae. Also, the tested strains are potential to produce exochitinase which could be suggested as another mode of action for its antifungal activity. GC-MS analysis of S. cerevisiae 117 extracellular secondary metabolites revealed the existence of 4-Hydroxyphenethyl alcohol (46.32%), 4, 4-Dimethyloxazole (9.14%) and 1,2-Benzenedicarboxylic acid dioctyl ester (2.8%).

Letters in Applied Microbiology (2018). 68, 104--111

24-Epibrassinolide application enhances growth and biochemical aspects of squash under salt stress conditions

Galal, A

Department of Botany and Microbiology, Faculty of Science, Sohag University, Sohag, 82524, Egypt

Brassinosteroids (BRs) are considered to possess protective activity in plants exposed to various stresses. The present study was conducted to evaluate the effects of 24-epibrassinolide (EBL) on salt stressed summer squash cv. Eskandrani seedlings, whether it can alleviate the deleterious effects of salt stress in growing seedlings or not. For this, summer squash seeds were germinated in solidified half strength MS (Murashige and Skoog) medium supplemented with different concentrations and combinations of EBL (0, 5, 10 and 20 µM) and NaCl (0, 50, 100 and 150 mM). The different concentrations (5, 10, 20 µM) of EBL significantly increased germination percentage and seedling growth capacity and the greatest increase was observed at 10 µM EBL. EBL application significantly increased the contents of photosynthetic pigments, the relative water content and the uptake of K and Ca. However, the different concentrations (50, 100 and 150 mM) of NaCl significantly decreased the above-mentioned attributes. The different concentrations (50, 100 and 150 mM) of NaCl significantly increased the electrolyte leakage, the lipid peroxidation and the Na uptake, but the interaction between EBL and NaCl significantly decreased these parameters. The results of this study proved that the application of 24-epibrassinolide to growing squash seedlings under salt stress conditions reduced the deleterious effects of salt stress and increased the tolerance of seedlings to its detrimental effects.

Acta Biologica Hungarica. 69 (2), 182-196

The antibiotic peptaibol alamethicin from *Trichoderma permeabilises* Arabidopsis root apical meristem and epidermis but is antagonised by cellulase-induced resistance to alamethicin

Dotson BR, Soltan D, Schmidt J, Areskoug M, Rabe K, Swart C, Widell S, Rasmusson AG.
Sohag University, Botany Department, Faculty of Science, Sohag, 82524, Egypt

Trichoderma fungi live in the soil rhizosphere and are beneficial for plant growth and pathogen resistance. Several species and strains are currently used worldwide in co-cultivation with crops as a biocontrol alternative to chemical pesticides even though little is known about the exact mechanisms of the beneficial interaction. We earlier found alamethicin, a peptide antibiotic secreted by Trichoderma, to efficiently permeabilise cultured tobacco cells. However, pre-treatment with Trichoderma cellulase made the cells resistant to subsequent alamethicin, suggesting a potential mechanism for plant tolerance to *Trichoderma*, needed for mutualistic symbiosis. Results: We here investigated intact sterile-grown Arabidopsis thaliana seedlings germinated in water or growth medium. These could be permeabilised by alamethicin but not if pretreated with cellulase. By following the fluorescence from the membrane-impermeable DNA-binding probe propidium iodide, we found alamethicin to mainly permeabilise root tips, especially the apical meristem and epidermis cells, but not the root cap and basal meristem cells nor cortex cells. Alamethicin permeabilisation and cellulase-induced resistance were confirmed by developing a quantitative in situ assay based on NADP-isocitrate dehydrogenase accessibility. The combined assays also showed that hyperosmotic treatment after the cellulase pretreatment abolished the induced cellulase resistance. Conclusion: We here conclude the presence of cell-specific alamethicin permeabilisation, and cellulase-induced resistance to it, in root tip apical meristem and epidermis of the model organism A. thaliana. We suggest that contact between the plasma membrane and the cell wall is needed for the resistance to remain. Our results indicate a potential mode for the plant to avoid negative effects of alamethicin on plant growth and localises the point of potential damage and response. The results also open up for identification of plant genetic components essential for beneficial effects from Trichoderma on plants.

BMC Plant Biology. 18 (1), 165, 2018

Zoology

Long-Acting β2-Adrenoceptor Agonists Enhance Glucocorticoid Receptor (GR)-Mediated Transcription by Gene-Specific Mechanisms Rather Than Generic Effects via GR

Rider CF, Altonsy MO, Mostafa MM, Shah SV, Sasse S, Manson ML, Yan D, Kärrman-Mårdh C, Miller-Larsson A, Gerber AN, Giembycz MA, Newton R.

Abstract

In asthma, the clinical efficacy of inhaled corticosteroids (ICSs) is enhanced by long-acting β_2-adrenoceptor agonists (LABAs). ICSs, or more accurately, glucocorticoids, promote therapeutically relevant changes in gene expression, and, in primary human bronchial epithelial cells (pHBECs) and airway smooth muscle cells, this genomic effect can be enhanced by a LABA. Modeling this interaction in human bronchial airway epithelial BEAS-2B cells transfected with a 2× glucocorticoid response element (2×GRE)-driven luciferase reporter showed glucocorticoid-induced transcription to be enhanced 2- to 3-fold by LABA. This glucocorticoid receptor (GR; NR3C1)-dependent effect occurred rapidly, was insensitive to protein synthesis inhibition, and was maximal when glucocorticoid and LABA were added concurrently. The ability of LABA to enhance GR-mediated transcription was not associated with changes in GR expression, serine (Ser^{203}, Ser^{211}, Ser^{226}) phosphorylation, ligand affinity, or nuclear translocation. Chromatin immunoprecipitation demonstrated that glucocorticoid-induced recruitment of GR to the integrated 2×GRE reporter and multiple gene loci, whose mRNAs were unaffected or enhanced by LABA, was also unchanged by LABA. Transcriptomic analysis revealed glucocorticoid-induced mRNAs were variably enhanced, unaffected, or repressed by LABA. Thus, events leading to GR binding at target genes are not the primary explanation for how LABAs modulate GR-mediatedtranscription. As many glucocorticoid-induced genes are independently induced by LABA, gene-specific control by GR- and LABA-activated transcription factors may explain these observations. Because LABAs promote similar effects in pHBECs, therapeutic relevance is likely. These data illustrate the need to understand gene function(s), and the mechanisms leading to gene-specific induction, if existing ICS/LABA combination therapies are to be improved.

Mol Pharmacol. 2018 Sep;94(3):1031-1046. doi: 10.1124/mol.118.112755. Epub 2018 Jun 29.

An Ethylenediamine-based Switch to Render the Polyzwitterion Cationic at Tumorous pH for Effective Tumor Accumulation of Coated Nanomaterials

Abdul-Hackam Ranneh, Hiroyasu Takemoto, Shunya Sakuma, Aziz Awaad, Takahiro Nomoto, Yuki Mochida, Makoto Matsui, Keishiro Tomoda, Mitsuru Naito, and Nobuhiro Nishiyama.

Abstract

Polyzwitterions are employed as coating polymers for biomaterials to induce an antifouling property on the surface. Fine-tuning the betaine structure switches the antifouling property to be interactive with anionic tissue constituents in response to a tumorous pH gradient. The ethylenediamine moiety in the carboxybetaine enabled stepwise protonation and initiated the di-protonation process around tumorous pH (6.5). The net charge of the developed polyzwitterion (PGlu(DET-Car)) was thus neutral at pH 7.4 for antifouling, but was cationic at pH 6.5 for interaction with anionic constituents. Quantum dots coated with PGlu(DET-Car) exhibited comparable stealth and enhanced tumor accumulation relative to the PEG system. The present study provides a novel design of smart switchable polyzwitterion based on a precise control of the net charge.

Angew Chem Int Ed Engl. 2018, 57, 5057 - 5061

Systematic in vivo study of NiO nanowires and nanospheres: biodegradation, uptake and biological impacts.

Alaraby M, Hernández A, Marcos R.

Abstract

High aspect ratio nanomaterials (NM) have a promising future in medicine and industry as a unique category of NM. Consequently, it is important to evaluate their potential biological side-effects before crediting their use. To understand the mechanisms of degradation, internalisation, and interaction with different biological targets, we used the in vivo model Drosophila melanogaster to obtain a systematic and complete study on high aspect ratio Ni nanowires (NiNW), compared with low aspect ratio Ni nanospheres (NiNS), and $NiSO_4$ as a model of agent releasing nickel ions. The distinguished shape of nanowires showed changes in their characteristics after oral administration until they reached the intestinal lumen, where their diameter decreased significantly. For the first time, we confirmed the internalization of needle-shaped materials via perforation of the intestinal barrier. Moreover, the results showed that D. melanogaster is a valid and effective tool in studies related to magnetic resonance imaging (MRI). Additionally, NiNM induced DNA damage and molecular changes at the gene expression level, in association with increase in oxidative stress levels. Notably, the observed negative effects were related to nickel as a metal rather than to its shape, since the effects induced by the three Ni forms were notably similar. In addition, independent of their form, Ni compounds did not induce toxic or mutagenic impacts. Our Drosophila model can be used to understand different phenomena related to high aspect ratio NM exposure, such as degradation, internalization and interaction with different targets.

Nanotoxicology. 2018 Sep 25:1-18. doi: 10.1080/17435390. 2018. 1513091. [Epub ahead of print]

Toxic and Genotoxic Effects of Silver Nanoparticles in Drosophila.

Alaraby M, Romero S, Hernández A, Marcos R.

Abstract

The in vivo model Drosophila melanogaster was used here to determine the detrimental effects induced by silver nanoparticles (AgNPs) exposure. The main aim was to explore its interaction with the intestinal barrier and the genotoxic effects induced in hemocytes. The observed effects were compared with those obtained by silver nitrate, as an agent acting via the release of silver ions. Larvae were fed in food media containing both forms of silver. Results indicated that silver nitrate was more toxic than AgNPs when the viability "egg-to-adult" was determined. Depigmentation was observed in adults including those exposed to nontoxic concentrations, as indicative of exposure action. Interestingly, AgNPs were able to cross the intestinal barrier affecting hemocytes that show significant increases in the levels of intracellular reactive oxygen species. Additionally, significant levels of genotoxic damage, as determined by the comet assay, were also induced. When the expression of different stress-response genes was determined, for both AgNPs and silver nitrate, significant upregulation of Sod2 and p53 genes was observed. Our results confirm for the first time that in an in vivo model as Drosophila, AgNPs are able to cross the intestinal barriers and produce primary DNA damage (comet assay) via oxidative stress induction. In general, the effects induced by silver nitrate were more pronounced than those induced by AgNPs what would emphasize the role of silver ions in the observed effects.

Environ Mol Mutagen. 2018 Oct 24. doi: 10.1002/em.22262. [Epub ahead of print]

Electrical excitability of roach (Rutilus rutilus) ventricular myocytes: effects of extracellular K^+, temperature and pacing frequency

Badr, A., Abu-Amra, E.S., El-Sayed, M.F. and Vornanen, M.

Abstract

Exercise, capture, and handling stress in fish can elevate extracellular K^+ concentration ($[K^+]_o$) with potential impact on heart function in a temperature- and frequency-dependent manner. To this end, the effects of $[K^+]_o$ on the excitability of ventricular myocytes of winter-acclimatized roach (Rutilus rutilus) (4 ± 0.5°C) were examined at different test temperatures and varying pacing rates. Frequencies corresponding to in vivo heart rates at 4°C (0.37 Hz), 14°C (1.16 Hz), and 24°C (1.96 Hz) had no significant effect on the excitability of ventricular myocytes. Acute increase of temperature from 4 to 14°C did not affect excitability, but a further rise to 24 markedly decreased excitability: stimulus current and critical depolarization needed to elicit an action potential (AP) were ~25 and 14% higher, respectively, at 24°C than at 4°C and 14°C ($P < 0.05$). This depression could be due to temperature-related mismatch between inward Na^+ and outward K^+currents. In contrast, an increase of $[K^+]_o$ from 3 to 5.4 or 8 mM at 24°C reduced the stimulus current needed to trigger AP. However, other aspects of excitability were strongly depressed by high $[K^+]_o$: maximum rate of AP upstroke and AP duration were drastically (89 and 50%, respectively) reduced at 8 mM $[K^+]_o$ in comparison with 3 mM ($P < 0.05$). As an extreme case, some myocytes completely failed to elicit all-or-none AP at 8 mM $[K^+]_o$ at 24°C. Also, amplitude and overshoot of AP were reduced by elevation of $[K^+]_o$ ($P < 0.05$). Although high $[K^+]_o$antagonizes the negative effects of high temperature on excitation threshold, the precipitous depression of the rate of AP upstroke and complete loss of excitability in some myocytes suggest that the combination of high temperature and high $[K^+]_o$ will severely impair ventricular excitability in roach.

American Journal of Physiology-Regulatory, Integrative and Comparative Physiology.

Insulin-like 3 expression and fibrosis induction after intra-testicular injection of magnetic nanoparticles in rat testis and the ameliorative role of Echinacea purpurea extract

Aziz Awaad, Mohamed A. Adly, Doaa Hosny

Abstract

The World Health Organization has approved magnetic nanoparticles (MNP) for use as a contrast agent for magnetic resonance imaging or tumor hyperthermia treatment. MNP are toxic over time after intra-testicular injection. A clear strategy to ameliorate the toxic side effects of MNP in normal tissues after medical application has not yet been developed. We used an extract of Echinacea purpurea (EP) as a natural source of antioxidant and free radical scavenging product for detoxification of MNP in testicular tissues. MNP localization in the interstitial area of testicular tissue reduced the expression of insulin-like factor 3 (INSL3) proteins as well as serum testosterone levels. Further, MNP caused accumulation of both collagen and elastin in the interstitial area and increased the thickness of the tunica albuginea. Injection of MNP during administration of EP extract for short periods slightly reduced the toxic side effects of MNP. After extended exposure to EP extract, INSL3 expression and testosterone returned to near control levels. Also, collagen and elastin accumulation caused by MNP was reduced after extended exposure to EP extract. We believe that the ameliorative effect of EP extract is due to its antioxidant properties.

Biotechnic & Histochemistry 2018, 93(2): 118–132, doi: 10.1080/10520295.2017.1399465.

Effects of seasonal acclimatization on thermal tolerance of inward currents in roach (*Rutilus rutilus*) cardiac myocytes

Badr, A., Korajoki, H., Abu-Amra, E.S., El-Sayed, M.F. and Vornanen, M.

Abstract

To test the hypothesis of temperature-dependent deterioration of electrical excitability (TDEE) (Vornanen, J Exp Biol 219:1941–1952, 2016), the role of sodium (I_{Na}) and calcium (I_{Ca}) currents in heat tolerance of cardiac excitability was examined in a eurythermic fish, the roach (*Rutilus rutilus*). Densities of cardiac I_{Ca} and I_{Na} and their acute heat tolerance were measured in winter-acclimatized (WiR) and summer-acclimatized (SuR) fish maintained in the laboratory at 4 ± 1 and 18 ± 1 °C, respectively. A robust L-type Ca^{2+} current (I_{CaL}), but no T-type Ca^{2+}current, was present in roach atrial and ventricular myocytes. Peak density of I_{CaL} was smaller in atrial (-1.97 ± 0.14 and -1.75 ± 0.19 pA/pF for WiR and SuR, respectively) than ventricular myocytes (-4.00 ± 0.59 and -2.88 ± 0.47 pA/pF for WiR and SuR, respectively) ($p < 0.05$), but current density and heat tolerance of I_{CaL} did not change between seasons in either cell type. In contrast to I_{Ca}, marked differences appeared in I_{Na} between WiR and SuR. I_{Na} density was 38% higher in WiR than SuR atrial myocytes (-80.03 ± 5.92 vs. -49.77 ± 4.72 pA/pF; $p < 0.05$) and 48% higher in WiR than SuR ventricular myocytes (-39.25 ± 3.06 vs. -20.03 ± 1.79 pA/pF; $p < 0.05$). The winter increase in I_{Na} density was associated with 55% (1.70 ± 0.27 vs. 0.77 ± 0.12) and 54% (1.08 ± 0.19 vs. 0.50 ± 0.10) up-regulation of the total Na^+ channel (*scn4* + *scn5* + *scn8*) transcripts in atrium and ventricle, respectively ($p < 0.05$). Heat tolerance of atrial I_{Na} was lower in WiR with a breakpoint temperature of 20.3 ± 1.2 °C than in SuR (23.8 ± 0.7 °C) ($p < 0.05$). The response of I_{Na} to seasonal acclimatization conforms to the TDEE hypothesis. The lower heat tolerance of I_{Na} in WiR is consistent with the lower heat tolerance of in vivo heart rate in WiR in comparison to SuR, but the match is not quantitatively perfect, suggesting that other factors in addition to I_{Na} may be involved.

Journal of Comparative Physiology B, 188(2), pp.255-269.

Spleen immunotoxicities induced by intra-testicular injection of magnetic nanoparticles and the role of Echinacea purpurea extract: a histological and immunohistochemical study

Aziz Awaad, Mohamed A. Adly, Doaa Hosny

Abstract

Recently, magnetic nanoparticles (MNP) have been used in several medical applications. High accumulations of MNP can be found in spleen and liver after different injection routes. Immunotoxicities produced by MNP in spleen, a lymphoid organ, need more investigations. This study investigated biodistribution, histological and immune responses to MNP in spleen after intra-testicular injection. Echinacea purpurea (EP) extract has immune stimulation and anti-oxidant properties. Investigation was done on the role of EP reduction of immunotoxicities produced by MNP in the spleen. After intra-testicular injection, MNP reached spleen parenchyma through blood circulation. Long term EP administration induced mild iron accumulation resulting from red blood cell (RBC) lysis. The opposite was observed when MNP treatment during EP administration significantly reduced lysed RBC iron in the spleen as well as MNP iron. It is possible the chelating properties of EP molecules possibly explained the presence of inert iron complexes from RBC in the spleen after EP administration only. The presence of MNP induced severe splenic cell degeneration and hemorrhage. The treatment with MNP combined with EP administration reduced these abnormalities. Additionally, anti-oxidant properties of EP and presence of MNP iron in the spleen had a role in activating macrophages to recycle all splenic iron. However, F4/80+, immunoglobulin A (IgA)+ and Ulex europaeus agglutinin I (UEAI)+ expressions significantly decreased when MNP were injected without EP. Otherwise, long term EP treatment maintained normal function of these cells.

Journal of Histotechnology, May, 2018, (41)3; 94-110. doi.org/10.1080/01478885.2018.1472857.

Ameliorative effect of bee venom and its extracted bradykinin-potentiating factor on neurological alteration induced by acrylamide and chips administration

Lashein, F.E.D.M., Amra, E.S.A., Seleem, A.A. and Badr, A.H.

Abstract

Acrylamide is reported for its toxicity on the central and the peripheral nervous system and causes paralysis. Bee venom (BV) and bradykinin-potentiating factor (BPF) have been documented for their potential therapeutic effects as anti-neuroinflammation. The study aimed to ameliorate the neurotoxic effects of acrylamide or chips by using BV or its extracted BPF. Mice were divided into 15 subgroups: control (G1.1, G1.2, G1.3) at 30, 45, and 60 days, respectively; acrylamide- (10 mg/kg b.w.; orally daily) administered subgroup for 30 days (G2.1), 45 days (G2.2), and 60 days (G2.3); chips feeding group (1/3 of daily diet) for 30 days (G3.1), 45 days (G3.2), and 60 days (G3.3); bee venom-treated group for 60 days (1.319 mg/kg b.w.) (G4.1); BPF-treated group for 60 days (2.314 mg/kg b.w.) (G4.2), day after the other day; and acrylamide- or chips-administered groups combined either with BV (G5.1, G6.1) or BPF treatment (G5.2, G6.2) for 60 days. The results indicated that the approximate LD50 for BV and BPF equal to 13.19 mg/kg and 23.14 mg/kg, respectively, and the extracted BPF contains 15 amino acids. Also, the results showed abnormal gait in mice of acrylamide-administered groups which was accompanied by histopathological changes in the hippocampus, cerebellum, and cerebral cortex. A marked gradual increase of alpha-synuclein expression was noted at the studied region in the acrylamide- and chips-treated groups at 60 days of treatment as compared to control. Both BV- and BPF-treated groups either separately or in co-administration with acrylamide or with chips did not show any histopathological changes in the studied regions with downregulated expression of alpha-synuclein. The study concluded the neuroprotective effect of BV and its extracted BPF against neurotoxicity induced by acrylamide or chips administration.

The Journal of Basic and Applied Zoology, 79(1), p.35.

Counter effect of bee venom and its extracted bradykinin-potentiating factor on acrylamide and chips administration-induced complications in the liver and kidney of male mice

Amra, E.S.A., Lashein, F.E.D.M., Seleem, A.A. and Badr, A.H.

Abstract

Acrylamide has been reported to induce hepato- and nephrotoxicity. The present investigation aims to alleviate the dangerous effects at the histopathological and physiological levels of acrylamide by bee venom and its extracted bradykinin-potentiating factor (BPF). Seventy-five adult male mice were divided into 15 groups: a control (G1) 15 animals for 30 (G1.1), 45 (G 1.2), and 60 (G 1.3) days of experimental periods; acrylamide-administered G2.1, G2.2, and G2.3 received acrylamide orally (10 mg/kg b.w) daily for 30, 45, and 60 days. Chips-administered G3.1, G3.2, and G3.3 were fed one third of its daily diet by chips for 30, 45, and 60 days. Bee venom- and BPF-treated G4.1 and G4.2 were i.p. injected with bee venom (1.319 mg/kg b.w.) and BPF (2.314 mg/kg b.w.), respectively, day after the other day for 60 days. G5.1 and G5.2 received acrylamide orally (10 mg/kg b.w) combined either with i.p. by bee venom (1.319 mg/kg b.w.) or BPF (2.314 mg/kg b.w.) respectively day after the other day for 60 days. G6.1 and G6.2 were fed one third of its daily diet by chips for 60 days combined either with i.p. by bee venom (1.319 mg/kg b.w.) or with BPF (2.314 mg/kg b.w.), respectively, day after the other day for 60 days.

The Journal of Basic and Applied Zoology, 79(1), p.34.

Histological and ultrastructural studies of spermatogenesis of freshwater mite, *Unionicola aegyptiaca* (Acari, Unionicolidae)

Ramadan, S.A., Ismail, T.G. and Mustafa, A. N.

Abstract

The male genital system of the water mite, *Unionicola aegyptiaca* consists of an accessory gland, two spherical testes, two vasa deferentia, common vas deferens, an ejaculatory complex and spermatopositor (penis) and is supported with the male genital skeleton. It is evident that each testis is enclosed in a very thin amorphous layer (basal lamina) and consists of a germinal part, in which spermatogenesis take place for sperms development, and a glandular part which consists of a massive complex of glandular cells. The glandular cells of the accessory gland and glandular part of each testis secret testicular secretions which delivered into the lumen of the testis and contribute to sperm cell aggregation and sperm movement. The sperm development of *Unionicola aegyptiaca* includes spermatogonia, primary and secondary spermatocytes, spermatids and sperms. Fine structures of these stages show mitochondria, rough endoplasmic reticulum, free ribosomes and cytoplasmic vacuoles in their cytoplasm. Transmission electron micrographs show that the mature sperm consists of three parts; head, middle piece and a short tail.

Egypt. J. Zool., 69: 191-206.

Expression of alpha-synuclein during eye development of Bufo arabicus.

Seleem, A.A. and Lashein, F.E.D.M.

Abstract

Alpha-synuclein contributes to neurodegenerative diseases that are characterized with the increase of its expression and collectively known as synucleinopathies such as Parkinson's disease and dementia with Lewy's bodies. A healthy balance of alpha-synuclein is important for preventing synucleinopathies, whereas the normal physiological role of alpha-synuclein is still under investigation. The present study was designed to evaluate the involvement of alpha-synuclein in the eye of Bufo arabicus during development, metamorphosis and adult stage. Different larval and adult stages of Bufo arabicus were obtained for histological and immunofluorescent expression of alpha-synuclein during eye development. The results showed that alphasynuclein expression was associated with differentiation and migration of periocular mesenchyme cells that will form the trabecular meshwork. Also, alphasynuclein expression was detected in the ciliary body at the adult stage. This study confirmed an additional role of alpha-synuclein during the development of the anterior eye chamber. On the other hand, synuclein expressions in Bufo arabicus under study helps improve our knowledge about gene conservation studies and the mechanisms by which the anterior chamber of the vertebrate eye is differentiated during development. Also, synuclein might be considered as an evolutionary conserved gene expression during eye development of Bufo arabicus.

Current Science, 115(7), pp.1305-1311.

Ameliorative Roles of Vitamins C, E and DMSA on Hepatic and Renal Functions Against Lead Toxicity in Male Albino Rats

Mohamed F.El-Sayed, Sarry Kh. Abdel – Kgaffar, Amin Abddou Seleem, Ramy A. Mohamed.

Abstract

This study was carried out to estimate the toxic effect of lead acetate on hepatic and renal functions of rats , and the possible ameliorative effect of both vitamin C and E , and their combination with DMSA against lead intoxication . Thirty male albino rats were divided into five groups and administrated the following treatments for six weeks . group 1 received drinking water and served as control; group 2 received 100 ppm lead acetate ; group 3 received 100 ppm lead acetate combined with 50 mg/kg b.wt of DMSA (ip) ; group 4 received 100 ppm lead acetate plus 160 mg/kg b.wt of vitamin C combined with 50 mg / kg b.wt of vitamin E; group 5 received in addition to lead acetate both vitamin C and E plus DMSA in the same previous dose . Lead acetate administrated induced a significant decrease in plasma alkaline phosphatase (ALP) , total proteins and plasma albumin , while it induced a significant increase in the plasma level of acid phosphatase (AP) , compared to the control. Significant elevation in the plasma level of urea , total lipids and triglycerides as a result of lead exposed were also observed , compared with control . DMSA , vitamin C combined with vitamin E , and DMSA combined with both vitamin C and E induced a significant elevation in the plasma level of ALP , total proteins and albumin respectively , whereas a significant decrease in the plasma level of AP , urea , total lipids and triglycerides , respectively were observed . Thus , lead acetate induced toxic effect in hepatorenal functions , whereas , administration of DMSA ,vitamin C plus E and also DMSA combined with both vitamins C and E could ameliorate the toxic effect of lead acetate on the kidney function and to somewhat on the liver function .

J. Pharm. Appl. Chem., 4, No. 1, - (2018)

Description of two new species of aquatic oribatid mites (Family: Malaconothridae, Genus: Malaconothrus) from Sohag Governorate,

Ramadan, S.A., Ismail, T.G. and Mustafa, A. N

Abstract

Two oribatid mite species belonging to the genus *Malaconothrus*, namely *Malaconothrus ramadani* sp. n. and *Malaconothrus transversus* sp. n., were described as two new species. They were collected from the roots of the floating aquatic plant, *Eichhornia crassipes* in River Nile, Girga city, Sohag Governorate, Egypt. The first species, *Malaconothrus ramadani* sp. n., is clearly characterized by zigzag-like lateral margins of the notogaster, nine thick dorsal folds (2 longitudinal and 7 protruded transverse), eight ventral thick oblique folds (7 longitudinal and 1 transverse) and the genital plates carry four pairs of simple setae. Also, it has five and six distinct dorsal and ventral processes, respectively. The second species, *Malaconothrus transversus* sp. n., is characterized by the presence of six flattened dorsal transverse folds and five ventral oblique folds (4 longitudinal and 1 transverse).

Egypt. Egypt. J. Zool., 2018 in press.

Studies on the Abundance, Temporal Distribution and Diversity of Spiders (Arachnida: Araneae) Associated with Lemon Trees, Sohag Governorate, Egypt

Fathey E. Soliman, Tarek G. Ismail, Alaa Y. Moustafa and Safa M. El-Masry

Abstract:

Spiders have an important role in the agroecosystems. They are effective in suppressing the pest populations as biological controllers. This study aimed to study the abundance, temporal distribution and diversity of spiders in an agriculture research site at Jazirat Shandweel, Sohag Governorate, Egypt. The sampling was carried out monthly from January to December 2016 using the beating and hand picking methods. One thousand, seven hundred and twenty-nine individuals were identified and classified into fifteen species belonging to fifteen genera and twelve families. The temporal variations in spider families revealed that; four families; Theridiidae, Eutichuridae, Salticidae and Linyphiidae, were the most abundant. Spider's community was classified into two categories; hunting spiders and the webbuilding ones. The hunting spiders were more abundant than the web building ones. The most species-rich family was Salticidae, while the most individuals-rich family was Theridiidae. The Shannon index exhibits the monthly variation in spider diversity that ranged between 0.83 and 2.28. The evenness index values were high and ranged between 0.4 and 0.95 revealing absence of dominance of a single species.

J. Eco. Heal. Env. 6, No. 3, 107-120 (2018)

Spiders (Arachnida: Araneae) of Jazirat Shandweel District, Sohag Governorate, Egypt

Fathey E. Soliman, Alaa Y. Moustafa, Tarek G. Ismail & Safa M. El-Masry

Abstract

This study gives highlights on the biodiversity of spiders in an olive trees orchard, a lemon trees orchard, and webs of Cyrtophora citricola at Jazirat Shandweel District, Sohag Governorate, Egypt. In addition, it gives a preliminary list of spiders based on the main taxonomic characters. The sampling was carried out weekly or monthly during the period: September, 2015 to January, 2018 using the beating net and hand picking methods. A total of 6237 individuals were collected, identified, and classified into: 30 species belonging to 29 genera and 21 families; among them, three families, 18 genera, and 11 species are listed in addition to other unidentified species. Keywords: Araneae, Biodiversity, Identification, Sohag Governorate, Taxonomic keys.

Serket (2018) vol. 16(3): 133-160.

Identification of some trematode cercariae collected from six marine snail species of the genus nerita

Amaal hassan, muslimah al-solami1 , sabah m. Hassan

Abstract

Transmission of trematode cercariae depends mainly on the presence of marine snails as an intermediate host for zoonotic diseases. Parasitic infections in marine snails are poorly discussed. The current study was aimed to investigate the collected snails and determine the prevalence of larval trematode infections as well as identifying the cercarial types from January to December 2016. A total of 549 marine snails belonging to the genus, Nerita were randomly collected from Obhor bay, Red Sea at Jeddah city, Saudi Arabia. To harvest cercariae, snails were exposed to artificial light and the non-shedding snails were crushed. Eight distinct cercariae were identified as well as their sporocysts. Seven of them were found belonging to non-virgulate xiphidiocercaria: Ascorhytis charadriformis, cercariae, Haematoloechus similis, Litorina saxatilis V, Litorina saxatilis VII, Maritrema lingulla, Microphallus similis, Microphalliae and one ocellate furcocercous. The most prevalent type of cercariae was Maritrema lingulla (16.96%). The described cercariae are part of a diverse group of about eight trematode species inhabiting marine Nerita snails as first intermediate hosts. Such studies can assist in collecting data on disease distribution in the sympatric fish and the configuration of trematodes transmission by snails and eventually, in the avoidance and control of the subsequent fish and human diseases. Key words: Marine snails, Nerita, Sporocyst, Cercariae, Trematoda, Red Sea

Journal of the Egyptian Society of Parasitology, Vol.48, No.2, August 2018

Role of Parasitic Helminths in Bioremediating Some Heavy Metal Accumulation in the Tissues of Lethrinus mahsena

Amaal Hassan, Samia Moharram , Hanan El Helaly

Fish take up metals from the aquatic ecosystem and accumulate it in their muscle tissues and organs. The aim of the present study was to determine the role of intestinal helminths in bioremediating the accumulation of some heavy metals in the muscle tissues of the emperor fish, Lethrinu smahsena. A total of 130 fish were collected randomly from Raas Mehsen in the Red Sea, Jeddah coast, during the period of November 2015 to May 2016. The percent of total infection in L. mahsena fish was found to be 62%. Four species of Trematoda, one cestode larva and three species of Nematoda were recorded from the small intestine. Element concentrations in the infected and non-infected fish and parasites were analyzed using flame atomic absorption spectrometry. Mean concentration of individual heavy metals in trematode parasites was in the order of As> Fe> Zn> Pb> Cu> Cd. For cestodes, it was As > Fe> Zn> Pb> Cu> Cd. While in nematodes, it was in the order of As> Fe> Zn> Pb> Cd> Cu. Most heavy metals exhibit a significant decrease in fish tissues infected with helminthes. Bioaccumulation factors indicated much higher concentrating capacity of cestode parasites than fish organs. Thereby, cestode and nematode infections in marine fish could be considered to be a biological indicator of heavy metal pollution and at the same time could also minimize the bioaccumulation of heavy metals in fish tissues

Turkish Journal of Fisheries and Aquatic Sciences 18: 435-443 (2018)

Meristic and Morphometric Characteristics of five-lined snapper, *Lutjanus quinquelineatus* (Bloch, 1790) from the Red Sea, Egypt

Faiza . M. Soliman , Sahar. F. Mehanna, Hamdy .A. Soliman and Taha. S. Baker

A**bstract**

In the present study, 120 fish samples (64 male and 56 female) of five-lined snapper, *Lutjanus quinquelineatus* of variable sizes were used for demonstration the morphometric and meristic characteristics of this species in the Egyptian Red Sea, Hurghada fishing area. The total length varied from 15.3 to 28.7 cm in males and from 16.0 to 31.7 cm in females while their weights ranged between 44 and 378 g in males and between 48 and 512 g in females. This fish species showed constant meristic characters. Statistical interpretation of morphometric data indicated that there is direct relationship between total body length with head length (HL), snout length (SnL), eye diameter (ED) and length of caudal peduncle (CPL). The meristic characters like dorsal fin rays, anal fin rays, lateral line scales, gill rakers on lower arm and scales in transversal line were counted. The results revealed that there is no sexual dimorphism in *L. quinquelineatus* from Hurghada fishing area.

Egyptian Journal of Aquatic Biology & Fisheries

Oxidative stress and histomorphological markers in the offspring of *Poecilia reticulate* maternally exposed to metallic and nanoformulated copper

Hamdy A. M. Soliman and Sohair M. M. Ragab

Abstract

The goal of present study is to determine whether metals or nanomaterials are transferred from exposed pregnant females of viviparous fishes to their developing offspring and the subsequent potential effects on the oxidative stress and histomorphological indicators. Gravid females of guppies (Poecilia reticulata) exposed to 1 mg/l copper sulfate (CuSO4) or copper oxide nanoparticles (CuO-NPs) for 17 to 25 days depending on giving birth. Once a female gave birth, the female and her newborn offspring were analyzed for copper concentrations while some oxidative stress parameters and histopathology were performed for the newborn offspring. There were no malformations or histopathological lesions observed in the newborn offspring of guppies exposed for either CuSO4 or CuO-NPs. Also, there was no maternal metal transfer for either CuSO4 or CuO-NPs while females exposed to copper sulfate only showed significantly higher concentrations of Cu compared to control group. In addition, there were non-significant changes in catalase compared to control group. While, glutathione decreased significantly in offspring their mothers exposed to CuO-NPs only compared to control group. In addition, superoxide radical and lipid peroxidation increased significantly in offspring their mothers exposed to CuSO4only compared to control group. The findings of the present study indicated that the offspring were more sensitive to CuSO4 than CuO-NPs. Although absence of metal Cu in the tissues of offspring as well as lack of morphological abnormalities and histopathology, maternal transfer of Cu metabolites may be suggested to be the causative factor for some oxidative stress.

Egyptian Journal of Aquatic Biology & Fisheries ISSN 1110 - 6131 Vol. 22(2): 51- 60 (2018)

Modulatory effects of green tea extract against the hepatotoxic effects of 4-nonylphenol in catfish (Clarias gariepinus)

Alaa El-Din H. Sayed, Hamdy A.M. Soliman

Abstract

The antioxidant role of the green tea (Camellia sinensis) extract (GTE) was examined to remedy the toxic effects of (0.2 mg l−1) 4-nonylphenol(4-NP). Biochemical parameters, antioxidant enzymes, liver lipid peroxidation (LPO), DNA fragmentation, and apoptosis as well as histopathology of liver of African catfish Clarias gariepinus were considered. Catfishes were divided into four groups: first group (control), second group (0.2 mg l−1 of 4- NP), third group (0.2 mg l−1of 4-NP +100 mg GTE l−1water), and fourth group (0.2 mg l−1 of 4-NP +200 mg GTE l−1water). The results showed that significant increments of serum glucose, AST, ALT, total protein, total lipids, cholesterol, G6PDH, and cortisol. Meanwhile, serum acetylcholinesterase, ALP, and LDH were significantly reduced. In addition, antioxidant enzymes (SOD, CAT, GST, and TAC) levels were reduced in 4-NP treated fish compared to control. Also, there were significant increments in hepatic LPO, DNA fragmentation, and apoptotic erythrocytes in 4-NP treated fish compared to control. Liver of 4-NP treated fish showed some histopathological alterations such as, vacuolization in hepatocytes, congestion in central vein, infiltration of mononuclear inflammatory cells, and necrosis as well as depletion of glycogen content of liver. Addition of green tea extract into the water restored the alterations in most of those biomarkers induced by 4-NP. We concluded that, GTE has a protective role against hepatic failure, depletion of antioxidant defense, and genotoxicity induced 4-NP in C. gariepinus.

Ecotoxicology and Environmental Safety 149 (2018) 159–165

UVA-induced neurotoxicity in Japanese medaka (Oryzias latipes)

Sayed AEH, Soliman HAM, Mitani H.

Abstract

Ultraviolet radiation-induced neurodegeneration has been studied in the early stages of development in fish, but not extensively in the adult stage. The present study aimed at investigating the effects of ultraviolet radiation-A (UVA) in adult Japanese medaka (Oryzias latipes). The brain, spinal cord, and retina were examined histopathologically as nervous system target organs. Japanese medaka fish were exposed to 15, 30, and 60 min day-1 UVA for 3 days, and samples were obtained 24 h and 14 days after UVA exposure. Neurohistopathological alterations in brain tissue included vacuoles, blood congestion, degeneration of neuropils, and pyknotic nuclei in neurons. Alterations in the spinal cord included neuronal cell degeneration, reduction in the spinal cord area, and degeneration of Mauthner cells. Retinal tissue showed vacuolation in the nerve fiber layer (NFL), pyknotic nuclei in the ganglion cell layer (GCL), and decreased cell populations particularly in the inner nuclear layer (INL) and GCL. The degree of degeneration was dependent on the duration of UVA exposure. The signs of degeneration decreased gradually and disappeared completely after the 14-day recovery period. In addition, p53-deficient medaka fish were more tolerant than were wild-type (Hd-rR) Japanese medaka. In conclusion, UV radiation induced neurodegeneration in the brain, spinal cord, and retina of adult Japanese medaka (Oryzias latipes) but their normal histological architecture reappeared in these tissues after 14 days.

Photochem Photobiol Sci. 2018

Effect of geographic location and sexual dimorphism on shield shape of the Red Sea hermit crab Clibanarius signatus using the geometric morphometric approach

Ismail, T.G.,

Abstract:
The hermit crab Clibanarius signatus Heller, 1861 inhabits varied intertidal habitats of the Red Sea coast, such as rocky shores and mangrove littoral salt marshes. Shield-shape variation among three populations of C. signatus was analyzed with geometric morphometric methods. Shape variation was studied through multivariate analyses using configurations aligned by the generalized Procrustes analysis. Shape variation was explored through principal component analysis. The ordination of the populations and the sexes was investigated using discriminant analysis of canonical variables. Centroid size, as a measure of overall size, was used to estimate size variation among the three populations and the sexes. The results revealed the presence of shield-size variation among the three populations and confirmed the size sexual dimorphism in two populations. Moreover, the analysis revealed the occurrence of two morphotypes based on a covariation between shield shape and shape of occupied shells. The geographic distance was not a good predictor of shield shape. Cross-validation analyses correctly reclassified more than 70% of individuals and 66% of sexes to their correct group. It was suggested that association in shield-shell shape could be the result of the phenotypic plasticity of this species.
Canadian Journal of Zoology, 96(999), pp.667-679.

Localization of connective tissue growth factor (CTGF) and transforming growth factor beta-2 (TGF-β2) during eye development of four species of birds

Seleem, A.A., Sultan, A.R.S., Said, A., Shahat, M.M. and Moustafa, M.A.

Abstract
Connective tissue growth factor (CTGF) and transforming growth factor (TGF-β2) have essential roles for structure, function, growth, and production of extracellular matrix during eye development. The current study aim was to examine the localization of CTGF and TGF-β2 by immunohistochemical labeling during eye development in four different habitat species of Egyptian birds i.e. chicken (Gallus gallus domesticus), duck(Cairina moschata), quail (Coturnix coturnix), and egret (Bubulcus ibis). Fertilized eggs were obtained to access pre-and post-hatching stages of developing eye. CTGF and TGF-β2 were detected in the inner non-pigmented epithelium layer of ciliary body during eye development of studied birds. Moreover, CTGF was well expressed in the developing sclera, but not expressed in the developing retina. On the contrary, expression of TGF-β2 was detected in the developing retina but was not detected in the developing sclera. The pattern of expression and distribution of CTGF and TGF-β2 in ciliary body, retina and sclera concluded the important cellular function of these growth factors during eye development of studied birds.
Journal of Histotechnology, pp.1-13.

Zinc oxide nanoparticales induced histological, histochemical and genotoxicity effects in kidney of adult male rabbits

Tito N Habib, Hekmat O Abdel-Aziz and Eman E Ragab

Abstract

Our aim was to study the histological, histochemical and genotoxic effects of ZnO NPs on the kidney of adult male rabbits. Fifteen adult male rabbits were divided equally into three groups. Group I was the control group; group II was the low dose treated group, in which rabbits were intraperitonial injected with ZnO NPs (100 mg/kg/day) for 14 days; and in group III was the high dose treated group, rabbits were injected intra peritonially with ZnO NPs (250 mg/kg/day) for 14 day. At the end of the experiment, specimens from the kidney were taken and stained by H&E, PAS and Masson trichome stains. Also bone marrows were isolated for flow cytometry to study genotoxicy. ZnO NPs was nephrotoxic and led to prominent histopathological changes in the kidney. There were destructions of the renal tubules, in form of loss of brush border, vacuolation of cytoplasm and intratubular protein depositions. Also there was interstitial infiltration of inflammatory cells. The renal corpuscles were dilated and congested. There was increase in apoptotic cell rate of bone marrow samples and showed greater and distinct fragmentation or shearing DNA. ZnO NPs had cytotoxic and genotoxic effects in the kidney. It increased apoptotic rate of the bone marrow cells and fragmentation of DNA. ROS may be the main cause of cytotoxic effects. ZnO NPs was toxic in dose dependent manner.

J Ecosys Ecograph 2018, Volume: 8

Synthesis and effect of a new Terbium Gibberellic complex on the histopathological alteration induced by Gibberellic acid on liver and kidney of mice Mus Musculus

Seleem, A.A. and Hussein, B.H.

Abstract

The objective of this study was to synthesize Gibberellic lanthanide complex and evaluate its biological activity to reduce the Gibberellic acid toxicity on liver and kidney. The new bis (Gibberellic)-nitro-terbium(III) complex was characterized by different analytical methods: elemental analyses, Uv-vis, molar ratio, fluorescence, FT-IR, and TGA-DTA measurements. Thirty newborns were classified into three groups control, Gibberellic acid, and Terbium gibberellic acid complex. Livers and kidneys of studied groups proceed for general histology and immunohistochemical staining of Cyr61, cytochrome C, and TNFR2. From the absorption titration measurements, the binding constants of DNA with Tb(III)-(GA)2 complex and free ligand were found to be 3.9×10^4 and 2.1×10^3 M^{-1}, respectively, with the stoichiometry of 1:1. Hypochromism was observed from the absorption titration experiment which indicates the intercalation of Tb(III)-(GA)2 complex between the base pair of DNA. Gibberellic acid treated group showed alteration in the histological picture of livers and kidneys that accompanied with the reduction in the expression of Cyr61, cyt C, and TNFR2. The amelioration was observed in Gibberellic acid complex with Terbium group. The study concluded that Terbium gibberellic complex is less dangerous effects than Gibberellic acid alone. This article is protected by copyright. All rights reserved.

Chemical biology & drug design.

Antitumor effect of scorpion venom peptides in vivo of male rabbit and in vitro of DU145 cells of prostate cancer model

Nadia S Mahrous, Hemely A Hassan, Fayza M Ali and Tito N Habib

Abstract

The modern approach used to characterize various compounds from animal venoms, using advanced proteomic and genomic tools, has been denominated "venomics". Venoms from various scorpions have been reported to prevent propagation of different cell lines such as prostate cancer (DU-145), human leukemia and neuroblastoma. In the present study, antitumor effect of scorpion venom was detected in vivo of male rabbits and in vitro of PC-3 cell line using cell cycle profiling analysis, DNA fragmentation assay, and genetic and epigenetic variations by ELISA kits. The results showed that apoptosis was maximum at pre-G1, and cell growth arrest at G1 phase in group IV. Venom differentially up regulated gene expression of P53, BAX, BCL-2. DNA showed greater and distinct fragmentation in vivo and in vitro of prostate cancer (PC) than venom treated groups. From the previous result we have concluded that L. quinquestriatus' scorpion venom induced apoptosis and differentially modulated the expression of tumour suppressor genes and concomitantly repressing the expression of oncogenes in vivo of induced male rabbits with PC and in vitro of PC-3cell line.

J Ecosys Ecograph 2018, Volume: 8

Influences of olive leaf extract in the kidney of diabetic pregnant mice and their offspring

Hend A. Mohammed, Hanan A. Okail, Mona A. Ibrahim, and Nahed M. Emam

Abstract

Background: Phytotherapeutic treatment is used in the treatment of diabetes and its complications. The current study aims to evaluate the significant effect of supplementation of aqueous olive leaf extract (OLE) (Olea europaea) in the kidney of diabetic pregnant mice and their fetuses. Forty pregnant mice were divided into four groups contained 10 mice each after mating. The first group was the control (G1). The second group (GII) was intraperitoneally injected by a single dose of (240 mg/kg body weight) of streptozotocin (STZ). The third group (GIII) was administrated with a daily oral dose of extract of olive leaf extract (100 mg/kg) from days 1 to 18 of gestation. The fourth group (GIV) was injected intraperitoneally by a single dose of (240 mg/kg body weight) of STZ and post-treatment with oral dose of extract of olive leaves from days 1 to day 18 of gestation.Results: Both mothers and their fetuses of STZ-induced diabetic group showed a decrease in weight compared to control and diabetic group supplemented OLE extract. According to the biochemical and histopathological observations, the STZ-induced diabetic group showed a significant ($P < 0.05$) increase in serum urea and creatinine levels parallel with detectable histopathological changes in kidney tissues of pregnant mice and their fetuses. Moreover, there was a significant decrease in serum urea and creatinine ($P < 0.05$) of diabetic mother group under treatment with OLE as compared to diabetic mice. Also, histological findings showed improved renal architecture as reflected by reduced glomerular and tubular necrosis in pregnant mice and their fetuses when compared with control group. Also, there was an increase in the anti-angiotensin II (Ang II) immunoreactivity in renal tubules, intra-glomerular, and interstitial cells in the kidney tissue of STZ-induced diabetic group which was markedly improved by treatment with OLE.

Conclusion: Oral administration of aqueous olive leaf extract to diabetic pregnant mice and their fetuses has ameliorative effect on weight gain as well as kidney functions and has the ability to minimize the damage in the kidney and placental tissue caused by hyperglycemia, and this effect may be attributed to its antioxidant activity.

The Journal of Basic and Applied Zoology

Geology

Hydrocarbon type detection using the synthetic logs: A case study, Baba member, Gulf of Suez, Egypt

Abudeif, A.M.[b], Attia, M.M.[b], Al-Khashab, H.M.[b], Radwan, A.E.[a]

[a]*Exploration Department, Gulf of Suez Petroleum Company (GUPCO), Cairo, Egypt*

[b]*Geology Department, Faculty of Science, Sohag University, Sohag, Egypt*

Abstract

Lack of pressure data and/or one curve of the essential well logs such as density, neutron, sonic, resistivity and gamma ray curves in some reservoirs, is not preferred situation for the petrophysict, which will affect the petrophysical evaluation process and the reservoir characterization study. Four wells (A, B, C and D), in the area of interest, penetrated Baba sandstone zone in Badri field. The main challenge in the studied zone is the absence of pressure gradients and the density-neutron separation is not clear enough to judge the hydrocarbon type in all wells at the level of baba sandstone reservoir, where they are needed for the estimation of the hydrocarbon type (oil or gas). So it is preferred to use the three porosity logs to investigate the hydrocarbon type. The second challenge is constructing synthetic logs in the absence of the three main porosity logs. In this paper, all available data were used to estimate the hyocarbon type in two studied wells at the level of Baba sandstone zone, firstly by using well logging relationships between density and sonic in the wells which have sonic logs at the zone of interest, secondly by applying special petrophysical studies to help for estimation of hydrocarbon type. Crossplot technique was used to estimate the hydrocarbon type in the zone of interest using the synthetic sonic curve, original density curve, original neutron curve plus their derived porosity and variables values in the used well logging crossplots including some petrophysical crossplots, which can help in this situation. The results of this study revealed that, 1) the synthetic logs play a great role in solving of petrophysical and geological problems, 2) there is a good relationship between the density and sonic logs in the analogues (A and D) wells, and 3) the obtained synthetic sonic log makes a sense with lithology and other logs (neutron and gamma). Therefore, the synthetic sonic log, in corporation with the density and the neutron logs as well as the crossplots can detect the fluid type in the studied wells. The final result that the most likely hydrocarbon type in well (B) is oil while it has gas signature in well (C).

Journal of African Earth Sciences, 144, (2018), 176-182

A new species of Hypselaster (Echinoidea, Spatangoida) from the Middle Eocene Midawara Formation of the Eastern Desert, Egypt

Elattaar, A.A.

Geology Department, Sohag Faculty of Science, Sohag University, Sohag, 82524, Egypt

Abstract

The schizasterid echinoid genus Hypselaster Clark, 1917, is recorded for the first time from the Midawara Formation (Middle Eocene, Lutetian), which crops out east Maghagha area, east Nile Valley, Eastern Desert, Egypt. Except for Hypselaster sp. from the Upper Miocene (Messinian) of Morocco, no Hypselaster has been recorded in pan Africa. The material described in the present paper is considered to represent a new species (Hypselaster strougoi n. sp.) that is characterized by a medium, oval to subpentagonal test with distinct frontal sinus, a subcentral ethmolytic and wide apical disc (slightly behind the center of test) with two large and apart genital pores, an anteriorly excentric semilunal-shaped peristome, long, flexed and deeply sunken paired anterior petals, a longitudinally oval periproct in the topmost part of the oblique forwardly truncated posterior, and perforate, crenulated tubercles. Both peripetalous and incomplete latero-anal fascioles are present; the latero-anal fasciole is faint and incomplete laterally on the sides of the test.

Swiss Journal of Palaeontology, 137 (2), (2018), 379-387

Estimation of site effect using microtremor technique at 15th May City, Helwan, Egypt

Mohammed, M.A.[a], Abudeif, A.M.[a], Omar, K.A.[b], Attia, M.M.[a]

[a] *Faculty of Science, Geology Department, Sohag University, Sohag, Egypt*

[b] *National Research Institute of Astronomy and Geophysics (NRIAG), Helwan, Cairo, Egypt*

Abstract

Local site effect is an important feature of seismic hazards, which often causes amplification of ground motions and results in increasing the damage potential of earthquake. This paper presents an experimental study of microtremor data to investigate the dynamic characteristics of soil and structures at the 15th May City, southeast Cairo, Egypt. This city was constructed on Eocene sedimentary rocks of mainly limestone. Despite the newness of this city, their buildings suffer from structural damages, which mainly developed over the last two decades. Predicting the reasons of structural damage caused by earthquakes (including micro-earthquakes) is considered and became the main target of this study. The horizontal vertical spectral ratio (HVSR) analyses of ambient noise data at 54 sites were processed and interpreted using Geopsy Software to calculate the amplification factor and fundamental resonance frequency of each observation point. Three tests including the damping value, the horizontal spectrum rotate, and H/V rotate were undertaken to ensure that the peaks of spectral ratio are either natural or artificial origin. The vulnerability index (Kg) was estimated based on Nakamura's technique for assessing the seismic vulnerability index (SVI). The results indicate that the resonance frequency ranges between 1.36 and 1.607 Hz at the most measured stations, but it attained higher value up to 11 Hz at sites having high thicknesses of soft sediments. The lowest resonance frequencies occur in the areas of the deepest bedrock, whereas the higher resonance frequencies were observed in the areas of shallowest bedrock. The amplification factor ranges between 1.09 and 3.61 at most measured stations, but it became greater up to 5 in few locations. The northern west part of the area has thick soft sediments and may be more affected by earthquake damage because it contains SVI values ranging from 6.5 to 8.5, in consistent with the amplification factor and fundamental frequency results, while the other parts of the area are relatively safe because they contain low SVI values (0.5–4.3).

Arabian Journal of Geosciences, 11 (2), 1 (2018), Article number 16

Middle Eocene echinoids from El Sheikh Fadl-Ras Gharib stretch, Eastern Desert, Egypt: systematics, stratigraphy, palaeobiogeography

Elattaar, A.A.

Geology Department, Sohag Faculty of Science, Sohag University, Sohag, Egypt

Abstract

Twenty-two echinoid species (5 regular and 17 irregular) belonging to 14 genera, 10 families, 5 orders, and 3 subclasses are identified from the Middle Eocene succession cropping out in El Sheikh Fadl-Ras Gharib stretch, Eastern Desert. The echinoid fauna studied herein came from four sections: Gebel ElMehasham, South Gebel ElMehasham, Gebel ElMereir, and Gebel Qarara sections. The studied succession consists of three formations, from base to top Muweilih, Midawara, and Sath ElHadid, spanning the Middle Eocene (Lutetian and Bartonian), Lower-Middle Mokattamian (levels MK3 to MK6). The highest species diversity is recorded in the Midawara Formation (21 species), while the Muweilih Formation is barren of echinoid species. Four species are recorded for the first time in the studied area: Echinolampas cf. bastai Elattaar and Strougo 2001; Schizaster isidis Stefanini Boll Soc Geol Ital 38:39–63, 1919; Gillechinus humei (Fourtau 1908); and Eupatagus lefebvrei (de Loriol Memoires de la Societe de Physique et d'Histoire Naturelle de Geneve 27:58–148, 1880). One species consider to be new, Schizaster sp. (n. sp). Thirteen species are endemic to Egypt, and nine are common elsewhere in the world, in some countries of Europe, Africa, and Asia. Predation and malformation in growth are observed in two species: Schizaster humei Fourtau Mémoires de l'Institut Egyptien 6(2):93–175, 1909b and Eupatagus cossmanni (Lambert Mém Soc Géol Fr, Paléontol 9:1–57, 1902) as a shallow infaunal species. All the identified echinoid fauna herein has been examined and systematically described with the aim to know their stratigraphic and paleogeographic distribution.

Arabian Journal of Geosciences, 11 (12), 1 (2018), Article number 303

Detection of basaltic intrusion using geomagnetic survey on Kolit Fahdi, Eastern Desert, Egypt

Abudeif, A.M., Alkhashab, M.H., Saad, S.E.
Faculty of Science, Geology Department, Sohag University, Sohag, Egypt

Abstract

The aim of this study is to delineate the areal extent of and estimate depths to a basaltic intrusion – Fahdi domal structure (FDS) – in the western desert of Egypt. The study also shed light on the different phases of deformations associated with this intrusion. For this purpose, we integrate total field ground magnetic data and aeromagnetic data, collected for a wider area surrounding this dome, to characterize the basaltic intrusion in terms of depth and magnetic susceptibilities and evaluate the subsurface structure caused by this intrusion in the surrounding areas. The magnetic data was reduced to the North Pole to get RTP magnetic data with anomalies centered on the subsurface causative bodies. Different Filtering techniques were applied including; regional-residual separation using power spectrum method, downward continuation, structural trend analysis and depth estimation for the basement sources. The depths were calculated using power spectrum technique, analytical signal tool and Euler deconvolution. 2D and 3D modeling of RTP magnetic profiles were applied to validate the results of depth estimation. Apparent magnetic susceptibility values were also calculated and plotted as a contour map to delineate the subsurface distribution of rocks rich in magnetic minerals. The maps show large magnetic anomalies due to basaltic intrusion within the sedimentary rocks trending more or less NNW-SSE and high probability multi-phase nature of intrusion activities. The structural measurements include joints, folds and faults. Most of the measured faults are normal faults with vertical striations on their plains. Some of the measured joints were filled with calcite. These structures are often due to tension caused by uparching of the brittle limestone rocks to give the domal structure of Kolit Fahdi.

12th International Geological Conference in Jeddah (Feb 4-8, 2018), organized by the Saudi Geological Survey and the Saudi Society for Geosciences.

Karst Induced Geo-hazards in Egypt: Case study slope stability problems along some selected Desert Highways

Youssef, A.M.[1,2], El-Shater, A.[1], El-Khashab, M.H.[1], El-Haddad, B.A.[1]
[1]Geology Department, Faculty of Science, Sohag University, Sohag, Egypt, [2]Geological Hazards Department, Applied Geology Sector, Saudi Geological Survey, Jeddah, Kingdom of Saudi Arabia

Abstract

Karst environments are characterized by distinctive landforms related to dissolution characteristics. Karst terrains, frequently underlain by cavernous carbonate and/or evaporite rocks, may induce ground instability problems. Impacts and problems associated with karst are rapidly increasing as development expands upon the karst prone areas. This has led to an escalation of karst-related environmental and engineering problems such as landslides developed on rock cuts/slopes weakened by karstification features. In the current work, the effects of karstification and sinkholes on the stability of the rock cuts/slopes along some selected desert highways were evaluated. These highways represent the most used highways in Egypt, connecting most of the Governorates. They represent the backbone of Egyptian transportation and commercial traffic. Finally, the most optimum mitigation/remediation methods were summarized to decrease and minimize the consequences of slope instability.

Wasowski J., Giordan D., Lollino P. (eds) Engineering Geology and Geological Engineering for Sustainable Use of the Earth's Resources, Urbanization and Infrastructure Protection from Geohazards. GeoMEast 2017. Sustainable Civil Infrastructures. Springer, Cham

Engineering Applications of 2D Electrical Resistivity Tomography (TRT) For the proposed New Akhmim City, Sohag, Egypt

Abudeif, A.M.[1], FAT-HELBARY, R.E. [2], El-khashab, H.M. [1], Masoud, M.M. [1]

[1]Geology Department, Faculty of Science, Sohag University, (Sohag), Egypt

[2] Aswan Earthquake Research Center, P.O. Box 152 Aswan, Egypt

Abstract

Land reclaimed from water bodies or its equivalent (swamp, flood zones and abandon river channel) usually contain certain mechanically unstable geological formations (e.g. peat and clay) which are inimical to the foundation of engineering structures. Concerted effort must therefore be ensured to determine depth to competent layer (bedrock) across the proposed site as against conventional geotechnical test which is a point test. Complementary noninvasive geophysical methods must be carried out for any engineering construction so as to ensure stability of building construction and avoid the devastating effects of building collapse rampant of late. Thus, electrical resistivity tomography (ERT), constrained by percussion drilling, were used for the present study for addressing these subsurface engineering problems. The method is based on the assumption that subsurface geological materials have significant resistivity contrasts that can be identified based on measurements on the surface. The field geometry was made up of seven profiles using Wenner configuration, The results of the 2-D resistivity tomography along seven profiles with smallest electrode separation of 5.0m on a total length of 300 m was interpreted using Res2dinv software. The subsurface is characterized by three different resistivity zones, which were interpreted as gravel at the top, sand beneath it and clay beneath the sand layers. The ERT results was in consistent with the results of boreholes drilling in the study area The presence of Clay was correlated to the cause of chronic differential settlements of some engineering structures within the area. No serious structural features were detected as faults, karastification phenomena or caving. So the area is valid for construction proposes.

12th International Geological Conference in Jeddah (Feb 4-8, 2018), organized by the Saudi Geological Survey and the Saudi Society for Geosciences.

Alteration parameters affecting the Luxor Avenue of the Sphinxes-Egypt

El-Gohary M. [a], Redwan M. [b]

[a] Conservation Dept., Faculty of Archaeology, Sohag Univ., 82524 Sohag, Egypt

[b] Geology Dept., Faculty of Science, Sohag Univ., 82524 Sohag, Egypt

Abstract

Stone alteration in the environment is caused by various extrinsic disintegration agents, besides, their intrinsic properties “mineralogical composition, textures and internal structure”. Therefore, the purpose of the current study was to evaluate the weathering state affecting the Luxor Avenue of the Sphinxes by studying its chemical, mineralogical and physio-mechanical characteristics, in addition to morphological features. Scientific techniques, such as X-ray fluorescence (XRF), X-ray diffraction (XRD), Petrographical microscopy (PM), Cathodoluminescence (CL), Environmental Scanning Electron Microscope (ESEM) and micro energy-dispersive X-ray fluorescence (μ-EDXRF) were used. The results showed that quartz represents more than 96% of the sandstones and the main cement of the grains is quartz overgrowth. Alteration and formation of kaolinite was clearly observed. Halite, sylvite and bischofite were the main salts that affected the statues representing approx. 78.40%. The study also provided information about the different deterioration factors affected the Avenue of the Sphinxes namely; burial environment, solar effects, soil moisture and groundwater. These caused some deterioration forms such as soiling & crusting, breaking down most of the statues heads, saturation forms, salt crystallizations and stone abrasion. Cleaning, desalination and consolidation using different materials and techniques, in addition to reducing the human anthropogenic impacts are recommended for future conservation of the Luxor Avenue of the Sphinxes.

Science of The Total Environment, 626, (2018), 710-719

Evidence for rare-metal occurrences in the post-orogenic Pan-African Aswan pegmatite (southern Egypt): mineralogy, geochemistry and monazite dating

Abdelfadil, K.M.[1,3], Gharib, M.E. [2], Putiš, M.[3], Uher, P.[3]

[1]Sohag University, Faculty of Science, Department of Geology, 82524 Sohag, Egypt, [2]Helwan University, Faculty of Science, Geology Department, 11795 Cairo, Egypt, [3]Comenius University, Faculty of Natural Sciences, Department of Mineralogy and Petrology, Mlynská dolina, Ilkovičova 6, 842 15 Bratislava, Slovakia

Abstract

Pegmatite-hosted, rare-metal mineralization from Aswan area, southern Egypt, intruded the post-orogenic Pan-African granitic rocks and the associated tonalitic gneisses and biotite schists. Most of the pegmatites show a regular pattern of concentric zoning and present affinity to NYF (Nb-Y-F) family. These pegmatites consist mainly of Kfeldspar, albite, quartz, and subordinate muscovite, while the accessory minerals include columbite-(Fe), monazite-(Ce), xenotime-(Y), zircon, fluorapatite, and magnetite. Compositions of Nb-Ta minerals show enrichment of Ti, Sc and fractionation Fe/Mn and Nb/Ta. These features indicate primary magmatic fractionation of these elements into the highly evolved pegmatite melts, rather than to assimilation from the country rocks. Chemical U-Th-Pb dating of monazite from the studied pegmatites yielded post-orogenic Pan-African age (578 ± 5 Ma). This age is younger than the previously estimated U-Pb zircon ages for the tonalitic gneisses and the associated granitic country rocks of the Aswan area (622 ± 11 Ma- 595 ± 11 Ma; Finger et al. 2008) which the studied pegmatite intruded all of them. The analysed monazite-(Ce) displays the dominant LREE phosphate end-member composition and show large variations in composition from the border to the core zone of the studied pegmatites. Monazite-(Ce) from the border zone has higher ThO2 (2.7–9.5 wt.%), Y2O3 (0.1–3.9 wt.%), Nd2O3 (11.0–14.3 wt.%), Sm2O3 (2.4–3.9 wt.%), Gd2O3 (1.3–3.1 wt.%) with marked lowering in La2O3 (9.3–12.8 wt.%), Ce2O3 (23.2–29.4 wt.%) and slightly negative Eu anomalies relative to the monazite-(Ce) from core zone. This data proved the effective role of fractional crystallization in formation of the studied pegmatites.

5th Central-European Mineralogical Conference, June 26 – 30, Banská Štiavnica, Slovakia.

Provenance studies of Kalabsha kaolin deposits, Egypt: a petrographical and geochemical approach

Saber, E.-S., Ali, M., El-Sheikh, A.

Geology Department, Faculty of Science, Sohag University, Sohag, 82524, Egypt

Abstract

The present study focuses on the kaolin deposit in Kalabsha area south Western Desert of Egypt in an attempt to determine its possible source, tectonic setting, and weathering history by means of integrated petrographical and geochemical approaches. The petrographical study was worked by microscopic investigation and supported by X-ray diffraction analysis. X-ray fluorescence and inductively coupled plasma-mass spectrophotometry methods were used for the determination of the bulk elemental composition. Mineralogical analysis revealed that kaolinite is the main clay mineral component indicating a severe chemical weathering of Al-rich source rocks and complete leaching under warm, semiarid climatic conditions. The nonclay minerals are represented by quartz, iron oxides and hydroxides, Ti-bearing minerals, and zircon. Geochemical data show a prevalence of SiO_2 and Al_2O_3 and enrichment of Hf, Nb, Ta, Th, U, and Zr that support the kaolinitic nature of the deposits and their derivation from a felsic granitic terrain. The high values of the chemical index of alteration and the lower values of the index of compositional variability also suggest an intensive weathered source area and the geochemical maturity of the sediments. Other relevant geochemical discriminant functions and plots reveal felsic igneous parent rock for the kaolin deposits. Q-mode hierarchical cluster analysis combined with the normalized rare earth element patterns played a crucial role in unraveling the origin of the studied deposits. The results show that the most probable source rock of the Kalabsha kaolin deposits is the intense weathering of relatively proximal Adara Adatalob granites and their similar rock types in the Arabian-Nubian Shield from the south Eastern Desert of Egypt.

Arabian Journal of Geosciences, 11 (13), 1 (2018), Article number 339

Late Neoproterozoic adakitic lavas in the Arabian-Nubian shield, Sinai Peninsula, Egypt

Abdelfadil, K. M[a], Obeid, M. A[b,c], Azer, M. K[d,e], Asimow, P.D[e]

[a]Geology Department, Faculty of Science, Sohag University, Sohag, Egypt, [b]Geology Department, Faculty of Science, Fayoum University, P.O. Box 63514, Fayoum, Egypt, [c]Faculty of Petroleum and Mining Sciences, Alexandria University (Matrouh Branch), Egypt, [d]Geological Sciences Department, National Research Centre, 12622 Dokki, Cairo, Egypt, [e]Division of Geological & Planetary Sciences, California Institute of Technology, Pasadena, CA 91125, United States

Abstract

The Sahiya and Khashabi volcano-sedimentary successions are exposed near the southern tip of the Sinai Peninsula, the northernmost segment of the Arabian-Nubian Shield (ANS). These Neoproterozoic successions include a series of intermediate to acidic lavas and associated pyroclastic deposits. Field observations and geochemical data reveal two distinct eruptive phases. The lavas representing each phase are intercalated with volcaniclastic greywackes and siltstones. The first eruptive phase, well exposed at Wadi Sahiya, includes basaltic andesite, andesite and dacite with minor rhyolite. The rocks of this sequence are at most weakly deformed and slightly metamorphosed. The second eruptive phase, well exposed at Wadi Khashabi, includes only undeformed and unmetamorphosed dacite and rhyolite. The two volcano-sedimentary successions were separated and dismembered during intrusion of post-collisional calc-alkaline and alkaline granites. Geochemical compositions of the Sahiya and Khashabi volcanic rocks confirm the field data indicating discrete phases of magmatism, however all the compositions observed might plausibly be derived from a common source and be related to one another dominantly through fractional crystallization. The low and variable Mg# values (55–33) measured in the basaltic andesites and andesites preclude their equilibration with a mantle source. Rather, even the most primitive observed lavas are already the products of significant fractional crystallization, dominated by removal of amphibole and plagioclase. Continued fractionation eventually produced dacite and rhyolite marked by significant depletion in Y and HREE. The gradual appearance of negative Nb-Ta anomalies with increasing SiO2 through both suites suggests at least some component of progressive crustal contamination. The medium- to high-K calc-alkaline character of the Sahiya and Khashabi volcanics could be explained either by their formation at an active continental margin or by a two-stage model that appeals to re-melting of arc material in a post-collisional setting. The Wadi Sahiya basaltic andesite and andesite samples exhibit the defining chemical characteristics of adakites: high Sr (>700 ppm), low Y (<16 ppm), high Sr/Y (>20) and low Yb (<1.8 ppm). Although this signature can be associated with slab melting, here we show that it reflects partial melting of lithospheric mantle beneath thickened continental arc crust. The early eruptive phase, exposed at Sahiya, was erupted on an active continental margin, whereas the later Khashabi succession marks the transition to a post-collisional stage.

Journal of Asian Earth Sciences, 158 (2018), 301-323

Characterisation of the Egyptian Pliocene bentonite from the Sohag region for pharmaceutical use

Elshater, A.[a], Elhaddad, A.[a], Elattaar, A.[a], Abugharbia, M.[b], Soliman, W.[a]

[a]Geology Department, Faculty of Science, Sohag University, Sohag, Egypt

[b]Botany Department, Faculty of Science, Sohag University, Sohag, Egypt

Abstract

This paper aims to prepare purified Na-bentonite with improved properties for its use in the pharmaceutical industry. Calcium bentonite from the Sohag region of Egypt was activated with various proportions of sodium carbonate (2, 3, 5 and 8 wt.%). Additionally, bentonite was purified by sedimentation to eliminate impurities, especially quartz. The results of X-ray diffraction (XRD) and swelling volume data confirmed that raw bentonite was converted to sodium bentonite using 5% Na2CO3. The sodium bentonite (M5) obtained by activation met the chemical and microbiological requirements set by the pharmacopoeias regarding toxic trace elemental contents (As, Pb and Cd), the absence of E. coli, the total contents of aerobic microbes and physicochemical properties such as swelling volume, pH and sedimentation volume. Therefore, (M5) bentonite can be designated as being potentially appropriate for pharmaceutical applications. The cation exchange capacity (CEC), surface area, porosity, pH, gel formation and swelling volume data indicated that M5 bentonite could be used to formulate oral suspensions and in topical application.

Arabian Journal of Geosciences, 11 (14), 1 (2018), Article number 385

Geotechnical properties of Precambrian carbonate, Saudi Arabia

El-Sayed Sedek Abu Seif[1,2], Abdulelah A. Bahabri[1], Abd El-Hamed El-Shater Abd El-Hamed[2]

[1]Faculty of Earth Sciences, King Abdulaziz University, Jeddah, Saudi Arabia

[2]Geology Department, Faculty of Science, Sohag University, Sohag, Egypt

Abstract

The effect of post depositional processes (e.g., diagenesis) on geotechnical properties of the studied Fatima carbonates has been evaluated on 32 oriented samples of Precambrian carbonate of Fatima Group, Jeddah, Saudi Arabia where Fatima carbonate considered as the oldest sedimentary rock unit. Fatima carbonate sequence represents the middle part of Fatima Group and attains 90–130 m thick. Fatima carbonate composes mainly of alternating cycles of highly deformed, folded, and faulted stromatolitic carbonates. Algal laminates with scattered dolomite pseudomorphs are recorded within these carbonates and are shown clearly in cut-slabs. The laminae are millimetric in thickness. The Fatima carbonate has a relative abundance of nearly uniform-sized dolomite crystals. Dolomite crystal are represented by small-sized rhombs of euhedral, subhedral, and non-rhombic. The larger euhedral rhomb-shaped dolomite crystals are occurred as cavity filling dolomite. The silicification features are recognized as patches of cryptocrystalline quartz replacing laminated carbonates. It is believed that this type of silicification represents late diagenetic stage and not influenced by the depositional environment or by physicochemical conditions of water. XRD charts indicate that the Fatima carbonate is consisted mainly of dolomite, quartz, and minor constitutes of gypsum. These carbonates are mostly barren in marine fossils and it is clear that these carbonates were deposited within restricted (lagoonal) marine environment. The rock unit weight values of the studied Fatima carbonate range from 29.429 to 25.993 kN/m3. The total porosity varies from 9.147 to 6.112%. The uniaxial compressive strength (UCS, measured by Schmidt Hammer) values of Fatima carbonate range from 22.6 to 110 MPa for the horizontal direction and from 19.7 to 71.8 MPa for the vertical direction). The abovementioned results implicate that the studied Fatima carbonate rock samples are classified as medium to strong rocks.

Arabian Journal of Geosciences, 11 (17), (2018), Article number 500

Pan-African rare-earth bearing paragneiss, South-eastern desert, Egypt: geochemistry and monazite age dating

Abdelfadil, K.M.[1,2], Putiš, M.[2], Ondrejka, M. [2], Saleh, G.[3]

[1]Sohag University, Faculty of Science, Department of Geology, 82524 Sohag, Egypt, [2]Comenius University, Faculty of Natural Sciences, Department of Mineralogy and Petrology, Mlynská dolina, Ilkovičo va 6, 842 15 Bratislava, Slovakia, [3]Nuclear Materials Authority, P.O. Box 530, El Maadi, Cairo, Egypt

Abstract

The studied gneiss of Abu Rusheid is located about 90 km SW from Marsa Alam City (South-eastern desert, Egypt) covering about 3 km2 with low to medium facies metamorphism. It accommodates rare-element (Nb, Sn, Zr, and REE) mineralization. Chemical composition of the samples was determined by ICP-ES and ICP-MS and detailed mineralogical study using EPMA and LA-ICP-MS have been achieved. The gneiss is strongly enriched in REE. Chondrite-normalized REE patterns illustrated enrichment in HREE in studied rock relative to LRRE and strong Eu negative anomalies. The enrichment in HREE relative to LREE reflects the abundant presence of zircon, monazite- (Ce), xenotime-(Y), and fluorite. Zircon contains high Hf, Th and Yb contents. Columbite is homogenous and weakly zoned and classified as columbite-(Fe) with moderate Mn/(Mn+Fe) ratio (0.35–0.49) and very low Ta/(Ta+Nb) (0.01–0.07) ratio. The EMPA U–Th–Pb dating on monazite from the studied gneiss yields two ages: (i) deformation age of 659 ± 3.5 Ma recorded by monazite cores, and (ii) younger age of 575 ± 2.1 Ma obtained from its rims. The older age is comparable with previous age determination of zircon reported from similar rocks in the Eastern desert, indicating a thermal metamorphic peak at about 560 Ma during the convergence between East and West Gondwana, with simultaneously widespread calc-alkaline granitic intrusions (Loizenbauer et al. 2001). The younger age might represent a later event associated with the emplacement of post Pan-African granitic intrusions (Abdallah 2006, and references therein).

5th Central-European Mineralogical Conference, June 26 – 30, Banská Štiavnica, Slovakia.

Hydrologic analysis of the challenges facing water resources and sustainable development of Wadi Feiran basin, southern Sinai, Egypt

Ahmed, A.A.[a], Diab, M.S.[b]

[a]*Geology Department, Faculty of Science, Sohag University, Sohag, Egypt*

[b]*Geology Department, Faculty of Science, Menoufia University, Menoufia, Egypt*

Abstract

Wadi Feiran basin is one of the most promising areas in southern Sinai (Egypt) for establishing new communities and for growth in agriculture, tourism, and industry. The present challenges against development include water runoff hazards (flash flooding), the increasing water demand, and water scarcity and contamination. These challenges could be mitigated by efficient use of runoff and rainwater through appropriate management, thereby promoting sustainable development. Strategies include the mitigation of runoff hazards and promoting the natural and artificial recharge of aquifers. This study uses a watershed modeling system, geographic information system, and classification scheme to predict the effects of various mitigation options on the basin's water resources. Rainwater-harvesting techniques could save more than 77% of the basin's runoff (by volume), which could be used for storage and aquifer recharge. A guide map is provided that shows possible locations for the proposed mitigation options in the study basin. Appropriate measures should be undertaken urgently: mitigation of groundwater contamination (including effective sewage effluent management); regular monitoring of the municipal, industrial and agricultural processes that release contaminants; rationalization and regulation of the application of agro-chemicals to farmland; and regular monitoring of contaminants in groundwater. Stringent regulations should be implemented to prevent wastewater disposal to the aquifers in the study area.

Hydrogeology Journal, 26 (7), (2018), 2475-2493

Desertification Risk Assessment of Sand Dunes in Middle Egypt: A Geotechnical Environmental Study

El-Sayed Sedek Abu Seif [1,2] , Mohamed H. El-Khashab [2]

[1] *Faculty of Earth Sciences, King Abdulaziz University, Jeddah, Saudi Arabia*

[2] *Geology Department, Faculty of Science, Sohag University, Sohag, Egypt*

Abstract

The evaluation of aeolian desertification of sand dunes in north Assuit, Middle Egypt, has been achieved throughout a variety of detailed field investigations and laboratory measurements. The study area lies in hot dry desert climatic conditions where the sand dunes migration represents an effective threat cultivated lands, reclaimed lands, asphaltic roads and the systems of human distribution. Its mean annual rainfall is about 51mm. Except the Nile Valley, Egypt is mostly considered as dry desert lands so about 4% of its surface area is under plough. The study barchans are mainly composed of poorly graded sands and consist of fine sand, medium sand and a negligible amount of coarse sand, silts and clays. Compositionally, the studied sand dunes are mainly consist of quartz, rock fragments and negligible amounts of feldspars with the absence of any chemically active constitutes (e.g. chert, flint, chalcedony and dolomite). These sands are also free of organic matter. The removal of dune sands in hazardous sites considers a short-term solution method of the aeolian desertification problem.

Arabian Journal for Science and Engineering, 11 (17), (2018), 1-19